A Study of the Rapid Maxillary Expansion with the use of the Finite Element Method

by

Anastasios Kotinas

M.Sc., Dip.D.S., M.Orth. (RCS Edin)

DISSERTATION SUBMITTED FOR THE
Ph.D. IN ORTHODONTICS
AT THE
UNIVERSITY OF EDINBURGH
2007

DECLARATION

I, Anastasios Kotinas, declare that the following thesis was composed by the candidate and it is entirely my own work, with the exception of the help and guidance acknowledged in the text, and that the present work has not been submitted for any other degree or professional qualification except as specified.

A. Kotinas

Acknowledgements

I would like to express my sincere appreciation and gratitude once again to my supervisor Dr. J.P. McDonald; Consultant of the Orthodontic Department in the Victoria Hospital and Honorary Senior Lecturer of the Edinburgh University, for his priceless and substantial help and guidance in composing my thesis. I would also like to thank him for the information he kindly offered for the completion of the study groups of this work.

I wish also to thank Associate Professor Christoforos Provatidis; from the School of Mechanical Engineering of the National Technical University of Athens, but for his expertise and assistance in the development of the finite element model, the completion of this present study would have been impossible.

And at last but not least, I wish also to express my appreciation and gratefulness to my wife Marianna and my son Alex; for their substantial support and patience they showed all these years, without which, I would have found it difficult to complete successfully this work.

ABSTRACT

It is well documented in the literature that the contracted maxilla is commonly associated with nasal obstruction and mouthbreathing, forming what is known as "adenoid facies" or "long face" syndrome.

Midpalatal splitting at an early age produces separation of the maxillary halves with consequent widening of the nasal cavity and significant improvement in the Nasal Airway Resistance. Although clinicians agree about many of the indications for and outcomes of Rapid Maxillary Expansion, a review of the literature indicates that some disagreements persist in relation to the procedure.

The present study presents the development of a finite element model to simulate the craniofacial changes that occur during rapid maxillary expansion therapy. The mechanical model involves the entire human skull with the expansion device; the latter transforms the manual turns of the screw into orthodontic forces applied to the two maxillary halves through the anchor teeth of the appliance.

The behaviour of the finite element model was compared to the findings of a previous clinical study and to an *in-vitro* experiment in order to evaluate the qualitative and quantitative response of the craniofacial complex. The results refer to the opening pattern and associated displacements, stresses and strains on the cranium, the maxilla, the periodontal ligament and the anchor teeth. A parametric analysis of the finite element model was conducted for investigating the biomechanical effects of the procedure.

It appears feasible to simulate reliably the orthopaedic changes that occur in the nasomaxillary complex by the use of finite element analysis. The geometry of the model, as well as the midpalatal and the zygomaticomaxillary sutures and the articulation of the pterygoid process with the perpendicular plate of the palatine bone, play an important role in the degree and the manner of the maxillary separation. However, further research is required to define the material properties of the various craniofacial structures and consequently develop a finite element model which simulates the biomechanical aspects of the clinical procedure more accurately.

LIST OF CONTENTS

LIST OF TABLES

LIST OF FIGURES

LIST OF APENDICES

CHAPTER 1: INTRODUCTION

Rapid Maxillary Expansion is a clinical treatment modality that can be utilised in the treatment of maxillary deficiency to correct bilateral crossbite and to improve intra-nasal patency. The primary goal is to maximise orthopaedic and minimise orthodontic movement of teeth. To separate the maxillary halves at the median palatine suture, a splint attached to the anchoring teeth applies a high level of force to the maxillary basal bone (Isaacson *et al.*, 1964). This force splits the midpalatal suture in young adolescent patients and abducts the two maxillary halves laterally (Cleall *et al.*, 1965; Davis *et al.*, 1969; Haas, 1961; 1965; Wertz, 1970; Hicks, 1978; Timms, 1980; Memikoglu *et al.*, 1999).

Widening of the maxillary arch has been reported to be associated with a variety of effects in various craniofacial areas (Zimring *et al.*, 1965). Histological studies on animals demonstrated signs of increased cellular activity at various circumaxillary sutures (Starnbach *et al.*, 1964; 1966; Gardner *et al.*, 1971; Storey, 1973; Ten Cate *et al.*, 1977). Linge (1976) described the translation of forces into 'biological tissue reactions' in the suture following application of an external mechanical force. These biological tissue reactions include changes in the activity of cells and intercellular substances.

In the literature there is little information regarding the characteristics of the force, the areas of maximum concentration, the dissipation of the force, and finally the effects of this force on the various craniofacial sutures. Moreover, effective optimal treatment during orthodontic mechanotherapy requires that a clinician be aware of both the biological and biomechanical

response of the craniofacial skeleton to an applied force system (Tanne *et al.,* 1988a)

Various approaches have been developed to study the effect of orthopaedic force systems on the craniofacial complex. Animal research (Droschl, 1973; Nanda, 1978 and 1984; Jackson *et al.,* 1979) coupled with cephalometric studies using implants to measure the relative displacement of the craniofacial bones (Björk, 1955), *in vitro* studies employing strain gauges (Tanne *et al.,* 1985), photoelastic (Chaconas *et al.,* 1976) and holographic techniques (Pavlin *et al.,* 1984; Kragt *et al.,* 1986), have been used to characterise the mechanical behaviour of the craniofacial skeleton in response to the applied force system. Even though these studies have provided useful findings for clinical orthodontics, most of them have been limited to the precise evaluation of the biomechanical effect on the internal bony structures, including the sutures of the craniofacial complex. The displacements and stress-strain levels induced within the complex however have not been comprehensively researched (Tanne *et al.,* 1989).

In recent years, bioengineering has successfully employed the Finite Element Method (FEM) in developing model systems of structures in order to calculate both stresses and deflections due to applied forces (Turner *et al.*, 1956). In 1972, some fifteen years after the finite element method initiated a revolution in stress analyses of structures in engineering mechanics, this 'new method' was first introduced in the orthopaedic literature (Brekelmans *et al.,* 1972). Finite element method offers interesting possibilities in this respect, because it permits structural analysis of the patterns of externally induced stress and strain to be modelled as a system of composite, elastic materials (Korioth *et al.,* 1992). However, limitations to finite element modelling in the early '80s, were due to the assumptions and oversimplifications of material properties and skeletal geometry incorporated in those models. These simplifications were necessary as finite

element methods and CPU possibilities were restricted (Krabbel *et al.*, 1995).

These limitations are gradually improving through biomechanical research and advances in computer software and hardware. Consequently, the use of the Finite Element Method has expanded in all fields of medical and dental science. In recent years, Finite Element Analysis has been introduced in orthodontics as a powerful research tool for solving various structural mechanical problems. Analytical models of the craniofacial complex using the Finite Element Method have been developed in order to eliminate the shortcomings of conventional methods in orthodontic research (Khalil *et al.*, 1977; Knoell, 1977; McPherson *et al.*, 1980; Haskell *et al.*, 1986). There are two main methods of applying Finite Element Analysis in biomechanical studies. One is the analysis of stress and strain when any given force system is applied to the teeth or the cranial complex. The other is the evaluation of the subsequent craniofacial growth with particular relevance to the impact of such forces.

The aim of the present study was two-fold:

- To develop a three-dimensional anatomically accurate finite element model of the craniofacial complex with its structures, the appropriate physical characteristics and attributes of cortical and cancellous bone, sutures, teeth, and periodontal ligament together with the rapid maxillary expansion (R.M.E.) appliance for the FE analysis,
- To investigate the biomechanical reactions of the craniofacial bones to the heavy transverse orthopaedic forces generated by the RME appliance, with a view to quantifying the resultant stresses and displacements within the maxillary sutures, and hence to clarify the relationships of these displacements to biological phenomena such as suture separation, bone remodelling and tooth movement. The inherent characteristics of the force vectors will also be scrutinised.

The results of the Finite Element Analysis then to be compared to the findings of an earlier clinical study (McDonald, 1995).

CHAPTER 2: LITERATURE REVIEW

2.1. Rapid Maxillary Expansion

2.1.1. History

Orthodontic and rhinologic literature from 1860 (Angell, 1860) to 1930 reveals considerable controversy over the desirability and possibility of splitting the hard palate at the midsagittal suture as a means of widening the dental arch and the nasal cavity. In 1880, Kingsley described an appliance that could influence the position of the dentition in the upper jaw with the aid of extraoral forces. According to Pfaff (1905); Lohman (1915); and Derichsweiller (1953), the first rhinologist to be interested in the separation of the maxillary shelves was Eysell from Berlin, who, in 1886, suggested the possibility of influencing the inner configuration of the nose in this manner.

The compressed maxillary arch has also been of major concern to those who have interested themselves in the arrangement of the teeth. The causes of buccolingual discrepancies (i.e. narrow maxillary arch with unilateral or bilateral crossbite) could be either *genetic, environmental,* or *the result of abnormal function* (Harvold *et al.,* 1972; Graber, 1975) (i.e. mouthbreathing). In these cases, tooth movement alone cannot adequately accomplish the treatment objectives. The arch width must be increased by forceful separation of the maxillary shelves. Clinicians have increasingly included Rapid Maxillary Expansion in the treatment of their patients. Numerous appliances, fixed and removable, are used for the expansion of the dentomaxillary complex with the objective of placing the maxillary dental arch in a stable lateral position.

Midpalatal splitting with removable appliances is possible but not predictable. They can be used in the deciduous or early mixed dentition and must have sufficient retention to be stable during the expansion phase. The fixed split acrylic appliances (i.e. Arnold, Haas tissue-borne, Hyrax type appliances, Spolyar etc.) using spring loaded or nonspring-loaded jackscrews are most commonly encountered in the literature and more often used in the pre-adolescent children on a rapid or semirapid manner. The advocates of the tissue-borne fixed appliance believe that it causes a more parallel expansion force on the two maxillary halves and that the force is more evenly distributed to the teeth and the alveolar processes (Haas, 1961; 1970). A number of all metal fixed appliances have been used to accomplish slow expansion (i.e. Quad Helix, Coffin palatal arch), particularly in the deciduous and early mixed dentitions.

Although clinicians agree about many of the indications for and outcomes of Rapid Maxillary Expansion, a review of the literature indicates that various views and counterviens exist. Scientific research into the effects of rapid palatal expansion in animals and human subjects was not undertaken until the early 1960s. These studies showed that, by applying mechanical forces, not only the position of the dentition could be changed, but moreover that the growth of the entire maxillary complex could be modified by influencing sutural growth.

2.1.2. Techniques:

Removable expansion plates are not recommended if significant skeletal changes are required. Midpalatal splitting with such appliances is possible, but not predictable. The main problem of these appliances is the lack of rigidity (the resistance to rotation); the dentoalveolar components will tilt buccally hence diminishing the amount of basal bone expansion that is necessary. For these appliances to be effective, they must be used in the

deciduous or early mixed dentition and must have sufficient retention to be stable during the expansion phase (Skieller, 1964; Ivanovski, 1985).

The fixed split acrylic appliance consists of an expansion screw with acrylic abutting the alveolar ridges. The expansion screw can be either a spring loaded or nonspring-loaded jackscrew. The advocates of the tissue-borne fixed appliance believe that it causes a more parallel expansion force on the two maxillary halves and that the force is more evenly distributed on the teeth and the alveolar processes (Haas, 1961; 1970). The appliance is attached to the teeth with bands on the molars and first premolars.

For a more controlled expansion and a more assured palatal splitting, the use of sturdier appliances is recommended. The HYRAX, Haas, Derichsweiler or Biederman appliances utilise nonspring-loaded jackscrews with an all wire frame. This frame is soldered to the bands on the abutment teeth. The advocates of these appliances believe that they cause the least irritation to the palatal mucosa and are easier to keep clean. The Minne expander is a heavily caliber coil spring that is expanded by turning a nut to compress the coil. Two metal flanges perpendicular to the coil are soldered to the bands on the abutment teeth. Spring-loaded screws and the Minne expander may continue to exert expansion forces after completion of the expansion phase unless they are partially deactivated.

However, Barber and Sims (1981), Langford (1982) and Odenrick *et al.* (1982) all recorded marked buccal root resorption in first permanent premolars when these were used as buttresses for the Biederman type rapid maxillary expanding appliances. These defects tended to gradually repair when the pressure was relieved.

Silver/copper alloy cast cap splints, as described by Grossman (1963), have a number of advantages over band retained appliances. Cast splints which are extremely rigid, spread the load levels over the whole buccal tooth

bearing area and also relieve intercuspal locking whilst the expansion is taking place. More recently bonded full coverage appliances had been described (Mondro, 1976; Howe, 1982; Spolyar, 1984). The acrylic body used in the appliance design is preferred rather than an all wire framework as much of the expanding force is exerted against the alveolar process and base bone rather than purely teeth (Haas, 1961).

A number of all metal tooth-borne appliances have been used to expand arches. The Arnold expander, the Coffin palatal arch and the Quad Helix appliance have been used to accomplish "slow" palatal expansion, particularly in the deciduous and early mixed dentitions. Again, rigidity is of prime importance so these appliances which are attached only to the maxillary first molars can have limited effectiveness in cases such as cleft palate patients (Isaacson and Murphy, 1964). More recently, a two-point all metal rapid palatal expander was introduced with similar effects on the midpalatal suture and the dentition as did the four-point appliance (Lamparski *et al.,* 2003).

In older patients where the midpalatal suture is highly interdigitated, Rapid Maxillary Expansion can be accomplished by surgically moving the maxilla with lateral corticotomies (Lines, 1975), by surgically undermining the maxillae to release the areas of bony resistance (Glassman *et al.*, 1984; Alpern *et al.,* 1987), or by surgical separation of the palatal shelves (Bell *et al.,* 1976; Kraut, 1984). Mommaerts (1999) has described a technique of transpalatal distraction with a bone-borne titanium device for correction of maxillary transverse discrepancies.

The screws most commonly used in rapid maxillary expander appliances are Hyrax (Dentaurum 602-813), Glenross VI or Leone 620, all of which give between 11 and 18mm of expansion.

2.1.3. Forces developing during Rapid Maxillary Expansion treatment:

Orthodontic and orthopaedic forces often differ as to objectives, application, intensity, time and timing, and type. *An orthopaedic force must be of sufficient strength because it is dissipated over a wide area and is ideally utilized in the early growth of the individual.* RME forces can affect both the end result and associated side effects. Orthopaedic forces are usually intermittent and heavy, ranging from 500grm – 2000grm, the maximum load produced by a turn of the jackscrew and occurs at the time of turning the screw and begins to dissipate rapidly (Zimring and Isaacson, 1965).

It is difficult to measure compression or tension within the sutures, and there is no way to know theoretically what is required to alter growth. Clinical experience suggests that moderate amounts of force against the maxillary teeth can impede forward growth of the maxilla, but heavier force is needed for separation of sutures and growth stimulation. However, when force is applied to the teeth, only a small fraction of the pressure in the periodontal ligament is experienced at the sutures, because the area of the suture is so much larger.

In the studies of Isaacson *et al.,* (1964); horizontal, vertical and a combination of the two resulting in a buccal rotational force on the alveolar shelves of the maxilla, was measured in strains and then converted into force units using in vitro calibration curves. Isaacson, Wood and Ingram (1964) reported that 3 to 10 lb of force can be produced by single turns of the jackscrew appliance (i.e. 0.2mm lateral displacement) with cumulative loads of 20 lb or more after multiple daily turns. A year later Zimring and Isaacson (1965) measured maximum loads ranging from 16.6 pounds to 34.8 pounds during treatment. However, Hicks (1978) in a clinical study using the Minne-expander appliance produced measurable

separation of the maxillary segments. Using a 2 pound continuous load, he achieved 3.8 to 8.7mm of expansion during a 13-week period.

In 1995, Movassaghi *et al.* advanced the entire nasofrontal complex in rabbits using 0.54 Newton from a coil spring. Chin and Toch (1997) reported that 98 Newton was necessary to advance the midface in children and adolescents, which is near the force measured by bioengineers to elongate the tibia in adults (98 to 147 Newton) (Leong *et al.*, 1979). The force necessary to protract only the maxilla in older children and adults was measured between 5 and 20 Newton (Goh *et al.*, 1992; Major *et al.*, 1993). The average strain developed over treatment time demonstrates similar curvatures for both anterior (i.e. premolar) and posterior (i.e. molar) strains (Vardimon *et al.*, 1998). The mean expansion over treatment time showed a strong shape similarity to the mean strain diagram.

According to Newton's third law, the expansion force values recorded represent an indication of the resistance provided by the soft-tissue and/or osseous attachments to expansion. The magnitude of these resistance forces would be expected to vary according to a number of factors including the size of the displaced bone segments and elastic characteristics of the remaining tissue attachments, bone density and degree of ossification of the circummaxillary sutures (Remmler *et al.*, 1998). However, an equal amount of displacement produces a diverse magnitude of forces between patients or even in the same patient at different stages (i.e. before or after splitting the fibres of the midpalatal suture) of the Rapid Maxillary Expansion treatment. The resistance effect of the involved structures not only dictates the magnitude of force but could also alter the stability of the expanded dental arch.

An age differential was noted in the time required to dissipate loads produced by the appliance. Younger patients dissipated the load produced by a twice-daily activation schedule for a relatively longer period of time

than did the older patients. A smaller load was produced per activation in the younger patients as compared with the more mature patients. The presence of lower load values indicates only that the facial skeleton yielded to the expansion more readily and does not necessarily indicate that this is the optimal rate at which the expansion procedures should be carried out.

The Rapid Maxillary Expansion appliance is reactivated daily or in daily intervals and the initial force might decay to zero during these intermittent intervals. However, because no abrupt decrease in strain during the active phase was noticed, the theory of major resistance provided by the midpalatal suture which declines on splitting, could not be supported.

If the force does not decline to zero, residual force develops in the system. By definition a residual force is the force remaining between two consecutive activations before the onset of the second activation. The accumulation of residual forces suggests that the force magnitude could elevate over active treatment time.

Isaacson *et al.* (1964), and Zimring and Isaacson (1965) demonstrated that residual forces at the range of 1 to 11,5 pounds always develop during the active Rapid Maxillary Expansion phase, so maintaining a constant expansion force on the facial skeleton. During the retention phase, residual forces dissipate exponentially so that after 30 to 45 retention days, force magnitude decays almost to zero. On the other hand, Brosh *et al.,* (1998) found that strain level was preserved during the retention phase, apparently due to relapse strains. According to Brosh *et al.* (1998), the system will restore to zero strain only after the cessation of the relapse potential.

Intrasession and intersession strains and their pattern are most conceivably related to immediate or delayed responses of the maxillary complex. The immediate response probably occurs when the tooth moves in the periodontal ligament adjunct with some initial bending of the alveolar

process. The alveolar process bending occurs because screw displacement is greater than the periodontal ligament width. However, during the intermittent period, a second wave of delayed response appears, usually characterized by an increased resistance due to a later displacement of the maxillary complex affected by the circummaxillary sutures. The circummaxillary complex response is the major factor influencing the buildup of strain over treatment time. As a result, the maxillary complex undergoes displacement and tipping in various directions (not only transverse translation) introducing heavy and diverse moments in the system.

Residual forces have been shown also to depend on the patients age. The interarch expansion in patients with patent sutures and patients with advanced ossified circummaxillary sutures might be quite similar clinically (dental expansion can replace skeletal expansion in advanced ossified circummaxillary sutures), yet the strain level and pattern of development can differ substantially. Slower rates of expansion would also probably allow for physiological adjustment at the maxillary articulations, and would prevent the accumulation of large residual loads within the maxillary complex (Brosh *et al.,* 1998).

2.1.4. Possible Mechanisms for Maxillary Expansion:

Rapid maxillary expansion takes place when the lateral force applied to the teeth and maxillary alveolar processes exceeds the limits needed for orthodontic tooth movement. This pressure then acts as an orthopaedic force, compressing the periodontal ligament, deforming the alveolar processes, opening the mid-palatal suture and leading to bone apposition.

Advocates of "rapid" expansion (1 to 4 weeks total activation), believe that it results in minimum tooth movement (tipping), and maximum skeletal displacement. The theory is that with rapid force application to the

posterior teeth, there will not be enough time for tooth movement, the force being transferred to the suture and the suture opening whilst the teeth move only minimally relative to the supporting bone. Advocates of "slower" expansion (2 to 6 months) believe that it produces less tissue resistance in the circummaxillary structures and less tipping of the abutment teeth, as well as better bone formation in the intermaxillary suture, and that both factors help minimize postexpansion relapse (Isaacson *et al.,* 1964; Zimring & Isaacson, 1965; Storey, 1973).

When one is observing results of orthopaedic and orthodontic force systems applied to the maxillary complex, it can be seen that the most frequent effect is a posterior rotation of the maxilla, that is, a forward, downward tipping around the maxillary palatal region (Melsen, 1978; Haas, 1980; Nanda, 1980; Williams and Melsen, 1982). These observations can be explained by the complexity of the sutural area in the posterior part of the maxilla compared to the more simple sutures connecting the maxilla with the frontal, nasal, and zygomatic bones. The lateral tipping which occurs rapidly and the concomitant increase in palatal width suggests that it may not be due to teeth tipping within the alveolar process. Rather, it is probably the result of a rotation of the two palatal segments around the split midpalatal suture (Starnbach *et al.,* 1966). For this latter possibility to have occurred, a concurrent reorientation of the more remote facial bones would probably need to take place.

The aspect of rapid expansion that was not appreciated initially was that orthodontic tooth movement continues after the expansion is completed, until bone stability is achieved. In most orthodontic treatment, the teeth move relative to a stable bony base. It is possible, of course, for tooth movement to allow bony segments to reposition themselves while the teeth are held in the same relationship to each other, and this is what occurs during the approximately 3 months required for bony fill-in at the suture after rapid expansion (Ekström *et al.,* 1977). During this time, the dental

expansion is maintained, but the two halves of the maxilla tend towards approximation, which is possible because at the same time the teeth move laterally on their supporting bone (Proffit, 2000).

The maxilla grows by apposition of new bone at its posterior and superior sutures, in response to being forced anteriorly by the lengthening of the cranial base and pulled downward and anteriorly by the growth of the adjacent soft tissues (Krebs, 1964; Björk and Skieller, 1974). The maxilla always moves downward and anteriorly with Rapid Maxillary Expansion specifically because of the sutural orientation of the maxilla. The *"hafting zone"* (circummaxillary sutures) are disengaged by the tension created due to the Rapid Maxillary Expansion, and as the maxillae are forced apart and these sutures begin to open, the force produces an effect similar to growth, so that the maxilla moves downward and anteriorly (Haas, 1970). Denticulated sutures open, the bones slide, and the denticles bind like ratchets to prevent the return of the maxilla to its former position.

Another possible mechanism of maxillary movement is reminiscent of the septomaxillary ligament hypothesis in relation to maxillary growth. Ohshima (cited in Chang *et al.,* 1997) asserted that "new bony spicules deposited in a direction perpendicular to the inferior border of the vomer revealed evidence of a downward displacement of the maxilla". Ohshima implied that osteogenic activity at the vomeromaxillary suture pushes the maxilla downward or at least facilitates the downward displacement of the maxilla.

An additional mechanism has been proposed that involves structures distant from the circummaxillary sutural system. In Gardner and Kronmans' study (1971) with Rhesus monkeys, Rapid Maxillary Expansion produced 0,5-1mm of opening of the sphenooccipital synchodrosis. This finding may represent another mechanism by which the maxilla moves downward and forward.

Biederman (1973) suggested how the anterior maxilla at point 'A' can come forward with Rapid Maxillary Expansion therapy: if the Centre of Rotation (CRo) of the expansion is located at the posterior part of the maxilla at the junction between the hamular and pterygoid plates, then the paired maxillae rotate about these points and point 'A' comes forward. Biederman also proposed a mechanism for bite opening: if the maxilla disarticulates from the nasal bones and walls of the ethmoid then the bite closes. If those bones do not disarticulate but instead bend, then subsequent remodeling tips the palatal plane down at the posterior nasal spine, which causes an increase in the mandibular plane angle, thereby opening the bite.

Christiansen and Burstone (1969), have repeatedly shown that in order to forecast the movement of a constrained body (describing its centre of rotation), the equivalent force system at its centre of resistance must be known. Because Lee *et al.,* (1997) have identified the locations of the centres of resistance of the dentomaxillary complex in the sagittal and frontal views, one can relate the force systems of midpalatal sutural expansion to the centres of resistance of the attendant osseous structures. When an expansion force (F) is applied through activation of the Hyrax appliance, an equivalent moment and force result at the centres of resistance of each maxillary segment. The magnitude of the moment is equal to the perpendicular distance (Y) from each respective centre of resistance to the point of action of the expansion force, multiplied by the expansion force (F). The moment equivalent (FY) tends to cause the maxillary halves to rotate about their respective centres of resistance, while the expansion force (F) equivalent at the centre of resistance tends to translate the maxillary halves (Braun *et al.,* 2000). The net result is to provide centres of rotation in line with and superior to each centre of resistance. The osseous structures at the frontonasal suture would have to rapidly resorb to permit rotation of the maxillary halves about a point superior to the centre of resistance other than at the frontonasal suture. The centre of rotation is thus constrained to be at the frontonasal suture since

the resorption and reorganization at this suture would be a relatively lengthy process versus expansion at the midpalatal suture. The patterns on the zygoma are fundamentally translatory, implying a primary shearing stress in the zygomaticotemporal sutures, and primary compression and shearing stresses in the zygomaticomaxillary and zygomaticofrontal sutures. In the occlusal view the centre of rotation is calculated at the distal aspect of the maxillary midpalatal suture approximating the distal one third of the third molars, distal to the centres of resistance of the maxillary halves.

2.1.5. Skeletal Effects of the Rapid Maxillary Expansion treatment:

The bones of the craniofacial complex undergo many differential changes during growth. These changes, both in the amount and in the direction of bone growth, are primarily the result of inherent and genetically controlled cellular processes. Some of the changes are probably influenced by external factors such as muscle attachments and functional activity. In addition, the growth pattern of one bone may possibly be partially controlled by the growth of adjacent skeletal structures. In general, bones react to the stresses placed upon them. If the stresses change either in magnitude or in direction, then an alteration in the shape or structure of the bone or its relationship to adjacent bones can be expected as a result (Starnbach *et al.*, 1966).

2.1.5.1. Effects on the maxillary complex:

Rapid maxillary expansion occurs when the force applied to the teeth and the maxillary alveolar processes exceeds the limits needed for orthodontic tooth movement. As Bell (1982), has reported, if the applied transverse forces are of sufficient magnitude to overcome the bioelastic strength of the

sutural elements, orthopaedic separation of the maxillary segments, with a lateral shift of the two horizontal processes of the maxilla, can occur.

Haas in 1970, was among the first researchers who systemised the several aspects of rapid maxillary expansion:

- Anteroposteriorly, the opening of the midpalatal suture is initially scissors-like in nature (Inoue, 1970; Wertz, 1970), while if force continues for a longer period of time it produces a more parallel opening; inferosuperiorly, the opening is triangular with the apex being in the nasal cavity;
- As the suture opens, the crowns of the central incisors, considering that they are linked by elastic transseptal fibres, converge while the roots diverge and a diastema of 5mm on the average is found (or about ½ as great as the distance the screw had been opened). When the crowns come into contact, the continuing pull of the fibres causes the roots to converge toward their initial axial inclinations. During this cycle which usually takes about 4 months, the axial inclination of these teeth may vacillate as much as 50°;
- As the maxillae separate, the outer walls of the nasal cavity move laterally. Being attached to these walls, the concha retreat from the septum while the palatal processes swing inferiorly (Haas, 1965; Fried, 1971) at their free margin resulting in straightening of the deviated nasal septum and in increased intranasal capacity which facilitates nosebreathing in cases of nasal stenosis. These patients with the greatest degree of respiratory difficulty seem to notice the most improvement;
- The alveolar processes bend and move laterally with the maxillae. The effect is dental arch expansion. After stabilisation is terminated, any residual forces in the displaced tissues will act on the alveolar processes causing them to rebound (Isaacson *et al.,* 1964);

- When the midpalatal suture opens, the maxilla always moves forward and downward, specifically because of the sutural orientation of the maxilla (Haas, cited in Chang *et al.,* 1997; Chung and Font, 2004). The requisite expansion of the apical base is achieved by rotation of the halves of the maxilla in the frontal and horizontal planes. Thus, they move laterally with the fulcrum of rotation close to the frontonasal suture (Storey, 1973);
- The change in maxillary posture invariably causes a downward and backward rotation of the mandible which decreases the effective length of the mandible and increases the vertical dimension of the lower face (Chung and Font, 2004);
- More mobility of the maxilla for continued maxillary orthopaedic influence is thus created;
- In some cases, the previously low-positioned tongue[1] assumes normal posture (Starnbach *et al.,* 1966).

The magnitude of the opening varies greatly in different individuals and at different parts of the suture. Four components determine the interarch expansion: sutural displacement, alveolar process tipping and bending, tooth displacement and tooth tipping. The dental movement consists of tip and displacement. The skeletal change is more compound and is composed of sutural displacement, which is the result of sutural widening, and the alveolar process tipping and bending, which is affected by the interaction of the alveolar process with all circummaxillary sutures (tipping) and by the elastic mechanical property of bone *per se* (bending) (Vardimon *et al.,* 1998).

Krebs (1958; 1964) studied maxillary expansion with metallic implants. He placed implants in the alveolar process lingual to the upper canines and along the infrazygomatic ridge, buccal to the upper first molars. He found

[1] This may be due to the increased size of the palatal vault permitting the tongue to take a higher position, or the fact that the tongue has been trained to hold a loose fitting palatal retainer in place.

that the mean increase in intermolar distance measured on casts was 6mm, while the mean increase in infrazygomatic ridge implants was 3.7mm. In 20 of 23 patients examined, the increase in width of the basal zone of the maxilla was equal to or less than ½ the amount of dental arch expansion. He also found that the sutural opening was on average more than twice as large between the incisors than it was between the molars. On the other hand, Memikoglu *et al.* (1999) in a clinical study, indicated that the mean increase in maxillary base width was more than ½ the amount of intermolar expansion.

The suture opens wider and more rapidly anteriorly because of the buttressing effect of the other maxillary structures in the posterior regions (Isaacson *et al.,* 1964b; Gardner *et al.,* 1971; Vardimon *et al.,* 1998). Kudlick (1973), working on a human dried skull came to the conclusion that it was the sphenoid bone not the zygomatic arch that was the main buttress against maxillary expansion. He emphasized that the pterygoid plates of the sphenoid, although bilaterally positioned, do not have a mid-sagittal suture that allows them to be displaced laterally. This limiting effect of the pterygoid plates of the sphenoid minimizes dramatically the ability of the palatine bones to separate at the mid-sagittal plane. The pterygoid plates can only bend to a limited extent as pressure is applied to them, and their resistance to deformity increases dramatically in the parts closer to the cranial base where the plates are significantly more rigid (Timms, 1980). The most posterior part of the suture undergoes a negligible split, if at all. Holberg *et al.* (2006), using Finite Element Method, studied the stresses occured at the cranial base during rapid palatal suture expansion. They noticed that with increasing age, patient's bone elasticity decreases and consequently, lateral bending of the pterygoid process leads to a marked development of stress, particularly in the area of the sphenoid and the round foramen.

As the widening is greater in the anterior than the posterior segment, it forms a V-shaped expansion of the suture in the horizontal plane. However, it was found that "the suture opens in an antero-posterior direction, but rebuilds in a postero-anterior direction". This process is termed the 'zip' mechanism. Thus, the anterior region is more prone to relapse (Revelo *et al.,* 1994; Vardimon *et al.,* 1998).

With the initial alveolar bending and compression of the periodontal ligament, there is a definite change in the long axis of the posterior teeth (Thörne, 1956; Herold, 1989). Hicks (1978) found that the angulation between the right and left molars increased from 1° to 24° during expansion placing the palatine cusps in an extrusive relation with the lower molars. This tipping is usually accompanied by some extrusion, or the upper molars following the downward displacement of the maxilla (Byrum, 1971). Starnbach *et al.* (1966), however, in a histologic study noticed that the palatal processes, the alveolar processes and the teeth may have rotated as a unit around the disrupted midpalatal suture. In the anteroposterior dimension the rapid maxillary expansion appliance (Haas) does not induce any modification of the anchorage molars. Dental extrusion and consequent increase in dentoalveolar height contributes to the palatal depth change with rapid maxillary expansion (Davis, 1969). The expansion procedure imposes heavy forces on the roots of the anchor teeth and in association with the aforementioned tipping of these teeth, in few occasions root surface resorption was observed on the buccal side of the roots of first premolar teeth (Odenrick *et al.,* 1982). However, repair of the resorptive defects was found to occur exclusively with cellular cementum (Langford *et al.,* 1982).

The maxillary central incisors tend, also, to be extruded relative to the S-N plane and in 76% of cases they upright or tip lingually. This movement helps to close the diastema and also to shorten arch length. The lingual tipping of the incisors is thought to be caused by the stretched circumoral musculature (Wertz, 1970).

With the orthopedic expansion of the maxilla, the individual SNA variation ranged from -3,0° to +2,5° (da Silva *et al.,* 1991). These findings differ from the results of Haas, which ranged from 0,0° to +3,5°. In his work Haas found an anterior displacement in all of the 10 cases studied. This significant forward displacement of the maxilla observed by Haas may be related to the magnitude of the expansion achieved by the appliance or may be related to the skeletal resistance. In the early developmental stage, the least resistance of the facial structures to the expanded maxilla hinders its forward displacement during expansion. Haas, also, appraised this forward displacement of the maxilla by use of linear cephalometric measurements. He registered a 1,0mm to 4,0mm forward displacement of point A, although he used the facial plane (N-Pog) as a reference line. However, because of the mandibular spatial alterations that follow Rapid Maxillary Expansion procedures, this line does not represent a reliable reference base.

Krebs (1958), showed that the two halves of the maxilla rotated in both the sagittal and frontal planes, with the fulcrum of rotation in the frontal plane approximately at the frontomaxillary suture (Haas, 1961; Wertz, 1970; Hicks, 1978). Haas (1961) and Wertz (1970) and more recently Franchi *et al.,* (2002) found the maxilla to be more frequently rotated downward and forward resulting in an increase in the lower anterior facial height. Hicks (1978), using implants, found that the maxillae tip anywhere between -1° and +8° relative to each other. This tipping of the two maxillae results in less width increase at the sutural level than at the dental arch level. A few years later, Sarnäs *et al.* (1992) again with the use of implants, found that rotations and translations about and along the three cardinal axes of the head take place due to the left maxillary half relative to the right involving a complete re-orientation of the maxillae in space. The immediate effect of Rapid Maxillary Expansion was a rotation of the left maxillary bone about the vertical axis resulting in a V-shaped widening of the mid-palatal suture,

i.e. the anterior parts of the maxilla were separated more than the posterior parts. The effect of the rotation of the left maxillary bone about the sagittal axis was manifested by a wider separation inferiorly than superiorly. The greatest effect of the separation of the two maxillae was a rotation of the left maxilla about the transverse axis whereby the anterior part of the maxilla was displaced downwards. The final gain in width was small at the three reference points, but greatest at the farthest backwards and upwards reference point (ZYG). Contrary to all previous researchers, Ladner and Muhl (1995) showed that buccal tipping is not significant during rapid maxillary expansion.

Rapid expansion of the maxilla involves a complete rearrangement of all sutural surfaces surrounding the maxilla. As sutures can be expected to react to orthodontic forces in a manner similar to periodontal ligament, force per area would dictate the nature of tissue reaction. The area of the articulation surfaces of the palatomaxillary region is considerably larger than the surfaces of the fronto- and zygomaticomaxillary suture. It is, therefore, suggested that the centre of resistance of the maxillary complex may change during postnatal development, so that a shift toward the more complicated sutural area takes place from the juvenile to the adolescent period. Thus, orthopaedic forces may have a greater effect at an early age when optimal response can be expected.

The final position of the maxilla, after completion of expansion is unpredictable and it has been reported to return, partially (Haas, 1961) or completely (Wertz, 1970; Linder-Aronson *et al.,* 1979), to its original position. Moreover, Linder-Aronson in 1979 showed that the height of the palatal vault continues to increase after the end of active treatment and during the five years of post-retention observation period but it is not clear whether this is attributed to the Rapid Maxillary Expansion or to growth. The study also revealed increases in the anterior total facial height (6.6mm) and the lower facial height (3.7mm). However, the increases found in both

the total and lower anterior facial heights can be interpreted as a normal effect of growth during the 7 year total observation period.

2.1.5.2. Effects on the mandible:

The downward displacement of the maxilla has a direct effect in the spatial positioning of the mandible when related to the anterior cranial base. The mandible rotates downward and backward. This mandibular rotation induces other alterations such as opening the bite, occlusal plane inclination, increase in the mandibular plane angle, and a downward and backward displacement of the menton. There is some disagreement regarding the magnitude and the permanency of these changes (Wertz, 1970; Haas, 1970). The fairly consistent opening of the mandibular plane during Rapid Maxillary Expansion can be attributed to the disruption of the occlusion caused by extrusion and tipping of maxillary posterior teeth along with alveolar bending.

Review of the outcomes of short- and long-term studies shows that, overall, the mandibular dentition response to Rapid Maxillary Expansion was quite variable. This might be attributed to the lack of standardization for measurements of arch dimensions; differences in types of malocclusions, age ranges at the beginning of treatment, sample distributions and sizes, follow-ups and types of appliances used. However, Haas *et al.* (2001), recently restated what he had observed in his first clinical study 40 years ago: "When the maxillae are separated 12-14mm, noticeable spontaneous expansion will occur in the lower dental arch, due to altered muscle balance between the tongue and buccinator muscles as they affect the lower dental arch. That is, a permanent increase in maxillary apical base which leads to a spontaneous, permanent and significant increase in mandibular arch width."

Lima *et al.* (2004), recorded a significant increase of 0.97mm for intermolar width. This increase was similar to the majority of the mandibular intermolar widths previously reported (Wertz, 1970; Sandström *et al.,* 1988; Moussa *et al.,* 1995; Ulrich, 1997). For intercanine width, all studies reviewed showed large intercanine width increases, ranging from 0.5 to 5mm. Haas (1980) found stable increases up to 4 or 5mm. Gryson (1977) on the other hand, recorded changes in maxillary and mandibular intercanine and intermolar widths before and after expansion in 38 patients. The mean increase in the mandibular intermolar width was 0.4mm. However, there was no correlation between the change in mandibular intercanine and intermolar distances with respect to the increase in maxillary intercanine and intermolar distances.

Therefore, one can conclude that in general, the position of the mandibular dentition might be influenced more by maxillary skeletal morphology then by the size and shape of the mandible (Lima *et al.,* 2004). Consequently, Rapid Maxillary Expansion could influence the mandibular dentition, but the accompanying changes are neither pronounced nor predictable.

2.1.5.3. Effects on the adjacent facial structures:

Most bones involved in the craniofacial complex are united to the contiguous bones at sutures. An examination of the relationship of a maxillary bone to other facial bones reveals that it abuts 10 other osseous structures. Rapid Maxillary Expansion exerts considerable force against the two maxillary halves. This force has the potential to radiate outward and affect distant skeletal locations and consequently circummaxillary sutural growth may be promoted. Zimring and Isaacson (1965), reported pressure sensations in other areas which indicate that forces are probably there, but their magnitude and type (tension or pressure) remain unknown and unquantified.

Timms (1980), found a weak correlation between dental and basal movements and wide individual variations which may reflect the geometric morphology and the degrees of buttressing within the circummaxillary structures. Probably all these sutures offer resistance of different degrees depending on their location and orientation relative to the center and direction of force. Starnbach *et al.* (1966), noticed that sutures in the area of the nasal complex were disrupted. Cellular activity was greatest in the nasal area, the second most active suture was found to be the zygomatico-maxillary and some adjustment was noted in as remote an area as the zygomatico-temporal suture. Even though it was minimal in nature, this would tend to indicate that the zygomatic bone is being moved. In relation to Wolff's law of bone formation and stresses, this seems to point to force concentrations in these areas.

Chaconas and Caputo (1982) designed a three-dimensional anatomic model duplicated from a human skull and used different birefringent materials to simulate the various craniofacial structures. They compared five appliances – the Haas expander, Minne expander, Hyrax, Quad helix, and a removable expander. They found that each appliance produced different load-activation characteristics. Stresses produced by fixed appliances were concentrated in the anterior region of the palate, progressing posteriorly toward the palatine bones. These stresses radiated superiorly along the perpendicular plates of the palatine bones to deeper anatomic structures. The buttressing of the maxillary tuberosity with the pterygoid plates of the sphenoid bone allowed the forces to then radiate to the base of the medial pterygoid plate. From this region, the forces then branched superiorly toward the malar and zygomatic bones. Specifically, the areas of the zygomaticomaxillary and zygomaticotemporal sutures were affected. The forces then radiated superomedially toward the medial wall of the orbit and concentrated at the junction of the nasal and lacrymal bones.

The results of a three-dimensional finite element study of a human skull by Jafari *et al.* (2003) indicted that the transverse orthopaedic forces not only produced an expansive force at the intermaxillary suture but also high forces on various structures on the craniofacial complex, particularly the sphenoid and the zygomatic bones. The deep anatomical effects of these orthopaedic appliances were also observed by the high stress levels in the external walls of the orbit, frontozygomatic suture and frontal process of maxilla. Despite previous findings, Jafari *et al.* in their study (2003), showed that the bones which did not have a direct sutural articulation with the maxilla and palatine bones presented little or no displacement at all.

Although the main objective of Rapid Maxillary Expansion is to correct transverse deficiencies of the maxillary arch, its effects are not limited to the upper jaw. Rapid Maxillary Expansion may directly or indirectly affect all interconnected neighbouring structures such as, the mandible, nasal cavity, pharyngeal structures, temporomandibular joint, middle ear and pterygoid process of the sphenoid bone (Ceylan *et al.,* 1996). Another equally important factor is the soft-tissue complex that invests these skeletal structures. The muscles of mastication, the facial muscles, and the investing fascia are relatively elastic and can be stretched as the expansion force is applied. But the ability of the stretched muscles, ligaments, and fascia to permanently adapt to the new environment is a matter that deserves further investigation.

Therefore, the retention of rapid maxillary expansion cases probably does not necessarily depend totally on the presence of bone in the opened midpalatal suture. Rather, the retention of these cases more probably relies on the creation of a stable relationship at the articulations of the maxilla and the other bones of the facial skeleton. Even the deposition of new bone in the midpalatal suture does not necessarily insure the permanency of the treatment as long as forces are present at adjacent maxillary articulations for it is reasonable that relapse forces can cause the resorption

of this bone just as expansion forces caused its deposition. Moreover, retention of these cases holding the teeth alone does not appear to be a rational approach since forces present in the facial skeleton could conceivably cause the basal structures to relapse while the teeth were held at a constant width.

2.1.6. Rapid Maxillary Expansion and Nasal Airflow:

The reported direct benefits of Rapid Maxillary Expansion have included: correction of dental crossbites with relief of dental crowding (Hartgerink *et al.,* 1987; da Silva Filho *et al.,* 1995), improved conductive hearing loss due to middle ear and eustachian tube problems (Gray, 1975; Laptook, 1981) and improved breathing.

Anatomically there is an increase in the width of the nasal cavity immediately following expansion, particularly at the floor of the nose adjacent to the midpalatal suture (Haas, 1961; 1970; Starnbach *et al.,* 1966; Wertz, 1970). As the maxillae separate, the outer walls of the nasal cavity move in an outward and upward direction. The total effect is an increase in the intranasal capacity. The nasal cavity width gain averages 1.9mm, but can widen as much as 8 to 10mm at the level of inferior turbinates (Gray, 1975), while the more superior areas move medially (Pavlin *et al.,* 1984). In addition, high forces resulting from rapid maxillary expansion probably induce remodelling of the bones of the nasal cavity (Walters, 1975). Using computed tomography, Montgomery and associates (1979), found that the effects of Rapid Maxillary Expansion on the nasal cavity are not uniform and the changes in the nasal dimensions are progressively less toward the back of the nose.

Nasal airway resistance (NAR) accounts for approximately 50 per cent of total airway resistance. The nasal valve region is the narrowest segment of

the nasal airway and is the major flow-resistive segment (McCaffrey, 1993). Nasal airway resistance is a measure of airway adequacy (McDonald, 1995). Hershey, Stewart and Warren (1976), Turbyfill (1976), and Doruk *et al.* (2004), reported a reduction of nasal airway resistance by an average of 45% to 53% following Rapid Maxillary Expansion which remained stable during up to 1 year follow-up period. Warren (1979), believes that although the actual increase in binasal width is small, it should be remembered that airflow varies inversely as the fourth power of the radius of the tube through which it passes.

Wertz (1970), concluded that opening the midpalatal suture for the purpose of increasing nasal permeability cannot be justified unless the obstruction is shown to be in the lower anterior portion of the nasal cavity and accompanied by a relative maxillary arch width deficiency. Graber (1975), believes that the claims of improved nasal breathing apparently as a result of Rapid Maxillary Expansion are most likely only temporary. More important, 12-year-old children have considerably more lymphoid tissue than adults and the lymphoid tissues can act to block nasal breathing. Spontaneous regression of lymphoid tissues during growth automatically improves nasal breathing, even if nothing is done to the palate.

Therefore, it can be concluded that the effect of RME on the nasal airway will to a great extent depend on the cause, location, and the severity of the nasal obstruction.

2.1.7. Rapid Maxillary Expansion and the importance of age:

In general the opening of the midpalatal suture is smaller in adult patients (Korkhaus, 1953; Krebs, 1958; 1964). Growth at the midpalatal suture was thought to cease at the age of 3 years (Latham, 1971). By means of implants Björk and Skieller (1974), found that growth at the suture might

be occurring as late as 13 years of age. Persson and Thilander (1977), in a study on cadavers found that 5% of the suture was obliterated by age 25 years, yet the variation was such that a 15-year-old cadaver had an ossified suture, while a 27-year-old cadaver had an unossified suture. Similar variations in the degree of ossification of the midpalatal suture according to age were observed in a more recent research by Wehrbein *et al.* (2001). Thus, Rapid Maxillary Expansion feasibility should be based on the patient's sutural patency and not chronologic age.

Krebs (1964), suggested that the most marked effect of the rapid expansion therapy was recorded before and during the pubertal growth spurt. Thereafter the reaction in the midpalatal suture was apparently slower, but individual differences[2] can be noted. Most investigators (Krebs, 1958; Isaacson *et al.,* 1964; Zimring *et al.,* 1965; Wertz, 1970), agree that Rapid Maxillary Expansion with midpalatal splitting can be accomplished in both children and adults, but with advancing maturity, the rigidity of the skeletal components limits the extent and the stability of the expansion and the results are neither as predictable nor as stable (Bishara *et al.,* 1987). In other words, age may influence the amount of dental expansion achieved or may affect the relative contributions of the skeletal factors, consequently producing more dental movement than orthopaedic effects (Krebs, 1964; Ladner *et al.,* 1995). There is potential hazard of root resorption or of fenestration and dehiscence of the buccal cortical plate when Rapid Maxillary Expansion treatment is applied in sutural synostosis.

In adult subjects, forces are transmitted much more to the surrounding tissues because of the firm bony architecture and are divided over a larger sutural area because of the interdigitations (Wagemans *et al.,* 1988). Chaconas and Caputo (1982), illustrated photoelastically that there was

[2] Individual differences were evident in almost all studies. This could be attributed to the heterogenity of the study groups (i.e. both sexes, wide age range and skeletal maturity), as well as the variety of malocclusions and different degrees of cooperation with the treatment procedures.

stress in the area of the base of the medial pterygoid plates. If the maxilla is fused to these structures, as is the probable case in adult patients, intermaxillary expansion will be difficult to obtain. Therefore, higher level of forces have to be applied during expansion which can sometime cause fractures around the tuberosity area.

2.2. Finite Element Method

The Finite Element Method (F.E.M.) was introduced about 36 years ago as a method of stress analysis and was used to help resolve certain problems in structural mechanics associated with aircraft and motorcar design. Since then, along with the advent of modern computers, the F.E.M. has become a standard tool in engineering sciences to assess precisely local stress-strain distributions in geometrically complex structures (Turner *et al.,* 1956; Desai *et al.,* 1972; Bathe *et al.,* 1976; Zienkiewicz, 1977; Owen *et al.,* 1980; Cattaneo *et al.,* 2001).

The F.E.M. enables the solution of complicated problems which cannot be solved by ordinary closed form methods. FE modeling is an advanced numerical technique which solves a complex problem by redefining it as the summation of the solutions of a series of interrelated simpler problems. The method involves the subdivision or discretisation of the "*continuum*" (the structure under consideration) into a number of simply shaped regions called "*elements*" (i.e. hexahedral or prisms). No overlapping or gaps between elements are allowed. The finite elements are interconnected at specified points, called "*nodes*", on the element boundaries with defined degrees of freedom. This discretisation can occur in one, two or three dimensions, depending on the nature of the problem under consideration. Conclusion of the division process brings about an ensemble of nodes and elements that represents the morphological region of interest and is called "*mesh*". This division process, "*mesh generation*", is the most tedious and time-consuming process in the course of solution using Finite Element Method.

With F.E.M. procedure, the appropriate "*shape functions*" are next constructed. These functions are necessary to link the 3D configuration to

the process modelling equations. Since the actual variation of the field variable (i.e. displacement, stresses or strains) inside the continuum of the structure is not known, it is assumed that the variation of the field variable within the specific finite element can be represented by a selected mathematical function. The use of functions allows generation of a series of equilibrium equations (one per nodal degree of freedom) which, when appropriately summed across the entire geometry and solved simultaneously, define the structure response of the system being considered.

In translating the aforementioned mathematical description of the Finite Element Method into biological terms (Huiskes, 1983), the model as a geometric entity is defined first. This model is then (mathematically) divided into a number of blocks (elements), connected at specific locations (nodal points). The boundary conditions and loading configurations are numerically defined as displacements and forces, respectively, in boundary nodes. Every element is assigned one or more parameters (e.g. moduli of elasticity) that define its material (stiffness) behaviour.

Once material properties have been established, be they of a linear or non-linear nature, the data is then generated in matrix form to give a general equation as follows:

$$\mathbf{[k](d)=(r)}$$

where [k] is the element stiffness matrix, (d) the nodal displacement vector, and (r) the vector of elemental loads. A computer is then used to solve these equations for each of the elements simultaneously and to give the required reactions and displacements for the particular problem under consideration (Rao, 1982). In fact, the Finite Element Method program solves a large number of equations that govern force equilibrium at element nodes.

Precision in the results can only be achieved once geometry, material properties and boundary conditions are carefully delineated. In early studies, due to computer limitations and simplicity in the way that finite elements were made, most of the models were just two-dimensional constructions. Although this could be sufficient in some cases (FE parts with simple geometry and/or good symmetry), it was soon realized that a true three-dimensional FE model was the only method to assess realistic stress fields whenever an irregular and non-symmetrical object was to be studied (Huiskes, 1983).

FE analysis requires special care to be taken during the formation of the wire frame model, because mesh volumes should be created which provide reasonable geometric aspect ratio and behavior for the derived elements. To minimize approximation and thus to maximize model accuracy, one could theoretically subdivide a mesh volume into a large number of very small elements. Keyak and Skinner (1992), showed that the results of the Finite Element Analysis are very sensitive to element size, in particular in anatomical structures with highly variable modulus (i.e. trabecular bone). However, this greatly increases computer memory requirements and processing time. Another option is to manipulate the geometry by dividing contoured curves into smaller ones, thus creating more detailed mesh volumes. This option is however feasible only in regions with complex shapes or anticipated high gradients of material deformation. In doing so, one attempts to build mesh volumes where the creation of a smaller number of elements will provide sufficient accuracy without loss of structural response (Korioth *et al.,* 1992).

Although Finite Element Method applied for engineering analysis has long been well documented, it is only recently that it has been introduced into the study of cranial morphometrics (Bookstein, 1978; 1984; Cheverud *et al.*, 1983; Moss *et al.*, 1983; 1985). Due to the complex and irregular shapes that normally characterize biological structures, and due to the analytical

assistance provided by the extension of a method capable of subdividing biological structures into many smaller elements, that will permit independent analysis of each, the Finite Element Method has been widely used for assessing stresses and strains in normal bone (Huiskes *et al.*, 1983).

For the study of form, the customary methods most commonly used concern the comparison of the values of skeletal size and shape in a single skull, or group of skulls with those of some standard or control values, with time (age) held constant (Moss, 1975). Traditional growth studies based on cephalometric measurements uniformly involve the choice of a single point to serve as the center of a registered system and the selection of a line connecting two points for orientation of comparisons between films. By defining a point as the center, a registration system is built around that point. The location of the centre (registration point) becomes an unvarying entity, unchanged in all comparisons, and the apparent change of all other points occur only in relation to it. When growth is studied in a registered system, the nature of the system dictates that growth does not occur at the center and that all other points grow away from the center in a direction influenced by the adopted orientation (Richtsmeier *et al.*, 1986). If, instead of manipulating the line of orientation, a different point was chosen as the center of registration, yet another trajectory for each point would be produced.

On the other hand, the techniques normally used to record the biomechanical events which accompany functional loading of human structures are highly invasive. Consequently, computer modelling in combination with the modern imaging techniques which permit the generation of enough sectional profiles to characterize the osseous and dental structures, offers a promising alternative approach in this regard, with the additional ability to predict regional stresses and strains in inaccessible locations (Korioth *et al.*, 1992). Finite element methods are mathematically

equipped to capture the material, physical and response characteristics of the component craniofacial tissues. However, the arbitrary selection of different boundary conditions in the different studies also makes comparison between them very difficult.

Patient-specific physical models of craniofacial anatomy have been created recently using CT-based CAD-CAM technology (Remmler *et al.,* 1998); however, such fabrications neither capture the material properties nor the mechanical characteristics of human tissues. Moreover, CAD-CAM models lack the natural stress relaxation characteristics typically displayed by soft tissues subjected to incremental force application.

The craniofacial skeleton and surrounding tissues have undergone finite element engineering analysis in five major areas of research: crash and impact studies (Ruan *et al.,* 1994; Krabbel *et al.,* 1995; Voo *et al.,* 1996), bone mechanics of osseointegrated dental implants (Meroueh *et al.,* 1987; Bidez *et al.,* 1992; Meijer *et al.*, 1993), soft tissue surgical modelling (Larabee *et al.,* 1986a; 1986b; 1986c; Akita *et al.,* 1993; Pieper *et al.,* 1995), mechanical response of the mandible during physiologic function (Knoell, 1977; Farah *et al.,* 1988; Hart *et al.,* 1992; Korioth *et al.,* 1992) and finally, in orthodontics and dentofacial orthopaedics (Tanne *et al.,* 1988; 1989; 1995). In orthodontics F.E.M. is used to study the stresses and strains within a given force system applied to tooth movement or craniofacial complex, and to evaluate craniofacial growth, especially its particular application to cephalometric analysis (Desai & Abel, 1972; Bathe & Wilson, 1976; Owen & Hinton, 1980; Moss *et al.*, 1981; 1985; Richtsmeier & Cheverud, 1986). It is also widely used in the dental materials field (Wright & Yettram, 1978; Cook *et al.*, 1982; Rubin *et al.*, 1983).

2.2.1. Finite Element Method and Orthopedics:

Originally applied to structural and architectural analysis, Finite Element Method was introduced in medical sciences in the field of orthopaedics in 1972 (Brekelmans *et al.,* 1972), to evaluate stresses in human bones. The mathematical tools available for stress analyses in classic mechanics, however, were not very suitable for the highly irregular structural properties of bones. Hence, the powerful Finite Element Method became the logical choice to fill the gap, due to its unique capability to evaluate stresses in structures of complex shape, loading and material behaviour.

Nevertheless, this initial application of the Finite Element Method could have gone relatively unnoticed, due to its rather academic nature in orthopaedic basic sciences, had it not been for a rapidly growing interest in artificial joint replacements and new methods of fracture fixation. New questions and new methods have created a stimulating environment for the utilisation of the Finite Element Method in orthopaedic biomechanics, and its applications have grown exponentially in the last decade (Huiskes and Chao, 1983). Finite element analysis is at present being used to investigate the stress-related architecture of bone and remodelling processes (Weinans *et al.,* 1992), to test and to optimize artificial joint designs and fracture fixation devices, and to study the mechanical behavior of tissues such as articular cartilage and intervertebral discs.

When a structure is loaded, stresses are generated in its' component materials. The distribution of these stresses, their magnitudes and orientations throughout the structure, depend not only on the loading configuration, but also on the geometry of the structure and the properties of its materials. In addition, the stresses are influenced by the interaction of the structure with its environment and by physical conditions at boundaries between different materials. In a theoretical stress analysis the stress distribution is evaluated by using a mathematical model. In such a model,

that mimics the real structure to a certain degree of refinement, the structural aspects[3] are described mathematically. The mathematical descriptions can be more or less accurate, depending on the level of refinement required, and are usually based on experimentally determined data. In the solution procedure, the structural descriptions are combined in mathematical equations based on theories of solid mechanics and these are resolved to give the stresses present.

It is assumed that the morphology of bone relates to its internal mechanical loads. The process which regulates this relationship is called bone modelling or remodelling. It is believed that bone has the ability to adapt itself to the loading conditions to which it is exposed. Several attempts to quantify this process have been reported in the literature and several investigators tried to describe this process mathematically, in order to accurately predict bone formation or resorption (Frost, 1964a; 1964b; 1988; Kummer, 1972; Cowin *et al.,* 1976). For qualitative predictions it is necessary that the internal mechanical load in the bone structure can be determined accurately in terms of stresses and strains, for which the Finite Element Method is an effective tool (Huiskes *et al.,* 1983). By combining mathematical bone-remodelling descriptions with finite element models, quantitative predictions about bone formation and resorption in realistic bone structures can be made (Hart *et al.,* 1984; Fyhrie *et al.,* 1986; Huiskes *et al.,* 1987; 1989a; 1989b; 1991; Carter *et al.,* 1989; Beaupre *et al.,* 1990). These models are all based on the principle that bone remodelling is induced by a local mechanical signal which activates the regulating cells (osteoblasts and osteoclasts).

The femur (thigh bone) is the bone historically most frequently analysed (Wolff, 1870 and Koch, 1917; cited by Enlow, 1968) due to its common involvement in orthopaedic treatments, such as prosthetic replacement of the hip joint. The early Finite Element Method was adopted for stress analysis

[3] Loading, geometry, material properties, boundary and interface conditions

of the femur by Brekelmans *et al.* (1972) and Rybicki *et al.* (1972). The first efforts were not so much directed at a specific problem, but aimed at demonstrating the method and its possibilities. A good example (Huiskes *et al.,* 1983) of a problem-oriented approach in which the Finite Element Method can play a significant role, was the work by Brown *et al.* (1980). Other examples of problem-oriented studies, employing relatively simple Finite Element Method models, are those pertaining to bone growth and remodelling (Hayes *et al.,* 1982).

A number of Finite Element Method stress analyses of bones have been designed for problems of fracture and fracture fixation, including problems of bone remodelling. The mechanical characteristics of the fracture fixation devices are important due to strength requirements and the influence of their fixation rigidity on the fracture healing process. Use of the Finite Element Method in an analysis of a bone-fracture plate complex was first reported by Rybicki *et al.* (1974) although very little information was provided at that time. Further Finite Element Method studies of bone-plated fractures were carried out by Simon *et al.* (1977), Woo *et al.* (1977), Levine and Stoneking (1980), Claes *et al.* (1982), Carter *et al.* (1981). In addition to internal fixation devices, external fixation was also analysed (Chao *et al.,* 1981; 1982; Crippen *et al.,* 1981). However, because of the large variety in fracture types and surgical procedures in patients, it is questionable whether an 'anatomic' 3-D model is really helpful in analysing these structures, specifically when non-linear effects are taken into account. To aim for general information on a relative basis would seem more realistic in this case (Huiskes *et al.,* 1983).

Whole bones other than the femur were investigated as well, but to a lesser extent. Artificial joint design and fixation is probably the most popular application of the Finite Element Method in orthopaedic biomechanics. The mechanical problems involved in joint implants are more demanding due to long life expectancy and the severe but unknown loading

and boundary conditions imposed within the body. The femoral component of total hip replacement in general consists of a spherical head connected to a straight or curved stem fixed within the medullary canal of the proximal femur, using acrylic cement as a filler. Three-dimensional, 2-D and beam analyses of this structure have been widely published (Andriacchi *et al.,* 1976; Kwak *et al.,* 1979; Yettram *et al.,* 1979; 1980; Cook *et al.,* 1980; Sih *et al.,* 1981; Skinner *et al.,* 1982). Axisymmetric geometry, applying 3-D elements, was assumed by Bartel and Ulsoy (1975) and by Huiskes *et al.,* (1978). 'Anatomic' models applying the 3-D Finite Element method with varying degrees of refinement have been investigated by Scholten *et al.* (1978), Valliappan *et al.* (1980), Hampton *et al.* (1980), Lewis *et al.* (1981), Tarr *et al.* (1982) and Vichnin and Batterman (1982).

Finite Element Method analyses in artificial knee-joint design and fixation became more frequent in the late seventies. With some exceptions, all studies have dealt with the tibial component fixation exclusively, which indeed is the part giving the most problems in actual patients. Two-dimensional (Lewis, 1977; Hayes, 1978; Vichnin *et al.,* 1979; Askew *et al.,* 1981), 3-dimensional and axisymmetric models (Campen *et al.,* 1979; Croon *et al.,* 1982) were again used to analyse the tibial fixation alone or with the femoral stem (Roehrle *et al.,* 1982), of hinged and non-hinged prostheses. Most of these studies were directed at the function of the central post, used to fixate the plateau in the tibia.

Analyses of prosthetic components other than in the hip and knee joints have been rare. Finite Element analyses of the soft tissues in the musculoskeletal system have been limited to articular cartilage and the intervertebral discs in the spine. Finite Element Method analyses of soft tissues other than those mentioned are quite common in related fields, as for instance cardiovascular biomechanics. Where the musculoskeletal system is concerned, the Finite Element Method has been used to some extent in the fields of crash biomechanics and product liability for modelling the

spine, skull and rib cage. In orthopaedic biomechanics, a final area of the application of the Finite Element Method as a universal numerical tool to solve differential field equations lies in problems of heat and mass transfer (Huiskes *et al.,* 1983).

There is no question that the Finite Element Method has established itself as an important research tool in orthopaedic biomechanics which has opened new fields of investigation, and even triggered a renewed interest in basic orthopaedic science.

2.2.2. Finite Element Method applied to General Dentistry:

Many efforts have been made to analyze the stresses in the human tooth, its environs, and artificial tooth replacements and supports. A survey of the literature in this area reveals a multitude of applications for such research:

- The shape and design of restorations, crowns, dental implants, retention pins, partial dentures and bridges. More recently Finite Element Analysis has been introduced in bracket design and development (Ghosh *et al.,* 1995; Knox *et al.,* 2000);
- The interactions of bone, periodontal ligament and tooth;
- The study of thermal and setting effects and resulting residual stresses in restorations and crowns;
- The effect of forces on teeth that have been restored with various filling materials;
- The physical, biochemical and biologic effects of chewing forces.

The problem of tooth stresses is very complicated because of the non-homogenous character of tooth material and the irregularity of tooth contours. The tooth structure is composed of several different materials: enamel, dentin, pulp, cementum, periodontal ligament and bone. Each of these has widely varying properties. The problem is further complicated by

large variations (both in magnitude and direction) of chewing forces (Rubin *et al.,* 1983).

Conventional methods lends itself to investigation by recourse to *in vitro* physical testing. However, such methods necessarily involve expensive and sophisticated equipment together with much time and expenditure in the setting up of each individual experiment.

It has been recognized for some time that analytical solutions will not be amenable to these complex problems of analysis. Nevertheless, the important stress patterns can be determined by numerical procedures. Finite element stress analysis methods have been developed which will allow the investigation of complex geometries for elastic and viscous materials. Using these methods, a thorough examination of existing and new clinical procedures is possible in order that the complex stress patterns within the tissue, joining medium and prosthesis may be evaluated (William *et al.,* 1987).

Biomechanical influences play an important role in the longevity of bone around dental implants (Skalak, 1983). Forces on the abutments will be transferred to the implants and will lead to stress in the bone surrounding the implants. Bone tissue is known to remodel its structure in response to mechanical stress. The long-term function of a dental implant system will depend on the biomechanical interaction between bone and implant. With the Finite Element Method the mechanical behavior of the bone and the implant system can be evaluated (von Fraunhofer, 1975).

Several studies on the stress distribution around implants in the edentulous or partially edentulous jaw have been published. Some of them deal with the selection of an implant design which will cause a minimum of stress concentration in the bone when being loaded (Siegele *et al.,* 1985; Rieger *et al.,* 1989; van Rossen *et al.,* 1990). Others have been performed to study the

influence of the interface (bone-implant) behavior on the stress concentration (Borchers *et al.,* 1983).

Rubin *et al.* (1983) demonstrated the superiority of three-dimensional finite element analysis over the two-dimensional form by showing that the calculated stress induced in a tooth under load was actually less in the three-dimensional model: this was attributed to the concentrated nature of the load representation in the plane stress (two-dimensional) model.

2.2.3. Finite Element Method and Craniofacial Growth:

The ways in which the human craniofacial complex grows has received considerable attention by many researchers worldwide, ever since the first description of cephalometric radiography in 1931 by Brodie in the United States and Hofrath in Germany. In general, it is accepted that the face grows downwards and forwards relative to the cranium, but the growth of the various components of the face has been fraught with difficulties and controversy. To show that growth is occurring, a stable point of reference is needed from which measurements can be made, but no point within the skull can truly be shown to be absolutely stable. Gravely and Benzies (1974) have also showed that in tracing a cephalometric X-ray, errors of a single measurement are of a high order even when traced by an experienced orthodontist. We are faced therefore, not only with a structure or set of structures that is in a constant state of flux, but also with a method of measurement of changes due to treatment or growth that does not lend itself to a high degree of accuracy.

Björk (1951) summarised the difficulties inherent in the use of the lateral cephalograms for the study of craniofacial growth as follows: Cross-sectional studies indicate general growth tendencies in the population as a whole, while, longitudinal studies indicate individual growth and

development. Lateral cephalograms are two-dimensional representations of three-dimensional growing structures. Moreover, the selection of specific reference planes presupposes that they are not affected by growth changes (Bookstein, 1982; 1983; 1984). Changes in craniofacial form rarely occur at traditional cephalometric datum points and are seldom confined to straight lines (Moyers and Bookstein, 1979). In fact, cephalometric changes follow complex translational movements depicting localised appositional and resorptive changes between the datum points. By portraying craniofacial changes as vector displacements, therefore, conventional cephalometric techniques "misrepresent" morphologic change (Cheverud *et al.,* 1983; Richtsmeier and Cheverud, 1986). The work of Book and Lavelle (1988) indicated the need to evaluate cephalometric changes over very short areas in order to embrace subtle appositional and resorptive changes.

Due to intrinsic constraints of conventional cephalometrics, newer and more appropriate methods of craniofacial growth analysis are desirable (Moyers and Bookstein, 1979). The classic transformation grids spanning specific homologous points provide alternative evaluations of cephalometric change. Although these transformation grids have furnished invaluable pictorial insights into the distortions and transformations associated with cephalometric change, they have thus far proved resistant to mathematical description (Moorrees and Lebret, 1962).

Other methods have been proposed for the skull over the years, such as the allometric centred model (Moss *et al.,* 1983) and the growth network model (Moss *et al.,* 1984). The allometric centred model considers that there is only one unique centre of growth for the skull: this, however has not been shown to be the case, because it cannot take account of differing growth rates within line segments, and it cannot predict angular changes with growth (Moss *et al.,* 1983). The network model is a refinement of the allometric centred model, in that it considers two or more centres of

growth within the skull. However, it is still based on allometric growth prediction, which has been shown to be limited.

Initially, tensor analysis has been employed as this method allowed visualisation of the magnitude and direction of the principal tensors (Battagel, 1995). However, tensor biometrics determines size- and shape-change only at specific landmarks. Finite Element Morphometry is a technique that describes morphological alterations with respect to anatomical landmarks (Cheverud *et al.,* 1983; Richtsmeier and Cheverud, 1986; Lozanoff and Diewert, 1986; 1989; Moss *et al.*, 1986; McAlarney *et al.,* 1992; Lozanoff *et al.,* 1994; Sameshima and Melnick, 1994). Using this technique, change in morphology is viewed as a deformation of an initial geometric configuration, whose boundaries are formed by edges that connect anatomical landmarks, into a final form. Deformation of the initial geometry is depicted graphically as a set of principal tensors (perpendicular stretch/strain extensions defining the degree of deformation) within the initial geometric configuration (Singh *et al.,* 1997). It should be noted that morphometric techniques attempt to numerically characterise biological phenomena and, consequently, they can be used only to generate hypotheses regarding underlying developmental mechanisms.

During the 1980s, the finite element method was applied as a new approach to the analysis of cephalograms (Bookstein, 1982; Moss *et al.,* 1985; Richtsmeier and Cheverud, 1986). Finite Element Method can be used to describe the kinematics of other types of growth (e.g. additive [accretionary] growth), as well as the multiplicative growth that both the allometric centred and network models describe. However, it is first necessary to know the ways in which the craniofacial complex grows in order that it might be modelled adequately in the computer program for the Finite Element Method.

The mathematical modelling of craniofacial growth uses the concept of continuum mechanics based upon two separate ideas (Moss *et al.,* 1985):

- first, that a growth tensor is a fundamental descriptor of growth;
- second, that the Finite Element Method allows a convenient and systematic approximation of the mean growth tensor within finite elements, using the data obtained from a relatively small number of points within each element.

In the Finite Element Method, the cephalometric datum points are considered to be stable. Thus appositional and resorptive changes in the tissues between the datum points are assumed to result in these points moving further away from or closer to one another. The Finite Element Method therefore facilitates measurement of the morphologic changes in the tissues between the datum points without reference to arbitrary reference points or planes. This is accomplished by simultaneous registration on all datum points delineated on the cephalograph. In the Finite Element Method, the cephalometric datum points, termed nodal points, are selected to represent the craniofacial skeleton as fully as possible. Ideally, nodal points should be anatomic.

However, the introduction of this new method does not solve the problems related to prediction of growth changes (Athanasiou, 1995). The following should be taken into consideration:

1. The method requires accurate and precise measurement of the known landmarks in the system. As used by Moss *et al.,* (1985) and Bookstein *et al.,* (1985), the landmarks are obtained by conventional cephalometric methods, usually without replication which makes them just as crude and error-prone as those of conventional cephalometrics.
2. The utility of Finite Element Analysis in the analysis of growth and development processes has not been tested except to compare its findings with those of conventional methods.

3. As used by Bookstein *et al.,* (1985) and Moss *et al.,* (1985), the nodes surrounding the elements straddle sutures and even extend from the calvarium to the mandible. This violates the usual assumption of Finite Element Analysis that within each element the structure is homogenous.
4. Also, finite element analysis in the prediction of facial growth can be misapplied; the Finite Element Method is in essence developed to measure stresses and strain within a structure under mechanical loads, as opposed to linear, curvilinear, or logarithmic displacements of the growing skull in which mechanical loading is minimal or non-existent.

Furthermore, the complexity of facial growth in man has been considered and demonstrated by many authors (van der Klaauw, 1945; Scott, 1954; Bjork, 1955, 1969; Isotupa *et al.,* 1965; Moss, 1968; Koski, 1968; Moss *et al.*, 1980; Musson, 1985; Haskell *et al.,* 1986; Motoyoshi *et al.,* 2002). A substantial amount of literature has shown convincingly that most biologic growth in general, and craniofacial skeletal growth in particular, often is both anisotropic and nonlinear. Growth is anisotropic because it must include shape changes as well as size changes, and it is nonlinear because the changes in lengths and angles are not small.

The limitations of investigative methods such as cephalometry have been stated and compared with finite element analysis as a tool for predicting facial growth (Moyers and Bookstein, 1979; Bookstein, 1982; Cheverud *et al.,* 1983; Moss *et al.,* 1985; Lavelle, 1989). The application of Finite Element Method to the problem of facial growth has many possibilities. Such a system, combined perhaps with analogous mechanisms, could give a very accurate forecast of facial growth for large groups of ethnically homogeneous subjects. The accuracy of such methods is dependant on the sophistication of the computer systems involved, the fineness of the finite element mesh, and the nature of the particular problem under consideration.

In the case of the single patient, however, after the "fourth dimension", time, we still have to consider the "fifth dimension" of growth-individual variation.

However, in clinical practice, with the human skull there is a finite limit to the number of points that can be obtained reliably. Hence the Finite Element Method cannot provide an absolute description of growth; it can and does, however, often provide one that is significantly finer than that of any customary roentgenographic cephalometry and, because of its intrinsic invariance, is always more biologically correct.

In conclusion, the prediction of facial growth seems destined to be confined to the addition of average growth increments onto the existing pattern, as proposed by Björk and Skieller (1972) and Houston (1979).

2.2.4. Finite Element Method and Orthodontic Tooth Movement:

A number of devices and methods have been used over the years in order to measure occlusal changes from study models. The symmetrograph, designed by Korkhaus in 1930, is a rather crude machine capable of making profile tracings of the palate via a modified pantograph. The Optocom, first described by van der Linden in 1972, is somewhat more accurate and sophisticated, in that it can be used for three-dimensional assessment of study casts. A microscope with cross-wires makes measurements of casts from the occlusal aspect and treats this as being in the X and Y axis. To make measurements in the Z axis, the model has to be reoriented in the machine, a computer program integrating the two separate readings, which makes measurement very time-consuming.

Stereophotogrammetry, on the other hand, uses a stereo-pair of photographs of a three-dimensional object, which, when viewed in a stereocomparator,

gives an illusion of depth, which can then be measured. Originally described in 1870, it received its greatest application in World War I when it was used to produce very accurate maps from aerial photographs. By linking the measurement system to a microcomputer, the readings can be stored and analysed. In the analysis of orthodontic tooth movement, Jones, Ang, and Houston (1980) summarised the difficulties inherent in the use of X-rays and study models in that there is no absolutely stable base to which measurements can be related. Moreover, errors in the transfer of control points between models, or in their measurement, especially if a facebow transfer is used, will compound the difficulty in making an accurate assessment.

In the following years and in order to overcome the aforementioned problems, the reflex metrograph (Jones, 1987) was introduced into the study of tooth movement. This instrument translates points in space by a three-dimensional sliding rod mechanism into digital information which can be stored on a computer disc, eliminating the need for cameras, photographs, and other expensive equipment used in other image analysis systems, the measurements being made directly from the models. It is a valid and accurate method of assessing occlusal changes in large serial studies.

However, in clinical orthodontics, tooth movement is the result of various force systems that are applied by means of a fixed or removable appliance to the crown of the tooth. A great number of studies have been conducted to investigate biological and biomechanical changes in the periodontal ligament resulting from these force systems. The response of the tooth is complex, occurring in two stages, the first being an initial displacement as the periodontal ligament and bone absorb the initial loading, then as time passes the bone responds to the changed state of stress/strain with bone resorption/apposition in the areas of pressure/tension due to the action of osteoclasts/osteoblasts, respectively. In other words, these studies have indicated that orthodontic forces produce stresses and strains in the ligament

and that these biomechanical components further induce cellular (i.e. biological) reactions in the periodontal membrane and remodelling of the alveolar bone

When considering the distortion of bone and other supporting tissues, as well as the stresses that may be developed within them due to orthodontic movement, many difficulties present themselves, the most important of which is that it is impossible to compare the "before" and "after" position of the bone adjacent to the relevant tooth. This sort of behavior has not previously been modelled using engineering laws. The complex nature of the structural layout of the tooth further leads to complications. Not only are the surface boundaries of the tooth complex, but so also is the internal geometry.

As teeth tend to be of a regular, if not precisely geometrical, shape, interest in describing their behavior under loading by mathematical means began in 1933 with Synge's paper to the Royal Society of London, in which the periodontal ligament was considered as an incompressible membrane. The calculations derived from this theory satisfactorily explained the tightness of the teeth and gave values for the centre of rotation that agreed well with observed values. Hay (1939) modified this somewhat by considering that the membrane was compressible, and the bulk modulus of water was used as a measure of compressibility. The values obtained from this investigation differed little from Synge's findings. Gabel (1956) further investigated the functions of the fibres of the periodontal ligament simplifying Synge's theory into a combined fibre and incompressible membrane hypothesis. Daly *et al.* (1974) in a study of tooth mobility, showed that the periodontal ligament exhibited an instantaneous elastic response followed by a delayed elastic response and also that it behaves in a linear fashion below 0.01 Nt/mm^2 torque.

In order to predict the behavior of a mathematical model, we must know the physical properties of the materials of which the model is composed: enamel, dentine, pulp, periodontal ligament, cancellous and cortical bone. These mathematical and mechanical analyses describe accurately the behavior of rigid and flexible bodies, however, the structures to which they apply are biological in nature, composed of tissues that are multiphasic, of irregular shape, whose physical characteristics can alter with age, nutritional status, and endocrine and metabolic changes. The response of similar teeth to similar forces is different, even within the same dentition. The mechanical appliances available are themselves subject to the effects of force and force decay, and while a high degree of the original treatment plan can be achieved for a patient, the vectors of the resultant forces usually result in movement inaccuracy at various stages of treatment, which must be corrected later.

As early as 1957, Evans criticised the methodology inherent in mechanical and mathematical modeling of bodily structures such as bones:

- The formulae used in such analyses are based on the assumption that an even distribution of force will occur in the cross-section, a situation that does not occur in bone.
- A bone is not an evenly formed body, whereas the theory of columns and beams are based on the assumption that the body being analysed is of a uniform shape throughout and composed of homogenous material.
- The results of mathematical studies deal with two dimensions instead of three.

These criticisms are valid also for teeth and dental structures. In the mathematical analyses considered above, McGuinness (1990) added the following criticisms to those of Evans:

- The only formulae derived were those for the centres of rotation and resistance.

- No studies have described the deformations or the stress gradients occurring in the dental tissues due to force applications.

The advantages of the Finite Element Method over other methods (particularly the photoelastic method and holographic technique) are many, in particular, the relative ease of modelling complex irregular geometries of natural tissue and biomaterials. It is also a straight forward process to allow for the nonhomogenous, anisotropic properties of natural materials. Moreover, photoelastic and holographic techniques have limitations in measuring internal stresses and/or strains in the periodontium, maintaining the periodontal tissues intact. For this reason, Finite Element Method has been employed recently in the field of dentistry.

Yettram, Wright and Houston (1977) were among the first in the UK to explore the use of finite element analysis in orthodontic tooth movement, by constructing a two-dimensional model of an upper central incisor and determining the instantaneous centre of rotation (ICR) of the root relative to different loading applications of the crown. Halazonetis (1996) used a similar two-dimensional model to determine periodontal ligament stress distribution following force application at varying distances from the centre of resistance of a maxillary incisor.

Using more complex three dimensional models Tanne and Sakuda (1983), Tanne (1987), Tanne, Sakuda and Burnstone (1987), Inoue *et al.* (1988), McGuinness *et al.,* (1990, 1991), Tanne *et al.* (1992) and Wilson *et al.,* (1992, 1994) have studied moment to force ratios and stress distributions during orthodontic tooth movement. Tipping, torquing and uprighting movements produced varying stress distributions from the cervix to the apex, while bodily movements produced homogenous stress induction in the periodontium. The nature of principal stress distributions in the periodontal ligament was highly coincident with histological findings in terms of site specific tension and compression of the periodontal ligament and alveolar

bone remodelling. Moreover, Tanne *et al.* (1991) showed that patterns of initial displacement of a tooth may be influenced by such anatomic variables as dimensions of the tooth and alveolar bone, variations in root length, widths of the periodontal ligament space, and mechanical properties of the periodontium. It is of clinical significance to understand optimal force considerations for each individual patient.

The models used by various authors to analyze the problems of tooth movement were two and three dimensional instantaneous (essentially static) models. Middleton *et al.* (1996) developed an initial longer-term time-dependent (continuous/dynamic) finite element model of a maxillary canine tooth in order to study tooth movement and the process of bone remodelling around the tooth. More recently, Verna *et al.,* (2004) while studying the role of microcracks in the alveolar bone for the initiation of bone remodelling mechanism after application of an orthodontic load, they conferred non-linear properties to the periodontal ligament and different values of Young's modulus under different loading situations.

2.2.5. Finite Element Method and Orthopaedic Forces to the Craniofacial Complex:

Traditional cephalometric analyses facilitate only cursory craniofacial evaluation. When a more rigorous geometric technique, in the form of finite element analysis, was applied to a retrospective series of lateral cephalographs taken before and after the completion of the orthodontic therapy, however, complex craniofacial size and shape changes were apparent (Lavelle, 1988). One of the major impediments to accurate cephalometric evaluation stems from the method of quantification (Ricketts *et al.,* 1972; Williams *et al.,* 1985). Based upon linear, angular or coordinate data, traditional cephalometric appraisals combine size and shape parameters together. The scientific validity remains obscure, regardless of their

subsequent statistical analysis (Bookstein, 1982). Moreover, biomechanical stresses or strains in the craniofacial skeleton cannot be investigated in detail by conventional methods. These components may be key determinants for bone remodelling. Therefore, it is of clinical significance to understand the biomechanical response of the complex to therapeutic forces when compared to actual morphological changes of the skeleton.

In the field of dentofacial orthopaedics, various techniques have been employed to evaluate the stress distribution induced within the craniofacial complex. However, it is not always possible with these methods to quantify stress or strain in an internal area of living structures. It is difficult to apply strain gauge techniques to the craniofacial skeleton without causing tissue damage. Furthermore, photoelastic and holographic techniques have a limitation when measuring the biomechanical components induced within the structure (Tanne *et al.,* 1991).

A technique applicable to biomechanical investigation for stress or strain within biological tissues is needed. The Finite Element Method is applicable to the biomechanical study of strains and stresses generated in the internal structures. The initial attempts to introduce Finite Element Method in the study of the craniofacial complex date back to the 1970's, when the first mathematical models of a dried *in vitro* human mandible were developed (Gupta *et al.,* 1973). From a biomechanics viewpoint, the *in vitro* condition was selected since it preserved anatomical definition, facilitated model development and expedited experimental verification. Model geometry was derived from physical measurements taken of mandible specimens using a sectioning and mapping technique and the initial models contained limited anatomical description. The materials simulated in that models included more often cortical and cancellous bone.

Miyasaka *et al.* (1986) and Tanne *et al.* (1989; 1991; 1996) have examined the reactions of the craniofacial complex during the application of

protraction headgear, orthopaedic chin cup forces and conventional headgear forces by using the Finite Element Method analysis. A human dry skull was sliced into 14 sections parallel to the Frankfort plane and these sections were consequently used to create a two-dimensional finite element model. Their model consisted of 2918 nodes and 1776 solid elements and included 18 sutural systems. The results indicated that, from a biomechanical aspect, many variables in the force system are pertinent to displacement and stress in the periodontium and bony structures for both orthodontic and orthopaedic treatments. Among these variables, the direction of force may be of great importance in determining the nature of displacement of the nasomaxillary complex as in the case of orthodontic tooth movement. Sutural response, the stresses in the sutural interfaces in particular, is a key determinant of therapeutic change of the craniofacial complex. A few years later, Tanaka, Tanne and Sakuda (1994; 1995) constructed a three-dimensional finite element model of the mandible including the temporomandibular joint with a similar method to that used to construct craniofacial complex for finite element analysis for the stresses developed in the area during functional loading.

The application of the finite element method to the human jaw has so far been compromised by oversimplifications of material properties and skeletal geometry, especially in the dentoalveolar complex (Gupta *et al.,* 1973; Knoell, 1977; McPherson & Kriewall, 1980; Lewis *et al.*, 1980; Ferré *et al.,* 1985; Umetani *et al.,* 1988; Van Buskirk *et al.,* 1988). For instance, if bone tissue is modelled as being elastically isotropic rather than orthotropic, a maximum error of up to 45° in the prediction of the orientation of the principal axes of stress is possible (Cowin and Hart, 1990).

Finite Element Method analysis has been used to evaluate treatment effects of various treatment modalities in diverse malocclusions (Lavelle, 1989; Tanne *et al.,*1993; 1996; Cangialosi *et al.*, 1994; Sung *et al.,* 2003; Chang *et al.,* 2004). Obviously knowledge of how a particular craniofacial structure

responds to a given treatment modality would be of great value in treatment planning.

Automated and manual CT edge detection methods have been implemented by clinicians and engineers to quantify intracranial volume (Gault *et al.*, 1988; Posnick *et al.*, 1992; Gosain *et al.*, 1995) and develop craniofacial finite element models (Tanne *et al.*, 1988; 1989; 1995; Krabbel *et al.*, 1995; Voo *et al.*, 1996; Korioth *et al.*, 1997). In the past, simple monoplanar edge detection techniques (Hobatho *et al.*, 1991) have sufficed for orthopaedic CT/FEA analyses of tubular bones of the lower extremities which, architecturally, are less complex than the cranium. However, strain validation studies involving the more complicated anatomy of the cranium demand more elaborate triplanar edge detection algorithms to provide the necessary spatial resolution of the model. The variation of craniofacial anatomy over the human cranium becomes an important factor when finite element analysis results are compared to clinical data.

The first attempts to create a three-dimensional finite element model of a part of the craniofacial complex using CT scans date back to 1992, when Hart *et al.* and Korioth *et al.* constructed a model of the human mandible in order to calculate the mechanical response to functional loading.

The first attempts to use eightnoded hexahedral elements for the construction of the finite element meshes, have shown that the surfaces of these models are characterised by abrupt transitions and right angles (Fyhrie *et al.*, 1992; Hollister and Kikuchi, 1992; van Rietbergen *et al.*, 1995). Jacobs *et al.* (1993), have found that surface strains at the boundaries of these digital image-based meshes are less accurate than those of smooth meshes and that the decreased solution quality may not necessarily improve with mesh refinement. Guldberg and Hollister (1994) acknowledged that digital image-based meshes produce increased error at surfaces, but suggested that the error was acceptable relative to other inaccuracies such as material

property uncertainty. In earlier research, Hollister *et al.* (1992), found that digital image-based meshes require a minimum of 2-4 elements across the thickness of relevant structures to produce solutions with less than 10% error. Unfortunately, as computational resources are often limited, attaining this minimal mesh density in all parts of a geometrically complex mesh may not be feasible.

However recently, a technique which directly converts image voxels to eightnoded hexahedral elements with automated smoothing of all surfaces and material interfaces, has been developed (Camacho *et al.,* 1997). The smoothing algorithm produces a more accurate overall surface geometry at the cost of distorting the individual elements' brick shape which is optimal for element stress calculations. Solution errors are decreased as a result of this algorithm indicating that errors resulting from an irregular representation of the surface geometry are greater than those introduced by surface element distortion. In applications where surface quantities are of particular interest (i.e. bone surface remodelling), this mesh generation technique provides an improved solution over previous methods.

Another important factor for the accuracy of the Finite Element Analysis, as shown by Keyak and Skinner (1992), is the size of the elements used for the construction of the mesh. They noticed that there was a general decrease in the level of stress and strain when element size was increased and consequently, the elements must be very small to represent the sharp variations in mechanical properties that exist in bone. This sensitivity to element size implies that quantitative comparisons of the stresses/strains predicted by different Finite Element Models may not be meaningful if the elements in those models are not the same size. On the other hand, qualitative comparisons may be made.

The principal advantage enjoyed by the Finite Element Method is that it overcomes the intrinsic constraints of any method of roentgenographic

cephalometry and that its numerical descriptions of growth behaviour are reference frame invariant. The Finite Element Method, due to the basic concept behind the method, has also the following advantages for solving displacement-related problems:

- arbitrary structural geometries can readily be modelled with the use of elements;
- arbitrary accommodation of boundary conditions and loading;
- capability of modelling differing internal material properties;
- close resemblance of the actual structure;
- and finally, does not involve the tracing error, the identification of the points error, the measurement error and the poor repeatability of the conventional cephalometry.

Moreover, the description of changes provided by the F.E.M. is significantly finer than that of the roentgenographic cephalometry and, because its intrinsic invariance, is always more biologically correct (Moss *et al.*; 1985).

The price of the increased accuracy, however, is that more homologous points need to be located. We must therefore be content to view the chosen elements as analytical constructs and consider them to be as closely representative of biological entities as possible (Richtsmeier *et al.*, 1986). At the same time, maximizing model accuracy by subdividing a mesh volume into a large number of very small elements, will increase greatly computer memory requirements and processing time. However, this is necessary only in regions with complex shapes or anticipated high gradients of material deformation. Otherwise, smaller number of elements will provide sufficient accuracy without loss of biological detail or structural response (Korioth *et al.*, 1992).

CHAPTER 3: SUBJECTS AND METHODOLOGY

3.1. Experimental Technique

A human dry skull of an adult subject with the maxillary alveolar crest well represented but with the teeth missing, without the mandible and with no evident craniofacial anomaly was used to construct the Finite Element Model. The anatomy of the cranium was obtained by using the computer tomography (CT) technique.

The cranium was supported on a wooden base in order to avoid distortion during the procedure of imaging and was introduced into the tomograph orientated at an angle to the Frankfort Horizontal. Every effort was made to eliminate any movement of the head caused by the machine during the radiographic procedure and to allow for scan slices to be completely parallel and in the exact distance between them. 98 CT-images parallel to each other were initially taken at 1,5mm intervals by a Siemens Somatom Plus 4® Computer Tomograph. The sections covered the area of the skull and the craniofacial complex.

The type of Computer Tomograph used had the possibility to save all the information obtained during the imaging procedure as raw data on an optical disc, or as tiff files (i.e. type of image files) on 3,5" floppy discs. The advantage of the technique is that scanning and digitizing of the images is not required, thus avoiding further method errors.

The raw data obtained by the Computer Tomograph were processed and three-dimensional coordinates of the geometric points which define the bones of the skull were obtained and saved in an IGES file. The CT sections were read into a commercially availabe, visualization computer

software MIMICS/MEDCAD® (Materialise's Interactive Medical Image Control System) by Materialise N.V., Leuven, Belgium.

The next step was to create from the coordinates of the geometric points, the 3-D Finite Element Model of the skull on which the Finite Element Analysis will be performed. In order to do that, the data obtained from the Computer Tomograph and saved in an IGES file had to be further processed using a CAD/CAE software with the assistance of the Assistant Professor of the Department of Mechanical Engineering, Mechanical Design and Control Systems, National Technical University of Athens (Greece); Mr. Christoforos Provatidis.

The IGES file was introduced in Autocad which is a CAD type software (i.e. Computer Aided Design software) and converted in a .dxf file. This represents an interface to download the data in a CAE type software (i.e. Computer Aided Engineering software) in which the Finite Element Analysis will be performed. The software chosen was the ALGOR® version III 12.10 (ALGOR.com) which is less demanding in computer power and therefore is compatible with PC's (**Figure 1**).

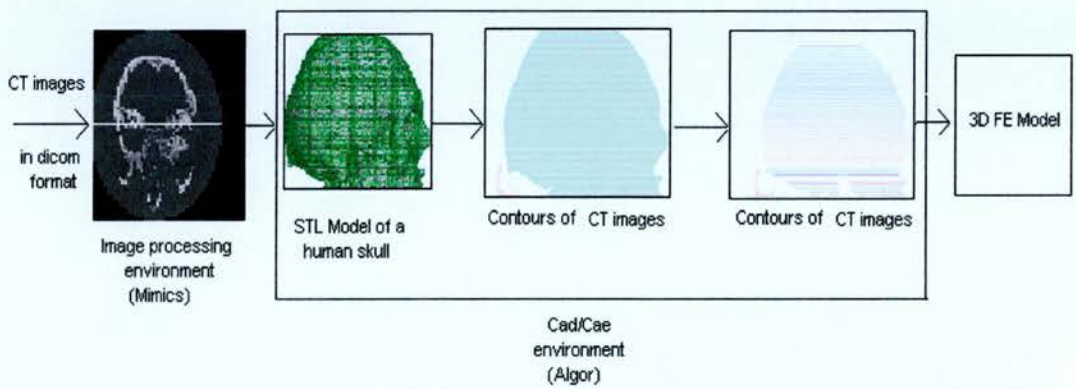

Fig. 1: The workflow diagram for the generation of 3D Finite Element Model.

The model of the craniofacial skeleton presented in **Figure 2** is the initial result of a rapid prototyping process (MIMICS/MEDCAD®). The model of the skull derived included an enormous number of nodes and elements (i.e. 75444 nodes and 1582833 elements) and also included a number of invalid nodes. Therefore, the model of the skull created was too complicated for further investigation, making it also impossible to identify anatomical structures of the head.

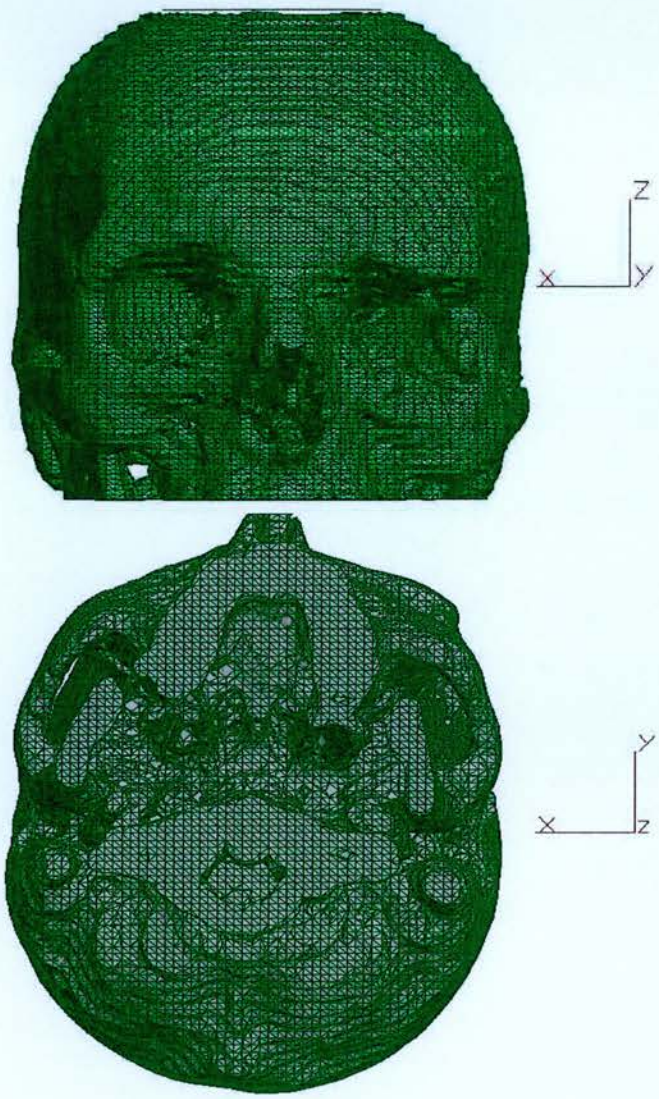

Fig. 2. The frontal and basal view of the skull after reconstruction from the CT sections (i.e. rapid prototyping process) into the ALGOR software program.

Consequently, from the initial 98 sections, 51 sections were chosen to construct a new model with the following two criteria:

- firstly, each section was "described" by a number of points with a common z-coordinate. Between two neighboring points, straight lines were drawn passing through these points in order to circumscribe each section by a number of straight lines. One of the difficulties that occurred was that there was no information about the geometry of the skull in-between the tomographic sections. However, due to the large number of sections and the small distance between them, and taking into account the continuous character of the division of elements of the succeeding slices, it was possible to reproduce the geometry of the skull with sufficient accuracy. The distance between two succeeding sections was 3mm except for the nasomaxillary region where the distance was 1.5mm in order to increase accuracy in the area of application of the expansion force.
- Secondly, the true anatomy of the nasomaxillary complex was respected.

The reduction of the number of sections had also another advantage, the reduction of the time required for the mathematical calculations. The selection of sections was done by ALGOR® software to identify the coordinates at the start and the end of each line and save all the data as an eagle file (.egl). This was an easier, more flexible and more accurate method compared to manual identification of the sections. Using a lisp program the inverse procedure has taken place, whereby the program could read the data obtained and represent graphically the lines between the two nodes. The whole model was rebuilt and the result was an .esd file with the number of sections as represented in **Figure 3**. The sections presented are only those sections that were finally used for the construction of the finite element model with the main objective not to lose any important geometric information.

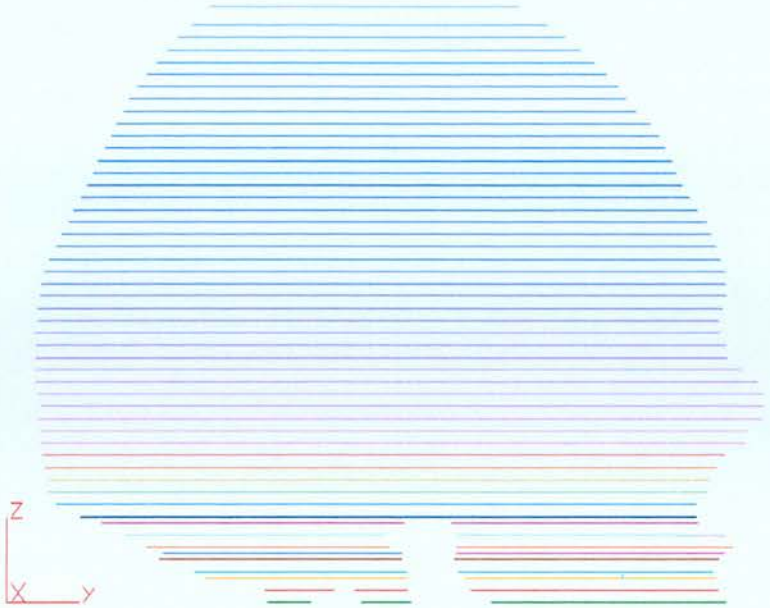

Fig. 3. The amount of sections finally chosen for the creation of the Finite Element Model of the skull (right view). Each section is represented with a different layer (colour).

The lining of the bone anatomy of some of the sections with different z-values that were finally selected to be used in the construction of the model is presented in Appendix (**App. 1-4**). The model was then divided in finite elements to construct the mesh. Dividing each selected section into finite elements interconnected with straight lines which follow the initial anatomy, resulted in a new section that mimics the initial section but is not identical. The sections presented in **App 5-8** correspond to the sections presented in the **App. 1-4** after this process taken place. It is important to note that the division of each section into finite elements is based on the outer geometry of the skull.

The construction of the mesh was done automatically by the software where the geometry of the model was simple, by converting the lines into splines, and manually where the anatomy was more complex. The bone

was then divided into different groups based on its mechanical properties. These bones were the maxilla, the zygomatic bone, the palatal bone, the sphenoid and the nasal bones. The separation of the various bones was at the level of the sutures (i.e. maxillozygomatic; nasomaxillary; frontomaxillary; maxilloethmoidal suture and as well as the suture between the maxilla and the lacrimal bone). Modelling of the midpalatal and the pterygopalatine and maxillopalatine sutures was also done. Each suture was identified by a different colour in order to make the changes in their mechanical properties during the finite element analysis of the model easier.

For the construction of the teeth, the z-axis (Z=0) was lowered by Z=3 and the maxillary dental arch was added artificially respecting the proportional relationship of the teeth to the whole skull. Initially the model consisted of the outer surface of the skull and the teeth and was constructed with plate elements. The model as resulted from this process is shown in Appendix (**Figures 4 - 5**).

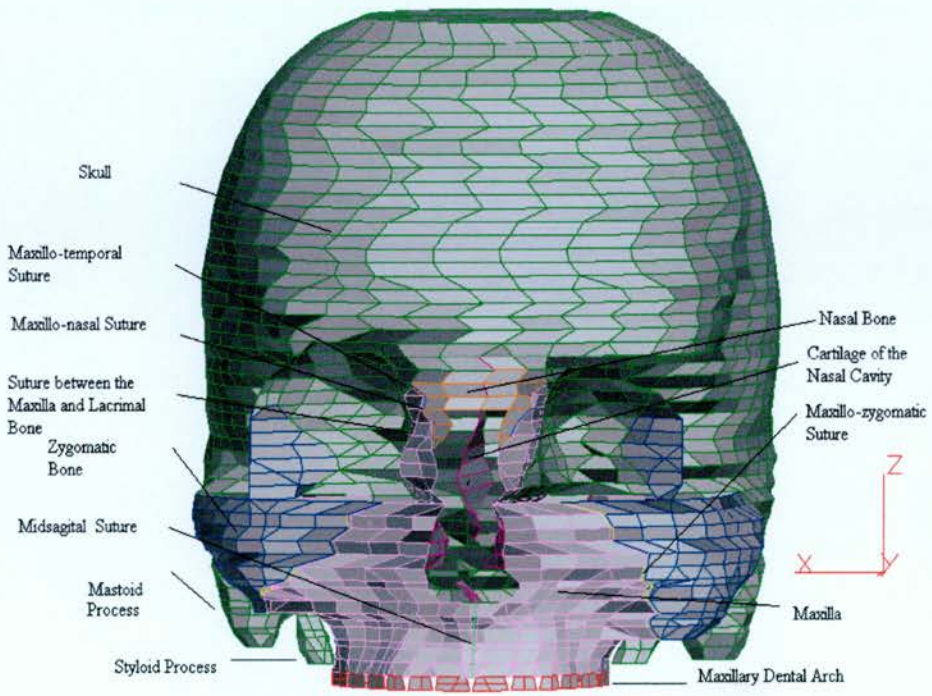

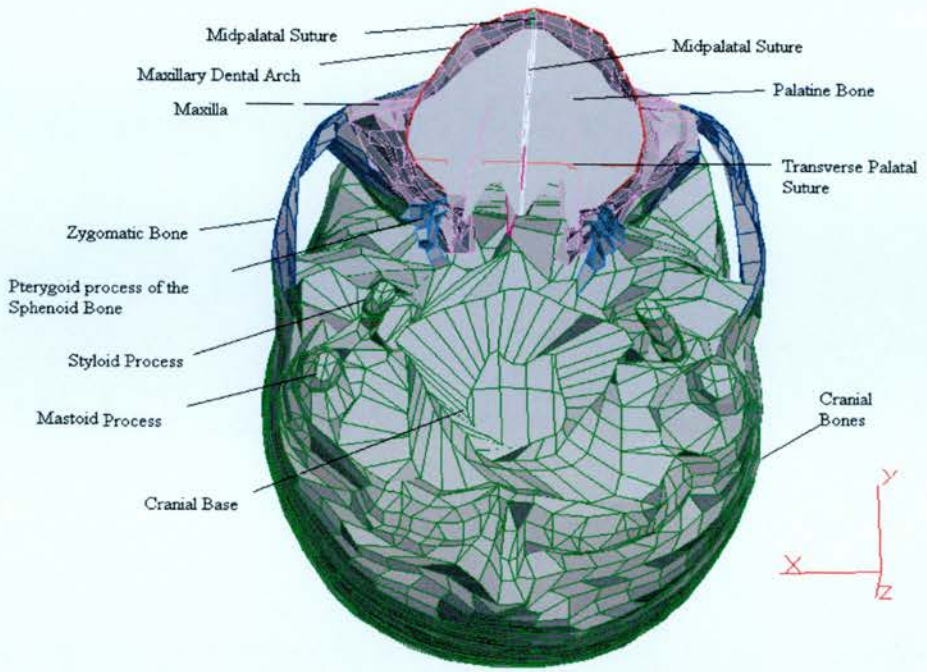

Fig. 4. The initial Finite Element Model of the dry skull (frontal and basal view).

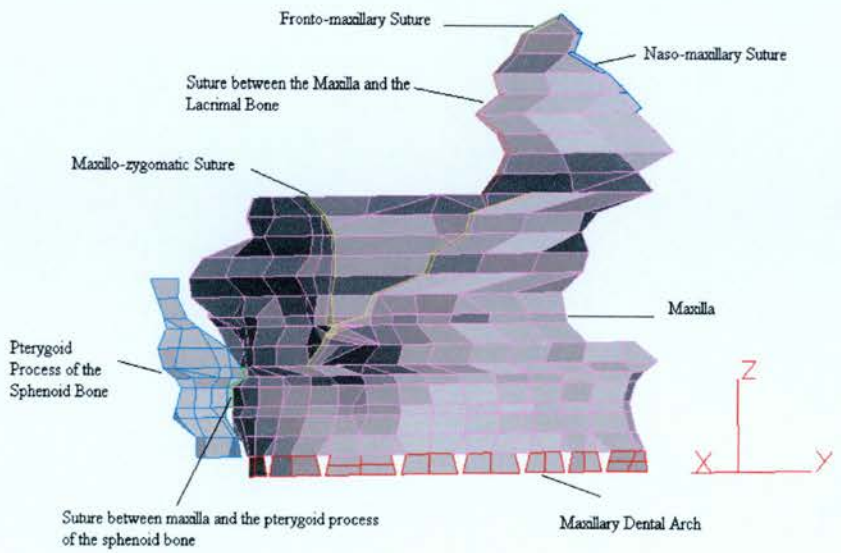

Fig. 5. Right view of the initial Finite Element Model of the maxilla

After constructing the mesh of the nasomaxillary and the craniofacial complex, the model of the RME appliance was manually added. Different types of maxillary expansion devices have been used by clinicians for rapid maxillary expansion of the mid-palatal suture. The RME model used in the present study consisted of the Hyrax screw and the two symmetric acrylic halves. For the modelling of the acrylic part, brick elements were used; for the Hyrax screw, plate and beam elements were preferred. The brick elements were chosen because the acrylic part of the appliance was considered as a homogenous material, and the beam elements for the Hyrax screw were chosen due to the cylindrical shape of the original. The model of the Hyrax screw was given the material properties of steel in that steel possesses the highest proportion of the alloys used in its construction. The model of the Rapid Maxillary Expansion appliance was supported on the first premolar and first permanent molar teeth (**Figure 6**).

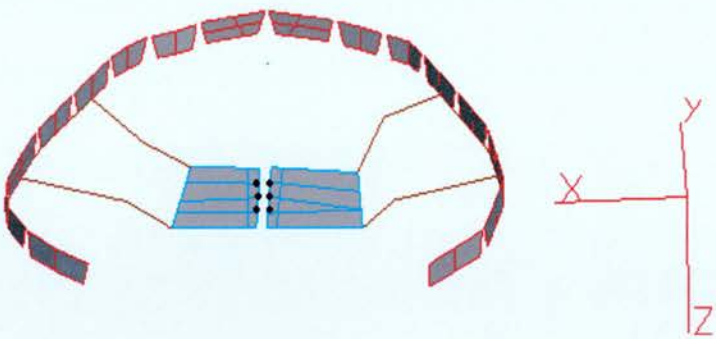

Fig. 6. The initial Finite Element Model of the Rapid Maxillary Expansion appliance (i.e. the HYRAX screw without the acrylic plates) fitted on the maxillary dentition. The black dots represent the nodes on which the external load of the expansion forces will be applied on the model.

In **Figure** 7 presents the model of the Rapid Maxillary Expansion appliance fitted on the model of the maxilla and in **Figure 8** the Finite Element Model of the skull after the addition of the teeth and the appliance. The model consisted from 5288 nodes and 5697 elements.

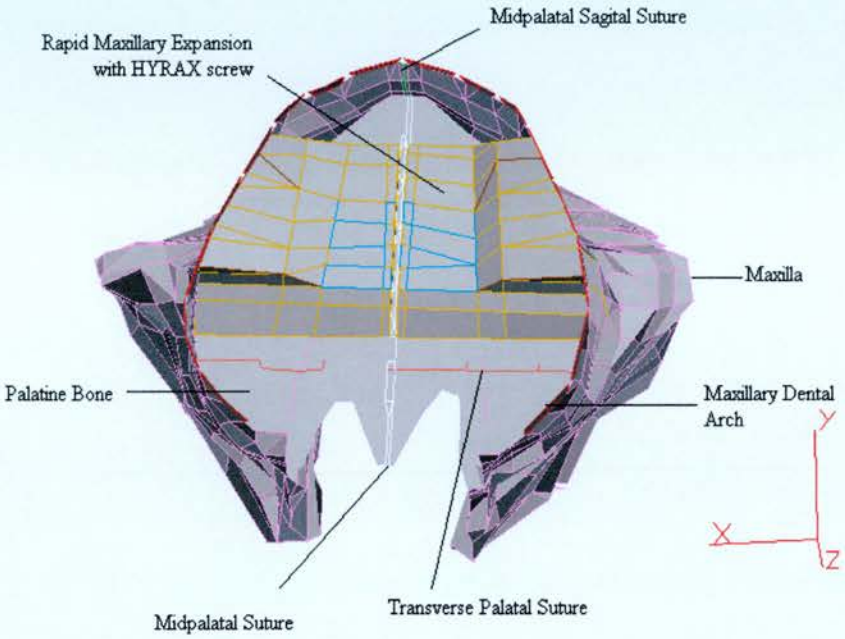

Fig. 7. Placement of the Rapid Maxillary Expansion appliance on the maxillary dental arch (basal view)

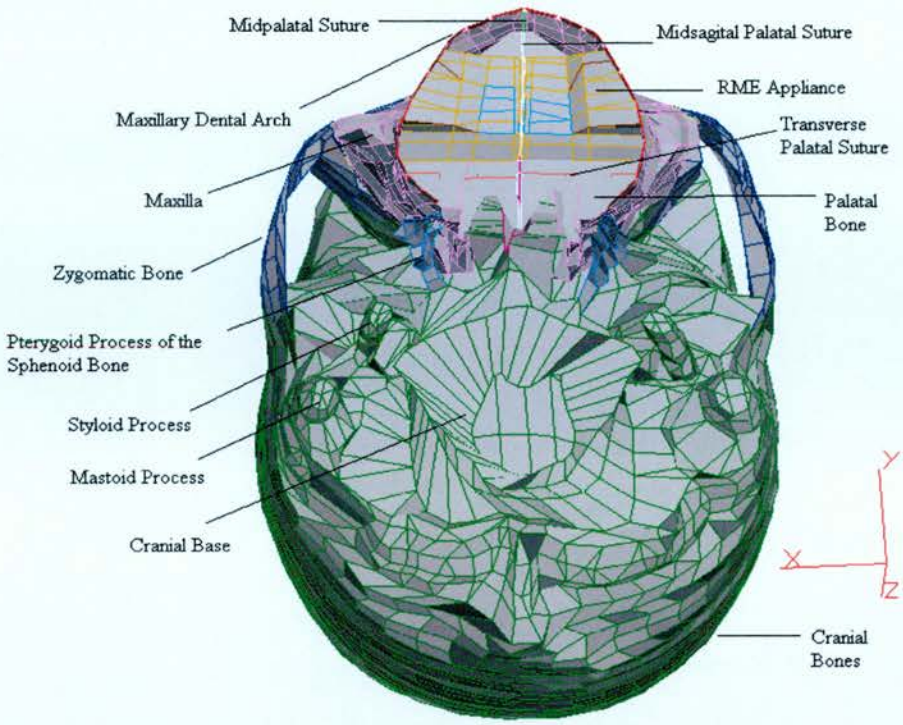

Fig. 8. Basal view of the Finite Element Model of the dry skull with the artificially added maxillary dentition and the Rapid Maxillary Expansion appliance in place.

The results of the Finite Element Analysis were compared with the clinical findings from a previously studied population (McDonald, 1995) as described in the following chapter.

3.2. Clinical Subjects

The clinical subjects used in this study originated from the East of Scotland, specifically from the Edinburgh and Fife areas. They were referred to the Orthodontic departments of either the Edinburgh Dental Hospital or the Victoria Hospital, Kirkcaldy by General Dental or Medical Practitioners or Hospital Specialists. The criteria for selection for the study were as follows:

- full transverse cusp crossbite
- no evidence of adenoidal blockage of nasopharynx
- no previous tonsilar, nasal or adenoidal surgery.

In addition to these basic selection criteria, for the purposes of this study all patients required complete medical and dental records including good Postero-Anterior and lateral cephalometric radiographs with Rapid Maxillary Expansion appliance in situ at the end of active expansion. From a total of 72 cases reported previously (McDonald, 1995), 49 were selected for the study.

3.3. Clinical Procedures

All clinical treatment had been undertaken previously by McDonald (1995). Full baseline records included study models, clinical photographs, orthopantomogram Postero-Anterior and lateral cephalometric radiographs and rhinomanometric measurements. The commencement of orthodontic treatment of the anomaly patients arose when the maxillary canines had erupted to allow the easy transition from Rapid Maxillary Expansion to fixed appliances to complete treatment. The Rapid Maxillary Expansion appliance used was a fixed split acrylic appliance supported with bands cemented on the first permanent premolars and molars, with the active expansion produced by a Hyrax screw (11mm or 18mm). The choice of

expansion screw depended on the estimated amount of expansion desired. Minor modifications of the appliance were used depending on orthodontic classification (McDonald, 1995).

Activation Regime

The appliance was activated by the parent 24 hours following cementation and the patients were reviewed regularly during active expansion. The following regime was typical for all patients. During the first week one-quarter turn three times a day, once after breakfast, school and before bed. During the second week this was reduced to one-quarter turn twice a day, after breakfast and before bed. Finally, for the third week the screw was turned one-quarter turn once a day in the mornings only. If necessary this was continued until the crossbite had been overcorrected so that the palatal cusps of the upper molars were riding up on the buccal cusps of the lowers.

When the required expansion was achieved, the expansion screw was locked in position with cold cure acrylic and the appliance was used as a retainer for three months. After active expansion the following records were repeated: clinical photographs, orthopantomogram Postero-Anterior and lateral cephalometric radiographs and rhinomanometric measurements. These records were used to analyse the skeletal, dental and nasal effects of RME in the anomaly sample.

3.4. Radiographs

All radiographs for the original study were taken at the Edinburgh Dental Hospital by a single trained Radiographer. Subjects were radiographed in natural head position as described by Solow and Tallgren (1976). The selection of the clinical subjects for the inclusion in this study was based

largely on the quality of Postero-Anterior and lateral cephalometric radiographs. Both sets of radiographs before and after RME were examined closely to ensure a clear image of a wide range of skeletal, dental and nasal structures.

The original lateral cephalometric radiographs were taken with the aid of a cephalostat and a Morito Pan X E2 Orthopantomogram. Trimax 3M blue-based fast radiographic film was used in a cassette with rare earth screen. Exposures were made at 80 kvolts for 8 seconds. Postero-Anterior cephalometric radiographs were taken using the same equipment after the patients allowed to reposition into natural head position. The film was exposed for 1.3 seconds at 80 kvolts (McDonald, 1995).

3.4.1. Digitising

A computer based system was used in this study to scan, to digitise and to measure skeletal, dental and nasal; linear and angular measurements. The computer hardware consisted of a Pentium II at 466 MHz IBM compatible personal computer, AGFA SNAPSCAN 1236usb scanner and a Hewlett-Packard Deskjet 980cxi professional series colour printer. The software used consisted of a commercially available cephalometric analysis program, Viewbox v2.60.02 (Manual version; Copyright © by Demetrios J. Halazonetis). This program has an extensive library of cephalometric landmarks and measurements together with a facility to create additional operator-generated landmarks and cephalometric measurements.

In a darkened room cephalometric radiographs were scanned and transferred to the cephalometric analysis software. Then a number of skeletal, dental and nasal landmarks were digitised with the use of the Microsoft Intellipoint® mouse.

3.4.1.1. Reference points used in digitising the lateral cephalometric radiographs:

A lateral cephalogram is one of the orthodontic records that provides information about the sagittal and vertical relations of:

- the craniofacial skeleton;
- the soft tissue profile;
- the dentition;
- the pharynx; and
- the cervical vertebrae.

These structures and their relationships to each other are scrutinised by means of linear and angular measurements as well as by the use of ratios based on the various cephalometric landmarks.

3.4.1.1.1. Skeletal Landmarks

A number of skeletal landmarks were chosen as candidates for investigation, the majority of these landmarks were taken from definitions by Downs (1948), Sassouni (1955), Coben (1955) and Athanasiou (1995). A list of the skeletal landmarks and definitions are given in **Appendix 9** and presented in **Figure 9**.

3.4.1.1.2. Dental Landmarks

Dental landmarks were based on definitions by Athanasiou (1995) and are shown in **Appendix 10** and in **Figure 9**.

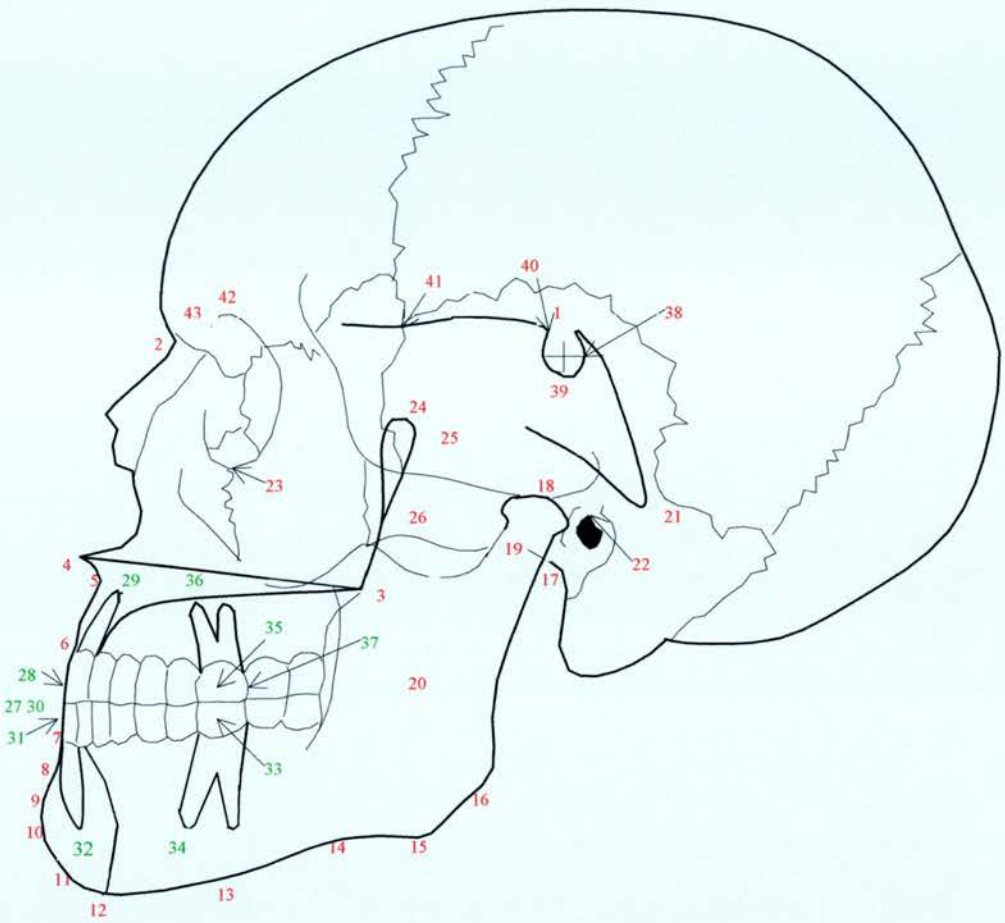

Fig. 9. Skeletal and Dental landmarks used in digitising lateral cephalometric radiographs (Numbers correspond to those given in Appendix 9 and 10). Red are skeletal landmarks, green are dental landmarks.

3.4.1.1.3. Soft Tissue Landmarks

Soft-tissue landmarks are used mainly to construct an aesthetic soft-tissue drawing and their exact location is not important since they are not used in any measurements. A list of the soft tissue landmarks and definitions are given in **Appendix 11** and presented in **Figure 10**.

The following orientations are provided by digitising software:

- FH at Fix 1,2: Places the radiograph with the Frankfort plane horizontal and Porion at the coordinates of point Fix1 (x=1000, y=650)
- Occlusal Horizontal: Orientates the radiograph so that the occlusal plane is horizontal
- SN at 7 degrees: Orientates the radiograph so that the Sella – Nasion line is at 7 degrees to the horizontal.

The measurements selected for analysis of the lateral cephalometric radiographs are given in the following **Table 1**. The reference lines and planes used in these measurements are presented in **Table 2.**

Linear Dimensions	Angular Dimensions	Dentoalveolar Relations
n-s	n-s-ba	Ils/NL
n-sp	n-s-ar	Ili/ML
n-gn	pm-s-ba	
s-ba	s-n-sp	
s-ar	s-n-ss	
s-pm	s-n-sm	
sp-me	s-n-pg	
sp-pm	ss-n-sm	
ss-pm	ss-n-pg	
is-sp	NSL/NL	
ii-me	NSL/ML	
	NL/ML	
	NSL/MBL	
	ML/RL	

Table 1. Lateral cephalometric measurements

Reference Line	Definition
MBL	Mandibular Base Line. The line through gnathion and condylion
ML	Mandibular Line. The tangent to the lower border of the mandible through gnathion and gonion
NL	Nasal Line. The line through sp and pm
NSL	Nasion-Sella line. The line through n and s.

Table 2. Reference lines and planes used in the analysis of the Lateral Cephalometric Radiographs

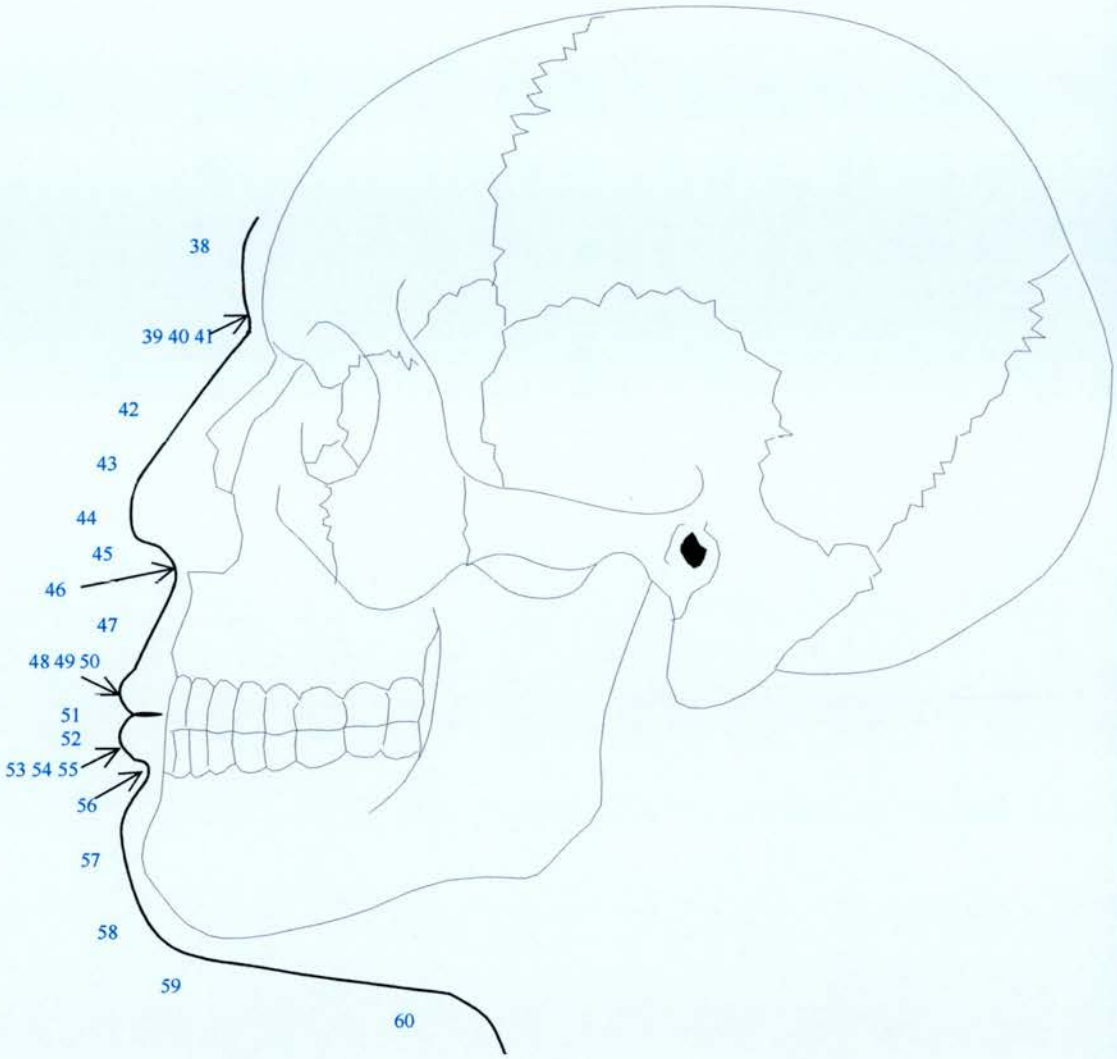

Fig. 10. Soft Tissue Landmarks used in digitising lateral cephalometric radiographs

3.4.1.2. Reference points used in digitising the postero-anterior cephalometric radiographs:

Landmarks and variables that can be identified on coronal planes of different depths in the same postero-anterior cephalogram can provide useful information concerning the vertical, transverse, and sagittal dimensions of the craniofacial skeleton.

There are 59 digitised points in the Frontal cephalogram definition file supplied with the Viewbox software. The definitions of the cephalometric points used in the study were taken by Grummons and Kappeyne van de Copello (1987), Athanasiou et al. (1992), da Silva et al. (1995) and Athanasiou (1995). These points are presented in **Figure 11** and **Appendix 12**. These points are symmetric for left and right except for the points in the median plane.

The following orientations are provided:

1. MSR fix: Places the radiograph with the MSR plane vertical and Crista Galli at the coordinates of point Fix1 (x=80, y=40)
2. MSR Vertical: Orientates the radiograph so that the MSR plane is vertical
3. Zygomatic Horizontal: Orientates the radiograph so that the Zygomatic plane is horizontal.

MSR is the midsagittal reference plane that passes through Crista Galli and Anterior Nasal Spine (Grummonds and Kappeyne van de Copello; 1987).

From these points a number of skeletal and dental transverse measurements were selected and are given in **Table 3**.

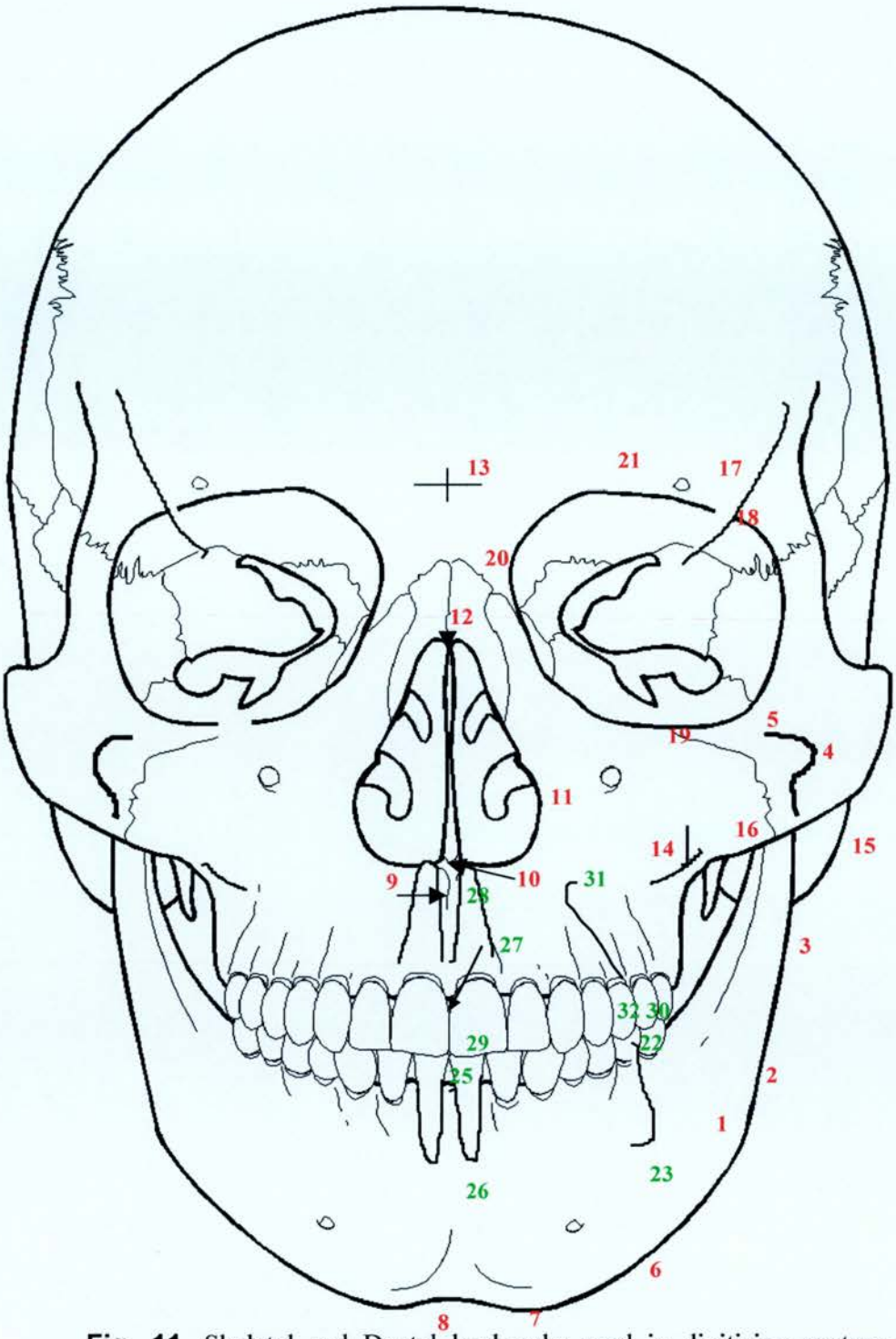

Fig. 11. Skeletal and Dental landmarks used in digitising postero-anterior cephalometric radiographs (Numbers correspond to those given in Appendix 12). Red are skeletal landmarks, green are dental landmarks.

Orbit Level	Nasal Level	Maxillary Level	Mandibular Level	Proportionality
LOR-LOL	MSR-MSL	EMR-EML	LMR-LML	NASDIM
MOR-MOL	CNR-CNL	UMR-UML	AGR-AGL	MAXDIM
LOR-UMR	CNR-CNM	MIR-C2		
LOL-UML	CNM-CNL	C2-MIL		
	MOR-CNR	MIR-MIL		
	MOL-CNL	CNR-EMR		
		CNL-EML		
		EMR-UMR		
		EML-UML		
		UMR-MIR		
		UML-MIL		

Table 3. Postero-Anterior Cephalometric Measurements

3.4.2. Method Error:

Method error for all linear and angular measurements and cross-sectional area calculations were accomplished using duplicate tracings of the anomaly sample before treatment according to Houston (1983). A period of at least four weeks elapsed between duplicate tracings and comparisons between the two sets of readings were carried out as follows. Systematic error was examined using a Student's t-test of all the variables. Random error was examined using the modification of Dahlberg's formula (1940) suggested by Houston (1983). The results of the method error for all linear, angular and cross-sectional area measurements are given in **Table 4** and **Table 5**.

Measurement	Variance T1 (Houston)	Error Variance/Total Variance	p	Comment
n-s	13,05	9,6%	0,399	NS
n-sp	25,74	7%	0,365	NS
n-gn	64,29	8,9%	0,428	NS
s-ba	9,14	10,3%	0,367	NS
s-ar	7,16	10%	0,459	NS
s-pm	15,82	9,9%	0,423	NS
sp-me	28,93	9,8%	0,478	NS
sp-pm	19,52	9,9%	0,377	NS
ss-pm	26,26	9%	0,335	NS
is-sp	7,65	9,4%	0,375	NS
ii-me	8,91	9,7%	0,386	NS
n-s-ba	47,1	4,5%	0,488	NS
n-s-ar	42,28	5,1%	0,480	NS
pm-s-ba	40,83	10,1%	0,426	NS
s-n-sp	35,63	9,4%	0,427	NS
s-n-ss	29,12	9,6%	0,373	NS
s-n-sm	37,43	8,1%	0,495	NS
s-n-pg	38,53	8.1%	0,463	NS
ss-n-sm	17,77	8,8%	0,289	NS
ss-n-pg	16,52	8,5%	0,344	NS
NSL/NL	19,8	8,4%	0,256	NS
NSL/ML	50,22	2,9%	0,456	NS
NL/ML	25,37	8.9%	0,429	NS
NSL/MBL	31,13	8,5%	0,433	NS
ML/RL	19,35	7,6%	0,354	NS
Ils/NL	41,88	7,1%	0,392	NS
Ili/ML	40,73	4,8%	0,457	NS

Table 4. Duplicate Determinants for Lateral Cephalometric Measurements

Measurement	Variance T1 (Houston)	Error Variance/Total Variance	p	Comment
LOR-LOL	30,99	8,3%	0,436	NS
MOR-MOL	13,21	5%	0,386	NS
LOL-UML	29,22	9%	0,47	NS
LOR-UMR	21,87	7,3%	0,449	NS
MSR-MSL	24,9	5,8%	0,391	NS
CNR-CNL	5,89	8,2%	0,378	NS
CNR-CNM	1,47	8%	0,356	NS
CNM-CNL	1,47	8%	0,356	NS
MOR-CNR	8,38	8%	0,288	NS
MOL-CNL	9,39	7,4%	0,401	NS
EMR-EML	18,56	8,4%	0,495	NS
UMR-UML	19,69	7,5%	0,426	NS
MIL-C2	0,05	2,5%	0,436	NS
MIR-C2	0,05	2,5%	0,436	NS
MIR-MIL	0,23	5,3%	0,322	NS
CNR-EMR	8,63	8,6%	0,443	NS
CNL-EML	7,4	7,4%	0,359	NS
EMR-UMR	17,79	6,7%	0,475	NS
EML-UML	23,46	7,9%	0,46	NS
UMR-MIR	12,92	7,8%	0,477	NS
MIL-UML	4,97	8,6%	0,374	NS
LMR-LML	8,11	5,8%	0,447	NS
AGR-AGL	15,75	7,3%	0,381	NS
NASDIM	13,98	9,5%	0,461	NS
MAXDIM	21,21	7,1%	0,419	NS

Table 5. Duplicate Determinants for Postero-Anterior Cephalometric Measurements

The results of the method error indicated there were no systematic differences found for all sets of measurements and that the majority of measurements were associated with percentage errors of around 10% or less. For the purposes of this study it was decided to keep the measurements related to the maxilla mainly because only the finite element model of the craniofacial and nasomaxillary complex was developed and the mandible was excluded from the model for the time being.

3.4.3. Statistical Analysis:

Lateral and postero-anterior cephalometric measurements of the clinical subjects, from both before and after treatment were tested for normality. As far as could be ascertained all measurements tested conformed to normal distribution. Parametric statistical tests were judged to be suitable for both within group and between group comparisons. Statistical tests were, also, applied in order to check whether the difference in the sample means was due to treatment or occurred coincidentally. Due to the number of comparisons that would be made ($N>30$); it was decided that the level of significance should be $p<0.05$ (**Appendix: 13.1**).

Finally, a 99,5% confidence interval for the true difference between the population means was then calculated (**Appendix: 13.2**). If the difference between the points that were finally used for comparison in the Finite Element Analysis is found within the limits of the confidence interval, it is then possible to define all these parameters that influence the clinical result of the Rapid Maxillary Expansion.

All statistical tests were accomplished using an Excell spreadsheet software package (Microsoft, USA). Formulae for statistical tests are given in **Appendix 13** and the results of the statistical analysis are presented in **Table 6** and **Table 7** with the underlined measurements indicating the findings with statistically significant differences in the before and after treatment measurements.

For the purposes of this study it was decided to use the four coloured measurements (i.e. CNR-CNL, EMR-EML, UMR-UML, MIR-MIL) from the postero-anterior cephalometric analysis which presented statistically significant differences in the before and after treatment analysis and were related to the transverse expansion and the separation of the two maxillary halves. The anatomical points of these four measurements were also easily reproducible on

the Finite Element Model. The confidence interval for $p<0.05$ was also statistically calculated for each of these four measurements in order to assess their upper and lower values and, consequently, make the comparison with the results of the Finite Element Analysis of the model of the dry skull more feasible (**Table 8**).

Lateral Cephalometric measurements	Before	SD	After	SD	Difference	p
Li to GoGn	84,11	6,43	84,16	6,01	0,05	0,927
MM	**31,98**	**4,86**	**33,15**	**5,10**	**1,17**	**0,001**
Ui to Palatal Angle	111,69	6,58	110,60	6,01	-1,09	0,081
N-ANS	54,87	3,62	55,96	3,82	1,09	0,003
SNPg	78,48	4,81	77,22	3,94	-1,26	0,002
SN to GoGn	**37,72**	**5,42**	**39,14**	**5,49**	**1,42**	**0,001**
ANS-Menton (dist)	**74,08**	**5,49**	**76,65**	**5,19**	**2,57**	**0,000**
ANS-PNS (dist)	54,80	3,67	55,88	3,31	1,08	0,017
ANS-Ui edge (dist)	31,57	2,71	31,74	2,77	0,17	0,318
Gn-Co (dist)	123,13	7,50	122,85	7,04	-0,28	0,520
Li-Menton (dist)	43,16	2,77	43,40	2,87	0,24	0,039
Na-Menton (dist)	**128,20**	**7,06**	**131,37**	**6,73**	**3,17**	**0,000**
S-Art (dist)	35,71	3,42	36,09	4,16	0,38	0,202
S-Ba (dist)	44,78	4,76	45,38	4,96	0,6	0,357
S-Na (dist)	74,79	3,43	75,01	3,83	0,22	0,391
S-PNS (dist)	49,16	3,19	49,73	2,88	0,57	0,003
Apoint-PNS (dist)	49,95	3,51	50,81	3,38	0,86	0,019
N-S-Ba	130,45	5,87	131,16	4,72	0,71	0,106
N-S-Ar	124,59	5,81	125,31	5,45	0,72	0,109
PNS-S-Ba	55,35	5,91	55,69	5,26	0,34	0,446
S-N-ANS	98,13	4,43	97,35	3,85	-0,78	0,156
Apoint-N-Pog	**1,47**	**3,38**	**-0,32**	**3,54**	**-1,79**	**0,000**
SN-MxPl	7,39	3,80	7,74	3,22	0,35	0,298
SN-GnCo	60,39	4,37	61,65	4,22	1,26	0,002
MndPl-Ramus	131,64	4,85	131,08	4,75	-0,56	0,134

Table 6. The results of the analysis of the Lateral Cephalometric radiographs of the clinical subjects.

Postero-Anterior Cephalometric measurements	Before	SD	After	SD	Difference	p
AGR-AGL	89,02	5,13	89,66	5,57	0,64	0,060
CNL-CNM	**15,6**	**1,22**	**16,43**	**1,30**	**0,83**	**0,000**
CNL-EML	21,01	3,01	20,65	2,59	-0,36	0,402
CNR-CNL	**31,2**	**2,46**	**32,86**	**2,62**	**1,66**	**0,000**
CNR-CNM	**15,6**	**1,22**	**16,43**	**1,30**	**0,83**	**0,000**
CNR-EMR	20,74	3,01	20,44	2,12	-0,3	0,469
EML-UML	12,73	4,81	13,2	3,61	0,47	0,545
EMR-EML	**61,49**	**4,04**	**63,96**	**3,58**	**2,47**	**0,000**
EMR-UMR	12,14	4,61	13,9	3,36	1,76	0,017
LMR-LML	60,75	4,17	60,77	4,17	0,02	0,973
LOL-UML	83,17	5,15	83,22	5,07	0,05	0,915
LOR-LOL	103,5	4,58	104,01	4,52	0,51	0,106
LOR-UMR	83,63	5,53	83,88	6,13	0,25	0,734
maxdim	1,01	0,03	1,01	0,03	0	0,135
MIL-C2	**0,57**	**0,34**	**1,11**	**0,69**	**0,54**	**0,000**
MIR-C2	**0,57**	**0,34**	**1,11**	**0,69**	**0,54**	**0,000**
MIR-MIL	**1,13**	**0,70**	**2,21**	**1,39**	**1,08**	**0,000**
MOL-CNL	43,19	3,58	43,51	3,53	0,32	0,365
MOL-CNR	51,2	3,18	52	2,89	0,8	0,003
MOL-EMR	71,27	4,44	71,74	3,60	0,47	0,352
MOR-CNL	50,46	3,55	51,42	3,33	0,96	0,004
MOR-CNR	41,62	3,55	42,38	3,41	0,76	0,030
MOR-EML	70,55	4,39	71,3	3,73	0,75	0,143
MOR-MOL	25,18	3,02	25,79	4,95	0,61	0,360
MSR-MSL	137,71	5,58	138	7,28	0,29	0,734
nasdim	1,02	0,05	1,01	0,04	-0,01	0,449
UML-MIL	**28,86**	**3,15**	**31,94**	**2,92**	**3,08**	**0,000**
UMR-MIR	**27,13**	**2,39**	**31,12**	**2,44**	**3,99**	**0,000**
UMR-UML	**54,66**	**3,34**	**63,55**	**4,52**	**8,89**	**0,000**

Table 7. The results of the analysis of the Postero-Anterior cephalometric radiographs of the clinical subjects.

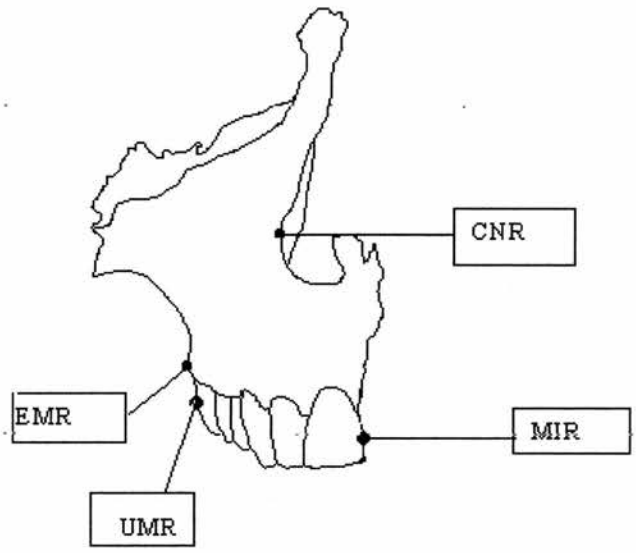

Measuring Points	Mean Differences measured on the P-A Cephs. $\Delta X = \bar{x}_{after} - \bar{x}_{before}$	Confidence Interval for the mean ($p < 0.005$) in mm
MIR-MIL	1.08	$0.49<\mu2-\mu1<1.66$
UMR-UML	8.89	$6.77<\mu2-\mu1<11$
EMR-EML	2.47	$0.43<\mu2-\mu1<4.5$
CNR-CNL	1.66	$0.3<\mu2-\mu1<3.01$

Table 8. Clinical measurements used for comparison with the results of the Finite Element Analysis.

3.5. Modelling improvements added to the initial Finite Element Model of the skull after pilot test:

In order to study all the biological phenomena that take place at the application of the method, a number of assumptions were made in the construction and the analysis of the finite element model developed in this study that may, in theory, lead to less precision in the results.

Weaknesses in the model included the lack of sophistication in modelling the anatomical structures and maxillary dentition; the lack of detailed knowledge regarding the material properties of the cancellous and cortical bone, the sutures and the structural parts of the Rapid Maxillary Expansion appliance; and the difficulty of knowing how to model the boundary conditions at the sutures. Other assumptions made during the Finite Element Analysis:

- In accordance with the approximations of earlier craniofacial Finite Element studies (Tanne *et al.,* 1988; 1989; 1991; 1995; Ruan *et al.,* 1994) we assumed linearly elastic and isotropic behavior for the full thickness of bone with an Elasticity modulus equal to 13700 Nt/mm^2;
- The maxilla is considered as a rigid body and consequently any bone bending while under force application is not considered;
- The entire sutural network behaves in an elastic manner, but different combinations of material properties creates individual participation in the behavior of the maxilla;
- The model was created using shell-plate elements for the bones of the skull and the sutures;
- The acrylic part of the Rapid Maxillary Expansion appliance was modelled with brick elements with Modulus of Elasticity equal to 2000 Nt/mm^2 (Verrue *et al.,* 2001);
- The metal part of the appliance was modelled using beam elements with Modulus of Elasticity equal to 206840 Nt / mm^2 as stainless steel (4130);
- The dentition was modelled with shell-plate elements with a Modulus of Elasticity equal to 20700 Nt/mm^2;

- The skull was packed at the cranial base along the foramen magnum (i.e. all degrees of freedom were constrained);
- The total mechanical load applied, resulted from the expansion caused by the displacement of the midline screw of the Rapid Maxillary Expansion appliance, is equal to 7.5mm.

The last assumption implies that separation of the maxillary halves is considered to be linear, the mechanical load of each turn of the screw is added algebraically to the preexistent load. In the clinical situation between each turn of the screw there is a relaxation period with consequent tissue rebound (Zimring and Isaacson; 1965), which is not taken under consideration in the initial calculations of the present study. Consequently, only displacements were initially calculated and not strain and stresses, because with the boundary condition of the 7,5mm opening of the Hyrax screw, the von Misses stresses developing in the craniofacial skeleton were much greater than the breaking point of the bone.

Therefore, after this pilot testing, some alterations were attempted to the existent Finite Element Model of the nasomaxillary complex in order to overcome some of the weaknesses of the initial study. And more specific, firstly, an attempt was made to study the tissue relaxation which exists in clinical situation. Secondly, the finite element mesh of the maxilla was changed and constructed with a combination of plate and brick elements (i.e. tetrahedral and hexahedral elements) so that the inner and outer cortical plates and the cancellous bone will be represented in the new model. The alveolar crest was also modelled. This reconstruction of the maxilla was critical in order to proceed with the third alteration of the model. The anchor teeth and their periodontal ligament were remodelled with more accurate anatomy, in order to study the tipping of these teeth within the periodontal space and the resultant bending of the alveolar crest, as the result of the heavy transverse force applied to the palatal side of these anchor teeth from the Hyrax screw of the appliance.

3.5.1. The simulation of tissue relaxation:

The computer software program used in the present study to perform the Finite Element Analysis (ALGOR) includes the meta-processor Superview which has the capability of saving the deformed model nullifying all tensions. The deformed model is renamed and saved from format.esd in a format.asd file. An attempt was made to apply the mechanical load gradually. On completion of each turn of the screw the new model created was saved with all anatomical changes caused by the expansion forces, and with all residual tensions nullified. However, only 14 turns of the screw were applied, because on the 15^{th} turn it was impossible to obtain a result. This is mainly due to two reasons. Firstly, the mathematical time required for calculating tensions and translations has increased from 10min for the first turn of the screw to 1 h 40min for the 14^{th} turn. Secondly, the structural elements were geometrically so greatly deformed, that in the 15^{th} turn was impossible to calculate the matrixes and consequently the displacements and tension distribution.

3.5.2. Anatomical modelling of the anchor teeth with the periodontal ligament:

In order to study the movement of the anchor teeth within the Periodontal Ligament, real models of a molar and a premolar tooth were used with the help of the "Coordinate Measurement Machine" (C.M.M.) to create the finite element mesh of these teeth (**Appendix 14**).

Each tooth was supported with the occlusal surface on a metal base, and silicone was used as the fixing medium. A selected point on the tooth surface was chosen as point 0 for the x,z,y coordinates and with the pin of the Coordinate Measurement Machine the whole tooth was scanned from the occlusal surface to the root apices (**Appendix 15**). The coordinates of all

points were introduced in a software program connected with the Coordinate Measurement Machine and were processed in a .dwg file and transferred to the pre-processor of the ALGOR computer software. The first image obtained is that of **Figure 12.**

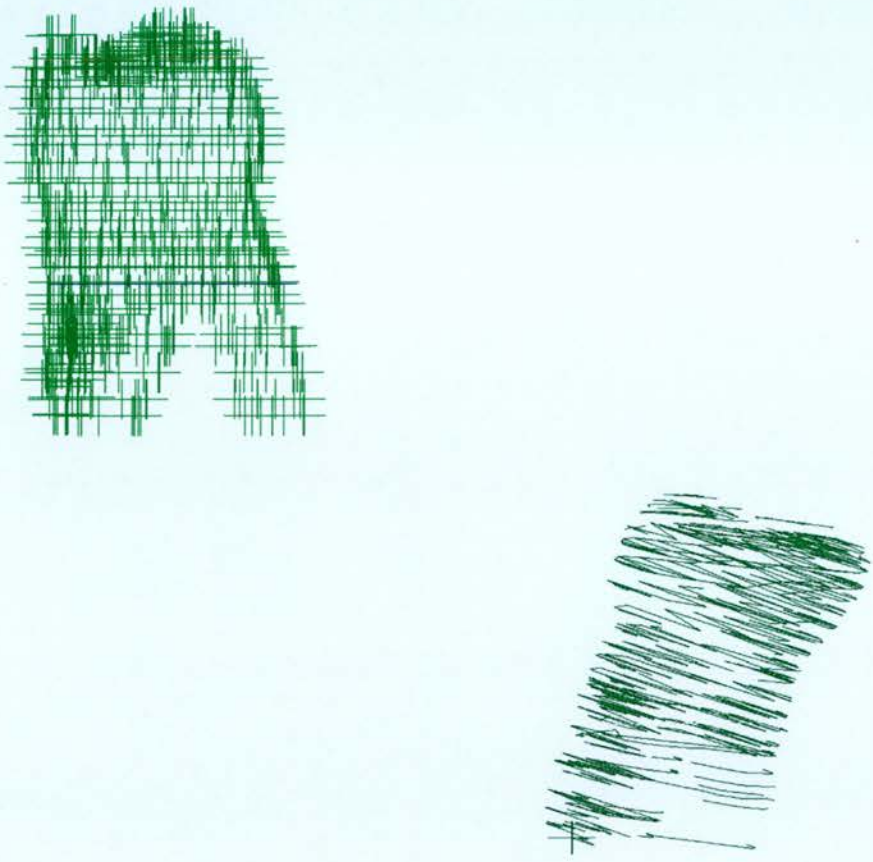

Fig. 12. Initial image of the first premolar and first molar maxillary teeth as resulted from the scanning by the Coordinate Measurement Machine.

This method presented a number of limitations:

- All points do not belong in the same vertical coordinate;
- The pin can define only points on the outer surface of the tooth which decreases the number of points available to accurately describe a horizontal section of the tooth;
- The occlusal surface couldn't be clearly defined because it was fixed with silicone on the metal base.

Therefore, with the help of the FORTRAN commercial computer software program, a restructure of all points was attempted respecting though the outer geometry of the tooth. Then, vertical coordinates were chosen with the following criteria:

a) To be defined by sufficient number of points;
b) The vertical coordinates of the teeth to coincide with the vertical coordinates of the maxilla when the tooth will be introduced into the FEM of the skull, or in other words the distance between them to be the same as in the FEM of the skull.

In order to obtain the model of the tooth, all points belonging to the same vertical coordinate were united with straight lines.

The Finite Element Model of the first maxillary premolar was created with brick elements and is presented in **Figure 13**. The next step was to create the Finite Element Model of the Periodontal Ligament of that tooth. Keeping the outer surface of the root of the tooth invariable and extending it by 0.25mm and with the use of brick elements; the finite element mesh of the Periodontal Ligament of the first maxillary premolar is created and presented in **Figure 13**

First Molar and its pdl

First Premolar and its pdl

Fig. 13. Three-dimensional finite element models of first premolar and first molar maxillary teeth including the periodontal ligaments artificially created.

The same method was followed in order to create the Finite Element Model of the distal anchor tooth of the Rapid Maxillary Expansion appliance with its Periodontal Ligament, the first maxillary molar. However, a customized software was prepared within the FORTRAN commercial software program which automatically united the points of each horizontal section (**Figures 12 - 13**).

3.5.3. Three dimensional reconstruction of the alveolar crest:

The next stage was to reconstruct the Finite Element Model of the alveolar crest occlusal to the palatal bone in order to make possible the insertion of the newly created models of the anchor teeth with their periodontal ligament. In that purpose, the initial Computer Tomograph scans were used to redraw with plate elements the outer and inner contour of the alveolar crest and maxilla (**Figure 14**).

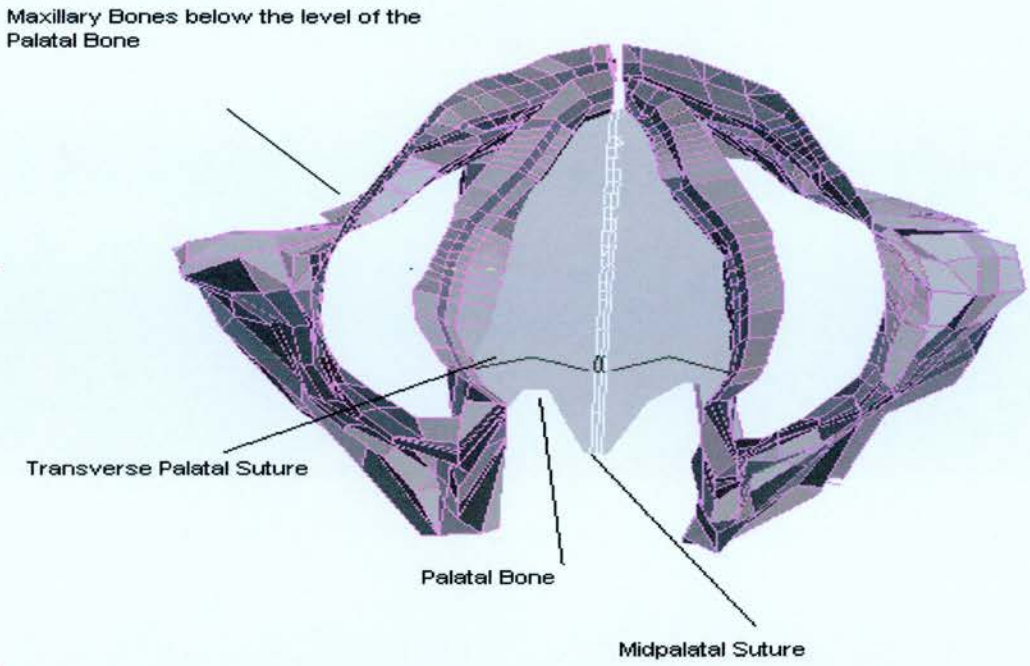

Fig. 14. The initial Finite Element Model of the alveolar crest.

Inside these new boundaries the models of the teeth with their periodontal ligament were inserted. The x, y and z coordinates of the teeth and Periodontal Ligament were adjusted to coincide with the coordinates of the Finite Element Model of the skull. The remaining space created between the Periodontal Ligament and the inner and outer contours of the alveolar crest, was reconstructed with brick elements. The plate elements simulated the cortical layer of the maxillary bones while the brick elements can be considered as the equivalent to the cancellous bone (**Figure 15 - 16**). Following the insertion of the anchor teeth, the Rapid Maxillary Expansion appliance was manually added (**Figure 17**).

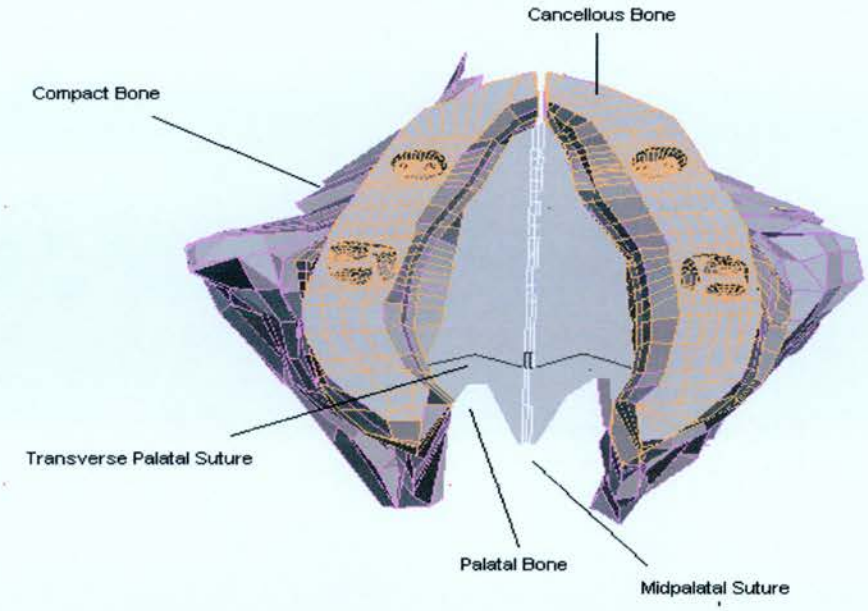

Fig. 15. The Finite Element Model of the reconstructed alveolar crest.

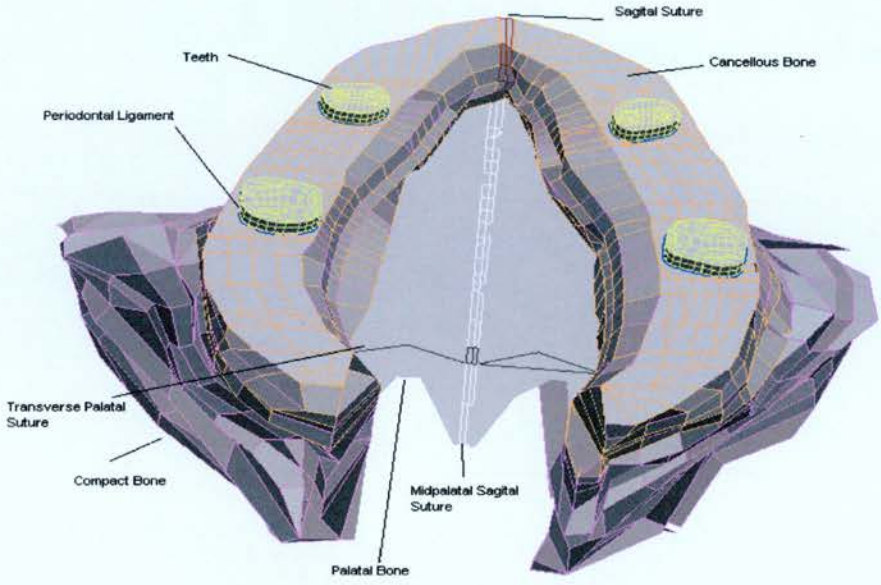

Fig. 16. The Finite Element Model of the reconstructed alveolar crest after the insertion of the anchor teeth with their corresponding periodontal ligament.

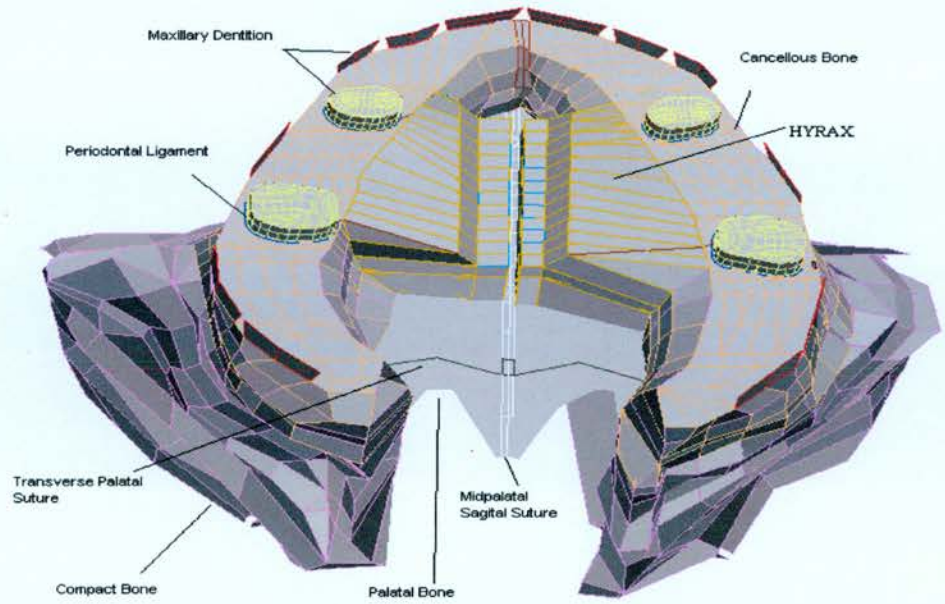

Fig. 17. The final Finite Element Model of the maxilla with the reconstructed three-dimensional alveolar crest, the anchor teeth, their periodontal ligament and the rapid maxillary expansion appliance in place.

Finally, the other bones of the skull were added and all cranial sutures were introduced in order to complete the geometry of the Finite Element Model of the skull. The improved Finite Element Model of the skull is composed of 10826 nodes and 14286 elements (**Figure 18**).

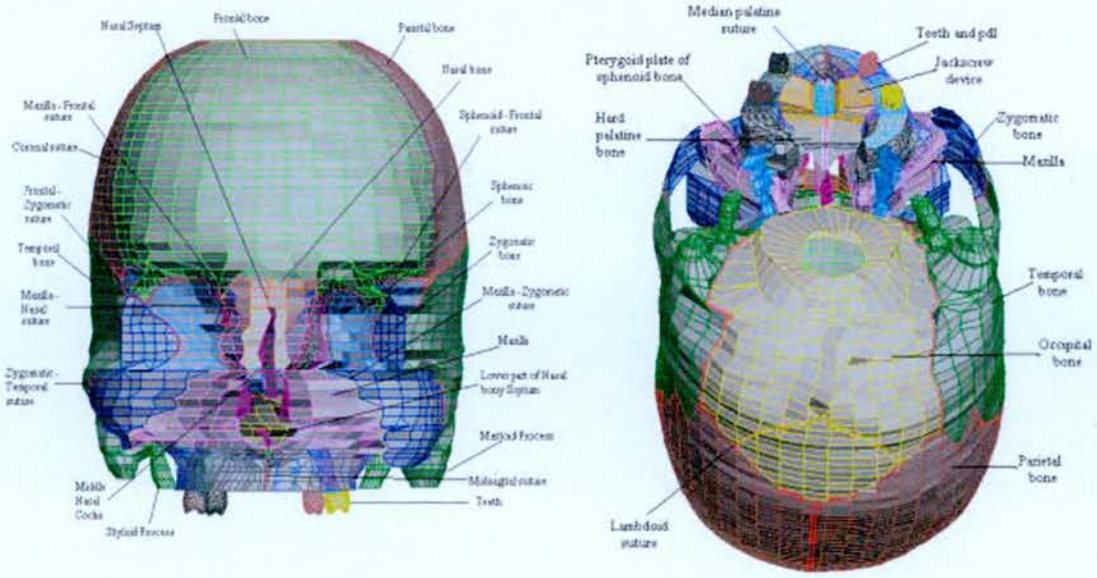

Fig. 18. The reconstructed three-dimensional Finite Element Model of the human skull including the sutures, the jackscrew device and the anchor teeth, which are banded to the jackscrew device, with their periodontal ligaments.

3.6. Experimental *(in vitro)* application of the Rapid Maxillary Expansion:

Quantitatively, the dry skull which undergoes rapid maxillary expansion does not behave in exactly the same way as *in vivo*, but it is possible to indicate the way the two maxillary halves separate during the application of the expansion force and how the effect of the force influences the other craniofacial structures. Therefore, it was considered necessary to apply the method of Rapid Maxillary Expansion on a dry skull in order to acquire more information on the distribution of the displacements, the order of suture separation, the areas of high stress, the linearity or not of the method. A description of the equipment and the method follows.

3.6.1. Measuring Equipment:

The same dry skull was supported on a custom made metal jig. Four holes were prepared in the occipital bone next to the articulation with the atlas and the skull was fixed with screws in a similar manner to that used in order to acquire the Computer Tomograph scans. The other end of the metal base was screwed to the table surface. The whole system was secured and the Rapid Maxillary Expansion appliance was cemented to the first permanent maxillary premolar and first permanent maxillary molar. These teeth were artificially constructed in the dental laboratory from heat cured acrylic after taking impression of the empty dental alveolus, in order to achieve a close fit of the root in the alveolus. The measuring devices used in the experiment are presented in **Appendix 16.**

In order to assess the changes observed at the dry skull after each turn of the screw of the Rapid Maxillary Expansion appliance, the same points were used as in the Postero-Anterior cephalometric and the Finite Element Analysis. Due to difficulties in definition of points EMR and EML, a metal marker was inserted bilaterally in the skull and its thickness was deducted from each measurement.

The experiment was also videotaped by a portable videocamera and a digital camera. The video images were saved in the PC in .avi format and for the processing of the video images the PCcard "Win TV 2000" was used **(Appendix 17).**

3.7. Objectives of the study:

1. To discuss the statement that *"when R.M.E. is undertaken, the anatomical structures of the nasomaxillary complex have no bearing on the force necessary to separate the midpalatal suture;"*

2. To discuss the statement that *"when R.M.E. is undertaken, the various maxillofacial sutures have no effect on the expansion of the maxillary segments;"*

3. To discuss the statement that *"when R.M.E. is undertaken, the amount of force needed to successfully complete the process is not dependant on the age of the patient and the level of ossification of the midline palatal suture."*

CHAPTER 4: RESULTS

4.1. First Approach (craniofacial.esd):

The skull was considered with 0 degrees of freedom at its base and expansion of 3.75mm was applied at each of the six (6) nodes of the Rapid Maxillary Expansion appliance **(craniofacial.esd)**. At the nodes of the Rapid Maxillary Expansion appliance we have movement only on the x-axis (the two halves of the appliance are moving away from each other). Material properties of the various components of the model are presented in **Table 10**.

The results of this initial application of the displacement at the level of the six (6) nodes of the rapid maxillary expansion appliance are presented in the following **Table 9** together with the clinical findings and the corresponding confidence interval.

Measuring Points	Differences measured by the FEA (mm)	Mean Differences measured on the P-A Cephs. $\Delta X = \bar{x}_{after} - \bar{x}_{before}$	Confidence Interval for the mean (P = 99.5%) in mm.
CNR - CNL	6.56	1.66	$0.3 < \mu_2 - \mu_1 < 3.01$
EMR - EML	6.55	2.47	$0.43 < \mu_2 - \mu_1 < 4.5$
UMR - UML	7.2	8.89	$6.77 < \mu_2 - \mu_1 < 11$
MIR - MIL	9.3	1.08	$0.49 < \mu_2 - \mu_1 < 1.66$

Table 9: Finite Element Analysis of **craniofacial.esd**

DESCRIPTION	COLOR - GROUP	THICKNESS (mm)	MODULUS OF ELASTICITY (Nt / mm^2)	POISSON's RATIO
Cranial Bones	1	5	13700	0.3
Teeth	2	5	20700	0.3
Acrylic	3	-	2000	0.3
RME (plate)	4	2.5	206840	0.3
RME (beam)	5	D = 2, t = 0.5	206840	0.3
Cartilage of Nasal Cavity	6	0.5	13700	0.3
Midpalatal Suture	7	3	1	0.3
Palatal Bone	8	3	13700	0.3
Zygomatic Bone	10	3	13700	0.3
Pterygoid Process of the Sphenoid Bone	11	2	13700	0.3
Maxillary Bone *	16	7	13700	0.3
Maxillary Bone **	17	9	13700	0.3
Nasal Bone	14	6	13700	0.3
Maxillo-zygomatic Suture	13	3	1	0.3
Naso-maxillary Suture	40	6	1	0.3
Temporo-maxillary Suture	100	5	1	0.3
Suture between the maxilla and the Lacrimal Bone	15	5	1	0.3
Suture between the maxilla and the pterygoid process of the sphenoid bone	80	2	1	0.3
Transverse palatal Suture	120	3	13700	0.3
Midsagital Suture	12	7	13700	0.3
* Maxillary Bone except of the alveolar crest.				
** Alveolar Crest of the maxillary bones.				

Table 10. Material properties assigned to the various components of the initial Finite Element Model of the craniofacial complex (**craniofacial.esd**)

It is clearly evident, that except the UMR-UML, all three other linear measurements were found greater than the clinical findings. Furthermore, they were even greater than the upper limit of the confidence interval for the clinical measurements, except as already mentioned, the measurement UMR-UML which was found smaller than the clinical situation and within the confidence interval. On the other hand, the qualitative behaviour of the model corresponded to the clinical findings. The maxilla expanded in a pyramidal manner with the base being at the level of the dentition and with the maximum opening at the level of the incisor teeth and decreasing posteriorly again in a pyramidal manner (**Figures 19 - 21**).

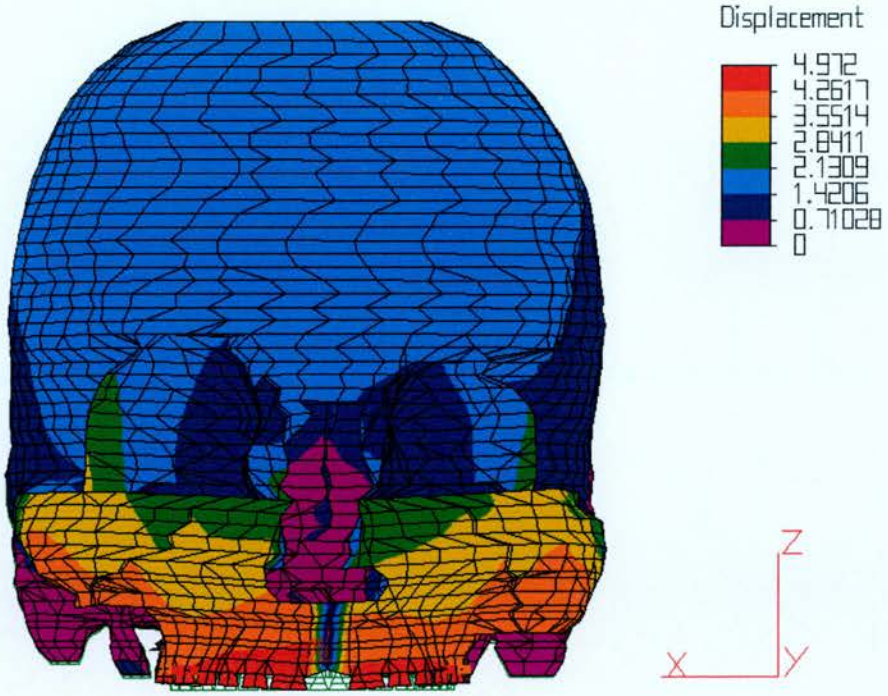

Fig. 19. Frontal view of the model (**craniofacial.esd**) after the initial application of the displacement at the level of the rapid maxillary expansion appliance.

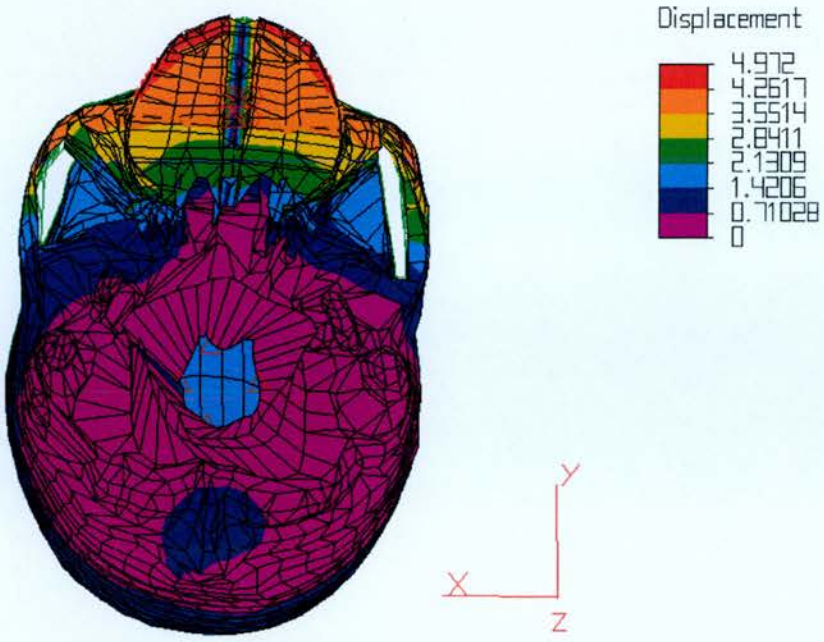

Fig. 20. Basal view of the model (**craniofacial.esd**) after the initial application of the displacement at the level of the rapid maxillary expansion appliance.

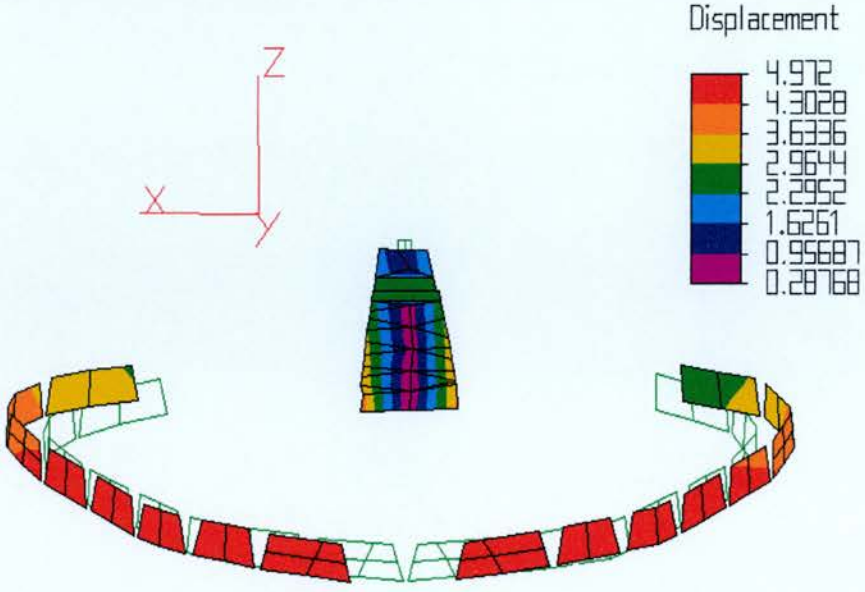

Fig. 21. Analytical view of the changes observed at the maxillary dentition and the midpalatal suture after the initial application of the displacement at the level of the rapid maxillary expansion appliance (**craniofacial.esd**).

4.2. The importance of the thickness of the bones and sutures (craniofacial 1.esd):

The thickness of the various bones of the skull and nasomaxillary complex was then measured in approximation with a Vernier Gauge and compared with the corresponding thickness of the same bones as measured electronically by the Finite Element software (**Table 12**). At the suture area it was given the smallest measured thickness of the adjacent bones. The material properties assigned to the various groups of this Finite Element Model of the dry skull are presented in **Table 13 (craniofacial 1.esd)**.

The skull was considered with 0 degrees of freedom at its base and expansion of 3.75mm was applied at each of the six (6) nodes of the Rapid Maxillary Expansion appliance. The results are presented in the following **Table 11** together with the clinical findings and the corresponding confidence interval.

Measuring Points	Differences measured by the FEA (mm)	Mean Differences measured on the P-A Cephs. $\Delta X = \bar{x}_{after} - \bar{x}_{before}$	Confidence Interval For the mean (P = 99.5%) in mm.
CNR - CNL	5.1	1.66	$0.3 < \mu_2 - \mu_1 < 3.01$
EMR - EML	5.53	2.47	$0.43 < \mu_2 - \mu_1 < 4.5$
UMR - UML	6.1	8.89	$6.77 < \mu_2 - \mu_1 < 11$
MIR - MIL	7.7	1.08	$0.49 < \mu_2 - \mu_1 < 1.66$

Table 11: Finite Element Analysis of **craniofacial 1.esd**

DESCRIPTION	THICKNESS (mm) (Computer measurements)	THICKNESS (mm) (Direct measurements)
Cranial Bones	5	14
Teeth	5	18.5
Cartilage of Nasal Cavity	0.5	0.5
Midpalatal Suture	3	3
Palatal Bone	3	3
Zygomatic Bone	3	10
Pterygoid Process of the Sphenoid Bone	2	6
Maxillary Bone *	7	8
Maxillary Bone **	9	19.5
Nasal Bone	6	8
Maxillo-zygomatic Suture	3	8
Naso-maxillary Suture	6	8
Temporo-maxillary Suture	5	8
Suture between the maxilla and the Lacrimal Bone	5	8
Suture between the maxilla and the pterygoid process of the sphenoid bone	2	6
Transverse palatal Suture	3	3
Midsagital Suture	7	8
* Maxillary bones superiorly to the alveolar crest and palatal bone		
** Maxillary bones at the level of the alveolar crest		

Table 12: Differences in thickness of the various anatomical structures as measured manually and automatically by the computer software

DESCRIPTION	COLOR – GROUP	THICKNESS (mm)	MODULUS OF ELASTICITY. (Nt / mm^2)	POISSON RATIO
Bones of the skull	1	14	13700	0.3
Teeth	2	18.5	20700	0.3
Acrylic	3	-	2000	0.3
RME (plate)	4	2.5	206840	0.3
RME (beam)	5	D = 2, t = 0.5	206840	0.3
Cartilage of the Nasal Cavity	6	0.5	13700	0.3
Midpalatal Suture	7	3	1	0.3
Palatal Bone	8	3	13700	0.3
Zygomatic Bone	10	10	13700	0.3
Pterygoid process of the Sphenoid Bone	11	6	13700	0.3
Maxillary Bones*.	16	8	13700	0.3
Maxillary Bones**	17	19.5	13700	0.3
Nasal Bones	14	8	13700	0.3
Maxillo-zygomatic Suture	13	8	1	0.3
Naso-maxillary Suture	40	8	1	0.3
Temporo-maxillary Suture	100	8	1	0.3
Suture between the maxilla and lacrimal bone	15	8	1	0.3
Suture between the maxilla and the pterygoid process of the sphenoid bone	80	6	1	0.3
Transverse palatal suture	120	3	13700	0.3
Sagital Suture	12	8	13700	0.3
* Maxillary bones except the alveolar crest.				
** Alveolar crest of the maxillary bone.				

Table 13. Material properties assigned to the various components of the Finite Element Model of the craniofacial complex (**craniofacial 1.esd**)

All four linear measurements were measured and found smaller by approximately 1mm each. Three of them (i.e. CNR-CNL; EMR-EML; MIR-MIL) were found closer to the uppermost limit of the confidence interval, whilst now, UMR-UML was found outside the lowermost limit of the confidence interval. The qualitative behaviour of the model corresponded to craniofacial.esd and the clinical findings (**Figures 22 - 23**). Consequently, the thickness of the various structures plays important role in the findings. Brings the results closer to the clinical findings, but however, they are still outside the confidence interval.

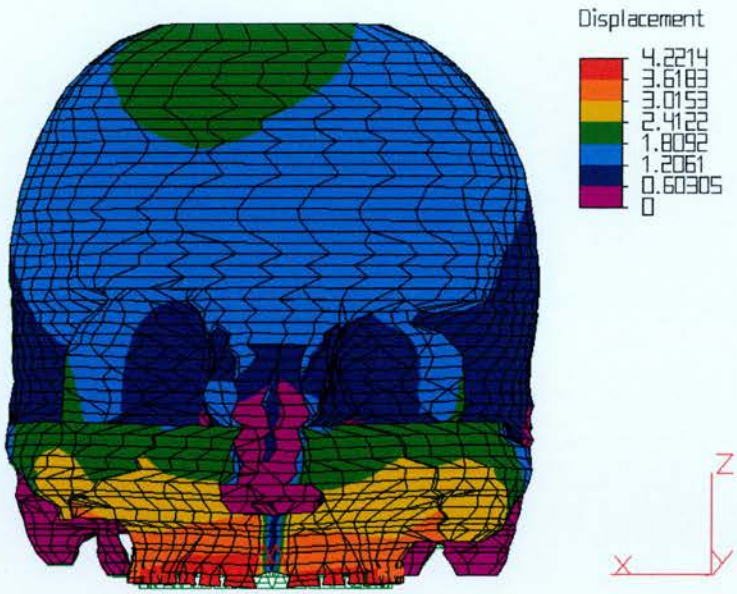

Fig. 22. Frontal view of the model (**craniofacial 1.esd**) with the displacements measured at the various structures of the skull.

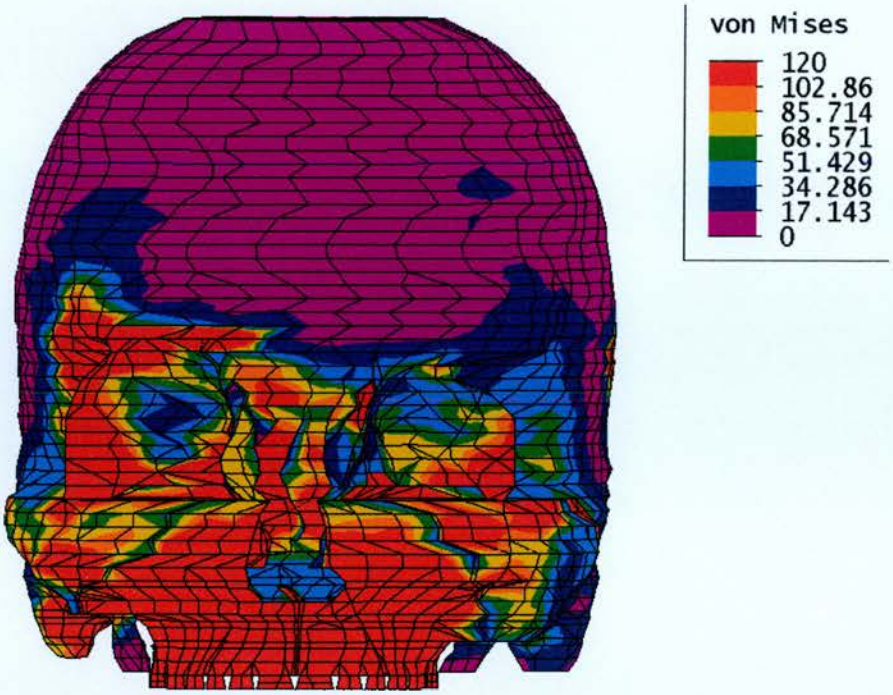

Fig. 23. Frontal view of the model (**craniofacial 1.esd**) with the von Mises stresses observed at the various structures of the skull.

4.3. The importance of the degree of ossification of the nasomaxillary sutures (craniofacial 2.esd – craniofacial 201.esd):

Another parameter that must be considered is the degree of ossification of the various circummaxillary sutures. It is still not clarified which sutures of the nasomaxillary complex remain open at the time of treatment and which are completely ossified or present varying degrees of ossification. In this section it was firstly assumed that all sutures are well ossified including the midpalatal and transverse palatal suture **(craniofacial 2.esd)**. Therefore the Modulus of Elasticity of the sutures equals that of the compact bone ($E = 13700$ Nt/mm^2).

The skull was considered with 0 degrees of freedom at its base and expansion of 3.75mm was applied at each of the six (6) nodes of the Rapid

Maxillary Expansion appliance. The results are presented in the following **Table 14** together with the clinical findings and the corresponding confidence interval.

Measuring Points	Differences measured by the FEA (mm)	Mean Differences measured on the P-A Cephs. $\Delta X = \bar{x}_{after} - \bar{x}_{before}$	Confidence Interval For the mean (P = 99.5%) in mm.
CNR - CNL	0.4	1.66	$0.3 < \mu_2 - \mu_1 < 3.01$
EMR - EML	2.1	2.47	$0.43 < \mu_2 - \mu_1 < 4.5$
UMR - UML	2.6	8.89	$6.77 < \mu_2 - \mu_1 < 11$
MIR - MIL	0.08	1.08	$0.49 < \mu_2 - \mu_1 < 1.66$

Table 14: Finite Element Analysis of **craniofacial 2.esd**

As it was expected, the displacements of the skeletal points were found significantly smaller, close to the lowermost limit of the confidence interval (i.e. CNR-CNL and EMR-EML). The expansion at the dental points (i.e. UMR-UML and MIR-MIL) was found far beyond the clinical findings (**Figure 24**).

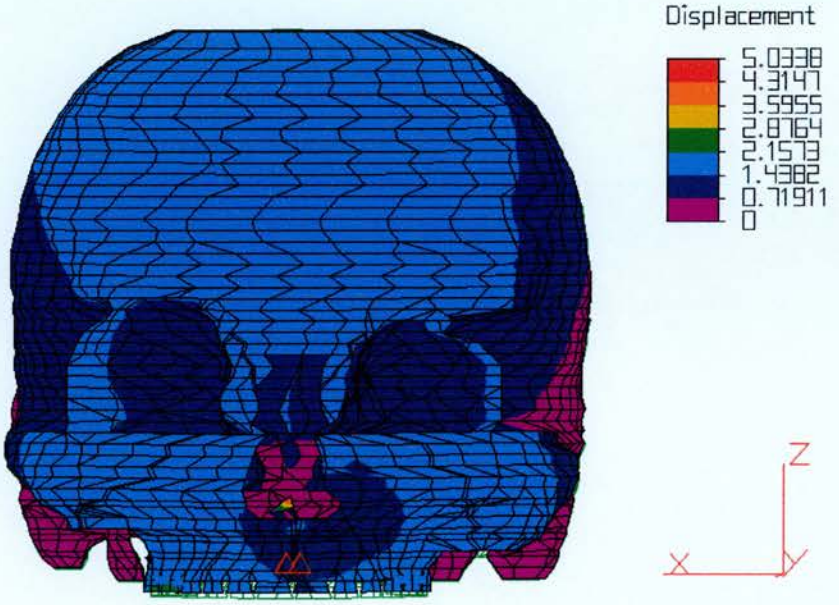

Fig. 24. Frontal view of the model (**craniofacial 2.esd**) with the displacements observed at the various structures of the dry skull when the circummaxillary sutures are considered totally ossified.

Then, it was assumed that the midpalatal and the transverse palatal sutures were totally unossified (i.e. open) whilst all other circummaxillary sutures were well ossified **(craniofacial 201.esd)**. Therefore, the Modulus of Elasticity of these two sutures was considered as $E = 1 Nt/mm^2$ while for all the other sutures equals that of the compact bone ($E = 13700\ Nt/mm^2$).

The skull was considered with 0 degrees of freedom at its base and expansion of 3.75mm was applied at each of the six (6) nodes of the Rapid Maxillary Expansion appliance. The results are presented in the following **Table 15** together with the clinical findings and the corresponding confidence interval.

Measuring Points	Differences measured by the FEA (mm)	Mean Differences measured on the P-A Cephs. $\Delta X = \bar{x}_{after} - \bar{x}_{before}$	Confidence Interval For the mean (P = 99.5%) in mm.
CNR - CNL	0.47	1.66	$0.3 < \mu_2 - \mu_1 < 3.01$
EMR - EML	2.8	2.47	$0.43 < \mu_2 - \mu_1 < 4.5$
UMR - UML	5.25	8.89	$6.77 < \mu_2 - \mu_1 < 11$
MIR - MIL	2.8	1.08	$0.49 < \mu_2 - \mu_1 < 1.66$

Table 15: Finite Element Analysis of **craniofacial 201.esd**

When the results in **Tables 14** and **15** were compared, it was clearly evident that the displacements of the skeletal points (i.e. CNR-CNL and EMR-EML) were not significantly different. However, the displacements of the dental points (i.e. UMR-UML and MIR–MIL) presented significant differences. The distance UMR–UML was doubled but again was smaller than the lowermost limit of the confidence interval, while the distance MIR-MIL was calculated 35 times greater and above the uppermost limit of the confidence interval (**Figures 25 - 26**).

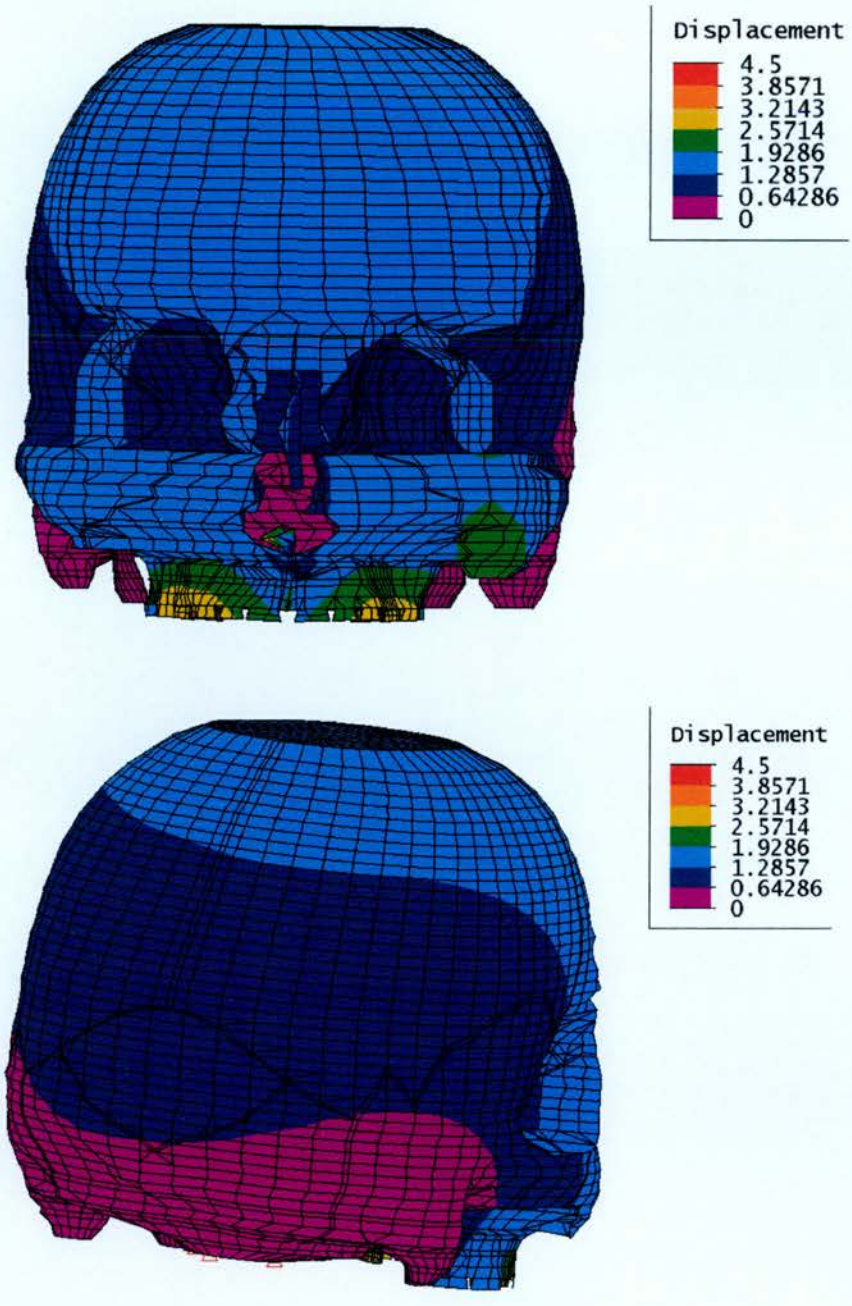

Fig. 25. Frontal and Posterior view of the model (**craniofacial 201.esd**) with the displacements observed at the various structures of the dry skull when the circummaxillary sutures are considered totally ossified except the midpalatal and transverse palatal sutures which are considered unossified.

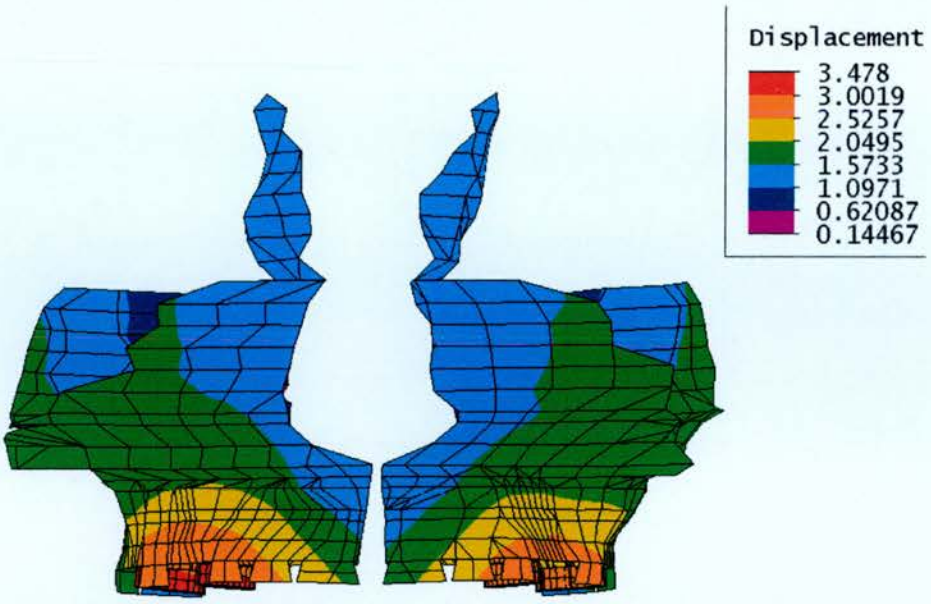

Fig. 26. Frontal view of the model of the maxilla (**craniofacial 201.esd**) with the displacements observed.

It can be suggested that the degree of ossification of the midpalatal and the transverse palatal sutures influences the outcome of the application of the expansion forces to the two maxillary halves. Consequently, and in order to better understand the biomechanics of the separation of the maxillary halves, a parametric analysis was required for assessing the role of the various nasomaxillary sutures and the other structures of the craniofacial complex.

On the other hand, it can be suggested that the sutures play an important role in absorption of the forces produced by the Rapid Maxillary Expansion. As it can be seen from the Finite Element Model of the skull (**Figure 27**), the tensions and stresses that develop during the application of the forces, decrease in a direct relationship to the distance, as they move away from the maxilla.

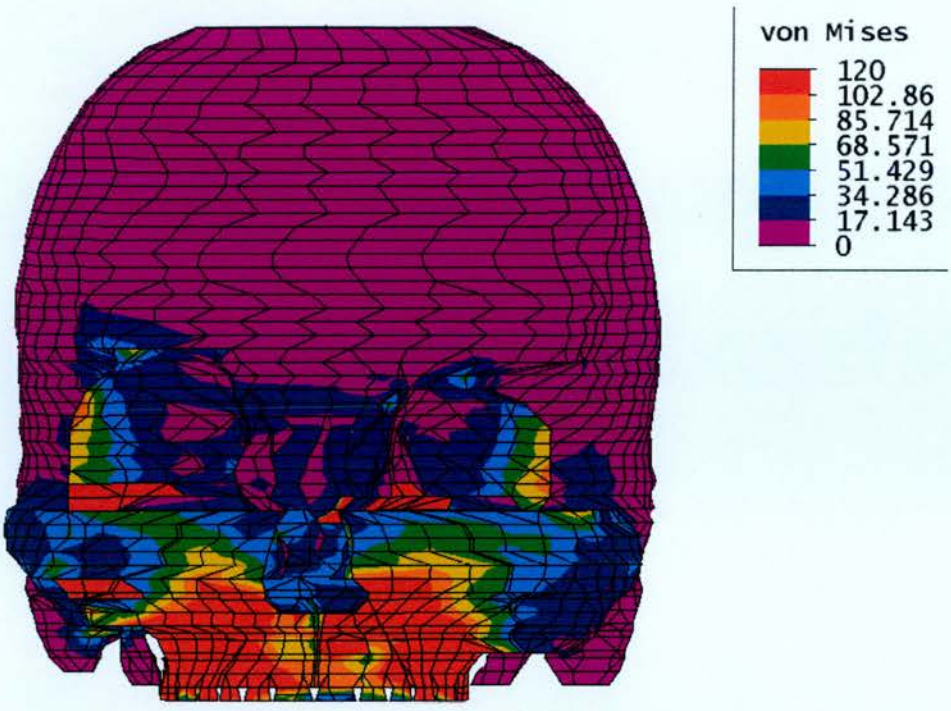

Fig. 27. Frontal view of the model (**craniofacial 2.esd**) with the von Mises stresses observed at the various structures of the dry skull when the craniofacial sutures are considered totally ossified.

4.4. The importance of the sagittal suture (craniofacial 3.esd - craniofacial 5.esd):

It was considered as sagittal suture, the frontal part of the midpalatal suture which lies between the central incisors; from the alveolar crest to the nasal cavity (**Figure 28**).

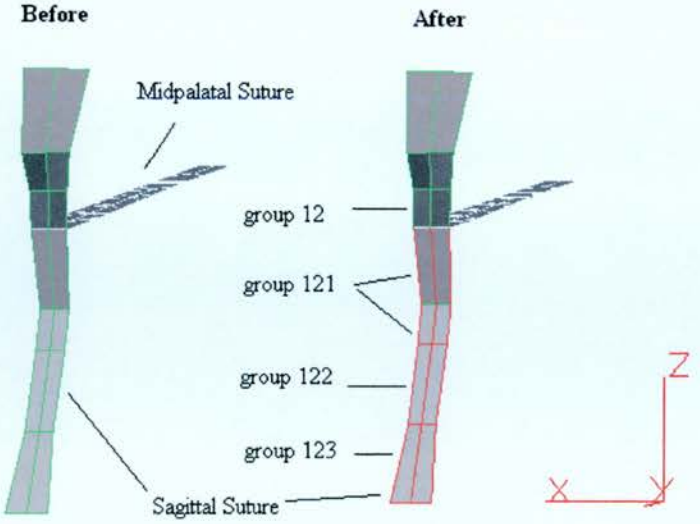

Fig. 28. The sagittal suture (**craniofacial 3.esd – craniofacial 5.esd**)

The separation of the dental points MIR-MIL may depend in part on the suture which separates the two halves of the maxilla at the frontal level and in part on the transeptal fibers. To appreciate the role of these structures in the separation of the frontal part of the maxilla during the Rapid Maxillary Expansion, the sagittal suture was subdivided at the level of the alveolar crest into three different groups with different material properties (i.e. groups 12; 121; 122). Group 123 will correspond to the transeptal fibers.

The skull was considered with 0 degrees of freedom at its base and expansion of 3.75mm was applied at each of the six (6) nodes of the Rapid Maxillary Expansion appliance. Considering all other circummaxillary sutures as totally unossified with E = 1 Nt/mm^2 and groups 12; 121; 122; 123 with **$E_{gr\ 12} = E_{gr\ 121} = E_{gr\ 122} = E_{gr\ 123}$ = 100 Nt/mm^2 (craniofacial 3.esd),** the results are presented in the following **Table 16** together with the clinical findings and the corresponding confidence interval.

Measuring Points	Differences measured by the FEA (mm)	Mean Differences measured on the P-A Cephs. $\Delta X = \bar{x}_{after} - \bar{x}_{before}$	Confidence Interval For the mean (P = 99.5%) in mm.
CNR - CNL	1.96	1.66	$0.3 < \mu_2 - \mu_1 < 3.01$
EMR - EML	4.6	2.47	$0.43 < \mu_2 - \mu_1 < 4.5$
UMR - UML	5.28	8.89	$6.77 < \mu_2 - \mu_1 < 11$
MIR - MIL	2.11	1.08	$0.49 < \mu_2 - \mu_1 < 1.66$

Table 16: Finite Element Analysis of **craniofacial 3.esd**

Considering all other circummaxillary sutures as open with E = 1 Nt/mm^2 and groups 12; 121; 122; 123; with $\mathbf{E_{gr\ 12} = E_{gr\ 121} = E_{gr\ 122} = E_{gr\ 123} = 1000\ Nt/mm^2}$ **(craniofacial 4.esd)** the results are presented in the following **Table 17** together with the clinical findings and the corresponding confidence interval.

Measuring Points	Differences measured by the FEA in mm.	Mean Differences measured on the P-A Cephs. $\Delta X = \bar{x}_{after} - \bar{x}_{before}$	Confidence Interval For the mean (P = 99.5%) in mm.
CNR - CNL	1.01	1.66	$0.3 < \mu_2 - \mu_1 < 3.01$
EMR - EML	4.22	2.47	$0.43 < \mu_2 - \mu_1 < 4.5$
UMR - UML	4.71	8.89	$6.77 < \mu_2 - \mu_1 < 11$
MIR - MIL	0.29	1.08	$0.49 < \mu_2 - \mu_1 < 1.66$

Table 17: Finite Element Analysis of **craniofacial 4.esd**

Considering all other circummaxillary sutures as open with E = 1 Nt/mm^2 and groups 12; 121; 122; 123; with $\mathbf{E_{gr\ 12} = E_{gr\ 121} = E_{gr\ 122} = E_{gr\ 123} = 13700\ Nt/mm^2}$ **(craniofacial 5.esd)** the results are presented in the following **Table 18** together with the clinical findings and the corresponding confidence interval.

Measuring Points	Differences measured by the FEA (mm)	Mean Differences measured on the P-A Cephs. $\Delta X = \bar{x}_{after} - \bar{x}_{before}$	Confidence Interval For the mean (P = 99.5%) in mm.
CNR - CNL	0.76	1.66	$0.3 < \mu_2 - \mu_1 < 3.01$
EMR - EML	4.03	2.47	$0.43 < \mu_2 - \mu_1 < 4.5$
UMR - UML	4.5	8.89	$6.77 < \mu_2 - \mu_1 < 11$
MIR - MIL	0.01	1.08	$0.49 < \mu_2 - \mu_1 < 1.66$

Table 18: Finite Element Analysis of **craniofacial 5.esd**

From the above findings it can be concluded that the sagittal suture plays an important role in the separation of the two maxillary halves. As sagittal suture ossifies, the separation of the points decreases.

When the modulus of elasticity of this suture becomes equal to that of the compact bone (E = 13700Nt/mm^2), the maxilla doesn't separate in a pyramidical manner. Therefore, for further study it was suggested that the suture at the time of Rapid Maxillary Expansion is unossified (E = 100 Nt/mm^2) and the separation of the central incisors depends on the material properties of the transeptal fibers.

4.5. The importance of the transeptal fibers (craniofacial 6.esd - craniofacial 9.esd).

To assess the role of the transeptal fibers, it was decided to keep the modulus of elasticity for the groups $E_{gr\ 12} = E_{gr\ 121} = E_{gr\ 122} = 100$ Nt/mm^2 (the sagittal suture was considered unossified; craniofacial 3.esd) and change the modulus of elasticity for the group 123 (this group corresponds in the Finite Element Model to the transeptal fibers) (**Figure 28**).

For **$E_{gr\ 123} = 100$ Nt/mm^2 (craniofacial 6.esd)** the results are presented in the following **Table 19** together with the clinical findings and the corresponding confidence interval.

Measuring Points	Differences measured by the FEA (mm)	Mean Differences measured on the P-A Cephs. $\Delta X = \bar{x}_{after} - \bar{x}_{before}$	Confidence Interval For the mean (P = 99.5%) in mm.
CNR - CNL	3.66	1.66	$0.3 < \mu_2 - \mu_1 < 3.01$
EMR - EML	4.9	2.47	$0.43 < \mu_2 - \mu_1 < 4.5$
UMR - UML	5.59	8.89	$6.77 < \mu_2 - \mu_1 < 11$
MIR - MIL	4.17	1.08	$0.49 < \mu_2 - \mu_1 < 1.66$

Table 19: Finite Element Analysis of **craniofacial 6.esd**

For $\mathbf{E_{gr\ 123} = 200\ Nt/mm^2}$ **(craniofacial 7.esd)** the results are presented in the following **Table 20** together with the clinical findings and the corresponding confidence interval.

Measuring Points	Differences measured by the FEA (mm)	Mean Differences measured on the P-A Cephs. $\Delta X = \bar{x}_{after} - \bar{x}_{before}$	Confidence Interval For the mean (P = 99.5%) in mm.
CNR - CNL	3.14	1.66	$0.3 < \mu_2 - \mu_1 < 3.01$
EMR - EML	4.84	2.47	$0.43 < \mu_2 - \mu_1 < 4.5$
UMR - UML	5.39	8.89	$6.77 < \mu_2 - \mu_1 < 11$
MIR - MIL	2.84	1.08	$0.49 < \mu_2 - \mu_1 < 1.66$

Table 20: Finite Element Analysis of **craniofacial 7.esd**

For $\mathbf{E_{gr\ 123} = 500\ Nt/mm^2}$ **(craniofacial 8.esd)** the results are presented in the following **Table 21** together with the clinical findings and the corresponding confidence interval.

Measuring Points	Differences measured by the FEA (mm)	Mean Differences measured on the P-A Cephs. $\Delta X = \bar{x}_{after} - \bar{x}_{before}$	Confidence Interval For the mean (P = 99.5%) in mm.
CNR - CNL	2.61	1.66	$0.3 < \mu_2 - \mu_1 < 3.01$
EMR - EML	4.62	2.47	$0.43 < \mu_2 - \mu_1 < 4.5$
UMR - UML	5.15	8.89	$6.77 < \mu_2 - \mu_1 < 11$
MIR - MIL	1.39	1.08	$0.49 < \mu_2 - \mu_1 < 1.66$

Table 21: Finite Element Analysis of **craniofacial 8.esd**

For $\mathbf{E_{gr\ 123} = 1000\ Nt/mm^2}$ **(craniofacial 9.esd)** the results are presented in the following **Table 22** together with the clinical findings and the corresponding confidence interval.

Measuring Points	Differences measured by the FEA (mm)	Mean Differences measured on the P-A Cephs. $\Delta X = \bar{x}_{after} - \bar{x}_{before}$	Confidence Interval For the mean (P = 99.5%) in mm.
CNR - CNL	2.38	1.66	$0.3 < \mu_2 - \mu_1 < 3.01$
EMR - EML	4.5	2.47	$0.43 < \mu_2 - \mu_1 < 4.5$
UMR - UML	5.01	8.89	$6.77 < \mu_2 - \mu_1 < 11$
MIR - MIL	0.6	1.08	$0.49 < \mu_2 - \mu_1 < 1.66$

Table 22: Finite Element Analysis of **craniofacial 9.esd**

As it can be seen from the above findings, the separation of MIR-MIL largly depends on the mechanical properties of the transeptal fibers. When $E_{gr\ 123}$ = 100 Nt/mm^2 the separation is 7.7mm, whereas, if $E_{gr\ 123}$ = 1000 Nt/mm^2 the separation is 0.6mm. However, the qualitative behavior of the Finite Element Model approximates that of the clinical findings for $E_{gr\ 123}$ = 500 Nt/mm^2 even though the measuring points UMR-UML and EMR-EML are outside the confidence interval. In conclusion, it can be suggested that this model better replicates the clinical situation.

The displacement of the points UMR-UML was smaller than clinical findings because the present Finite Element Model did not simulate the theoretical rotation/tipping of the molar teeth inside the periodontal ligament. This rotation will bend the alveolar crest inwards and move the EMR-EML within the confidence interval.

The displacement of the points EMR-EML may also be influenced by the separation of the sutures. In the following stages the influence of the various sutures will be investigated in turn.

4.6. The importance of the midpalatal suture (craniofacial 10.esd - craniofacial 12.esd):

From the research so far, it was concluded that the Finite Element Model of the dry skull simulates better the clinical situation if the Modulus of Elasticity of the transeptal fibers is $E_{gr\ 123} = 500\ Nt/mm^2$ and the sagittal suture is considered open (i.e. $E_{gr\ 12} = E_{gr\ 121} = E_{gr\ 122} = 100\ Nt/mm^2$) (craniofacial 8.esd). Parametric analysis will now be used to determine other factors that influence Rapid Maxillary Expansion.

Firstly, the role of the midpalatal suture will be studied. The skull was considered with 0 degrees of freedom at its base and expansion of 3.75mm was applied at each of the six (6) nodes of the Rapid Maxillary Expansion appliance. For the group that corresponds to the midpalatal suture, various values were given to the Modulus of Elasticity which represented varying degrees of ossification.

For $\mathbf{E_{gr\ 7} = 100\ Nt/mm^2}$ **(craniofacial 10.esd)** the results are presented in the following **Table 23** together with the clinical findings and the corresponding confidence interval.

Measuring Points	Differences measured by the FEA (mm)	Mean Differences measured on the P-A Cephs. $\Delta X = \bar{x}_{after} - \bar{x}_{before}$	Confidence Interval For the mean (P = 99.5%) in mm.
CNR - CNL	2.1	1.66	$0.3 < \mu_2 - \mu_1 < 3.01$
EMR - EML	4.03	2.47	$0.43 < \mu_2 - \mu_1 < 4.5$
UMR - UML	4.57	8.89	$6.77 < \mu_2 - \mu_1 < 11$
MIR - MIL	1.24	1.08	$0.49 < \mu_2 - \mu_1 < 1.66$

Table 23: Finite Element Analysis of **craniofacial 10.esd**

For $\mathbf{E_{gr\,7} = 1000\ Nt/mm^2}$ **(craniofacial 11.esd)** the results are presented in the following **Table 24** together with the clinical findings and the corresponding confidence interval.

Measuring Points	Differences measured by the FEA (mm)	Mean Differences measured on the P-A Cephs. $\Delta X = \bar{x}_{after} - \bar{x}_{before}$	Confidence Interval For the mean (P = 99.5%) in mm.
CNR - CNL	0.9	1.66	$0.3 < \mu_2 - \mu_1 < 3.01$
EMR - EML	3.03	2.47	$0.43 < \mu_2 - \mu_1 < 4.5$
UMR - UML	3.57	8.89	$6.77 < \mu_2 - \mu_1 < 11$
MIR - MIL	0.83	1.08	$0.49 < \mu_2 - \mu_1 < 1.66$

Table 24: Finite Element Analysis of **craniofacial 11.esd**

For $\mathbf{E_{gr\,7} = 13700\ Nt/mm^2}$ **(craniofacial 12.esd)** the results are presented in the following **Table 25** together with the clinical findings and the corresponding confidence interval.

Measuring Points	Differences measured by the FEA (mm)	Mean Differences measured on the P-A Cephs. $\Delta X = \bar{x}_{after} - \bar{x}_{before}$	Confidence Interval For the mean (P = 99.5%) in mm.
CNR - CNL	0.31	1.66	$0.3 < \mu_2 - \mu_1 < 3.01$
EMR - EML	2.62	2.47	$0.43 < \mu_2 - \mu_1 < 4.5$
UMR - UML	3.17	8.89	$6.77 < \mu_2 - \mu_1 < 11$
MIR - MIL	0.6	1.08	$0.49 < \mu_2 - \mu_1 < 1.66$

Table 25: Finite Element Analysis of **craniofacial 12.esd**

In all three models, the displacements were within the confidence intervals except of the UMR-UML. As the modulus of elasticity increases (i.e. the suture is considered ossified), the two maxillary halves separate with greater difficulty and in a non-pyramidical manner. In a similar manner the UMR-UML move away from the confidence interval. Therefore, it was concluded that the model which behaves similarly to the clinical situation is the model

which was investigated with the midpalatal suture assumed to be open (i.e. $E_{gr\,7} = 100\ Nt / mm^2$).

4.7. The importance of the transverse palatal suture (craniofacial 13.esd - craniofacial 15.esd):

Next, the role of the transverse palatal suture will be studied. From the research so far, it was concluded that the Finite Element Model of the dry skull which simulates better the clinical situation is **craniofacial 10.esd**. The skull was considered with 0 degrees of freedom at its base and expansion of 3.75mm was applied at each of the six (6) nodes of the Rapid Maxillary Expansion appliance. For the group that corresponds to the transverse palatal suture, various values were given to the Modulus of Elasticity which represented varying degrees of ossification.

For $\mathbf{E_{gr120} = 100\ Nt/mm^2}$ **(craniofacial 13.esd)** the results are presented in the following **Table 26** together with the clinical findings and the corresponding confidence interval.

Measuring Points	Differences measured by the FEA (mm)	Mean Differences measured on the P-A Cephs. $\Delta X = \bar{x}_{after} - \bar{x}_{before}$	Confidence Interval For the mean (P = 99.5%) in mm.
CNR-CNL	2.61	1.66	$0.3 < \mu_2 - \mu_1 < 3.01$
EMR-EML	4.58	2.47	$0.43 < \mu_2 - \mu_1 < 4.5$
UMR-UML	5.11	8.89	$6.77 < \mu_2 - \mu_1 < 11$
MIR-MIL	1.4	1.08	$0.49 < \mu_2 - \mu_1 < 1.66$

Table 26: Finite Element Analysis of **craniofacial 13.esd**

For $\mathbf{E_{gr\,7} = 1000\ Nt/mm^2}$ **(craniofacial 14.esd)** the results are presented in the following **Table 27** together with the clinical findings and the corresponding confidence interval.

Measuring Points	Differences measured by the FEA (mm)	Mean Differences measured on the P-A Cephs. $\Delta X = \bar{x}_{after} - \bar{x}_{before}$	Confidence Interval For the mean (P = 99.5%) in mm.
CNR-CNL	2.61	1.66	$0.3 < \mu_2 - \mu_1 < 3.01$
EMR-EML	4.35	2.47	$0.43 < \mu_2 - \mu_1 < 4.5$
UMR-UML	4.88	8.89	$6.77 < \mu_2 - \mu_1 < 11$
MIR-MIL	1.4	1.08	$0.49 < \mu_2 - \mu_1 < 1.66$

Table 27: Finite Element Analysis of **craniofacial 14.esd**

For $\mathbf{E_{gr\,7} = 13700\ Nt/mm^2}$ **(craniofacial 15.esd)** the results are presented in the following **Table 28** together with the clinical findings and the corresponding confidence interval.

Measuring Points	Differences measured by the FEA (mm)	Mean Differences measured on the P-A Cephs. $\Delta X = \bar{x}_{after} - \bar{x}_{before}$	Confidence Interval For the mean (P = 99.5%) in mm.
CNR-CNL	2.61	1.66	$0.3 < \mu_2 - \mu_1 < 3.01$
EMR-EML	3.82	2.47	$0.43 < \mu_2 - \mu_1 < 4.5$
UMR-UML	4.36	8.89	$6.77 < \mu_2 - \mu_1 < 11$
MIR-MIL	1.4	1.08	$0.49 < \mu_2 - \mu_1 < 1.66$

Table 28: Finite Element Analysis of **craniofacial 15.esd**

The transverse palatal suture appeared to influence the displacements of the points UMR-UML and EMR-EML as well as the way in which the midpalatal suture separates. When the modulus of elasticity for the transverse palatal suture increases, the midpalatal suture does not separate in a pyramidical manner. When $E_{gr\,120} = 13700\ Nt/mm^2$ the separation of the midpalatal suture is almost parallel (**Figure 29**). The displacements of the points CNR-CNL and MIR-MIL remain at the same level, whereas, the measuring points UMR-UML move away from the confidence interval. In conclusion, it was considered that the model with $E_{gr\,120} = 100\ Nt / mm^2$ (craniofacial 13.esd) behaves in a similar way to the clinical findings.

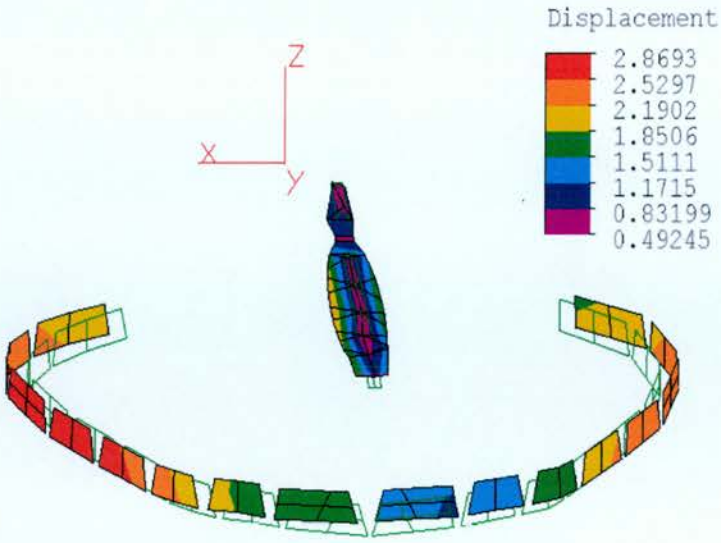

Fig. 29. Opening of the midpalatal suture (**craniofacial 15.esd**)

4.8. The importance of the suture between the maxilla and the lacrymal bone (craniofacial 16.esd - craniofacial 18.esd):

With the same method the effect of that suture on the separation of the two maxillary halves during Rapid Maxillary Expansion was investigated. From the research so far, it was concluded that the Finite Element Model of the dry skull which simulates better the clinical situation is **craniofacial 13.esd**. The skull was considered with 0 degrees of freedom at its base and expansion of 3.75mm was applied at each of the six (6) nodes of the Rapid Maxillary Expansion appliance.

The group that corresponds to the suture between the maxilla and the lacrymal bone it was tested with different modulus of elasticity (i.e. $E_{gr\ 15}$ = 100 Nt / mm^2 (craniofacial 16.esd); $E_{gr\ 15}$ = 1000 Nt / mm^2 (craniofacial 17.esd); and $E_{gr\ 15}$ = 13700 Nt / mm^2 (craniofacial 18.esd). With all three values there were very similar results, and it was concluded that this suture does not influence the behavior of the maxilla (**Table 29**).

Measuring Points	Differences measured by the FEA (mm)	Mean Differences measured on the P-A Cephs. $\Delta X = \bar{x}_{after} - \bar{x}_{before}$	Confidence Interval For the mean (P = 99.5%) in mm.
CNR-CNL	2.61	1.66	$0.3 < \mu_2 - \mu_1 < 3.01$
EMR-EML	4.62	2.47	$0.43 < \mu_2 - \mu_1 < 4.5$
UMR-UML	5.15	8.89	$6.77 < \mu_2 - \mu_1 < 11$
MIR-MIL	1.39	1.08	$0.49 < \mu_2 - \mu_1 < 1.66$

Table 29: Finite Element Analysis of **craniofacial 16.esd – craniofacial 18.esd**

4.9. The importance of the frontomaxillary suture (craniofacial 19.esd - craniofacial 21.esd):

From the research so far, it can be concluded that the Finite Element Model of the dry skull which simulates better the clinical situation is **craniofacial 13.esd**. The skull was considered with 0 degrees of freedom at its base and expansion of 3.75mm was applied at each of the six (6) nodes of the Rapid Maxillary Expansion appliance.

The group that corresponds to the frontomaxillary suture it was tested with different modulus of elasticity. For $E_{gr\ 100} = 100$ Nt / mm^2 (craniofacial 19.esd); $E_{gr\ 100} = 1000$ Nt / mm^2 (craniofacial 20.esd) and $E_{gr\ 100} = 13700$ Nt / mm^2 (craniofacial 21.esd) this suture does not seem to influence the separation of the maxilla during Rapid Maxillary Expansion (**Table 30**).

Measuring Points	Differences measured by the FEA (mm)	Mean Differences measured on the P-A Cephs. $\Delta X = \bar{x}_{after} - \bar{x}_{before}$	Confidence Interval For the mean (P = 99.5%) in mm.
CNR-CNL	2.61	1.66	$0.3 < \mu_2 - \mu_1 < 3.01$
EMR-EML	4.62	2.47	$0.43 < \mu_2 - \mu_1 < 4.5$
UMR-UML	5.15	8.89	$6.77 < \mu_2 - \mu_1 < 11$
MIR-MIL	1.39	1.08	$0.49 < \mu_2 - \mu_1 < 1.66$

Table 30: Finite Element Analysis of **craniofacial 19.esd – craniofacial 21.esd**

4.10. The importance of the nasomaxillary suture (craniofacial 22.esd - craniofacial 24.esd):

From the research so far, it can be concluded that the Finite Element Model of the dry skull which simulates better the clinical situation is **craniofacial 13.esd**. The skull was considered with 0 degrees of freedom at its base and expansion of 3.75mm was applied at each of the six (6) nodes of the Rapid Maxillary Expansion appliance.

The group that corresponds to the nasomaxillary suture it was tested with different modulus of elasticity. For $E_{gr\,40} = 100\ Nt/mm^2$ (craniofacial 22.esd); $E_{gr\,40} = 1000\ Nt/mm^2$ (craniofacial 23.esd) and $E_{gr\,40} = 13700\ Nt/mm^2$ (craniofacial 24.esd), as expected this suture appears to influence only the displacement of the points CNR-CNL, all other measuring points remaining unaffected (**Table 31**).

Measuring Points	Differences measured by the FEA (mm)	Mean Differences measured on the P-A Cephs. $\Delta X = \bar{x}_{after} - \bar{x}_{before}$	Confidence Interval For the mean (P = 99.5%) in mm.
CNR-CNL	2.5	1.66	$0.3 < \mu_2 - \mu_1 < 3.01$
EMR-EML	4.62	2.47	$0.43 < \mu_2 - \mu_1 < 4.5$
UMR-UML	5.15	8.89	$6.77 < \mu_2 - \mu_1 < 11$
MIR-MIL	1.39	1.08	$0.49 < \mu_2 - \mu_1 < 1.66$

Table 31: Finite Element Analysis of **craniofacial 22.esd – craniofacial 24.esd**

4.11. The importance of the suture between the pterygoid process of the sphenoid bone and the maxilla (craniofacial 25.esd - craniofacial 27.esd):

From the research so far, it was concluded that the Finite Element Model of the dry skull which simulates better the clinical situation is **craniofacial 13.esd**. The skull was considered with 0 degrees of freedom at its base and expansion of 3.75mm was applied at each of the six (6) nodes of the Rapid Maxillary Expansion appliance.

The group that corresponds to the suture between the pterygoid process of the sphenoid bone and the maxilla it was tested with different modulus of elasticity. For $E_{gr\ 80}$ = 100 Nt/mm^2 (craniofacial 25.esd); $E_{gr\ 80}$ = 1000 Nt/mm^2 (craniofacial 26.esd) and $E_{gr\ 80}$ = 13700 Nt/mm^2 (craniofacial 27.esd), this suture does not influence the behavior of the maxilla during Rapid Maxillary Expansion (**Table 32**).

Measuring Points	Differences measured by the FEA (mm)	Mean Differences measured on the P-A Cephs. $\Delta X = \bar{x}_{after} - \bar{x}_{before}$	Confidence Interval For the mean (P = 99.5%) in mm.
CNR-CNL	2.62	1.66	$0.3 < \mu_2 - \mu_1 < 3.01$
EMR-EML	4.59	2.47	$0.43 < \mu_2 - \mu_1 < 4.5$
UMR-UML	5.13	8.89	$6.77 < \mu_2 - \mu_1 < 11$
MIR-MIL	1.40	1.08	$0.49 < \mu_2 - \mu_1 < 1.66$

Table 32: Finite Element Analysis of **craniofacial 25.esd – craniofacial 27.esd**

From the above results, it can be suggested that the sutures between the maxilla and the lacrimal; frontal and pterygoid process of the sphenoid bone do not influence the qualitative behavior of the FEM and do not influence the displacements of the measuring points. Their importance is limited to the absorption of the forces created and transmitted by the Hyrax screw to the structures of the skull.

4.12. The importance of the maxillozygomatic suture (craniofacial 28.esd - craniofacial 30.esd):

In order to study the influence of the maxillozygomatic suture on the separation of the two maxillary halves during Rapid Maxillary Expansion it was assumed that all other sutures are unossified (i.e. $E = 100\ Nt/mm^2$). The Finite Element Model of the dry skull which simulates better the clinical situation is **craniofacial 13.esd**. The skull was considered with 0 degrees of freedom at its base and expansion of 3.75mm was applied at each of the six (6) nodes of the Rapid Maxillary Expansion appliance.

For $E_{gr13} = 100\ Nt/mm^2$ (craniofacial 28.esd) the results are presented in the following **Table 33** together with the clinical findings and the corresponding confidence interval.

Measuring Points	Differences measured by the FEA (mm)	Mean Differences measured on the P-A Cephs. $\Delta X = \bar{x}_{after} - \bar{x}_{before}$	Confidence Interval For the mean (P = 99.5%) in mm.
CNR-CNL	2.75	1.66	$0.3 < \mu_2 - \mu_1 < 3.01$
EMR-EML	4.46	2.47	$0.43 < \mu_2 - \mu_1 < 4.5$
UMR-UML	4.95	8.89	$6.77 < \mu_2 - \mu_1 < 11$
MIR-MIL	1.37	1.08	$0.49 < \mu_2 - \mu_1 < 1.66$

Table 33: Finite Element Analysis of **craniofacial 28.esd**

For $E_{gr13} = 1000\ Nt/mm^2$ (craniofacial 29.esd) the results are presented in the following **Table 34** together with the clinical findings and the corresponding confidence interval.

Measuring Points	Differences measured by the FEA (mm)	Mean Differences measured on the P-A Cephs. $\Delta X = \bar{x}_{after} - \bar{x}_{before}$	Confidence Interval For the mean (P = 99.5%) in mm.
CNR-CNL	2.75	1.66	$0.3 < \mu_2 - \mu_1 < 3.01$
EMR-EML	4.29	2.47	$0.43 < \mu_2 - \mu_1 < 4.5$
UMR-UML	4.8	8.89	$6.77 < \mu_2 - \mu_1 < 11$
MIR-MIL	1.36	1.08	$0.49 < \mu_2 - \mu_1 < 1.66$

Table 34: Finite Element Analysis of **craniofacial 29.esd**

For $E_{gr13} = 13700$ Nt/mm^2 (craniofacial 30.esd) the results are presented in the following **Table 35** together with the clinical findings and the corresponding confidence interval.

Measuring Points	Differences measured by the FEA (mm)	Mean Differences measured on the P-A Cephs. $\Delta X = \bar{x}_{after} - \bar{x}_{before}$	Confidence Interval For the mean (P = 99.5%) in mm.
CNR-CNL	2.75	1.66	$0.3 < \mu_2 - \mu_1 < 3.01$
EMR-EML	4.28	2.47	$0.43 < \mu_2 - \mu_1 < 4.5$
UMR-UML	4.76	8.89	$6.77 < \mu_2 - \mu_1 < 11$
MIR-MIL	1.36	1.08	$0.49 < \mu_2 - \mu_1 < 1.66$

Table 35: Finite Element Analysis of **craniofacial 30.esd**

From the above results, it can be suggested that the maxillozygomatic suture provides the greatest resistance to the separation of the maxillary halves during Rapid Maxillary Expansion. The Finite Element Analysis results which simulate better the clinical findings are those for $E_{gr\,13} = 13700$ Nt/mm^2 (i.e. the suture is considered ossified; **craniofacial 30.esd**) **(Figures 30 – 32)**.

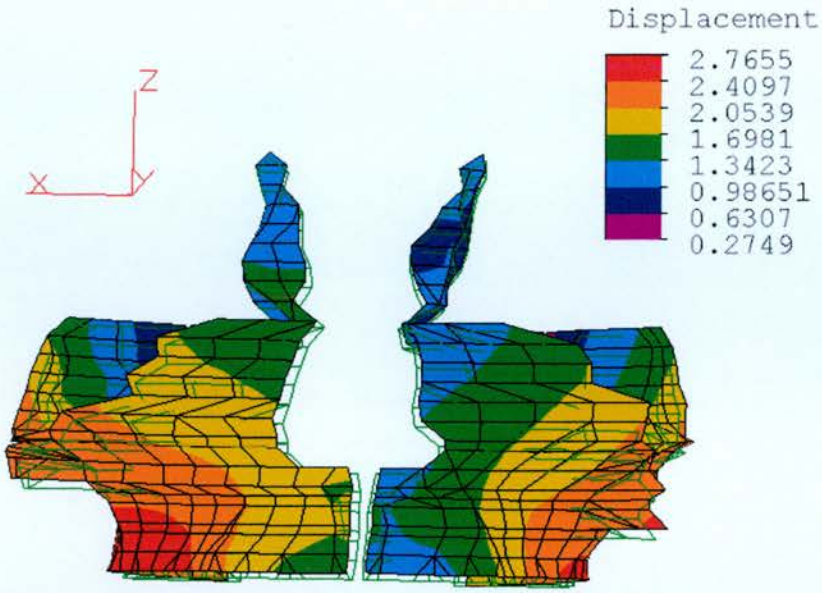

Fig. 30. Displacements calculated on the Finite Element Model of the maxilla (frontal view) (**craniofacial 30.esd**)

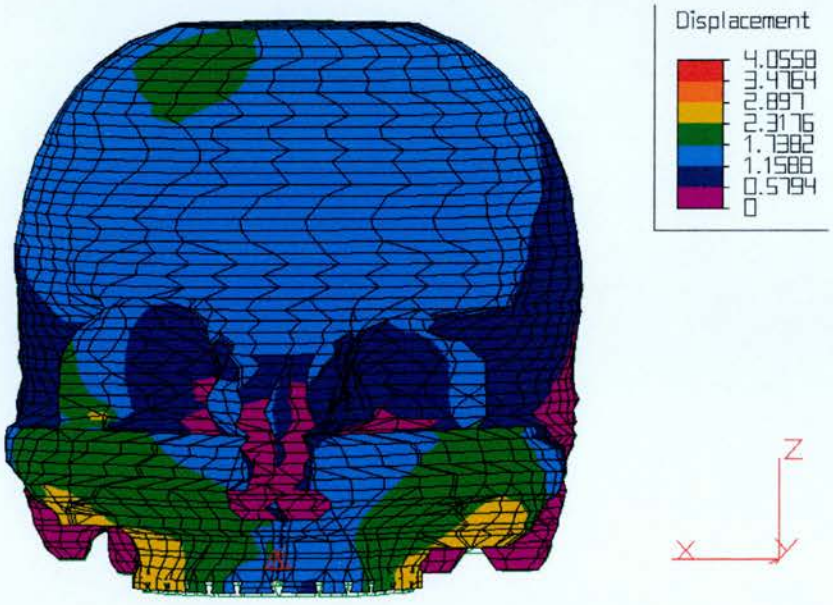

Fig. 31. Displacements calculated on the Finite Element Model of the skull (**craniofacial 30.esd**) (frontal view).

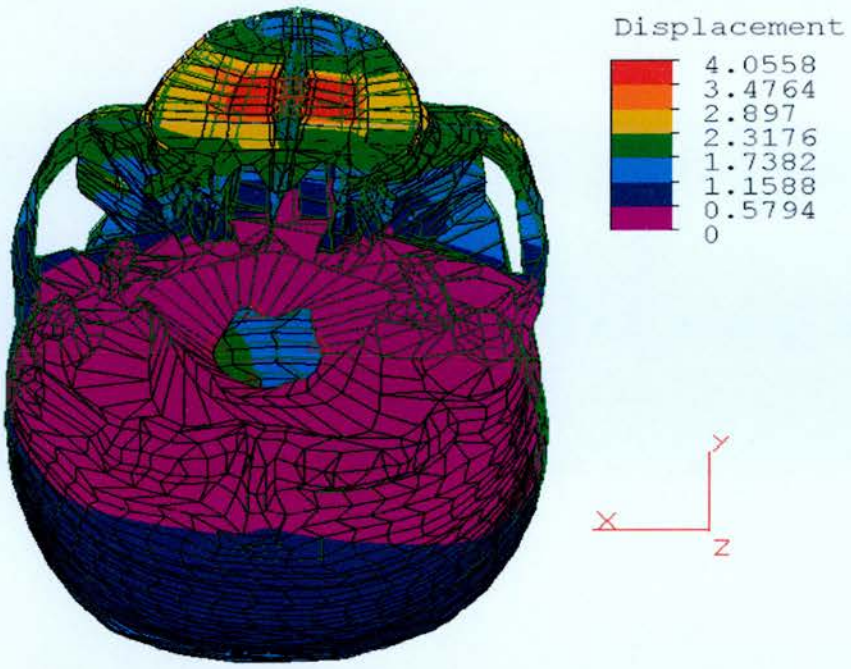

Fig. 32. Displacements calculated on the Finite Element Model of the skull (**craniofacial 30.esd**) (basal view).

4.13. The tissue rebound phenomenon (craniofacial 31.esd - craniofacial 44.esd):

After the first pilot runs, the parametric analysis of the Finite Element Model of the dry skull indicated that in order for the mathematical findings to be within the confidence interval of the clinical findings the transverse palatal suture, the midpalatal and the sagittal sutures must be patent, the maxillozygomatic suture should be ossified, and the interseptal fibers between the two central incisors must have a Modulus of Elasticity equal to 500 Nt / mm^2. In addition, the thickness of the various anatomical structures must be assigned with the real clinical values.

In the initial calculations of the present Finite Element Analysis, the separation of the maxillary halves is considered to be linear. The mechanical load of each turn of the screw is added algebraically to the preexistent load omitting the relaxation period with consequent tissue rebound which exists in the clinical situation between each turn of the screw.

Clinically, stress relaxation is characterized as a sharp elevation in tissue resistance force during the period of mechanical loading followed by a decay of this force until the next increment of activation. An attempt was made to add into the Finite Element Analysis the parameter of the relaxation period. Initially, the mechanical load was gradually applied. On completion of each turn of the screw a new model was created with all the anatomical changes caused by the expansion forces, and on which all the residual tension was nullified.

Using this method, only 14 turns of the screw were applied, because on the 15^{th} turn it was impossible to obtain a result due to the mathematical time required for calculating tensions and translations (i.e. for the first turn of the screw was 10min and for the 14^{th} turn was 1 h 40min) and due to the distortion suffered by the Finite Element Model. The results are presented in

the following tables (the model used initially was the craniofacial 30.esd) (**Table 36** and **Table 37**).

Ceph Points	Distance between points before RME (mm)	Distance between points (mm) Craniofacial 31.esd
CNR-CNL	22.578	22.7712
EMR-EML	66.978	67.039
UMR-UML	67.244	67.5653
MIR-MIL	1.48	1.57

Ceph Points	Distance between points (mm) Craniofacial 32.esd	Distance between points (mm) Craniofacial 33.esd
CNR-CNL	22.86	22.972
EMR-EML	67.44	67.64
UMR-UML	67.76	68.007
MIR-MIL	1.63	1.711

Ceph Points	Distance between points (mm) Craniofacial 34.esd	Distance between points (mm) Craniofacial 35.esd
CNR-CNL	23.11	23.267
EMR-EML	67.89	68.26
UMR-UML	68.305	68.603
MIR-MIL	1.77	1.87

Ceph Points	Distance between points (mm) Craniofacial 36.esd	Distance between points (mm) Craniofacial 37.esd
CNR-CNL	23.447	23.658
EMR-EML	68.455	68.78
UMR-UML	68.93	69.30
MIR-MIL	2.003	2.15

Ceph Points	Distance between points (mm) Craniofacial 38.esd	Distance between points (mm) Craniofacial 39.esd
CNR-CNL	23.903	24.176
EMR-EML	69.254	69.55
UMR-UML	69.709	70.14
MIR-MIL	2.33	2.54

Ceph Points	Distance between points (mm) Craniofacial 40.esd	Distance between points (mm) Craniofacial 41.esd
CNR-CNL	24.46	24.716
EMR-EML	70.07	70.46
UMR-UML	70.60	71.123
MIR-MIL	2.78	3.01

Ceph Points	Distance between points (mm). Craniofacial 42.esd	Distance between points (mm). Craniofacial 43.esd	Distance between points (mm). Craniofacial 44.esd
CNR-CNL	25.03	25.37	25.709
EMR-EML	70.909	71.358	71.8
UMR-UML	71.609	72.1	72.595
MIR-MIL	3.31	3.64	3.98

Table 36: Finite Element Analysis of **craniofacial 31.esd – craniofacial 44.esd**

Total changes between the measuring points:

Ceph Points	Total displacement during FEA in mm.
CNR-CNL	(25.709-22.578 =) **3.13**
EMR-EML	(71.8-66.978 =) **4.822**
UMR-UML	(72.595-67.244 =) **5.351**
MIR-MIL	(3.98-1.48 =) **2.5**

Table 37: Finite Element Analysis calculating tissue rebound

Using the same Finite Element Model of the dry skull as resulted from the earlier study (**craniofacial 30.esd**) and opening the screw by equal amount of turns (i.e. 14 turns x 0.25mm/turn = 3,50 mm of expansion) but without taking under consideration the tissue rebound phenomenon (craniofacial 70.esd), we get the following results (**Table 38**):

Ceph Points	Total displacement during FEA in mm. **(craniofacial 70.esd)** without tissue relaxation	Total displacement during FEA in mm. **(craniofacial 44.esd)** with tissue relaxation
CNR-CNL	**1.30**	**3.13**
EMR-EML	**2.03**	**4.822**
UMR-UML	**2.24**	**5.351**
MIR-MIL	**0.644**	**2.5**

Table 38: Comparison between the two models **(craniofacial 70.esd – craniofacial 44.esd)**

In the following Figures, the displacements of the four measuring distances are compared for each turn of the screw for the two different finite element models developed (craniofacial 30.esd and craniofacial 70.esd), with and without tissue relaxation.

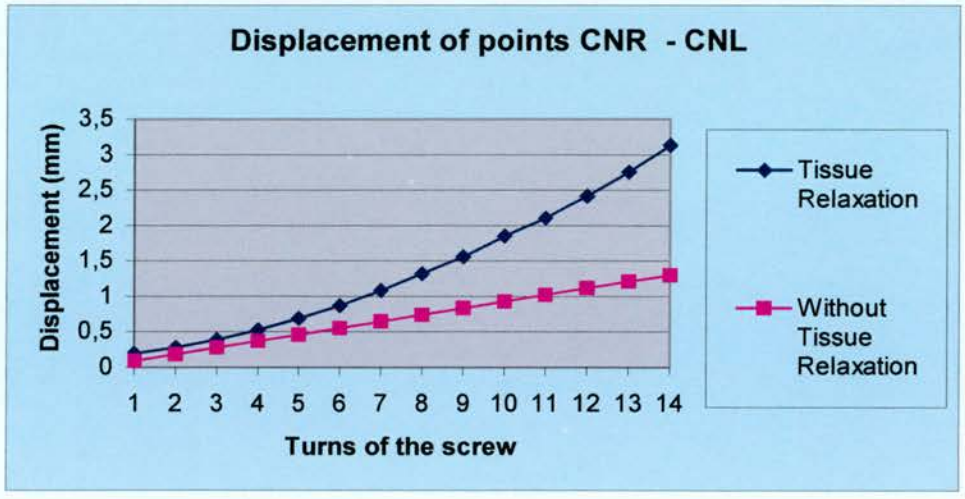

Fig. 33. Graphical presentation of the displacements for the points CNR-CNL **(craniofacial 30.esd – craniofacial 70.esd)**

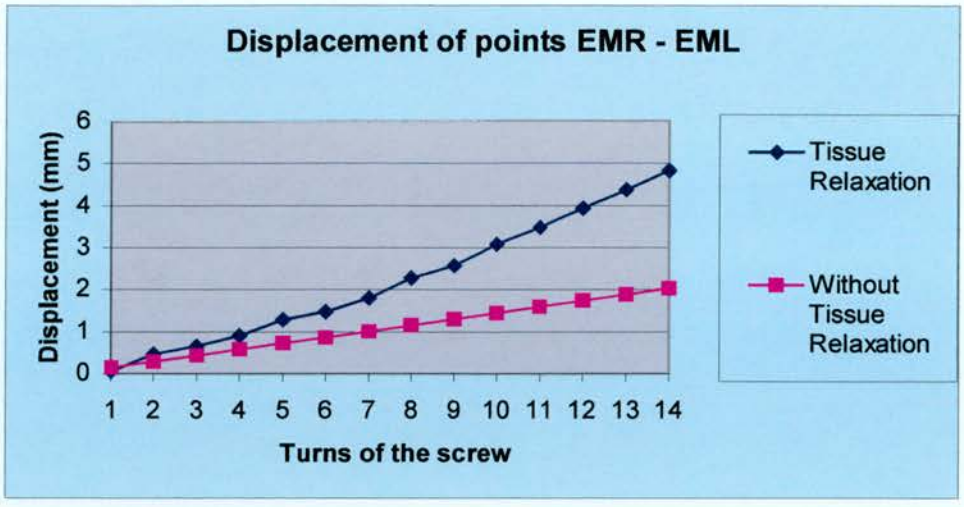

Fig. 34. Graphical presentation of the displacements for the points EMR-EML **(craniofacial 30.esd – craniofacial 70.esd)**

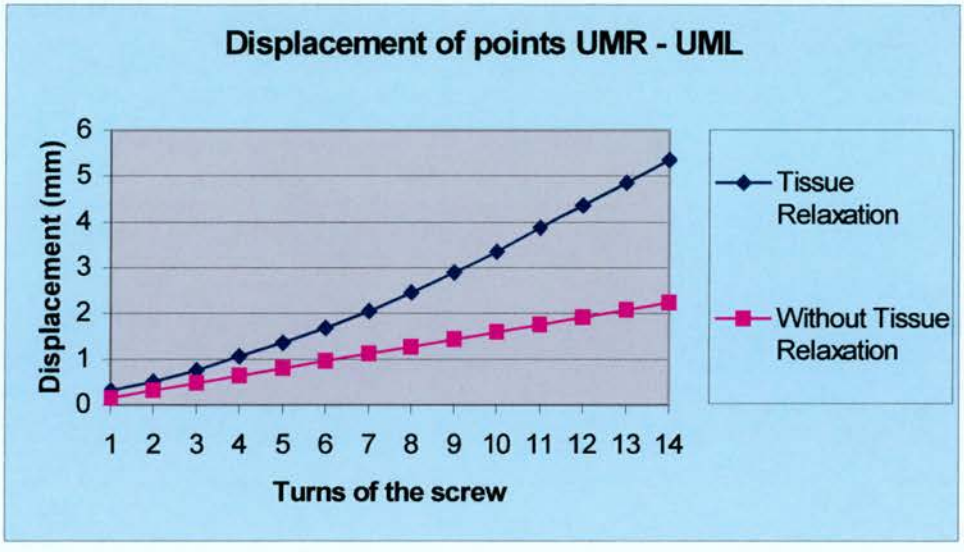

Fig. 35. Graphical presentation of the displacements for the points UMR-UML **(craniofacial 30.esd – craniofacial 70.esd)**

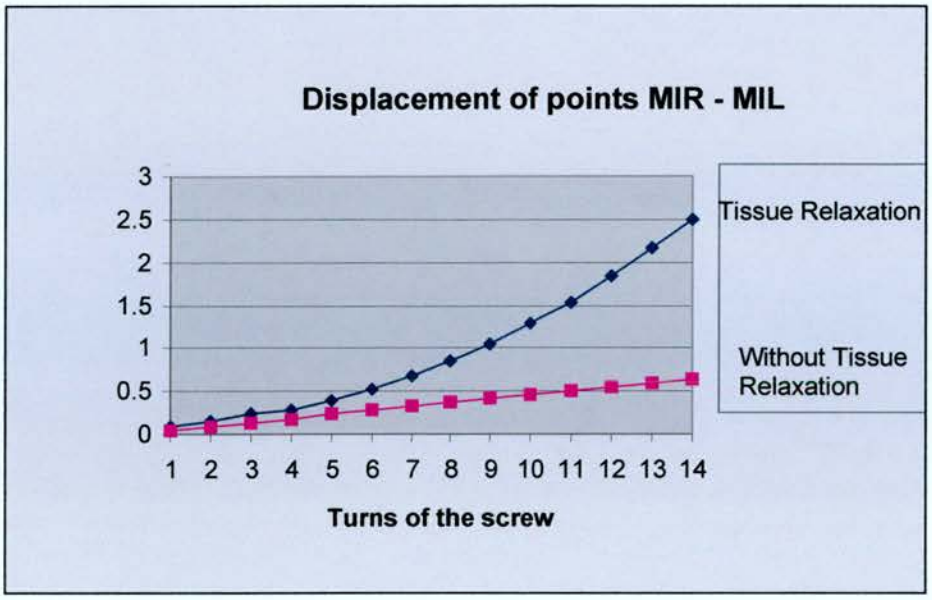

Fig. 36. Graphical presentation of the displacements for the points MIR-MIL **(craniofacial 30.esd – craniofacial 70.esd)**

From the above graphics it can be concluded that tissue relaxation plays significant role and influences the quantity and quality of the displacements of the various parts of the nasomaxillary complex. When tissue relaxation is not taken under consideration, the expansion is less and linear, while if an attempt is made to add in the analysis the phenomenon of tissue relaxation, the results show greater and non-linear separation of the maxillary halves.

4.14. The importance of modelling the neighbouring to the maxilla cranial bones for the results of the Finite Element Analysis (craniofacial 71.esd to craniofacial 72.esd):

In order to study the influence of the other craniofacial structures on the separation of the two maxillary halves during Rapid Maxillary Expansion the Finite Element Model of the dry skull which simulates better the clinical situation will be used **(craniofacial 30.esd)**. The sutures that articulate the

maxilla with the neighbouring bones were packed at their distal edge (i.e. degrees of Freedom = 0), with the bones present in the first analysis (craniofacial 71.esd) (**Figure 37**), and with the bones removed in the second analysis (craniofacial 72.esd) (**Figure 38**). Expansion of 3.75mm was applied at each of the six (6) nodes of the Rapid Maxillary Expansion appliance (**Table 39**).

Ceph Points	Displacement (mm). (craniofacial 30.esd)	Displacement (mm). (craniofacial 71.esd)	Displacement (mm). (craniofacial 72.esd)
CNR-CNL	2.75	0.87	0.79
EMR-EML	4.28	1.82	2.09
UMR-UML	4.76	2.29	2.57
MIR-MIL	1.36	0.94	0.92

Table 39: Finite Element Analysis of **craniofacial 71.esd – craniofacial 72.esd**

From the above findings it can be concluded that the presence or not of the bones influences the results of the Finite Element Analysis of the Rapid Maxillary Expansion, except of the displacement between the points MIR-MIL. However, it was thought that for the completeness of the model the anatomy of the craniofacial complex should be maintained.

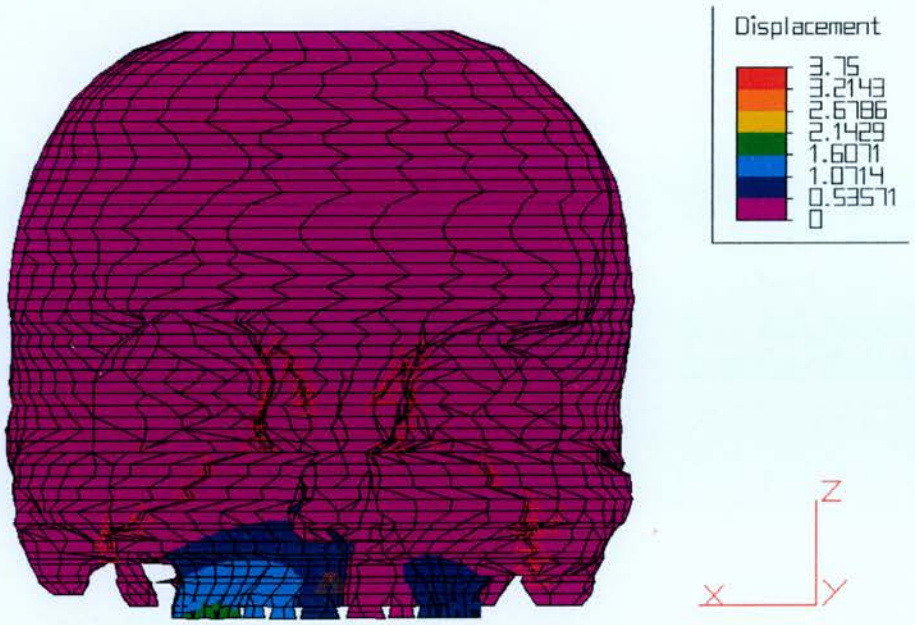

Fig. 37. craniofacial 71.esd

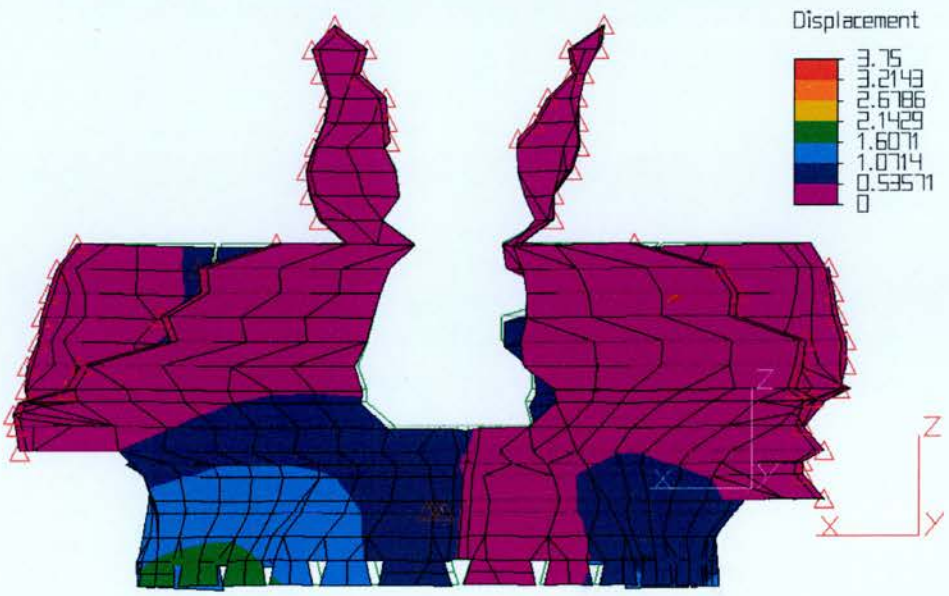

Fig. 38. craniofacial 72.esd

4.15 *In vitro* application of the Rapid Maxillary Expansion on a Dry Skull:

Even though the qualitative behavior of a dry skull which undergoes rapid maxillary expansion does not simulate with a high degree of accuracy the clinical situation, nevertheless, it is possible to indicate the way the two maxillary halves separate during the application of the expansion force and how the effect of the force influences the other craniofacial structures. Therefore, it was considered necessary to apply the method of Rapid Maxillary Expansion on a dry skull in order to acquire more information on the distribution of the displacements, the order of suture separation, as well as the areas of high stress concentration.

In **Appendix 18** the dry skull is shown before the application of the expansion forces with the Rapid Maxillary Expansion appliance cemented on the artificially constructed first maxillary premolars and the first permanent maxillary molars. After measuring the initial distance between the measuring points, the Hyrax type screw of the Rapid Maxillary Expansion appliance was turned and the two acrylic halves of the appliance was separated by 0.25mm. Consequently, a force is applied to the dry skull created by the expansion of the appliance.

After calculating the displacement between the measuring points, the same process was repeated, each time separating by another 0.25mm the two acrylic halves and adding another increment of force to the structures of the dry skull. After 6 ½ turns of the Hyrax screw of the Rapid Maxillary Expansion appliance, the resistance of the surrounding structures of the nasomaxillary complex to further expansion of the two maxillary halves was prohibitively high and prohibited any attempt to continue turning the screw (**Appendix 19**). The following day, however, a further attempt was made to continue the turns of the screw and the 7^{th} turn was completed and another ½ turn was

achieved. The displacements between the measuring points are presented in **Table 40** and **Table 41**.

Measuring Points	Distance between points in mm. (Start)	Distance between points in mm. (Turn 1)	Distance between points in mm. (Turn 2)	Distance between points in mm. (Turn 3)
CNR-CNL	20.57	20.57	20.67	20.77
EMR-EML	57.255	57.331	57.426	57.520
UMR-UML	54.13	54,19	54.38	54.39
MIR-MIL	1.41	1.70	1.91	2.17

Measuring Points	Distance between points in mm. (Turn 4)	Distance between points in mm. (Turn 5)	Distance between points in mm. (Turn 6)	Distance between points in mm. (Turn 6½)
CNR-CNL	20.80	20.90	21.13	21.17
EMR-EML	57.617	57.731	57.850	57.919
UMR-UML	54.49	54.49	54.57	54.72
MIR-MIL	2.30	2.49	2.67	2.82

Measuring Points	Distance between points in mm. (Turn 7)	Distance between points in mm. (Turn 7 ½)
CNR-CNL	21.22	21.28
EMR-EML	57.99	58.07
UMR-UML	54.85	54.91
MIR-MIL	2.98	3.11

Table 40: The results of the *in vitro* application of Rapid Maxillary Expansion.

Measuring Points	Total Displacement (mm)
CNR-CNL	**0.71**
EMR-EML	**0.815**
UMR-UML	**0.78**
MIR-MIL	**1.7**

Table 41: Total displacements occurred between the measuring points during *in vitro* application of the Rapid Maxillary Expansion.

4.16. Controlling the linearity of Rapid Maxillary Expansion methodology:

It was shown earlier that, if tissue relaxation period with consequent tissue rebound is added to the mathematical analysis, it influences significantly the displacements and the force distribution to the nasomaxillary and cranial structures. It also influences the linearity of the displacements.

However, clinically, the forces are not completely eliminated and residual forces are present between each turn of the screw. Moreover, the force value decreases after splitting of the midpalatal and the other sutures occurs. Therefore, the issue is to decide which of the two Finite Element Models simulates closer the clinical situation. In the following **Figures 39 – 42**, the findings of the Finite Element Analysis of the two models, with and without tissue relaxation, and these of the *in Vitro* experiment are presented. For comparative purposes in all three cases 7 turns of the screw are considered (limiting factor is the 7 turns of the screw that was carried out at the dry skull).

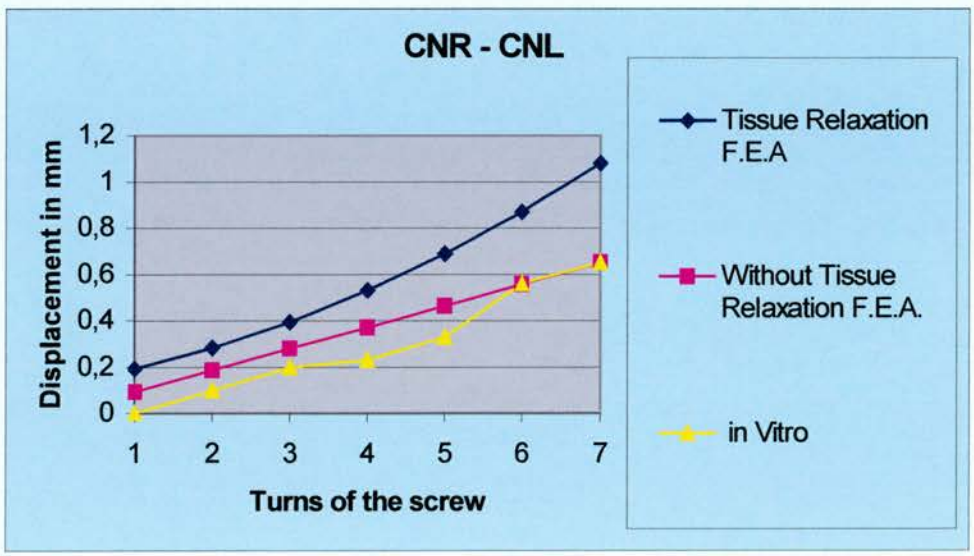

Fig. 39. Graphical comparison of the displacements for the points CNR-CNL

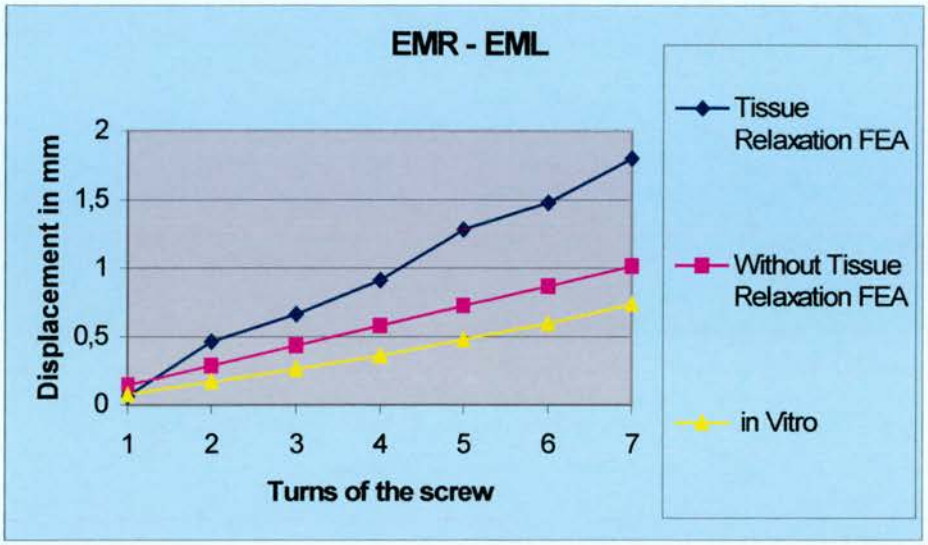

Fig. 40. Graphical comparison of the displacements for the points EMR-EML

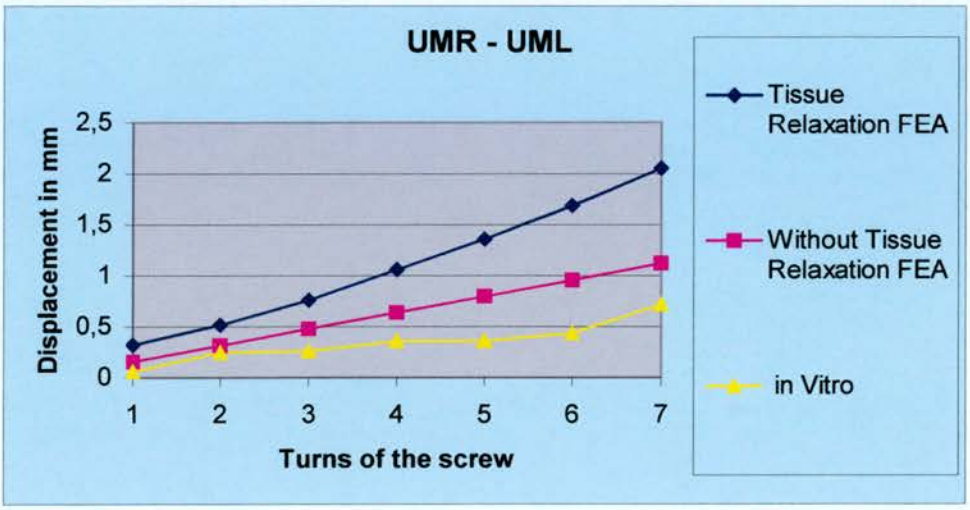

Fig. 41. Graphical comparison of the displacements for the points UMR-UML

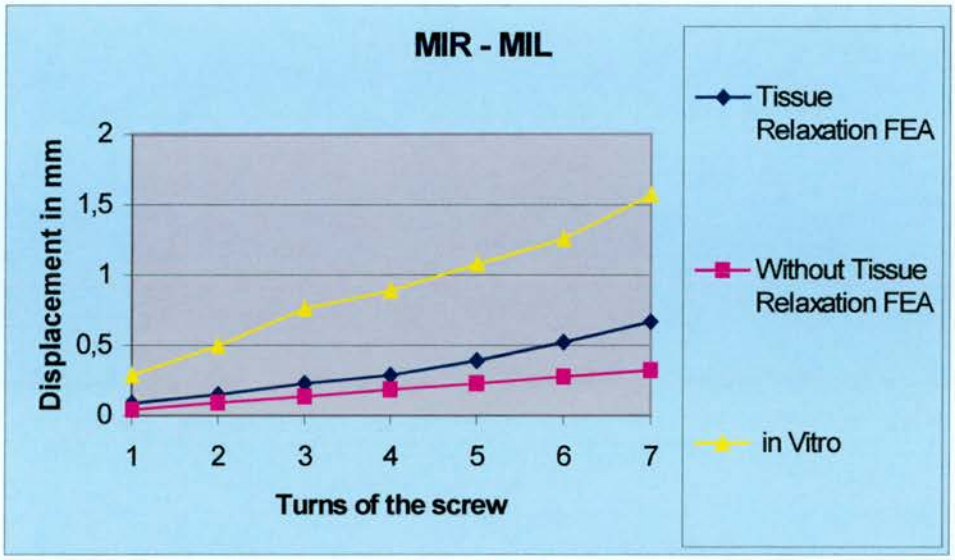

Fig. 42. Graphical comparison of the displacements for the points MIR-MIL

From the above **Figures 39 - 42** it can be concluded that the Curve of the *in vitro* experiment is closer to the linear curve of the Finite Element Analysis without consideration of the tissue rebound phenomenon, except for the measuring points MIR-MIL. Therefore, in further study of the Rapid Maxillary Expansion with the help of the Finite Element modelling of the skull, the behavior of the nasomaxillary complex is considered as linear with no tissue relaxation (in addition Finite Element Analysis as a computational method with CPU limitations of the present study, does not allow consideration for the tissue relaxation phenomenon for 30 turns of the screw).

4.17. Finite Element Analysis of the model summarizing all the aforementioned findings:

The Finite Element Model of the dry skull with the addition of the teeth, the associated periodontal ligament and the combination of cortical and cancellous bone in the maxilla (**Figure 18**) with limiting factors as resulted from the previous sections (**craniofacial 30.esd**) was tested. The results of the Finite Element Analysis (**craniofacial 300.esd**) are presented in the following **Table 42**.

Measuring Points	Dispalcement derived from FEA in mm (Craniofacial 30.esd)	Dispalcement derived from FEA in mm (Craniofacial 300.esd)	Mean Differences measured on the P-A cephs. $\Delta X = \bar{x}_{after} - \bar{x}_{before}$	Confidence Interval (P=99.5%) for the difference in Mean Values (mm).
CNR-CNL	2.75	3.29	1.66	$0.3 < \mu_2 - \mu_1 < 3.01$
EMR-EML	4.28	4.16	2.47	$0.43 < \mu_2 - \mu_1 < 4.5$
UMR-UML	4.76	5.34	8.89	$6.77 < \mu_2 - \mu_1 < 11$
MIR-MIL	1.36	1.92	1.08	$0.49 < \mu_2 - \mu_1 < 1.66$

Table 42: Finite Element Analysis of **craniofacial 300.esd**

Comparing the results of these two Finite Element Analysis, it is evident that modelling of the teeth and the periodontal ligament, as well as using brick elements for the cancellous bone of the maxilla, alters the displacement and the force distribution at the points EMR-EML and UMR-UML as it was suggested in the previous sections. The qualitative behavior of the new Finite Element Model is similar to the clinical situation as described in the literature, but now the displacement of points CNR-CNL and MIR-MIL is outside the confidence interval for $p<0.05$.

If now, it is considered that all the circummaxillary sutures are still patent (Modulus of Elasticity = 1 Nt/mm^2); the transeptal fibers between the two central incisors are elastic (i.e. have the same Modulus of Elasticity) and that the

other cranial sutures are totally ossified (**craniofacial 303.esd**), the results are presented in **Table 43**.

Measuring Points	Dispalcement derived from FEA in mm (Craniofacial 300.esd)	Dispalcement derived from FEA in mm (Craniofacial 303.esd)	Mean Differences measured on the P-A cephs. $\Delta X = \bar{x}_{after} - \bar{x}_{before}$	Confidence Interval (P=99.5%) for the difference in Mean Values (mm).
CNR-CNL	3.29	4.27	1.66	$0.3 < \mu_2 - \mu_1 < 3.01$
EMR-EML	4.16	4.66	2.47	$0.43 < \mu_2 - \mu_1 < 4.5$
UMR-UML	5.34	5.94	8.89	$6.77 < \mu_2 - \mu_1 < 11$
MIR-MIL	1.92	6.65	1.08	$0.49 < \mu_2 - \mu_1 < 1.66$

Table 43: Finite Element Analysis of **craniofacial 303.esd**

If it is assumed that all sutures of the Finite Element Model are elastic (i.e. open; with Modulus of Elasticity = 1Nt/mm²) (**craniofacial 304.esd**); the results are presented in **Table 44**.

Measuring Points	Dispalcement derived from FEA in mm (Craniofacial 303.esd)	Dispalcement derived from FEA in mm (Craniofacial 304.esd)	Mean Differences measured on the P-A cephs. $\Delta X = \bar{x}_{after} - \bar{x}_{before}$	Confidence Interval (P=99.5%) for the difference in Mean Values (mm).
CNR-CNL	4.27	5.8	1.66	$0.3 < \mu_2 - \mu_1 < 3.01$
EMR-EML	4.66	5.01	2.47	$0.43 < \mu_2 - \mu_1 < 4.5$
UMR-UML	5.94	6.24	8.89	$6.77 < \mu_2 - \mu_1 < 11$
MIR-MIL	6.65	8.05	1.08	$0.49 < \mu_2 - \mu_1 < 1.66$

Table 44: Finite Element Analysis of **craniofacial 304.esd**

From the results presented in **Table 44** it can be concluded that for **craniofacial 304.esd** model, measuring point displacements are outside confidence interval for $p<0.05$. However, for both models (i.e. with and without open sutures) the difference is not statistically significant and therefore, to perform parametric analysis for all sutures of the craniofacial complex separately is not justified.

In **Figures 43 – 48** the results of the stress distribution and displacements of the Finite Element Analysis for **craniofacial 304.esd** are presented. In these figures, the stresses are greater than in clinical practice because they do not include the tissue relaxation phenomenon. Therefore, stress distribution during Finite Element Analysis can lead only to qualitative conclusions and not to quantitative.

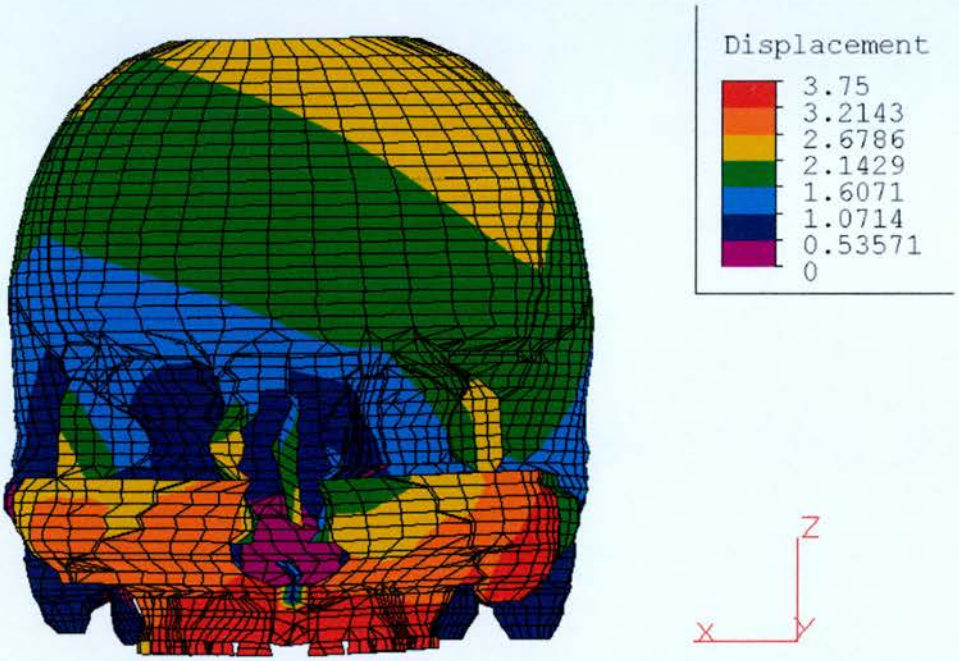

Fig. 43. Frontal view of the model of the skull (**craniofacial 304.esd**) with the displacements observed after application of the rapid maxillary expansion.

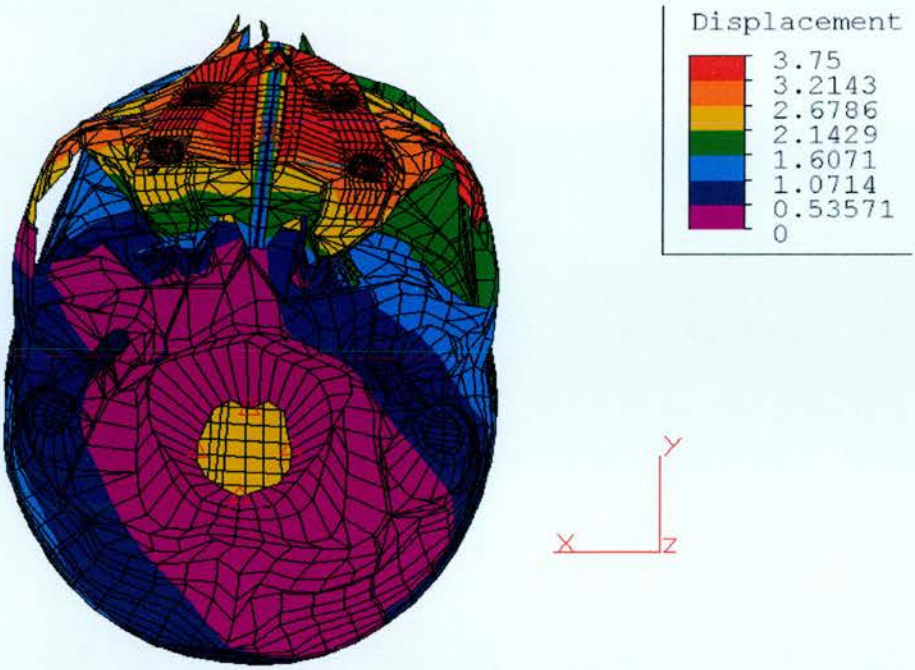

Fig. 44. Basal view of the model of the skull (**craniofacial 304.esd**) with the displacements observed after application of the rapid maxillary expansion.

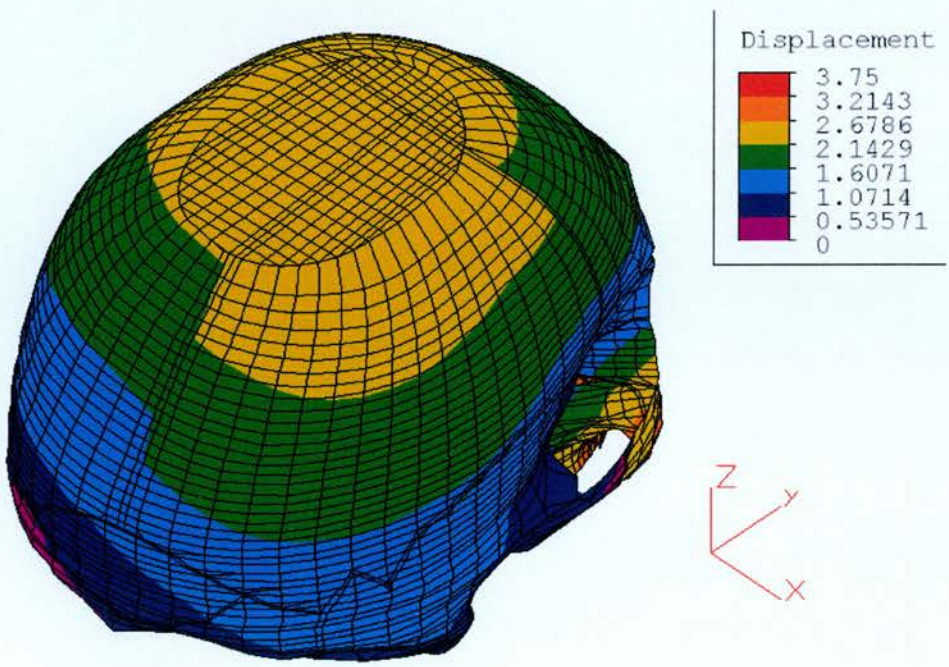

Fig. 45. Side view of the model of the skull (**craniofacial 304.esd**) with the displacements observed after application of the rapid maxillary expansion.

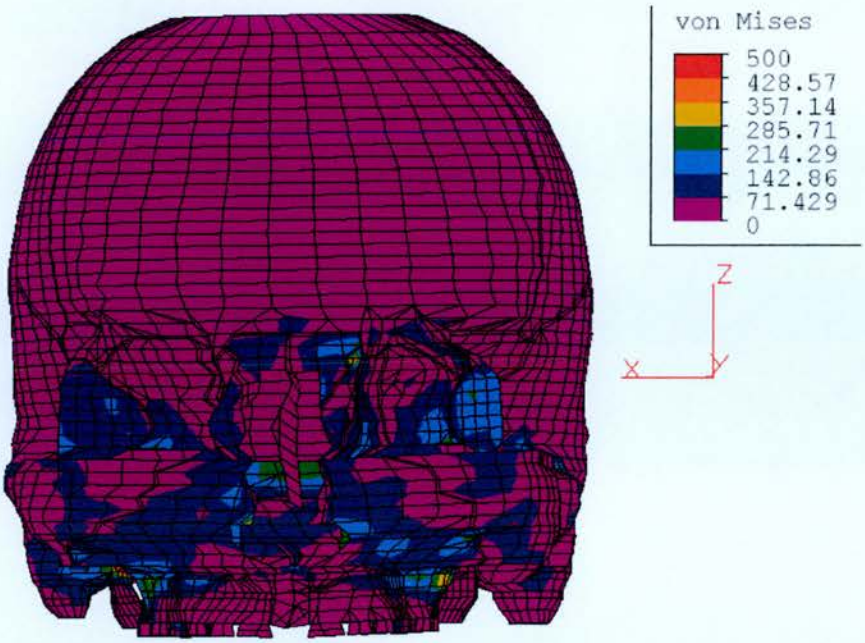

Fig. 46. Frontal view of the model of the skull (**craniofacial 304.esd**) with the distribution of von Mises stresses observed after application of the rapid maxillary expansion.

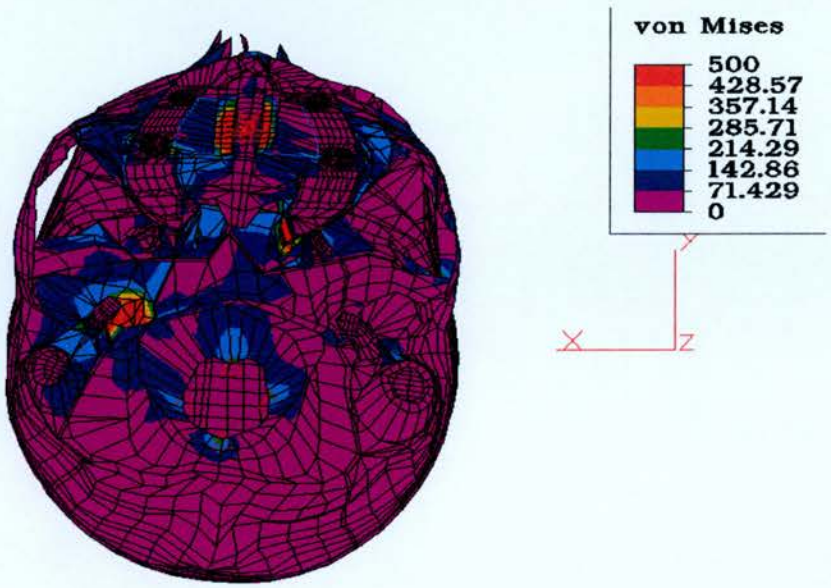

Fig. 47. Basal view of the model of the skull (**craniofacial 304.esd**) with the distribution of von Mises stresses observed after application of the rapid maxillary expansion.

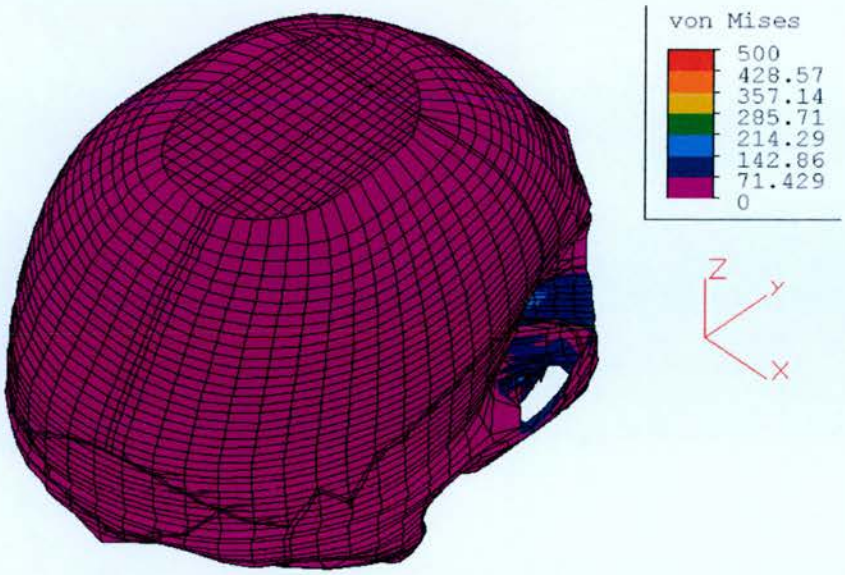

Fig. 48. Side view of the model of the skull (**craniofacial 304.esd**) with the distribution of von Mises stresses observed after application of the rapid maxillary expansion.

However, it gives a clear indication as to the areas which undergo higher levels of strain. The areas with the highest level of strain are, the two maxillary halves where the external load is applied and the suture between the temporal and the occipital bone near to the styloid process (**Figure 49**). The area near the styloid process presents high stress levels in the *in Vitro* experiment with the dry skull too, as it can be seen in **Figure 49**.

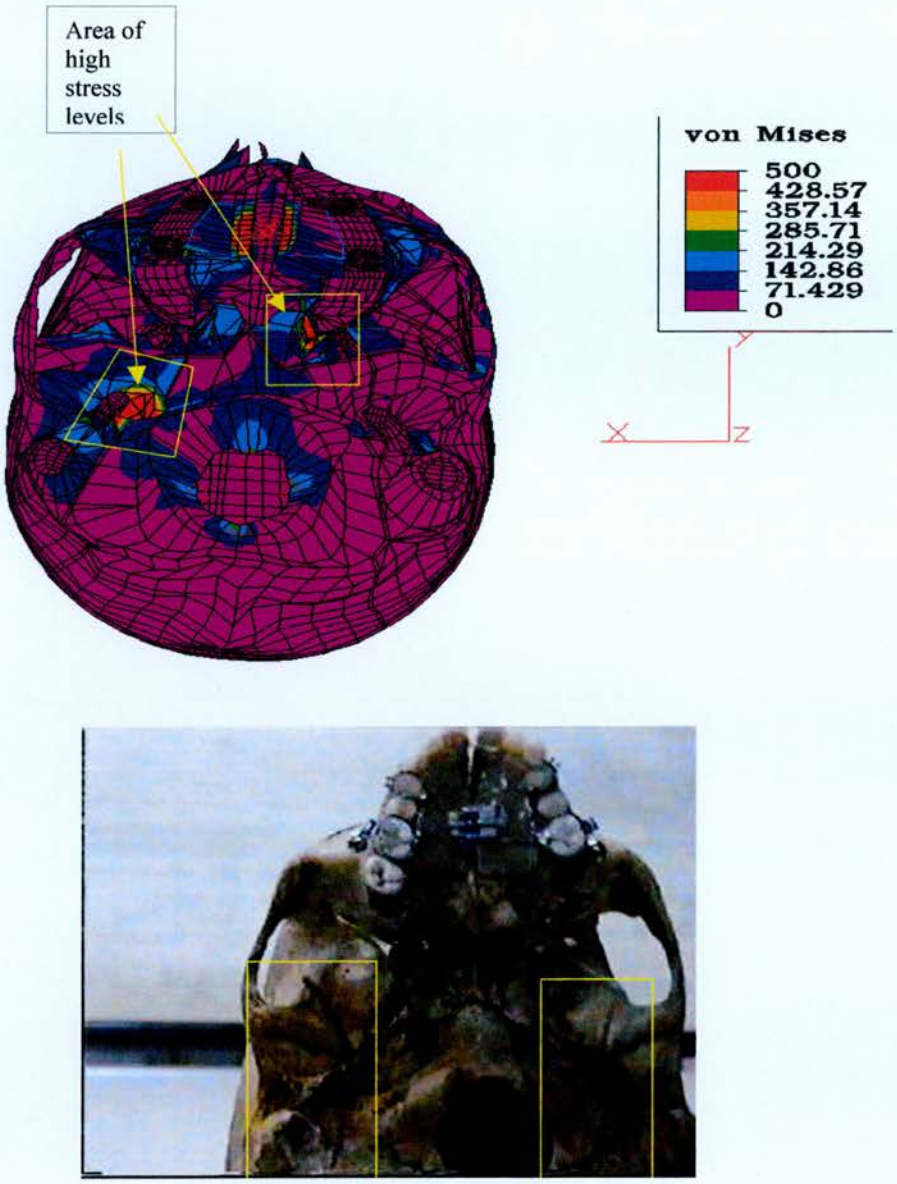

Fig. 49. The stress levels in the area of the styloid process and the articulation of the pterygoid process with the perpendicular plate of the palatine bone.

It was attempted to isolate the Finite Element Analysis at the level of the anchor teeth and their periodontal ligament. The results of the displacements and the stress distribution in this area are presented in **Figures 50 – 53**. It is suggested that the stresses developed at the compact bone at the level of the first maxillary molar are higher than those developed at the level of the first maxillary premolar. It is also evident that the stresses developed at the level of the crown of the first maxillary molar are higher than those developed at its roots, while the stresses developed at the crown of the first maxillary premolar are lower than those developed at its roots. For both teeth the stresses developed at the level of the periodontal ligament appear to be low.

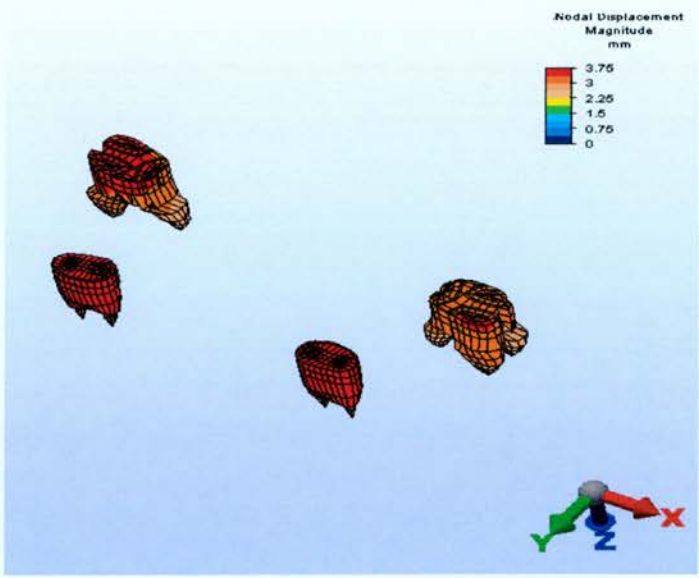

Fig. 50. The displacements calculated at the anchor teeth (**craniofacial 304.esd**)

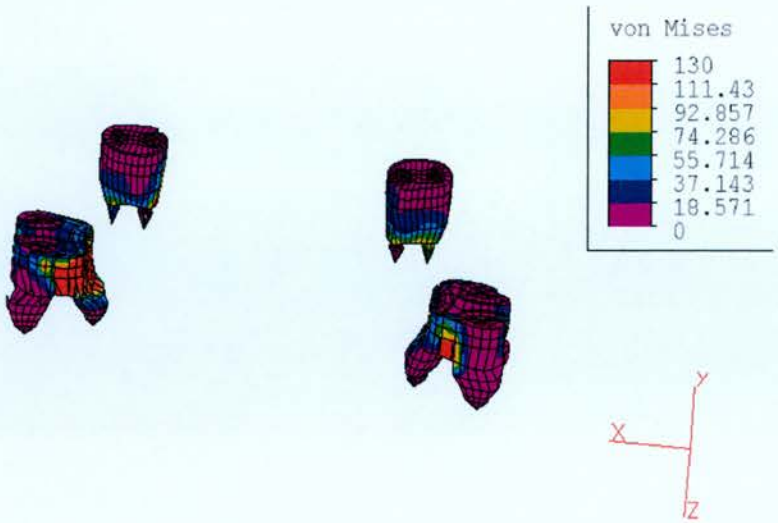

Fig. 51. The von Mises stress distribution at the level of the anchor teeth **(craniofacial 304.esd)**

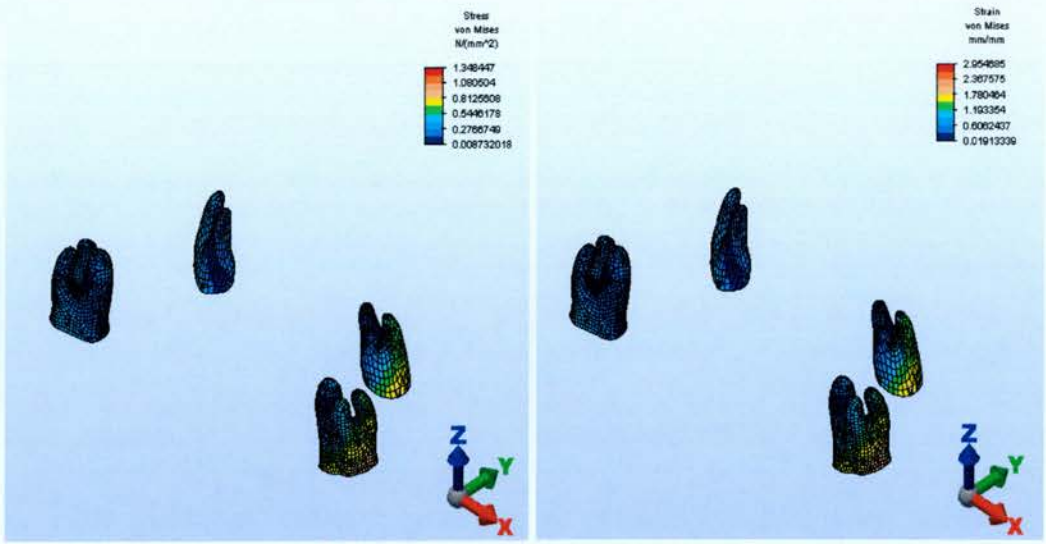

Fig. 52. The von Mises stress and strain distribution at the level of the periodontal ligament of the anchor teeth **(craniofacial 304.esd)**

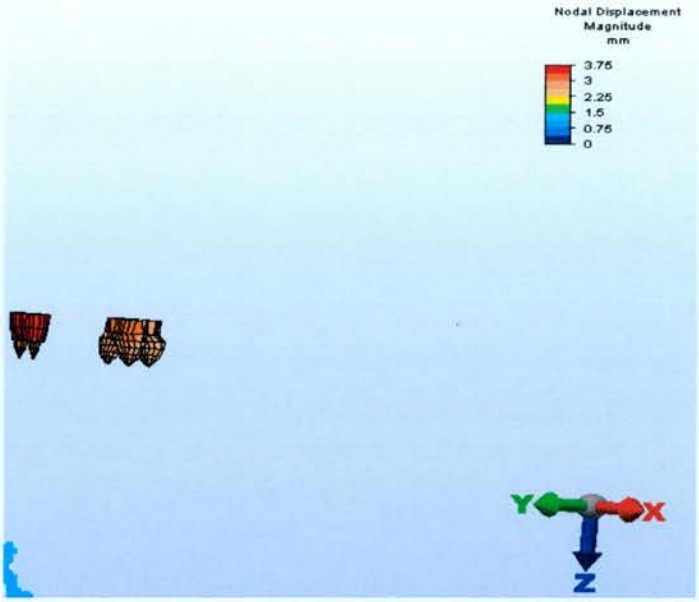

Fig. 53. The displacements calculated at the level of the periodontal ligament of the anchor teeth (**craniofacial 304.esd**).

Finally, the displacements in all three directions of the space (i.e. coordinates x & y & z) for the various structures of the craniofacial complex are presented in **Table 45 (Figure 54)**.

Nr of structure	Structure	Displacement in Coordinate x (mm)	Displacement in Coordinate y (mm)	Displacement in Coordinate z (mm)
1	Frontal Bone	1.21016	-0.653813	0.829488
2	Nasal Bone	1.08992	-0.269686	0.852184
3	Superior-Anterior part of the Zygomatic Bone	1.36753	-1.00547	0.597623
4	Anterior part of the Zygomatic Arc	2.41277	-1.01632	0.44457
5	Posterior part of the Zygomatic Arc	1.33357	-2.04456	-0.336717
6	Central Incisors	3.83753	-0.293361	-0.0792668
7	Maxilla between Central and Lateral Incisors	3.43732	0.103065	0.0144367
8	Maxilla at the area of the Canine	3.44332	0.009937	0.231798
9	Maxilla at the Molar area	1.86847	-0.501648	0.379685
10	Mastoid Process	-0.173771	-0.135207	-0.932057
11	Inferior part of the pterygoid process	0.146537	0.0823573	1.52458
12	Middle part of the pterygoid process	0.73912	-0.0967077	1.27505
13	Superior part of the pterygoid process	0.292489	-0.29004	1.01372
14	Parietal Bone	1.05656	-0.721427	-0.888499
15	Occipital Bone	0.184623	-0.327109	-0.782978

Table 45: Displacements measured at the various craniofacial structures in all three directions of space.

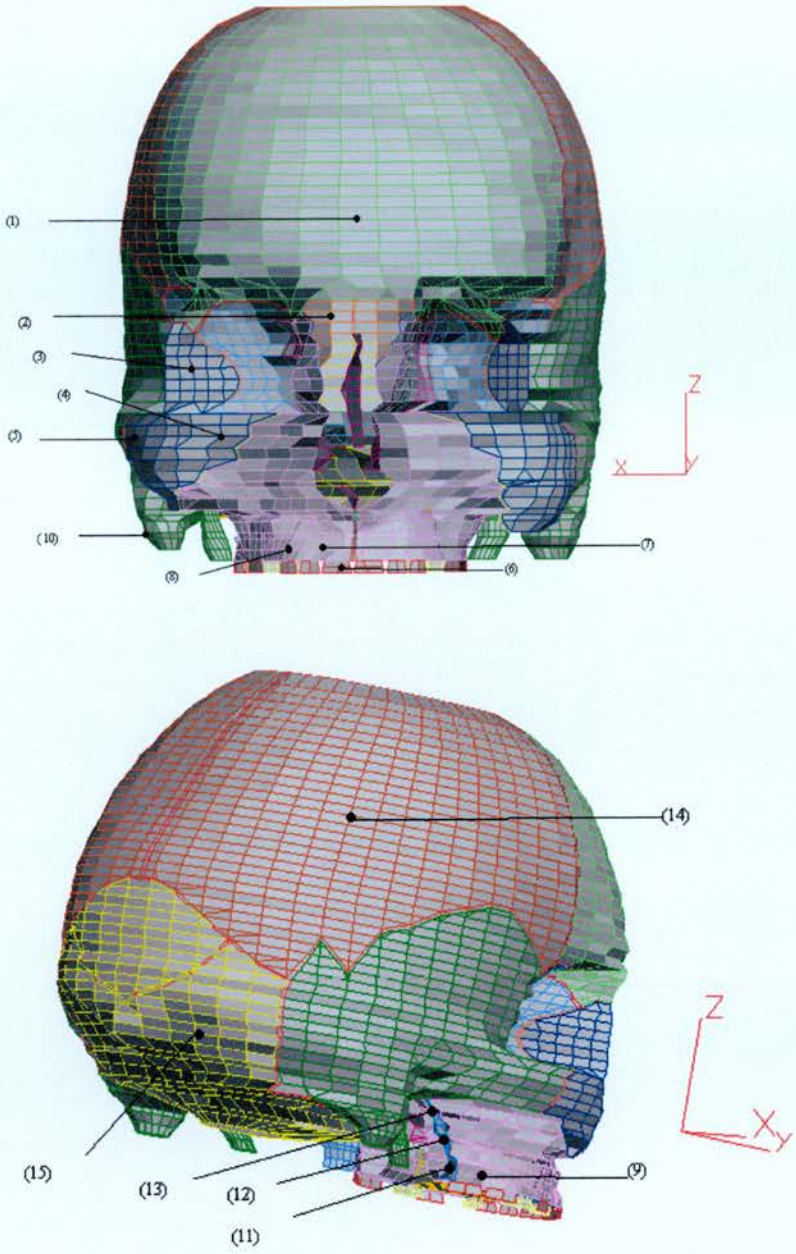

Fig. 54. The craniofacial structures at which displacements are measured

In **Figures 55 - 57** the results of the displacements in the three spatial directions of the various structural components of the Finite Element Model of the skull are presented.

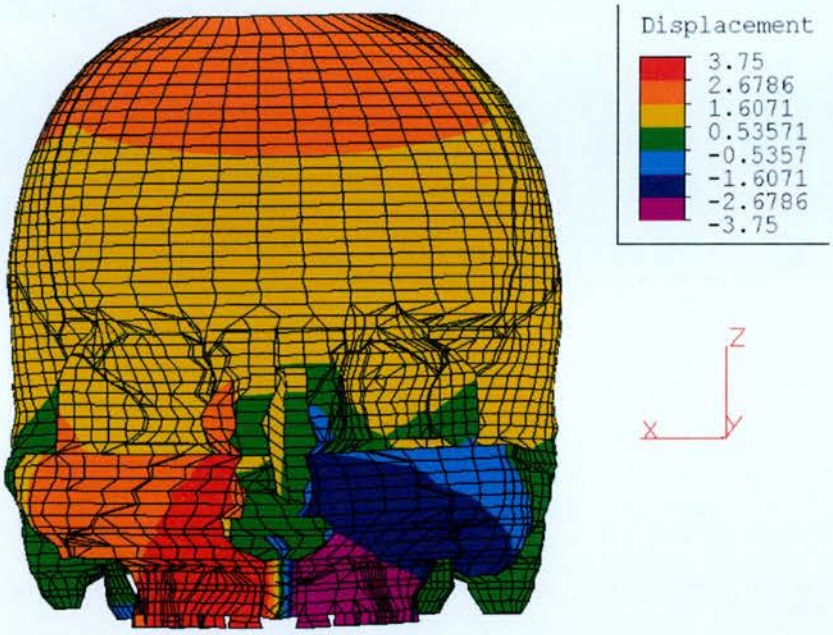

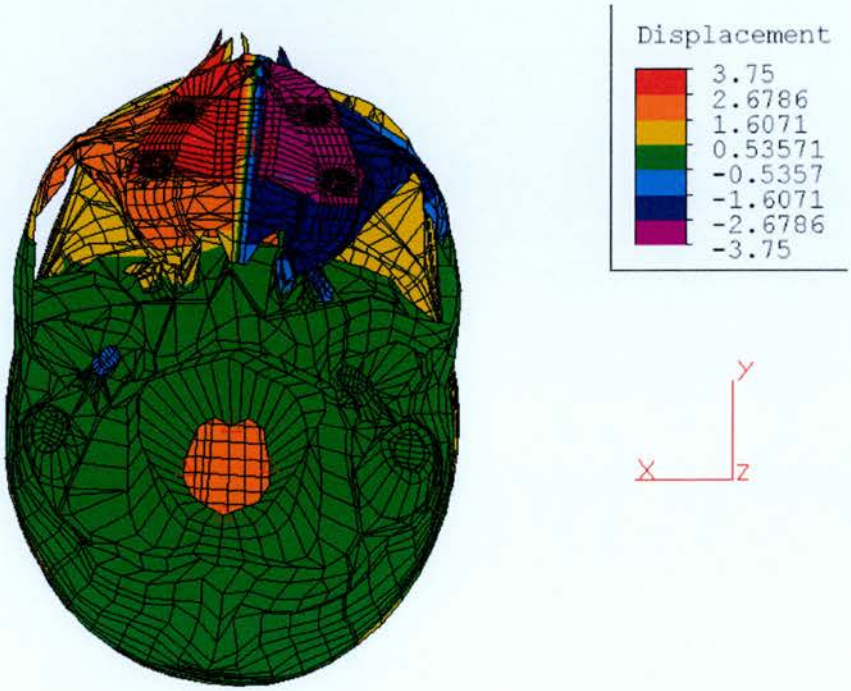

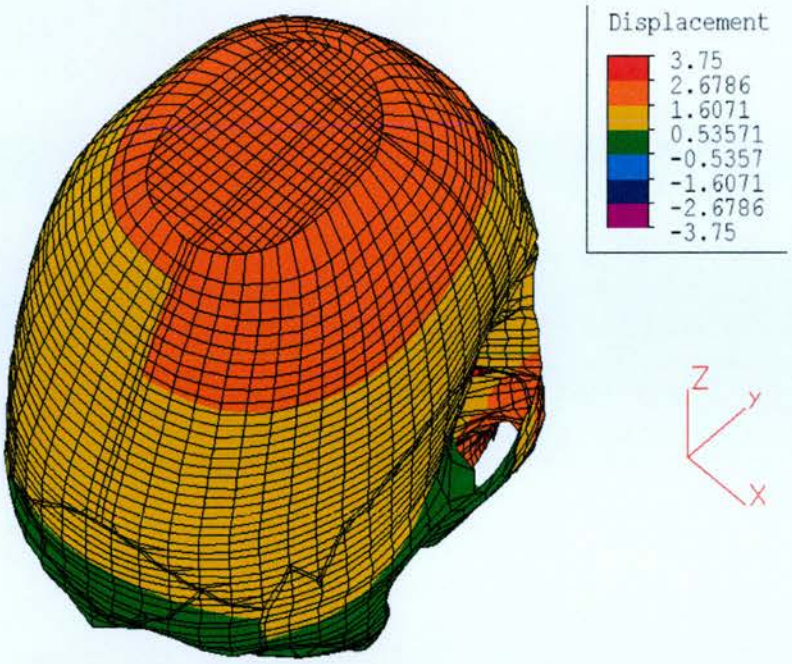

Fig. 55. The displacements measured at the various craniofacial structures in the x-coordinate (frontal, basal and side views)

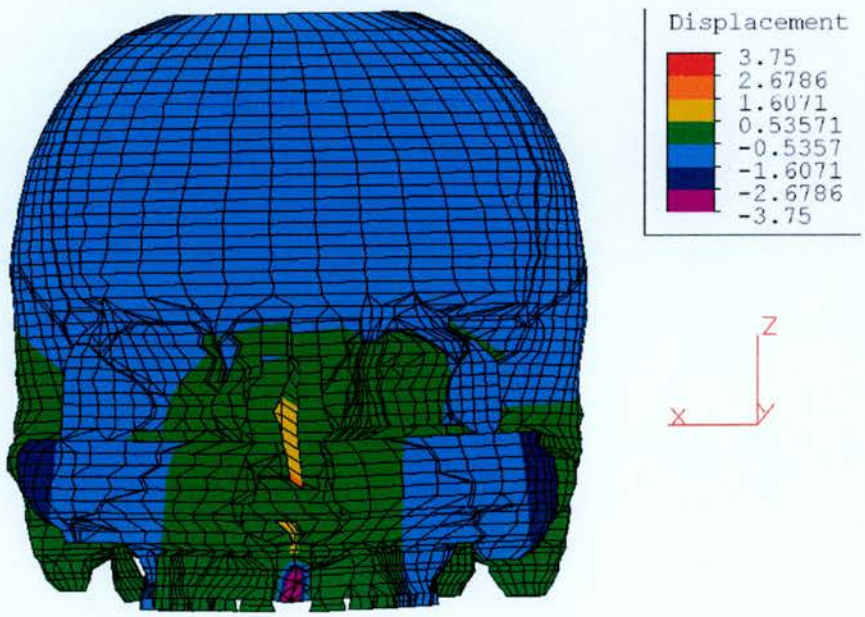

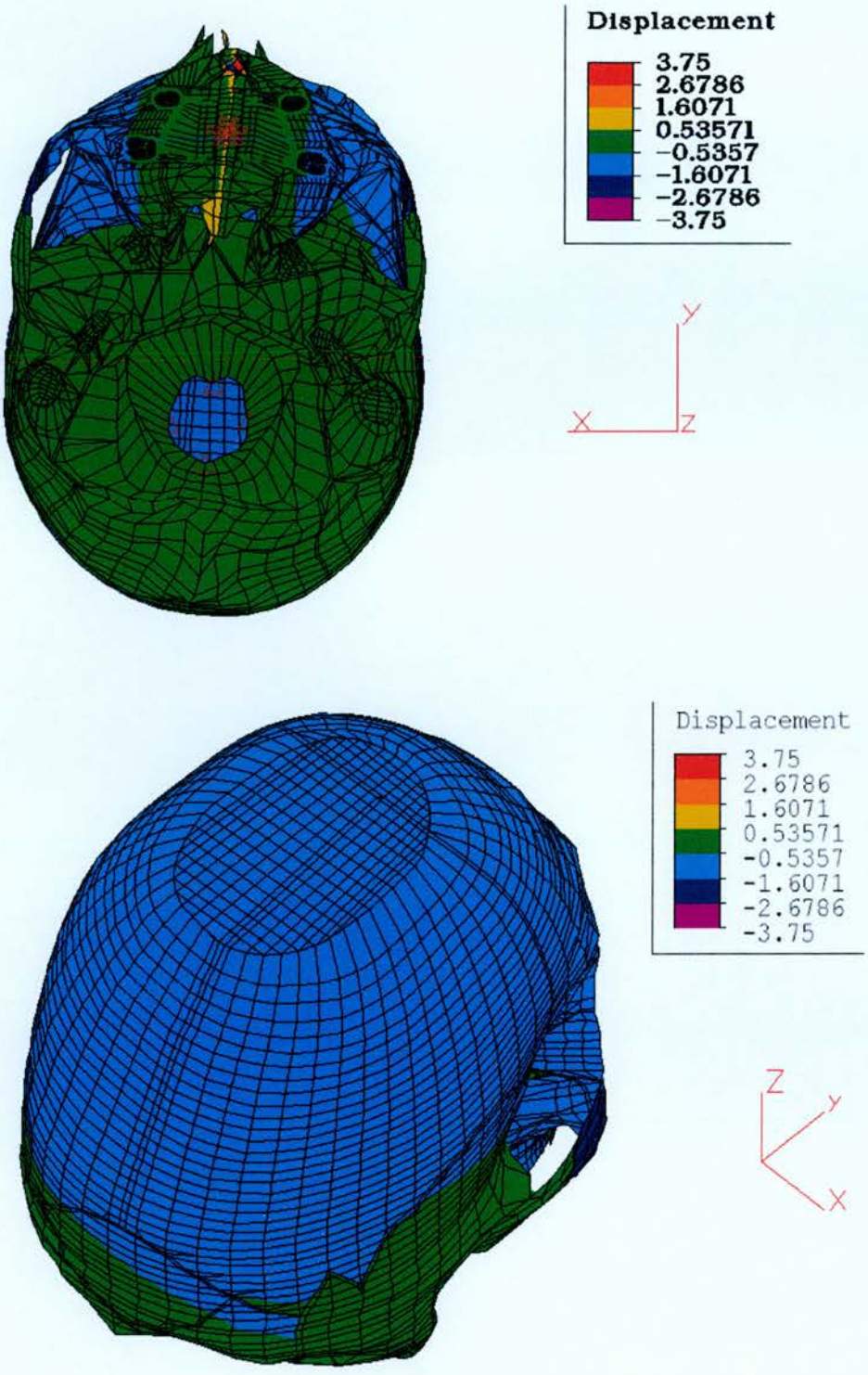

Fig. 56. The displacements measured at the various craniofacial structures in the y-coordinate (frontal, basal and side views)

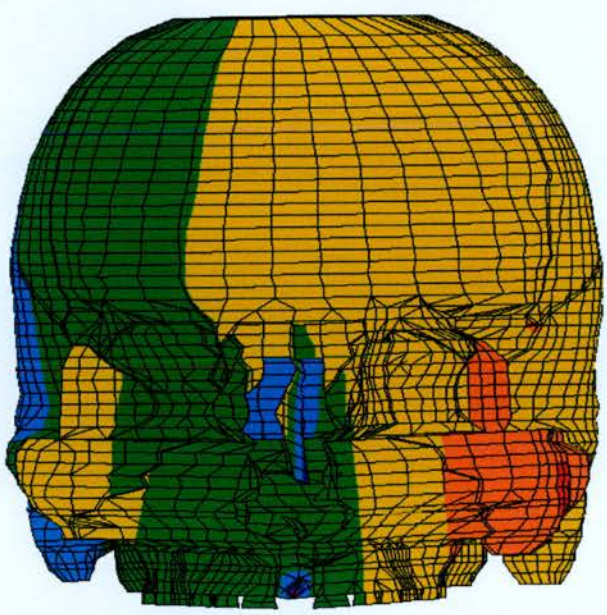
Displacement
3.75
2.6786
1.6071
0.53571
-0.5357
-1.6071
-2.6786
-3.75
Z
X
Y

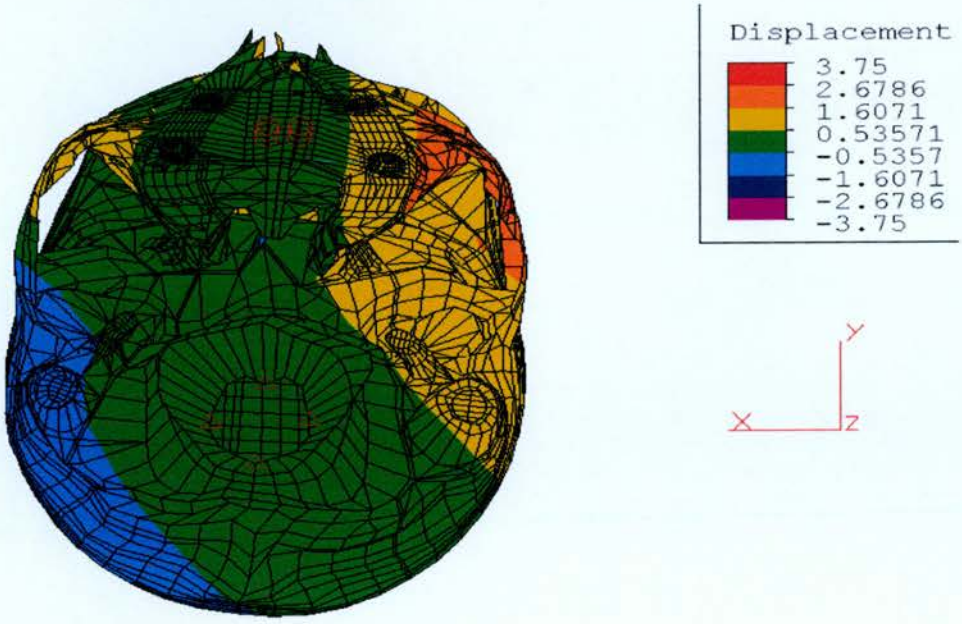
Displacement
3.75
2.6786
1.6071
0.53571
-0.5357
-1.6071
-2.6786
-3.75
Y
X
Z

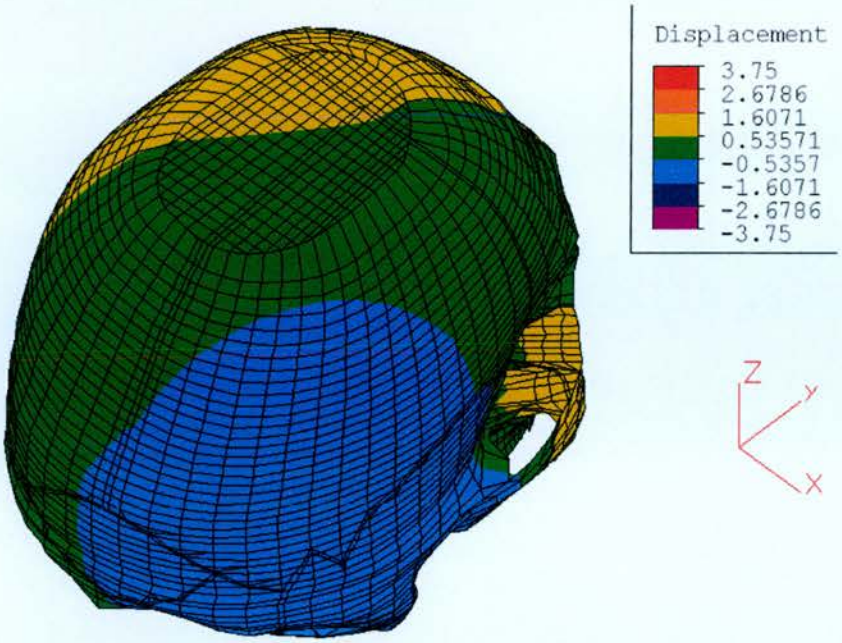

Fig. 57. The displacements measured at the various craniofacial structures in the z-coordinate (frontal, basal and side views)

CHAPTER 5: DISCUSSION

5.1. General comments on study design:

To discuss the objectives of the study, this section will begin with comments on study design, on the Finite Element Analysis and the Finite Element model used. There then follows an analysis of the method errors which were encountered and finally a discussion of the results.

This study was based on the initial construction of a Finite Element Model (F.E.M.) of the human craniofacial complex, the experimental application of the method of Rapid Maxillary Expansion and the consequent Finite Element Analysis. The results of the Finite Element Analysis were compared with the clinical findings from a previous research project based in the Edinburgh and Fife area (McDonald, 1995).

5.1.1. Experimental construction of the F.E.M. of the human craniofacial complex:

Although previous studies have provided detailed knowledge regarding the Rapid Maxillary Expansion (R.M.E.) technique, the effects of the procedure still remain unclear due to the limited evaluation of the biomechanical effects on the internal structures of the craniofacial complex. Several studies have been conducted to investigate histologically, morphologically and biomechanically the response of the craniofacial complex to R.M.E. However, it would be difficult to assess the mechanical reaction of the craniofacial bones to complex loading in three-dimensional space using conventional methods, namely, strain gauge (Tanne *et al.,* 1985), photoelastic (Chaconas and Caputo, 1982) or holographic (Pavlin and Vukicevic, 1984)

techniques. In addition, it has been suggested that by using roentgenographic cephalometric methods (RCM) only anecdotal observations are possible and RCMs are incapable of correctly depicting, in detail, time-related changes or changes in location of biological shapes (Moyers and Bookstein, 1979).

The Finite Element Method is a standard tool used in engineering sciences to assess precisely local stress-strain distributions in geometrically complex structures. The Finite Element Model provides the freedom to simulate orthodontic force systems applied clinically and makes it practicable to clarify biomechanical state variables such as displacements, strains and stresses induced in living structures by various external forces in three-dimensional space.

The value of Finite Element Analysis entirely depends on element density and the accuracy of geometry, material properties and loading conditions. Compared with automotive applications, geometric data for most human parts is not available. Furthermore, biological material properties must be converted into numerical material properties, suitable for the finite element program code.

The application of finite element modelling to biomechanics requires different methods to design a model with accurate geometry and material properties. For the construction of the Finite Element Model of the craniofacial complex, a human dry skull of an adult subject with no evident craniofacial anomaly and with the alveolar crest well represented was used. This human dry skull was selected, because in clinical inspection all anatomical details were maintained in an excellent condition, a criterion which was crucial for obtaining the geometry of the model. On the other hand, the age of the subject does not play a significant role, since the material properties of the various anatomical structures and sutures will be given different values during the parametric analysis, which reflect different

stages in the growth and development of the human skull. The geometry of the cranium was obtained by using the computer tomography (CT) technique.

Details of Finite Element Models developed using CT scanning have been previously published (Hart *et al.*, 1992). Computer tomography represents a well established method of medical imaging with high quality sagittal sections of the inner structure of the body. It has a number of advantages over previous reconstruction methods, particularly the ability to automatically locate object-boundary outlines and produce shaped three-dimensional images of reconstructed data (Moaddab *et al.*, 1985; Sprawls, 1990; Mehta *et al.*, 1997). Hart and his co-workers (1992) used two different methods to obtain the digitised description of mandibular geometry, and suggested that the non-destructive method based on CT scans presented certain advantages compared to a technique that involved embedding the mandible in a plastic resin and cutting serial sections (**Table 46**).

Embed mandible in plastic, cut serial sections
Advantages:
1. Accuracy of information regarding cross-sectional geometry and the orientation and distribution of trabecular bone
Disadvantages:
1. Loss of bone material due to sawing
2. Difficulty in obtaining uniform thickness with thin sections
3. Destruction of the specimen
4. Time and effort required for specimen preparation, and geometry digitization
Digital edge detection based on CT scans
Advantages:
1. Accuracy of cross-sectional geometry, accuracy and speed of digitisation
2. Preservation of the specimen
Disadvantages:
1. Uncertainty regarding trabecular bone orientation
2. Need access to a CT scanner

Table 46: Comparison of model generation methods. (Hart *et al.*, 1992)

Qualitative comparisons of the serial cuts and the CT scans showed that only minor positional errors (on the order of 1mm) were introduced by the CT scans (Hart *et al.,* 1992).

In the literature there have been several attempts to develop (semi)-automated methods to build up Finite Element Models from CT data. Some of these methods are characterised by direct conversion of CT image voxels to eight-node hexahedral elements. This could potentially lead to some problems such as a huge number of elements in the model (van Rietbergen *et al.,* 1999) and abrupt transitions in the model's external shape. The latter could lead to inaccurate results especially in the elements lying close to bone surface (Marks and Gardner, 1993; Camacho *et al.*, 1997).

In order to minimize this, alternative methods using data retrieved from standard clinical CT scanner to build up a smooth three-dimensional Finite Element model were used. The biggest advantage of the three-dimensional reconstruction technique is its capacity to rotate the reconstructed object in any direction, thus allowing the operator to observe it from any angle he wishes.

In the present study data retrieved from a standard clinical Computer Tomograph (Siemens Somatom Plus 4® Computer Tomograph) were used to build up a three-dimensional Finite Element Model in the preprocessor (CAD) of a Finite Element program. The Computer Tomograph used had the capacity to save all the information obtained during the imaging procedure as raw data on an optical disc, or as tiff files (i.e. type of image files) on 3.5" floppy discs. The advantage of this technique is that digitizing of the images is not required, thus avoiding further compounding method errors.

The sections were parallel in the horizontal planes and covered the area of the skull and the craniofacial complex. The next step was to create from

the coordinates of the geometric points, the 3-D Finite Element Model of the skull on which the Finite Element Analysis will be performed. Using commercial software, the raw data obtained by the Tomograph was processed and an initial mathematical model was constructed which consisted of a large number of nodes and elements (i.e. 75444 nodes and 1582833 elements) and also included a number of invalid nodes. The model of the skull created was too complex for further investigation, making it also impossible to identify the anatomical structures of the head. In order to overcome the difficulties raised from the enormous amount of data, the points that were characterised with the same z-coordinate were selected from the initial .IGES file.

Consequently, from the initial 98 sections, 51 sections were chosen to construct a new model using the following two criteriae:

1. Each section was "described" by a number of points with a common z-coordinate. Between two neighbouring points, straight lines were drawn passing through these points in order to circumscribe each section by a number of straight lines. One of the difficulties that occurred was that there was no information about the geometry of the skull between the tomographic sections. However, due to the large number of sections and the small distance between them, and taking into account the continuous character of the division of elements of the succeeding slices, it was possible to reproduce the geometry of the skull with sufficient accuracy. The distance between successive sections was 3mm except in the nasomaxillary region where the distance was 1.5mm in order to increase accuracy in the area of application of the expansion force.
2. The true anatomy of the nasomaxillary complex was respected.

The reduction of the number of sections had also another advantage, that of reducing the time required for the mathematical calculations. This spacing of CT-images enables a higher geometric accuracy. The model was then automatically divided by ALGOR® software in finite elements to

construct the mesh. The division of each section into finite elements is based on the outer geometry of the skull. The construction of the mesh was done automatically by the software where the geometry of the model was simple, by converting the lines into splines, and manually where the anatomy was more complex.

In the strain validation analysis of a dry skull, accurate thickness representation is critical to the accuracy of the Finite Element Analysis predictions. For this purpose, solid parabolic tetrahedral elements provide a dimensionally precise means to represent the nonuniform thickness of the adult cranium through the inherent geometry of the mesh. If instead, shell elements are used, the variable wall thickness can not be directly represented through mesh geometry thereby requiring a strategy of thickness assignments for all element nodes as physical property designations.

Nevertheless, for a number of CT/FEA applications, the objectives of the analyses can be efficiently served with shell elements. In the present CT/FEA analysis, for the construction of the outer surface of the skull shell-plate elements were used in a semi-automeshed model to evaluate the effectiveness of transverse expansion of the nasomaxillary complex for patients in puberty. In comparison to the dry skull, the cranial model is more architecturally complex containing various tissues with different material properties. The objectives for this clinical CT/FEA analysis also differed in that the predictions sought the overall deformation of a heterogenous nasomaxillary and craniofacial skeleton subjected to force loading from the Hyrax screw of the Rapid Maxillary Expansion appliance. Since the strain in the paediatric model was incurred largely by the flexible syndesmotic network of soft tissues connecting the cranial bones (i.e. cranial sutures), bone strain was not of great importance to the deformation of the model. Therefore, by using a shell mesh additional elements were spared for the biomechanically more important representation of the

maxillary dentition and the Rapid Maxillary Expansion appliance, as well as the craniofacial connecting sutures (Remmler *et al.,* 1998).

Shell-plate elements are plain, flat surface structures with a thickness that is very small compared to their other dimensions. In finite element modelling of a plate, what is modelled is the mid-surface which is a plane parallel to the plate surfaces that divides the thickness into equal halves. They combine bending and membrane actions (i.e. in-plane), and were chosen because they are considered superior when the number of elements is reduced, whilst brick elements as studied by Tanne *et al.* (1987), cannot describe bending effects, especially if only one element is used across the bone thickness (Işeri *et al.,* 1998). In addition, the mathematical calculations are easier when forces are applied perpendicularly to their surface. Moreover, in the present study displacements were calculated rather than strain and stress; therefore, modelling with plates results in light and economical structures. Quadrilateral elements exhibit higher accuracy than triangular elements, while triangular elements should be preferred in the part of the structure that is close to irregular boundaries. Shell elements are understood as flat plate elements used to model curved surfaces. The bone was then divided into different groups based on its mechanical properties, the separation of the various bones being at the level of the sutures. Each suture was identified by a different colour in order to make the changes in their mechanical properties during the finite element analysis of the model easier to identify.

In the latter, more detailed, construction of the Finite Element Model of the facial skeleton, automatic mesh generation techniques (ALGOR®) were used to construct the mesh of the maxilla below the level of the palatal bone and the alveolar crest. These techniques favour a combination of tetrahedral and hexahedral elements over only brick elements to create detailed models of three-dimensional systems with complex geometries. The thickness of the model was increased, according to the geometric

dimensions of the respective part so that an equivalent stiffness effect was simulated.

The tetrahedron can be viewed as an extension of the triangle in the third dimension, while the hexahedron can be considered as the counterpart of the planar quadrilateral extended in the third dimension. The hexahedral element has the same geometric shape as the eight-node brick element. They differ, however, in their theoretical formulation and computational accuracy. Commonly used tetrahedral and hexahedral elements have only three translational degrees-of-freedom per node. The accuracy of tetrahedral and hexahedral elements is increased by introducing additional nodes at mid-sides. In practical applications, use of tetrahedral elements requires some caution to develop models without leaving any "holes" in them. In general, hexahedral elements are more accurate than tetrahedral elements. Nevertheless, tetrahedral elements are more versatile since they allow modelling of intricate geometries and facilitate transition from coarsely meshed regions to finely meshed regions in a model. In most cases, combination of tetrahedral and hexahedral elements provides the optimum mesh.

The maxillary dento-alveolar arch and the model of the R.M.E. appliance were added artificially with respect to the proportional relationship of the teeth to the whole skull. In the initial Finite Element Model, the teeth were also modelled with shell elements, which is a somewhat crude idealisation but resulted in a light and economical structure. In the second Finite Element Model with the more refined mesh, brick elements were used to construct the Finite Element Model of the First Maxillary Premolars and the First Maxillary Molar teeth on which the Rapid Maxillary Expansion appliance was supported. The periodontal space of these teeth was built manually by extending the external surface of their roots by 0.25mm. Brick elements were chosen because they provide information about the variation of stresses and deformations along their thickness and, consequently, are

able to calculate bone bending and tooth rotations within the width of the maxillary alveolar crest.

The appliance device modelled in the present study simulates the type of Rapid Maxillary Expansion appliance which consists of a Hyrax screw and two symmetric acrylic halves and is banded on the anchor teeth. For the modelling of the acrylic part, brick elements were used; for the Hyrax screw, plate and beam elements were preferred.

The brick elements were chosen because the acrylic part of the appliance was considered as a homogenous material, with a thickness comparable to the other two dimensions. Moreover, solid elements can provide information about the three-dimensional variation of stresses and deformations within the component. Beam elements for modelling the Hyrax screw were chosen due to the cylindrical shape of the original and also due to their propensity to undertake shear and moment (i.e. bending) in addition to tension and compression. When solid elements are interconnected with beam or plate and shell elements, attention should be paid to preserve the rotational degrees-of-freedom at the common nodes. This can be easily achieved by artificially extending the beam and plate elements into the solid elements. The model of the Hyrax screw was given the material properties of steel in that steel possesses the highest proportion of the alloys used in its construction. The model of the R.M.E. appliance was supported on the first premolar and first permanent molar teeth.

The initial model constructed only from plate-shell elements, consisted from 3761 nodes, 4121 elements and 3906 degrees of freedom. Refinement was achieved using both automatic routines and a local smaller average element size at the level of the maxilla below the palatal bone and the alveolar crest, resulting in a new Finite Element Model of the craniofacial skeleton which consisted from 10826 nodes, 14286 elements and 47091 degrees of freedom. The accuracy of a finite element model depends on the refinement

of the mesh, and accurate results are being calculated for nodal displacements with the most refined mesh (Hart *et al.,* 1992). Other researchers (Işeri *et al,* 1998; Cattaneo *et al,* 2001) found, using a standard convergence study, that the statistical difference between the results obtained by a medium mesh (i.e. 5892 degrees of freedom; Işeri *et al,* 1998) and a fine mesh (i.e. 12882 degrees of freedom; Işeri *et al,* 1998) were not significant. Consequently, the mesh density of the present model should provide sufficiently accurate results.

Finite element analysis appears to be the most appropriate technique for analysing the complex geometric and mechanical properties of human structures. Limitations to finite element modelling in the early 1980s were due to the assumptions and approximations incorporated in those models (Krabbel and Appel, 1995). These simplifications were necessary as finite element methods and CPU possibilities were restricted. However, the human neurocranium remains a geometrically complex structure that features internal voids and branching structures and an extensive network of sutures that interconnect the bones of the craniofacial skeleton. It consists of an external cortical layer and internal cancellous bone which blend one into another rather than demarcating sharply, and vary greatly both in relative thickness and density (Melvin *et al.,* 1969; McElhaney *et al.,* 1970; Hubbard, 1971). Consequently, the computer model is limited by our detailed knowledge of the physical properties of human tissues (Middleton *et al.,* 1996). Moreover, in the present study teeth were added to the model and the various components of the Rapid Maxillary Expansion appliance. Therefore, in order to study all the biological phenomena that take place at the application of the method, a number of assumptions were made in the construction and the analysis of the finite element model developed in this study that may, in theory, lead to less precision in the results:

- In accordance with the approximations of earlier craniofacial Finite Element studies (Tanne *et al.,* 1988; 1989; 1991; 1995; Ruan *et al.,*

1994) we assumed linearly elastic and isotropic behavior for the full thickness of bone with an Elasticity modulus equal to 13700 Nt / mm^2;

- The maxilla is considered as a rigid body and consequently any bone bending while under force application is not considered;
- The entire sutural network behaves in an elastic manner, but different combinations of material properties creates individual participation in the behavior of the maxilla;
- The model was created using shell-plate elements for the bones of the skull and the sutures;
- The acrylic part of the R.M.E. appliance was modelled with brick elements with Modulus of Elasticity equal to 2000 Nt/mm^2 (Verrue *et al.,* 2001);
- The metal part of the appliance was modelled using beam elements with Modulus of Elasticity equal to 206840 Nt/mm^2 as stainless steel (4130);
- The dentition was modelled with shell-plate elements with a Modulus of Elasticity equal to 20700 Nt/mm^2;
- The skull was packed at the cranial base along the foramen magnum (i.e. all degrees of freedom were constrained) and the total mechanical load applied resulted from the expansion caused by the displacement of the midline screw of the R.M.E. appliance equal to 7.5mm.

The last assumption implies that separation of the maxillary halves is considered to be linear, the mechanical load of each turn of the screw is added algebraically to the preexistent load. In the clinical situation between each turn of the screw there is a relaxation period with consequent tissue rebound (Zimring and Isaacson, 1965), which is not taken under consideration in the initial pilot testing of the present study. Only displacements were initially calculated and not strain and stresses, because with the boundary condition of the 7,5mm opening of the Hyrax screw, the von Misses stresses developing in the craniofacial skeleton were found to reach values as high as 550 MPa (in accordance to Işeri *et al.,* 1998) but

these values are dramatically greater than the breaking point of the bone. Consequently, despite that the linear model describes the displacement pattern quite well, the stress values are not realistic and the stress relaxation has to be taken into account in future studies.

Perceived shortcomings of the model included the lack of sophistication in modelling the anatomical structures and maxillary dentition; the lack of detailed knowledge regarding the material properties of the cancellous and cortical bone, the sutures and the structural parts of the Rapid Maxillary Expansion appliance; and the difficulty of knowing how to model the boundary conditions at the sutures. Therefore, the following discussion is aimed at providing answers to the questions regarding the qualitative behavior of the maxilla to the application of simulated orthodontic-orthopaedic loads, to quantify the resultant displacements and stresses within the maxillary sutures, and to discuss the relationships of these displacements to biological phenomena such as suture separation, bone remodelling and tooth movement.

5.1.2. Clinical subjects:

The most difficult problem is establishing confidence in the validity of the computed results – within the limitations imposed by the assumptions used in the analyses. This validity can be established only by comparison of the computed results with observed and measured responses (Huiskes *et al.*, 1981; Huiskes and Chao, 1983). Using clinical correlation studies and/or experimental investigations, the computed physical deformation values could be compared to either radiological or direct craniometric measurements. Clinico-mechanical discrepancies identified in such studies would probably motivate a re-examination of material and physical property values currently referenced in the bioengineering literature (Remmler *et al.*, 1998). Nonetheless, as emphasised in recent reviews of cranial and maxillofacial

Finite Element studies (Voo *et al.*, 1996; Korioth *et al.*, 1997), expectations of high accuracy in all regions of biologic models are rarely achievable. Therefore, the specific objectives of the study must be matched to available computational resources and the mesh design and boundary conditions optimised to shift the accuracy of the model toward regions of interest (Remmler *et al.*, 1998).

In order to verify the computed results, a number of radiologic measurements were undertaken on a group of clinical subjects. The clinical subjects used were selected from a previous research project based in the Edinburgh and Fife area (McDonald, 1995).

Clinical Subjects:

The clinical subjects used in this study originated from the East of Scotland, specifically from the Edinburgh and Fife areas. They were referred to the Orthodontic departments of either the Edinburgh Dental Hospital or the Victoria Hospital, Fife by General Dental or Medical Practitioners or Hospital Specialists. The criteria for selection for the study were as follows:

1) full transverse cusp buccal crossbite;
2) no evidence of adenoidal blockage of the nasopharynx;
3) no previous tonsilar, nasal or adenoidal surgery.

In addition to these basic selection criteria, for the purposes of this study all patients required complete medical and dental records including good postero-anterior and lateral cephalometric radiographs with R.M.E. *in situ* at the end of active expansion. It was felt important that the post-expansion radiograph should include the R.M.E. appliance *in situ* because this was the only way to ensure that the changes measured were due to maxillary expansion alone and not affected by any tendency towards relapse following

the removal of the appliance. From a total of 72 cases reported previously, 49 were selected for the study.

The clinical subjects contained 28 females and 21 males aged between 10-16 years. Sex distribution is expected to have little effect in the transverse widths and ratios as seen on the postero-anterior radiographs before treatment. Previous workers have commented on the similarity in postero-anterior transverse dimensions between the sexes (Athanasiou *et al.,* 1992). However in a study of the effects of rapid maxillary expansion, differences between the sexes may prove to be important as it is known that the facial skeleton increases its resistance to expansion significantly with increasing age and maturity (Zimring and Isaacson, 1965; Bell, 1982). As girls complete puberty earlier than boys, this may affect resistance to the forces of expansion. The pattern of expansion produced by R.M.E. may be expected to vary according to skeletal maturity and this may be assumed to occur on a highly individual basis.

5.1.3. Sources of errors:

There are three main sources of error that can arise from a cephalometric study (Athanasiou and Van der Meij, 1995). These are as follows:

1. Errors arising from radiological sources and x-ray projection;
2. Errors in identification of landmarks;
3. Errors inherent in the measuring systems used.

5.1.3.1. Radiology:

In order to minimise the effect of these sources of errors all cephalometric radiographs were taken at the same centre using the same equipment and by the same radiographer. This helped reduce systematic errors arising due to differences in equipment and technique. All subjects were radiographed

in natural head posture (NHP) for both lateral and postero-anterior cephalometric radiographs. Some practical problems may arise when using NHP for postero-anterior cephalometric registrations because the patient's head faces the cassette film. This makes it rather more difficult for the patient to look into a mirror and reproduce NHP (Athanasiou and Van der Meij, 1995).

Linear and angular measurements taken from cephalometric radiographs may be affected by rotations and tilting of the head within the cephalostat. According to Ishiguro *et al.* (1976), changes of up to +10° or -10° in tilt or left and right rotations may be tolerated as the associated errors are less than the method error. As a result, minor rotations and tilting of the head may be considered negligible factors in width or breadth measurements of a postero-anterior cephalogram. The use of a single trained Radiographer aware of all these problems helped reduce errors arising from these difficulties.

5.1.3.2. Digitising System and Landmark Identification:

A commercial software package (Viewbox Version 2.60 Copyright © Demetrios J. Halazonetis) was used in this study to measure transverse widths and cross-sectional areas on the tracings.

A number of skeletal landmarks and dental landmarks were chosen as candidates for investigation for both the frontal and the lateral cephalometric radiographs from the definition file supplied with the Viewbox software. The majority of these landmarks were taken from definitions by Downs (1948), Sassouni (1955), Coben (1955), Grummons and Kappeyne van de Copello (1987), Athanasiou *et al.* (1992); Athanasiou (1995) and da Silva *et al.* (1995). All of these landmarks were found to be well defined and easily identified on the radiographs.

It proved to be difficult to find any information on landmarks within the nasal cavity which may be the reason why the effects of the R.M.E. within the nasal cavity are so poorly understood. Previous investigators have commented that expansion due to R.M.E. extends well into the nasal cavity with the fulcrum of expansion being in the region of the frontonasal suture (Haas, 1961; Wertz, 1968; da Silva *et al.,* 1995). The main basis for this assumption would appear to be based on work with dry skulls rather than being demonstrated in vivo. Timms (1974) commented that the shape of expansion within the nasal cavity may not be strictly triangular with straight sides but may have a flat base and concave or sigmoidally shaped edges if the appliance used to achieve expansion is not sufficiently rigid. Cross and McDonald (2000) in a recent study used nasal templates constructed individually for every patient in order to assess changes in width of the nasal cavity due to rapid maxillary expansion. However, these templates can be affected by minor rotations especially in head tilt and this may explain why the majority of the cross-sectional and transverse measurements had high percentage errors and were discarded. Consequently, it is possible to compare only the qualitative behaviour of the maxilla in the transversal plane during the application of the expansion forces.

5.1.3.3. Method Error Analysis:

Method error for all linear and angular measurements and cross-sectional area calculations were accomplished using duplicate tracings of the anomaly sample before treatment according to Houston (1983). Systematic error was examined using a Student's t-test of all the variables. Random error was estimated using the modification of Dahlberg's formula suggested by Houston (1983). All skeletal and dental measurements were associated with an acceptable method error of less 10%.

For the purposes of this study it was decided to use the four measurements from the PA cephalometric analysis which presented statistically significant differences in the before and after treatment analysis and were related to the transverse expansion and the separation of the two maxillary halves. The anatomical points of these four measurements were also easily reproducible on the Finite Element Model.

5.2. Interpretation of results:

Human and animal studies describing rapid maxillary expansion (Haas, 1961, 1965, 1970; Wertz, 1970, 1977; Linder-Aronson and Lindgren, 1979; Timms, 1980; Adkins *et al.*, 1990; da Silva *et al.*, 1991, 1995) attributed the increase in the transverse dimensions of the upper arch to separate orthopaedic and orthodontic effects. The separation of the maxillae by splitting the median palatine suture constitute the orthopaedic effect, whereas the lateral movement of the posterior teeth and alveolar process are reported as the orthodontic effects. In the first few days of activation, the R.M.E. would be expected to result in compression of the periodontal ligament of the posterior teeth included in the device (Bishara and Staley, 1987; Ladner and Muhl, 1995). This in turn would cause bending of the alveolar bone and tipping of the anchor teeth. Continuing force would causes the suture to open and the maxillae to move apart laterally. As the posterior teeth may be expected to be carried laterally by the separating maxillary shelves, the separate orthodontic effects produced by the R.M.E. may be difficult to dissociate from the orthopaedic movement of the maxillae.

The effect of the expansion diminishes in a cranial direction (Krebs; 1964). Wertz (1970) also reported that the final shape of the separation of the maxillary halves was non-parallel, the wider aspect being anteriorly at the ANS and significantly narrower at the horizontal part of the palatine bone. Timms (1980) reported interhamular width increase suggesting that the

maxillae, palatine bones and the pterygoid process of sphenoid move apart during expansion. The expansion observed at the interhamular level was a percentage of the observed expansion of the maxillary molars suggesting non-parallel opening of the suture. The most impressive clinical effect of R.M.E. is the creation of a midline diastema as sutural separation occurs. Haas (1961) reported that the shape of the void created by separation was pyramidal with the base of this pyramid being at the occlusal level and the apex located somewhere in the nasal cavity.

In 1961 Haas reported that the maxilla was seen to move forwards and downwards. This was subsequently confirmed by Wertz (1970) who found that the maxilla was generally displaced downwards 1 - 2 mm and forwards 1.5 mm. Krebbs (1958) used metallic implants to demonstrate the rotation of the maxilla laterally and increased nasal cavity width following rapid maxillary expansion, while Wertz (1970) estimated that the fulcrum of the rotation to be near the frontonasal suture.

The anatomy of the midface is complex and the maxillae articulate with ten different bones within the facial structure and the anterior and middle cranial base. This complexity is responsible for the pyramidal shape of the expansion both anteroposteriorly and vertically. This was supported by findings of other workers (Wertz, 1970; da Silva *et al.*, 1995). Starnbach *et al.* (1966), demonstrated that during the early phases of R.M.E., the frontonasal, zygomatico-temporal and zygomatico-maxillary sutures all showed signs of increased cellular activity. Bishara and Staley (1987) suggested that the main resistance to mid-palatal suture opening is probably not in the suture itself, but in the surrounding structures in the sphenoid and zygomatic bones. Kudlick (1973) proposed that the sphenoid was the source of most of the resistance to lateral movement of the maxillae. He maintained that the pterygoid plates of the sphenoid limited the ability of the palatine bones to separate at the median palatine suture. Although bilaterally placed they are a single structure and do not have a suture. As

a consequence the pterygoid plates can only bend as a result of the expansion. Resistance to bending of the pterygoid plates is thought to increase as one approaches the cranial base (Timms, 1980). The zygomatic complex also offers some resistance to expansion (Haas, 1961) but these structures are thought to remodel and adjust to their expanded positions (Krebs, 1964).

The results, obtained with the present Finite Element Model, even though boundary conditions were at the upper and lower limits of the clinical situation for easier identification of the changes produced, were qualitatively similar when compared with the studies mentioned above.

After completing the construction of the Finite Element mesh, the model was introduced in a Computer Aided Engineering (CAE) software (ALGOR®), material properties were attributed (**Table 10**) and boundary conditions were applied. All degrees of freedom were constrained at the level of the occipital bone and foramen magnum and displacement in the transversal plane equal to 3.75mm was applied to each of the two acrylic halves of the R.M.E. appliance (**craniofacial.esd**). The calculated displacements at the four measuring points showed no statistical agreement with the homologous clinical measurements (**Table 9**), but however, there was qualitative similarity between clinical situation and the Finite Element Model predictions. Hence, the maxilla appears to expand in a pyramidal manner with the base of the pyramid at the level of maxillary dentition and the apex at the superior part of the nasal cavity, and with the maximum opening at the level of the incisor teeth and decreasing posteriorly.

In this initial approach, the thickness of the bone was measured automatically by the CAD software when the CT scans were introduced into the computer program. The measurements were taken at different points of each anatomical structure and a mean value was attributed to the

whole bone structure. However, these values were different than those measured later directly with a Vernier Gauge on the same dry skull (**Table 12**). The differences observed between the two measurements are due either to anatomical variation between different individuals, or to method error. The source of the method error can be either differences in the measuring points between the manual method and the computer software or due to scaling during the transfer of the electronic data from the optical disc of the computer tomograph to the CAD software (ALGOR).

Consequently, the first parameter to be tested was the effect of the thickness of the bone and of other anatomical structures on the qualitative and quantitative behaviour of the Finite Element Model of the nasomaxillary complex.

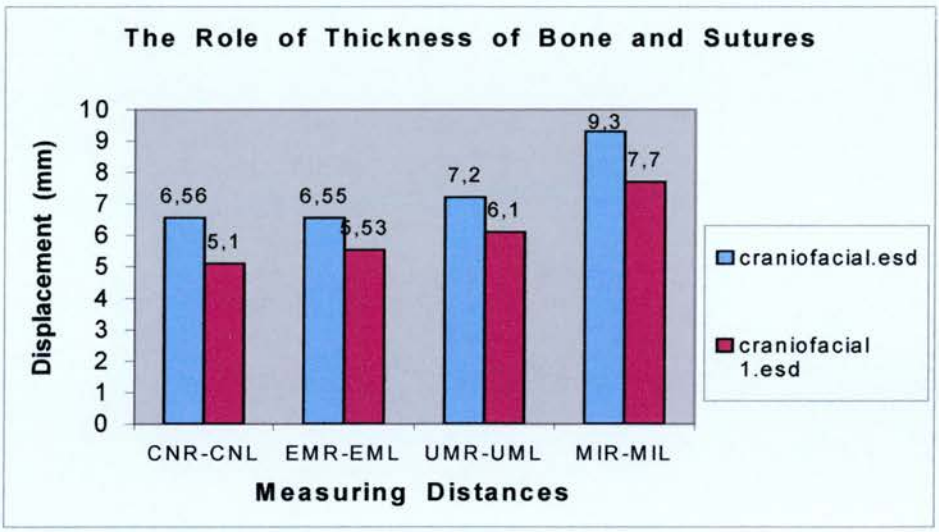

Fig. 58: Comparison between **craniofacial.esd** and **craniofacial 1.esd**

The statistical significant differences observed between the results of the two Finite Element Analysis (**Figure 58**) showed that when a mean value is attributed to the thickness of the various anatomical structures (i.e. model geometry), a systematic method error is introduced at the calculations which

distorts the results, while the qualitative behaviour of the nasomaxillary complex remains similar to the clinical situation. This systematic method error is due, firstly, to the fact that the bone thickness is variable throughout even in the same anatomical structure, and secondly, to the assumption that bone behaves like an isotropic material which does not take into consideration in the construction of the model the proportion between cortical and cancellous bone with different material properties. Therefore, when it was attempted to use the values for thickness of the bone as resulted from the manual measurements (**craniofacial 1.esd**), the displacements calculated at the four measuring distances are smaller and closer to the clinical findings, but, still outside the confidence interval. It can be suggested that model geometry plays an important role in the quantitative behaviour of the F.E.M., but is also influenced by other parameters.

Brin and associates (1981) in their study on cats, concluded that bone cells of old animals are less responsive to tensile forces than the corresponding cells in young animals. Moreover, although the edges of the expanded sutures in young animals showed layers of newly deposited bone, the same areas in adult animals were either devoid of new bone or showed minute amounts of new bone. In adult subjects forces are transmitted much more to the surrounding tissues because of the firm bony architecture and forces are divided over a larger sutural area because of the interdigitations (Wagemans *et al.,* 1988).

The next parameter to be tested was the effect of the various nasomaxillary sutures and the level of their ossification, hence, the importance of age in the clinical application of the R.M.E. technique. However, not yet clearly evidenced, due to human dissimilarity, is the exact level of ossification of each of the complex network of craniofacial sutures at the beginning of the Rapid Maxillary Expansion. Therefore, firstly, it was attempted to extrapolate the two extremes (i.e. all craniofacial sutures totally unossified –

craniofacial 1.esd; and all craniofacial sutures totally ossified – **craniofacial 2.esd**) in between which is reality (all other parameters being equal) (**Figure 59**).

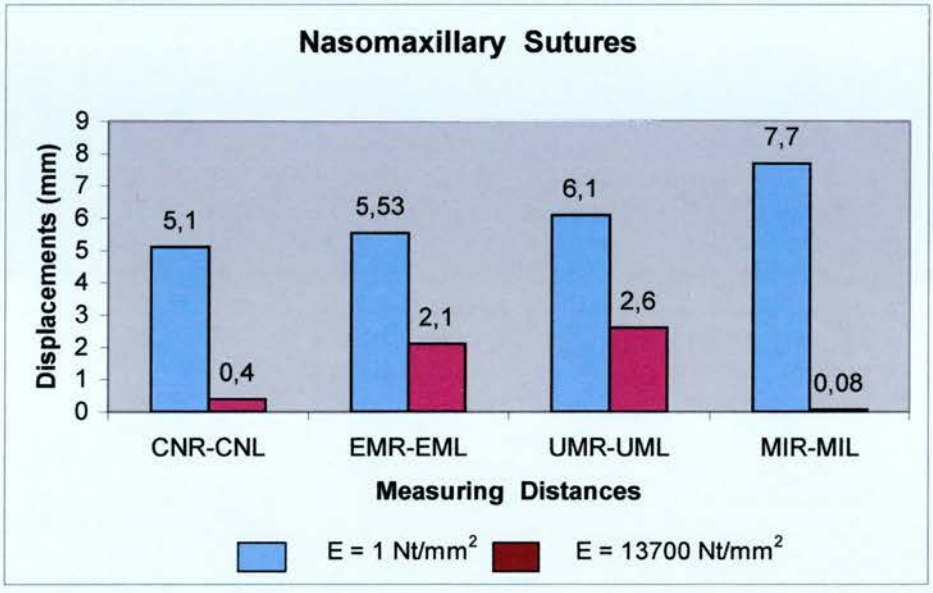

Fig. 59. Comparison between craniofacial 1.esd (E = 1 Nt/mm²) and craniofacial 2.esd (E = 13700 Nt/mm²)

It is evident that the expansion of the nasomaxillary complex was significantly less, with the exception of the points UMR-UML and EMR-EML. This can probably be explained by the fact that the R.M.E. device is attached to the maxillary first molars and the heavy expansion force applied directly to these teeth causes some tooth tipping, as well as bending of the alveolar bone in the posterior region. This can also be justified by the observation that, whilst in the Finite Element Analysis of the previous two models, the measuring expansion at the points CNR-CNL and EMR-EML was equal, in the third model there is a statistically significant difference between these two measurements, suggesting that when all sutures are considered ossified there is almost no expansion in the nasal cavity, only bending of the alveolar bone.

The morphology of the skeleton is known to reflect functional demand. The von Misses stress expresses the overall stress intensity, and its distribution gives an impression of the overall load transfer (Cattaneo *et al.,* 2003). Consequently, from the stress distribution observed in the Finite Element Model of the skull (**Figure 23**) and the way it is dissipated towards the postero-inferior part of the skull and away from the point of application of the heavy orthopaedic expansion forces, it can be inferred that the sutures play an important role as stress absorbers (Pritchard *et al.,* 1956). This function may be employed by the fibrous capsules surrounding the cambial zones. Moreover, the great vascularity of the middle zone might, in addition, serve as a hydrostatic cushion between the ends of the bone reinforcing the other protective measures against undue tensile mechanical stresses. Dissipation of forces is also observed but in a much reduced intensity in cases where all sutures are considered ossified (**Figure 27**). This could probably be explained by the nature of bone structure of the craniofacial complex. Within the irregular bones of the nasomaxillary complex, the cavity is filled with bony spicules arranged along the lines of the principal tensile and compressive stresses. Consequently, stresses are distributed along the areas which contain large proportions of cancellous bone and decrease rapidly in the areas which are constructed mainly by cortical bone (Johnson and Moore, 1997).

Then, it was attempted to assess separately the behavior each of the circummaxillary and midsagittal sutures in reaction to the expansion forces produced by the R.M.E. appliance.

Firstly, the frontal part of the midpalatal suture between the maxillary central incisors was studied in three different Finite Element Models (craniofacial 3.esd – craniofacial 5.esd). In each model it was given a different modulus of elasticity which represent different grades of maturation of the suture. During the Finite Element Analysis all other

circummaxillary sutures were considered not ossified in order to reduce the calculation time required from the computer software to perform the Finite Element Analysis (**Figure 60**).

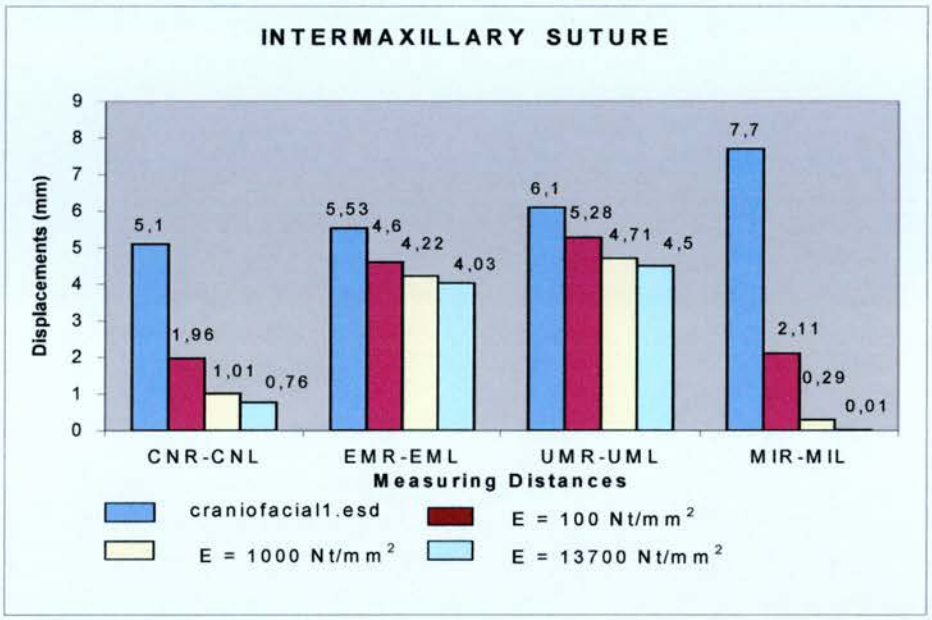

Fig. 60. Comparison between craniofacial 1.esd and craniofacial 3.esd (E = 100 Nt/mm²) – craniofacial 4.esd (E = 1000 Nt/mm²) – craniofacial 5.esd (E = 13700 Nt/mm²)

It is now accepted that the level of maturation of the sagittal suture between the maxillary central incisors plays an important role in the splitting of the anterior part of the maxilla, while the posterior part of the maxilla in the molar area (i.e. distances EMR-EML and UMR-UML) is least affected by that suture.

However, the diastema measured between the maxillary central incisors was greater than the uppermost limit of the confidence interval. The role of the transeptal fibers in the separation of the crowns of the incisors was discussed and it was thought that they impede the movement of the

crowns. Therefore, an attempt was made to simulate their effect by splitting the frontal part of the midpalatal suture in three groups and by giving different material properties in the lower occlusal third group (i.e. Egr=123) (**Figure 61**).

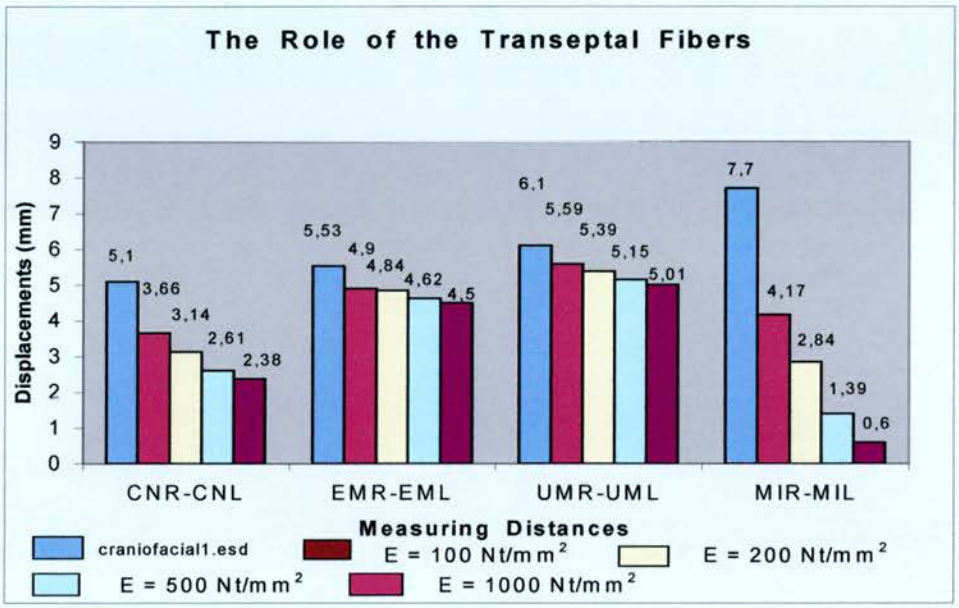

Fig. 61. Comparison between craniofacial 1.esd and craniofacial 6.esd (Egr123 = 100 Nt/mm²) – craniofacial 7.esd (Egr123 = 200 Nt/mm²) – craniofacial 8.esd (Egr123 = 500 Nt/mm²) – craniofacial 9.esd (Egr123 = 1000 Nt/mm²)

From the results of the Finite Element Analysis of the these four models it can be concluded that the transeptal fibres play an important role in inhibiting the separation of the crowns of the maxillary central incisors. In order to quantify this effect, however, the material properties, the physical characteristics and the clinical behaviour of all structures involved in the phenomenon must be defined. From the statistical analysis of the results it is suggested that models craniofacial 8.esd and craniofacial 9.esd are within the confidence interval of the clinical findings in three measurements (except UMR-UML). In order to decide on which model further Finite

Element Analysis will be applied, an attempt was made to compare the proportionality of the displacements. Finite Element Model **craniofacial 8.esd** (i.e. Egr 123=500Nt/mm²) presented the more symmetric displacements and therefore it was chosen to proceed with the analysis of the behaviour of the craniofacial complex during R.M.E. However, due to the number of assumptions made at the construction of the model, this is just an indicative value which suggests only that transeptal fibres possess different properties and characteristics than neighbouring structures and that they influence the separation of the crowns of the maxillary central incisors.

Another critical factor involved in the response of the maxilla to the expansion forces produced by the R.M.E. appliance is thought to be the midpalatal suture from the alveolar crest to the transverse palatal suture. Therefore, different material properties were attributed to that suture, from completely immature to completely ossified (i.e. craniofacial10.esd to craniofacial12.esd) (**Figure 62**).

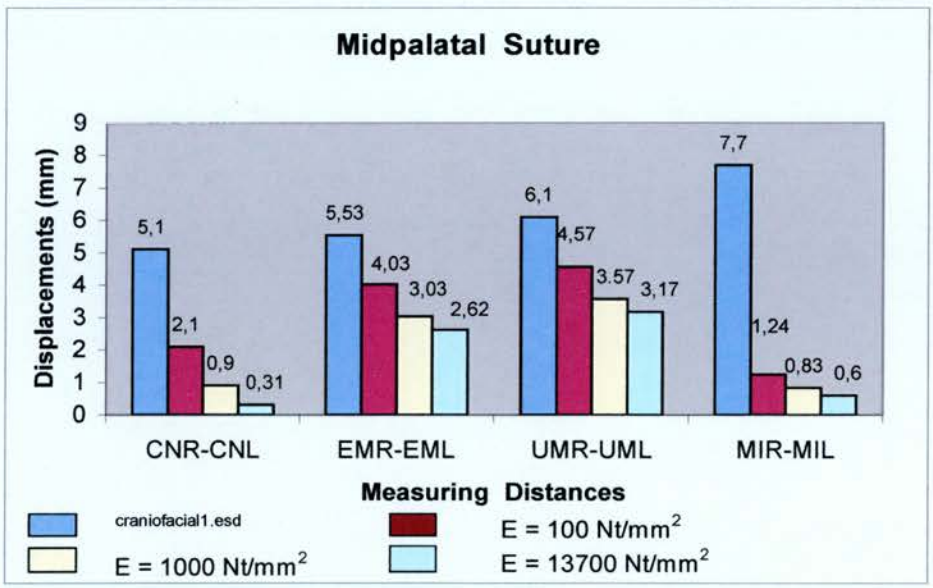

Fig. 62. Comparison between craniofacial 1.esd and craniofacial 10.esd (E = 100 Nt/mm²) – craniofacial 11.esd (E = 1000 Nt/mm²) – craniofacial 12.esd (E = 13700 Nt/mm²)

Even though in all three Finite Element Models the displacements measured are within the confidence interval (except for the UMR-UML), it is clearly evident that the less ossified the midpalatal suture the wider the expansion achieved. Moreover, in craniofacial 10.esd, where the suture is considered not ossified (Egr 7 = 100 Nt/mm^2), the difference measured for the distance UMR-UML is closer to the confidence interval of the clinical findings, while in the other two models it deviates significantly from that interval. It can be concluded that the earlier the treatment starts the more favourable skeletal response to expansion of the two maxillary halves occurs. This finding is in accordance with the clinical findings by other investigators who have reported difficulties in producing a separation of the maxillae at the midpalatal sutures during rapid expansion in adolescents who passed their pubertal growth spurts (Isaacson and Murphy, 1964; Krebs, 1964; Haas, 1965; 1970; Wertz, 1970). Increased resistance to expansion forces with increasing age is thought to be related to greater rigidity of the facial skeleton, and the morphology within the midpalatal suture may also contribute to increased resistance in older patients. Although this suture in human beings remains patent up to third or fourth decades of life, as early as 12 to 13 years of age bony interdigitations begin to form a mechanical interlocking of the maxillary segments (Melsen, 1972; 1975). As a result, separation of the maxilla by mechanical forces in young adolescents and adults would require the fracturing of these bony interdigitations (Hicks, 1978).

Another structure within the maxillary palate is the transverse palatal suture which is parallel to the vector of the expansion force applied by the R.M.E. appliance. Therefore it is important to investigate if the degree of its maturation affects the expansion produced by the appliance (**Figure 63**).

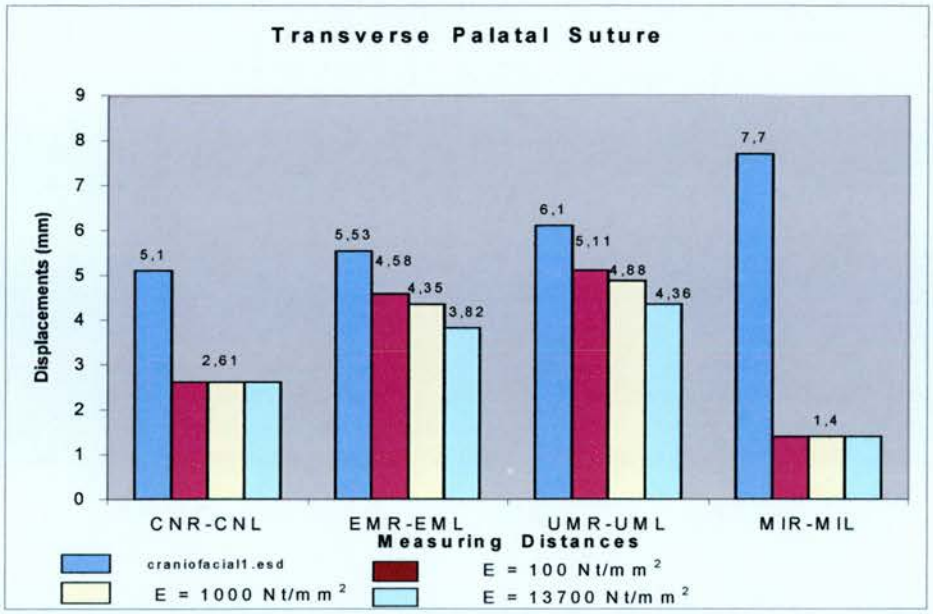

Fig. 63. Comparison between craniofacial 1.esd and craniofacial 13.esd (E = 100 Nt/mm²) – craniofacial 14.esd (E = 1000 Nt/mm²) – craniofacial 15.esd (E = 13700 Nt/mm²)

The differences in the displacements measured in the three distances (except UMR-UML) are within the confidence interval; the separation of the anterior part of the maxilla and the nasal cavity remain unaffected by the degree of ossification of the transverse maxillary suture. The posterior part of the maxilla is, however, influenced by the degree of maturation in the same manner as the other sutures studied. In other words, the greater the ossification, the less the separation of the two maxillary halves. Moreover, if the transverse palatal suture is considered completely ossified (i.e. Egr 120 = 13700 Nt/mm²), the separation of the midpalatal suture is not in a pyramidal manner and the greater displacements are observed in the dental arch (**Figure 21** & **Figure 29**).

Following this conclusion, an attempt was made to assess the importance of the circummaxillary sutures to the clinical response of the nasomaxillary

complex in relation to the force produced by the R.M.E. appliance. The suture of the maxillary bone with the lacrimal bone and the maxillo-frontal suture appear to have no significant influence in the separation process of the two maxillary segments. The naso-maxillary suture influences the separation within the nasal cavity as it is evidenced by the difference measured in the displacement of CNR-CNL.

Other important structures are considered to be the articulation of the pterygoid process of the sphenoid bone with the perpendicular plate of the palatine bone and the zygomatico-maxillary suture. Both have been incriminated as the major impediments in the separation of the maxilla and in particular in the non-parallel manner of its separation. Wertz (1970) suggested that the pterygoid plates of the sphenoid bone and the zygomatic arch offer the main resistance to the expansion force applied inferior to this buttressing and consequently minimizes dramatically the ability of the palatine bone to separate at the mid-sagittal plane. Timms (1980) suggested that the pterygoid plates can bend only to a limited extent as pressure is applied to them, and their resistance to bending increases in the parts closer to the cranial base. In skull material, it has been shown that the heavy interdigitation of the osseous surfaces between the palatine bone and the maxilla, and the pterygoid processes of sphenoid bone makes disarticulation difficult in the late juvenile and early adolescent periods (Melsen and Melsen, 1982). Işeri *et al.* (1998), on the other hand, showed that the inferior and middle parts of the pterygoid plates markedly displace or bend laterally, and high stresses develop particularly at the superior parts of the pterygoid plates of the sphenoid bone in the region close to the cranial base where the plates are more rigid.

The results of the present Finite Element Analysis suggest although, that the pterygoid processes of the sphenoid bone do not affect significantly the behaviour of the maxilla when different material properties are assigned to

the articulation since there is no difference in the displacements measured (**Figure 64**).

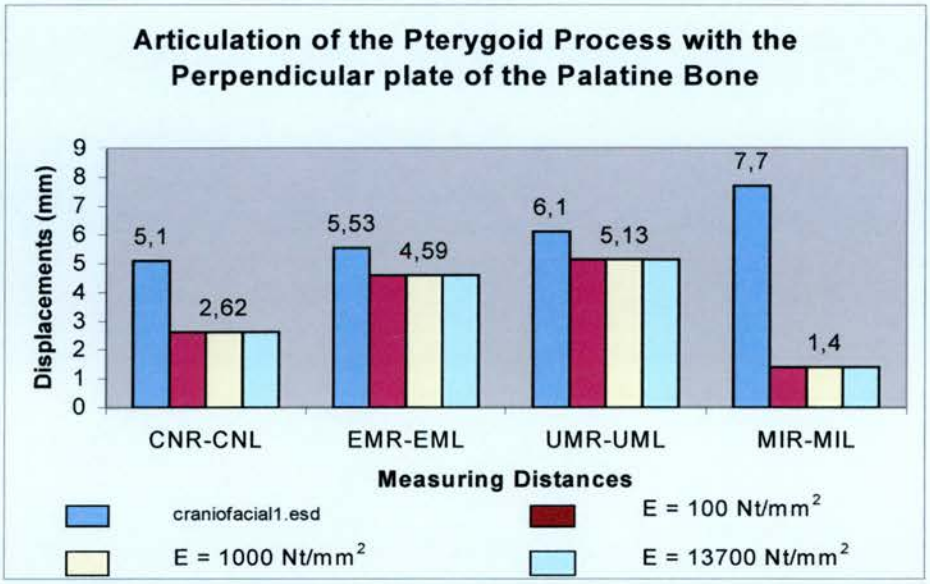

Fig. 64. Comparison between craniofacial 1.esd and craniofacial 25.esd (E = 100 Nt/mm²) – craniofacial 26.esd (E = 1000 Nt/mm²) – craniofacial 27.esd (E = 13700 Nt/mm²)

Unlike the articulation of the pterygoid process of the sphenoid bone with the perpendicular plate of the palatine bone, the zygomatico-maxillary suture and the zygomatic bone appear to be the main buttresses against the lateral movement of the maxillary halves especially in the molar region. Even though the maximum expansion posteriorly is achieved when the suture is considered not ossified, theoretically at the age of the treatment onset the suture is completely ossified, therefore **craniofacial 30.esd** model is considered as to be closer to the clinical situation (**Figure 65**).

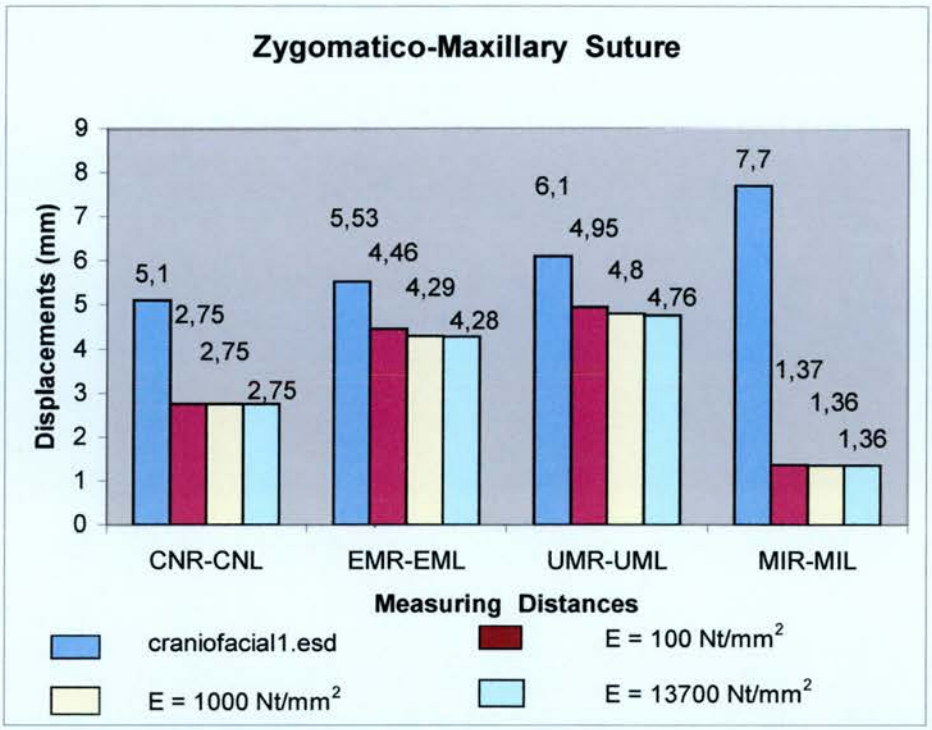

Fig. 65. Comparison between craniofacial 1.esd and craniofacial 28.esd (E = 100 Nt/mm²) – craniofacial 29.esd (E = 1000 Nt/mm²) – craniofacial 30.esd (E = 13700 Nt/mm²)

At this point, in order to continue the study, a first overall review of the Finite Element Analysis took place. In the case of the material properties of the various structures as shown by the comparison of the clinical findings and the findings from the Finite Element Model and presented in the **Table 47**, the qualitative behaviour of the maxilla is similar to that as described in the literature. The greatest widening was observed in the dento-alveolar areas, gradually decreasing through the upper structures (**Figures 31 - 32**). The separation of the two maxillary halves takes place in a pyramidal manner with the base of the pyramid at the level of the maxillary dentition and the apex at the superior part of the nasal cavity (**Figure 30**). The maxillary halves are displaced forward and downward with a degree of rotation around the axis of symmetry with the centre of

rotation located near the fronto-maxillary suture (Krebs, 1958; 1964; Haas, 1961; 1970; Wertz, 1968; 1970). The midpalatal suture expands, also in a pyramidal manner, with the widest part being anteriorly between the maxillary central incisors and the apex being posteriorly at the level of the transverse maxillary suture (Zimring & Isaacson, 1965). The separation of the maxillary halves is asymmetrical (Kudlick, 1973). Fried (1971) and Haas (1961, 1965) reported that the palatine processes of the maxilla were lowered as a result of the outward tilting of the maxillary halves, while on the other hand, Davis and Kronman (1969) noted that the palatine processes remained at their original height. However, neither of these findings can be supported by the present study because, one of the inherent difficulties of the study was the selection and definition of comparable measuring points between the cephalograms and the Finite Element Model in the area of the palate.

DESCRIPTION	COLOR-GROUP	THICKNESS (mm)	MODULUS OF ELASTICITY (Nt / mm^2)	POISSON's RATIO
Cranial Bones	1	14	13700	0.3
Teeth	2	18.5	20700	0.3
Acrylic	3	-	2000	0.3
RME (plate)	4	2.5	206840	0.3
RME (beam)	5	D=2, t = 0.5	206840	0.3
Cartilage of Nasal Cavity	6	0.5	13700	0.3
Midpalatal Suture	7	3	1	0.3
Palatal Bone	8	3	13700	0.3
Zygomatic Bone	10	10	13700	0.3
Pterygoid Process of the Sphenoid Bone	11	6	13700	0.3
Maxillary Bone *	16	8	13700	0.3
Maxillary Bone **	17	19.5	13700	0.3
Nasal Bone	14	8	13700	0.3
Maxillo-zygomatic Suture	13	8	13700	0.3
Naso-maxillary Suture	40	8	1	0.3
Temporo-maxillary Suture	100	8	1	0.3
Suture between the maxilla and the Lacrimal Bone	15	8	1	0.3
Suture between the maxilla and the pterygoid process of the sphenoid bone	80	6	1	0.3
Transverse palatal Suture	120	3	1	0.3
Midsagital Suture***	12	8	1	0.3
Midsagital Suture****	121	19.5	1	0.3
Midsagital Suture *****	122	19.5	1	0.3
Midsagital Suture ******	123	19.5	500	0.3
* Maxillary bone above the level of palatal bone.				
** Maxillary bone at the level of the alveolar crest.				
*** Sagittal suture at the nasal third (Fig. 28)				
**** Sagittal suture at the occlusal third (Fig. 28)				
***** Sagittal suture at the occlusal third (Fig. 28)				
****** Transeptal Fibers (Fig. 28)				

Table 47. Material properties assigned to the various components of the Finite Element Model of the craniofacial complex (**craniofacial 30.esd**)

Various investigators have shown that there is an increase in the width of the nasal cavity following expansion, particularly at the floor of the nose (Haas 1961; 1965; 1970; Wertz 1970). As the maxillae separate, the outer walls of the nasal cavity move laterally. The nasal cavity width gain averaged 1.9mm, but can widen as much as 8-10mm at the level of the inferior turbinates (Gray, 1975), while the more superior areas might move laterally (Pavlin and Vukicevic, 1984). Wetrz (1968) and McDonald (1995) confirmed the advantage of rapid palatal expansion in improving nasal air flow in patients with stenosis of the nasal airway. A numerical approach of the changes induced at the various levels of the nasal cavity in the present Finite Element Analysis, demonstrated that the width at the floor of the nose increased markedly compared with the superior parts (**Table 48**).

	Before RME	**After RME**	**Displacement**
At the alveolar crest between maxillary central Incisors.	1.65mm	9.54mm	7.89mm
At the midsagital suture at the floor of the nasal cavity.	3.08mm	8.17mm	5.09mm
CNR-CNL	22,59mm	27.33mm	4.75mm
At the middle part of the nasal cavity.	11.96mm	14.70mm	2,75mm
At the apex of the lateral wall of the nasal cavity.			0mm

Table 48: Displacements calculated in the nasal cavity of the Finite Element Model of the dry skull after Rapid Maxillary Expansion

It can be suggested that in order to maximize the expansion produced as the result of the orthopaedic force applied by the jackscrew device, the maxillary sutures should ideally be not ossified. However, the level of ossification of the midpalatal and the transverse palatal suture, as well as the zygomatico-maxillary suture, can be encountered for the V-shape separation of the two maxillary halves. In particular, the present study suggests that the main resistance to the expansion force is applied inferior to the zygomatic process and consequently minimizes dramatically the ability of the palatine bone to separate at the mid-sagittal plane. In general terms, it is a fortunate circumstance that this resistance is present, as pure parallel opening would move the frontal process of the maxilla bodily into the orbital cavity (Wertz, 1970).

By comparing the findings of the **craniofacial 30.esd** Finite Element Model of the skull and the clinical findings as resulted from the pre- and post-treatment postero-anterior cephalograms, it is concluded that displacements of points CNR-CNL, EMR-EML and MIR-MIL are greater in the Finite Element Analysis model than in the clinical situation but are within the confidence interval for $p<0.05$ and analogous if a proportional approach to the findings is attempted (**Table 49**).

	FEM	CLINICAL	FEM/CLINICAL
CNR-CNL	2,75	1,66	2,75/1,66 = **1,65**
EMR-EML	4,28	2,47	4,28/2,47 = **1,73**
MIR-MIL	1,36	1,08	1,36/1,08 = **1,26**
UMR-UML	4,76	8,89	4,76/8,89 = **0,53**

Table 49: Comparison between the clinical findings and the results of the Finite Element Analysis

In contrast to the previous three measuring distances, the difference in the displacement for the points UMR-UML is less than in clinical situation and outside the lower limit of the confidence interval. There is a difference in the qualitative and quantitative behavior of points UMR-UML.

Byrum (1971) and Hicks (1978) in their research noticed that maxillary central incisors and molars showed some extrusion. In the present study, however, only transverse displacements were calculated and consequently no conclusions can be drawn for any displacements in the other two spatial directions. Moreover, the Rapid Maxillary Expansion appliance used in the clinical study was a fixed split acrylic appliance anchored with bands on the posterior teeth and at the end of treatment postero-anterior cephalograms were taken with the appliance *in situ*, so effectively it would have been very difficult either to produce or to measure any vertical displacements of the buccal teeth.

In conclusion, it can be suggested, that the separation of the maxillary halves is a multifactorial phenomenon in which a large number of parameters are involved. Here, it should be emphasized that the statistical analysis of the results is used only as a study tool with the main purpose to make feasible the comparison between the clinical reality and the mathematical model, in other words, to control the validity of the Finite Element Model. However, this difference in the values between the Finite Element Method and clinical results can be explained by the systematic method errors introduced by the number of assumptions made at the construction of the Finite Element Model and by the fact that a dry skull was used to obtain the geometry and the thickness of the various anatomical structures of the skull instead of individual CT scans obtained from the clinical subjects involved in the study.

The geometry of the model and the thickness of the bony structures influences the quantitative behavior of the Finite Element Model. In this context, in order to facilitate the construction of an otherwise sufficiently complex model, initially, the outer geometry of the dry skull was used because it was easier identified from the CT sections, and not the mid-surface of the structures as the plate element theory defines. Another

parameter which influences the quantitative behavior of the Model and is not included in the first part of the mathematical analysis of the present study is the combination of cortical and cancellous bone in the bony structures of the craniofacial skeleton.

Consequently, and in order to overcome these inaccuracies of the Finite Element Model, some structural modifications were made to the Finite Element Model. Composite elements were used for the construction of nasomaxillary complex in order to give different material properties for the two different types of bone. The nasomaxillary complex was created with a combination of plate and brick elements. An outer and an inner layer were constructed using plate elements to simulate the cortical plates of the nasomaxillary complex and the space between them was filled with brick elements to simulate the cortical bone. This modification did not alter the values of thickness for the various bony structures of the Model from these obtained from CT scans and used in craniofacial 1.esd, but made easier the construction of the new Finite Element Model of the teeth and the periodontal ligament. This however, did not confer any significant change in the displacements of the measuring distances, as it can be seen in the following **Table 42**. This can be explained by the lack of knowledge relating to the extent of the cancellous bone and the thickness of the cortical layer which added systematic errors in the Finite Element Analysis.

The diastema created between the maxillary central incisors is greatly influenced by the existence of the transeptal fibers and their mechanical properties, while on the other hand, maxillary central incisors in the clinical group present a degree of anterior crowding due to the narrow skeletal bases. The difference observed for the distance UMR-UML between the clinical and the mathematical analysis findings, could be explained by the fact that the Finite Element Model does not take account of the tipping of the maxillary molar tooth within the periodontal ligament as the result of the heavy force applied palatal to the crown of the tooth from the

jackscrew of the Rapid Maxillary Expansion appliance (**Figure 66**). From the early years of this therapy it was believed that one possible mechanism for maxillary expansion was that, firstly, the appliance compresses the periodontal ligament, then bends the alveolar process, tips the anchor teeth and gradually opens the midpalatal suture (Derichsweiller, 1953).

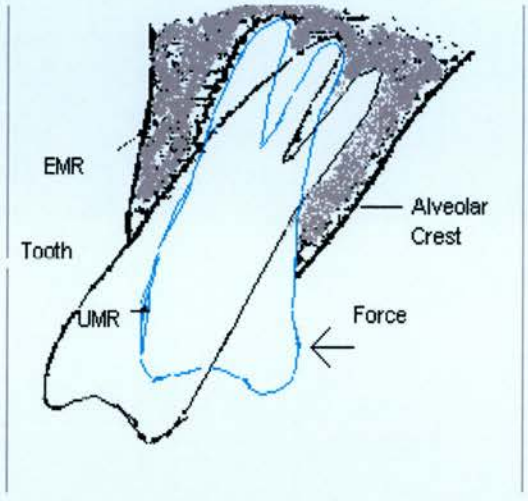

Fig. 66. Tipping of the tooth within the periodontal ligament

In order to overcome this problem the anchor teeth of the Rapid Maxillary Expansion appliance were remodelled with their correct anatomy using brick elements and introduced in the reconstructed maxilla. Moreover, the periodontal ligament of these teeth was also modelled (**Figure 13**) (Kronfed, 1931; Coolidge, 1937).

However, one should not forget the assumption made which implies that separation of the maxillary halves is considered to be linear, the mechanical load of each turn of the screw being added algebraically to the preexistent load omitting the relaxation period with consequent tissue rebound which exists in the clinical situation between each turn of the screw (Zimring and Isaacson, 1965), and is not taken into consideration in the initial calculations of the present study.

Clinically, stress relaxation is characterized as a sharp elevation in tissue resistance force during the period of mechanical loading followed by a decay of this force until the next increment of activation. When an attempt was made to add into the Finite Element Analysis the parameter of the relaxation period, it was concluded that it is closely related to the linearity of the maxillary expansion and influences significantly the displacements and the force distribution to the nasomaxillary and cranial structures.

Even though, the dry skull cannot reliably be used as a model to simulate the initial bone displacement *in vivo* (de Clerck *et al.,* 1990), it can still provide us with valuable qualitative information regarding the skeletal changes caused by the procedure. All craniofacial bones directly articulating with the maxilla were displaced to a lesser or greater degree, except the sphenoid bone, a finding which is in accordance with Kudlick's research (1973). Furthermore, all craniofacial sutures that are orientated perpendicular to the vector of the expansion force were separated. Similar findings were observed by Gardner and Kronman (1971) in their study in rhesus monkeys.

In **Figures 39 - 42** the findings of the FEA of the two Finite Element Models, with and without the relaxation period, and these of the *in vitro* experiment were presented. For comparative purposes in all three cases, 7 turns of the screw were considered (limiting factor is the 7 turns of the screw that were carried out on the dry skull). From these graphics it can be concluded that the curve of the dry skull is closer to the linear curve of the Finite Element Model when relaxation period is not taken into consideration, except for the measuring points MIR-MIL. This is not unexpected, because the dry skull, due to the lack of soft tissues and viability in general terms, does not present the tissue rebound phenomenon and each load is added algebraically to the preexistent force.

The displacement observed at the points MIR-MIL is greater at the dry skull than in the Finite Element Analysis due to the fact that the midsagittal suture separates first and unopposed at the dry skull under the expansion force of the Hyrax screw. These points represent dental points and their movement is influenced by the movement of the alveolar crest and by the existence of transeptal fibers which are not present at the dry skull.

The issue is therefore, to decide which of the two Finite Element Models simulates better the clinical situation. From a closer view it can be suggested that the Finite Element Model which takes into consideration the relaxation period simulates better the clinical reality, but when it was attempted to use mathematical extrapolation in order to calculate for this model the expansion for 30 turns of the screw, a large discrepancy between the clinical and this Finite Element Analysis numerical findings occured (the white arrow indicating the clinical findings) (**Figure 67 - 70**).

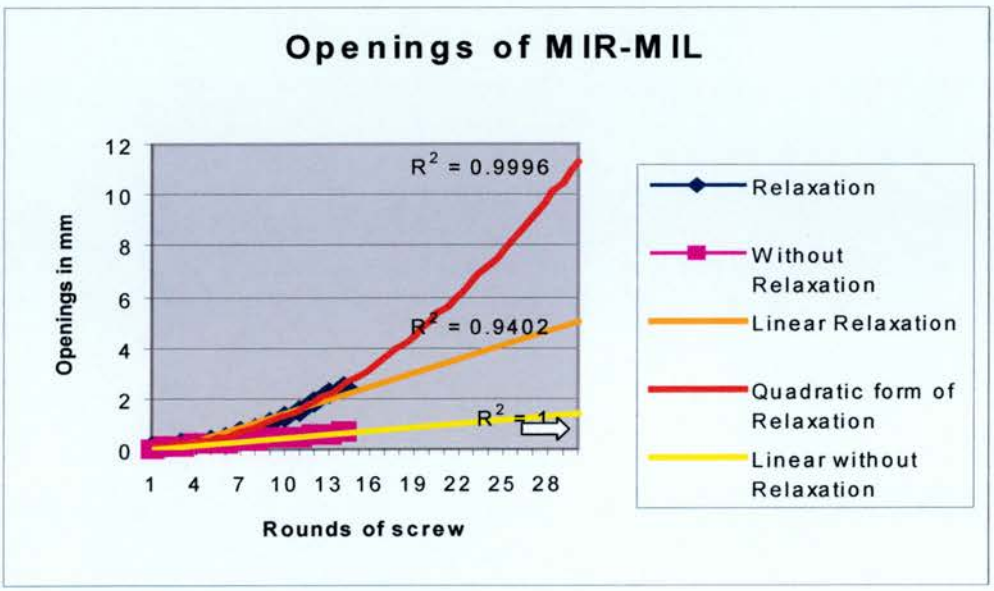

Fig. 67. Graphical presentation of mathematically calculated expansion for points MIR-MIL when tissue relaxation is taken under consideration into the Finite Element Analysis.

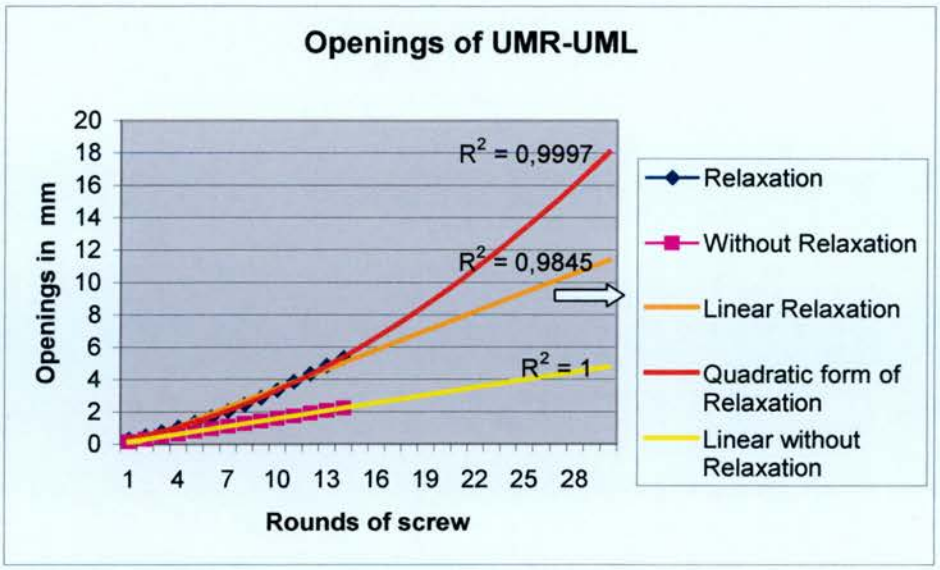

Fig. 68. Graphical presentation of mathematically calculated expansion for points UMR-UML when tissue relaxation is taken under consideration into the Finite Element Analysis.

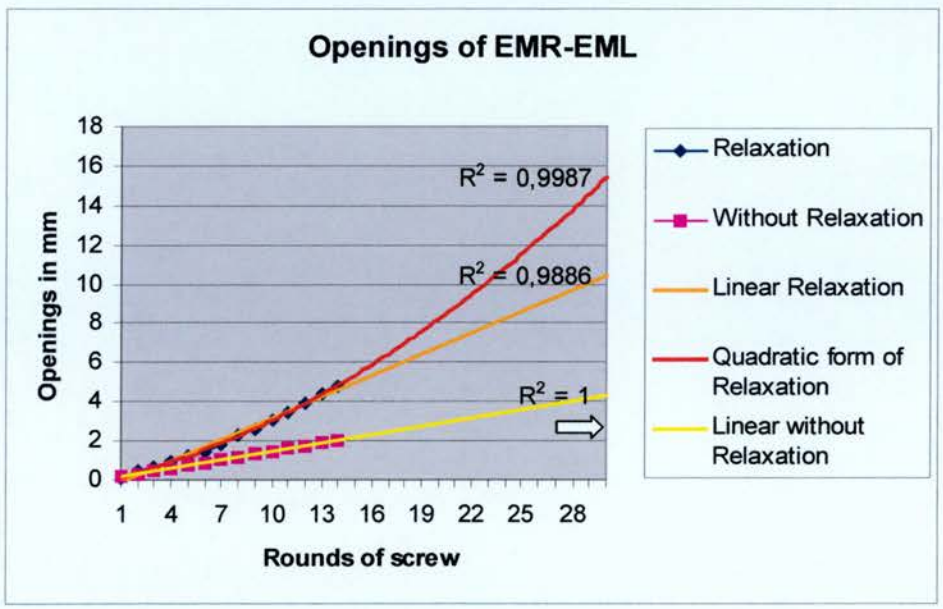

Fig. 69. Graphical presentation of mathematically calculated expansion for points EMR-EML when tissue relaxation is taken under consideration into the Finite Element Analysis.

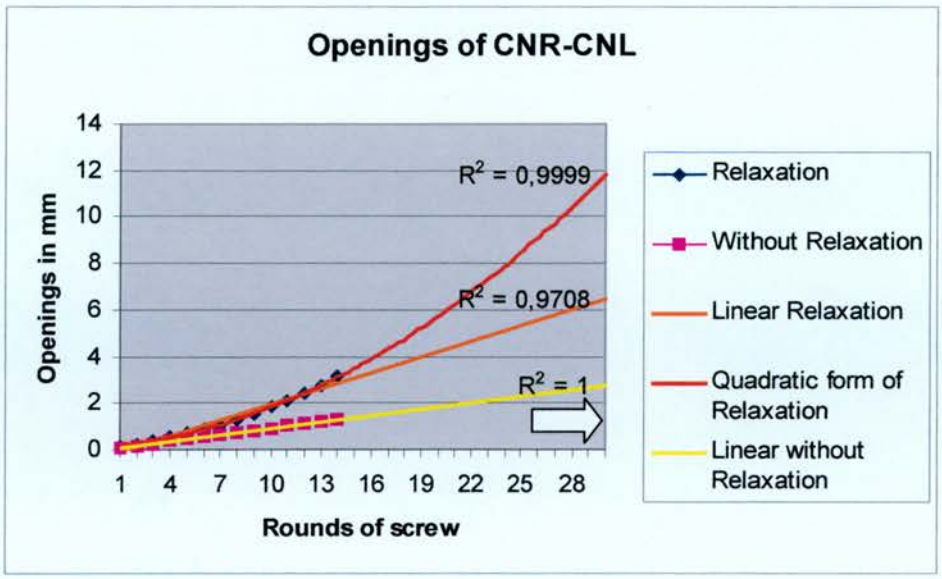

Fig. 70. Graphical presentation of mathematically calculated expansion for points CNR-CNL when tissue relaxation is taken under consideration into the Finite Element Analysis.

The differences observed at the magnitude of the displacements at CNR-CNL, EMR-EML, UMR-UML and MIR-MIL between the clinical measurements and the findings of the model which simulates the phenomenon of relaxation (craniofacial 44.esd), can be explained by the fact that clinically, between each turn of the screw, forces are not completely eliminated as was observed by Isaacson *et al.* (1964) (**Table 50**). A new force, which is not equal to the force exerted by the previous activation, is added with every turn of the screw. Consequently, the net force applied to the nasomaxillary complex by the Hyrax screw differs significantly from patient to patient and from turn to turn of the screw and hence must be influenced by a large number of parameters, including the resistance of the surrounding tissues and anatomical structures. Since the magnitude of the force is highly variable it was decided therefore to proceed with the Finite Element Analysis using the displacement of the parts of the screw rather than the force created.

Patient A 8,6 yr.	1st activation		+ 90 sec		+ 210 sec		Total net force		
	3,7 lb	0,2 lb decay (1 min)	2,5 lb	0,3 lb decay (1 min)	2,4 lb	2,2 lb decay (25,5 min)	5,9 lb over 29 min period		
Patient B 15,6 yr.	1st activation		+ 180 sec		+ 390 sec		Total net force		
	4,2 lb	2 lb decay (3 min)	8 lb	3 lb decay (3,5 min)	9,2 lb	9,1 lb decay (23 min)	7,3 lb over 30 min period		
Patient C 12 yr.	1st activation		+ 450 sec		+ 840 sec		Total net force		
	6,2 lb	1,8 lb decay (5,5 min)	5,4 lb	2,3 lb decay (5,5 min)	6 lb	4,4 lb decay (18,5 min)	9,1 lb over 32,5 min period		
Patient D 11 yr.	1st activation		+ 135 sec		+ 390 sec		+ 750 sec		Total net force
	4,1 lb	1,4 lb decay (2 min)	5,5 lb	2,2 lb decay (2,75 min)	3,2 lb	1,7 lb decay (4,5 min)	8 lb	4 lb decay (7,5 min)	11,5 lb over 21 min
Patient E 15,6 yr.	1st activation (1/2 turn of screw)		+ 90 sec (1/2 turn of screw)		+ 1830 sec (1/2 turn of screw)		Total net force		
	3,8 lb		7 lb	4,1 lb decay (27 min)	3,8 lb	1,7 lb decay (5 min)	8,8 lb over 35,5 min period		

Table 50: Force decay subsequent to the activation of the Rapid Maxillary Expansion appliance *(R.J. Isaacson, A.H. Ingram; Angle Orthodontist, 1964; 34: 261-270)*

Moreover, during the relaxation period, a degree of tissue rebound exists which causes some partial relapse of the expanded maxillary halves. Unfortunately, little is known about the quantitative and qualitative characteristics of that phenomenon and therefore this parameter cannot be introduced and calculated during the mathematical analysis. In the Finite Element Analysis the deformed state of the model after each turn of the screw is saved and an equal separation of the acrylic halves is added

algebraically to that state which causes further deformation of the Finite Element Model.

Further, it should not be overlooked that in the clinical situation the number of turns of the screw is greater than the 14 turns applied during the mathematical analysis, which highlights even more the difference in the displacements between the various analysis.

Therefore, in order to study further Rapid Maxillary Expansion with the improved Finite Element Model (with addition of the dentition, the associated periodontal ligament and the combination of cancellous-cortical bone in the maxilla (**Figure 18**)), the behavior of the nasomaxillary complex is considered as linear with no relaxation period (**craniofacial 300.esd**). All parameters and limiting factors were equal to those resulted from craniofacial 30.esd.

From the comparison of the results between the two Finite Element Models (**craniofacial 30.esd** and **craniofacial 300.esd**) for the same number of turns (30 turns) of the Hyrax screw (**Table 42**), it is evident that modelling of the teeth and the periodontal ligament, as well as using a combination of brick and plate elements to simulate the bone structure of the maxilla, alters the nature of the displacements for the points EMR-EML and UMR-UML. The anchor teeth, as it was suggested in the previous sections, under the influence of the expansion force, tip within the periodontal ligament and consequently cause a degree of alveolar lateral bending due to bone resiliency. These displacements now approach closer the clinical findings as presented in the literature (Haas, 1961; 1965; 1970; Wertz, 1970; Grimm, 1972; Hicks, 1978). This is represented graphically in **Figure 50** in which the nodal displacement at the level of the crown of the anchor teeth is somewhat greater than the nodal displacement at the level of the apex. Hicks (1978) found a definite change in the long axis of the posterior teeth with the angulation between them increasing from 1° to 24° during

expansion. This change is caused in part due to the tipping of the anchor teeth within the periodontal ligament, and partly due to the alveolar bending. Consequently, there is also an increase in dental arch width. The qualitative behavior of the new Finite Element Model is similar to the clinical situation as described in the literature, even though the displacement of points CNR-CNL and MIR-MIL are lying outside the 99.5% confidence interval.

In **Figures 51 - 52** it is presented an attempt to assess the von Misses stresses that develop at the level of the anchor teeth of the Rapid Maxillary Expansion appliance and the surrounding periodontal ligament. It can be suggested that at the level of the first permanent molar the stresses are higher than those that develop at the level of the first permanent premolar. This can be explained by the fact that the first permanent molars are placed further distally within the maxillary dental arch and closer to the zygomatic arch which represents one of the points with the greater resistance to the separation of the two maxillary halves. The separation of the midpalatal suture at this level is almost insignificant and therefore the external load created by the Hyrax screw of the appliance results in extremely high von Misses stresses at the mesio-linguo-distal side at the level of the cemento-enamel junction of the first maxillary permanent molars at the place where the bars of the Hyrax screw are soldered to the metal bands (Greenbaum and Zachrisson, 1982). Moreover, the placement of the screw is often closer to these teeth rather than anteriorly in the palate, again representing another factor in the increased stress levels that develop on these teeth. Since the separation of the maxillary halves at their distal end is minimal, the force applied to the mesio-linguo-distal side at the level of the cemento-enamel junction of the molar teeth by the screw, results in the aforementioned tipping of these teeth within the alveolae.

Furthermore, first permanent maxillary premolars encounter higher stress levels at the lingual marginal and middle parts of their roots than at their

crowns. This can be explained by the fact that in the premolar area the splitting of the midpalatal suture is greater due to less resistance from the other anatomical structures of the nasomaxillary complex. All the load created by the Hyrax screw is thus transmitted through the acrylic part of the appliance to that area and translated into pressure against the alveolar crest. Consequently, this pressure results in displacement of the maxillary halves. The pressure on the palatal side of the alveolar crest is expressed into high von Misses stresses on the lingual side of the roots of the first maxillary premolars in the Finite Element Model of the skull. The above findings are in accordance with the observations by Odenrick *et al.* (1982) about the resorption areas found on the first maxillary permanent premolars. They noticed extensive areas of resorption in the buccal marginal and buccal middle parts exactly opposite to the sites of tension observed during the present Finite Element Analysis.

In **Figure 52** the von Misses stresses that develop at the periodontal ligaments of the anchor teeth are presented, and which are comparatively lower than those developed at the teeth surface. This can be explained by the highly elastic material properties of the periodontal ligament. Clinically, the periodontal ligament of the anchor teeth under the forces created from the jackscrew of the appliance remodels in the areas of high tension and compression. Odenrick *et al.* (1982) observed on radiographic investigation, a widening of the periodontal space of maxillary first premolars. The remodelling of the periodontal ligament can, probably, be represented graphically by the nodal displacements observed at that level (**Figure 53**). These displacements when compared to the nodal displacements of the anchor teeth (**Figure 50**) appear to be approximately equal. In other words, the periodontal ligament as the result of the remodelling retains its initial dimensions.

More tests were performed on the improved Finite Element Model of the craniofacial complex and proved once again that all other sutures (except

the zygomatico-maxillary suture) do not play an important role in either the quantitative or qualitative behavior of the maxilla during the expansion procedure. Therefore, in practice, it is not always necessary to create a large Finite Element Model, but rather a reduced one which uses few degrees of freedom but, at the same time, it should reliably simulate the reality. For example, in the present study which requires to simulate the opening of the maxillae under the expansion forces, it is not necessary to model all maxillary details but rather a draft representation of the overall structure. On the other hand, it is of prime importance the choice of material properties and characteristics.

In **Figures 43 - 48**, the displacements and the distribution of maximal von Misses stresses at the various anatomical points of the craniofacial complex as resulted by the Finite Element Model, named as **craniofacial 304.esd**, were shown. It can be observed that the areas of high stress concentration are the palate, the articulation of the pterygoid process with the perpendicular plate of the palatine bone on the left side and the area of the right styloid process (**Figure 49**). The same findings were observed at the *in vitro* experiment with the dry skull with the difference that the separation at the level of the styloid process appears bilaterally. From the above findings, it is clear that, the articulation of the pterygoid process with the perpendicular plate of the palatine bone even though mathematically does not influence significantly the degree of separation of the maxillary halves shows a high concentration of stress values. This is probably due to its anatomical structure which does not include a median suture even though it is positioned in the middle cranial fossa and functions as a stop against the splitting of the midpalatal bone. In order to fully understand the role of the sphenoid bone, however, further research is required.

Işeri *et al.* (1998) observed a high stress concentration also at the external surface of the zygomatic bone and external wall of the orbit, around the

nasal bone and the antero-inferior wall of the nasal cavity. The differences observed greatly depend on the boundary conditions taken under consideration as well as on the geometry of the Finite Element Model constructed. In the aforementioned study only one half of the cranium was considered with respect to the sagittal plane passing between the orbit. Furthermore, shell elements of different thickness but with the same stiffness were used exclusively in order to construct all craniofacial structures, including the teeth. All sutures were assumed to have the same mechanical properties as the surrounding bone material except at the palatine bone, and all points of the cranium lying on the symmetry plane were constrained to have no motion perpendicular to this plane with the exception of the points at the palatine bone. These differences in the construction of the model and the assumptions made during the Finite Element Analysis may cause the differences in the stress distribution between these two models.

The external load from the jackscrew is applied directly at the level of the two maxillary halves in order to separate them and consequently the resultant stress concentration at the palate area is expectedly high. However, the asymmetric excessive loading on the left articulation of the pterygoid process with the perpendicular plate of the palatine bone and the right styloid process, can be caused by an asymmetric construction of the model. This finding is in accordance with the comments of Wertz (1970) on his research findings, that the skeletal effects in some cases may be more pronounced on one side than the other as a result of the individual skeletal architecture with the articulations of the maxilla on one side being more rigid than those found on the opposite side. Other investigators have mentioned or described this phenomenon in connection with rapid maxillary expansion (Krebs, 1958; Isaacson *et al.,* 1964; Starnbach *et al.,* 1964; Walters, 1975). The clinical significance of the asymmetrical skeletal separation of the maxillae has not been adequately investigated.

Nevertheless, this observation once again stresses the importance of accurate design of the geometry of the model under study.

It should be noted that von Misses stresses are higher than in the clinical situation since the relaxation period and consequent tissue rebound phenomenon are not considered. Therefore, the conclusions that can be drawn from this analysis are only useful in understanding the qualitative behavior of the craniofacial complex during Rapid Maxillary Expansion. However, qualitative research has its own scientific value. It can be used to generate hypotheses, development of patient-based measures, explaining research findings and informing future research.

CHAPTER 6: CONCLUSIONS

6.1. Conclusions:

It would appear feasible to simulate orthopaedic changes in the nasomaxillary complex by means of Finite Element Analysis. Modern imaging techniques permit the generation of sufficient sectional profiles to characterise the osseous and dental structures of the maxilla.

Due to the geometrical complexity of the anatomical and dentoalveolar structures, the development of a three-dimensional dentate maxillary model with the added complication of the Rapid Maxillary Expansion appliance, is not a straightforward procedure, for it demands manipulation of the original geometry to build volumetric shapes. At the present time the method developed still requires some manual input especially when applied to a bone with complex geometrical and structural characteristics, such as cortical and cancellous bone, dental enamel, dentine, the periodontal ligament, and the sutures. Published data was used to assign appropriate material characteristics to the Finite Element Model. Various restraints placed at the level of the craniofacial sutures permit formal analysis of the resulting deformations and forces at various, optional sites within the model. The morphology of the skeleton is known to reflect functional demand. Therefore, in order to study the biomechanical behavior of the maxilla during Rapid Maxillary Expansion using Finite Element Analysis, it is necessary to reproduce meticulously all the structures of the Craniofacial complex and to provide all the corresponding material properties. The assumptions made and the points where all degrees of freedom are constrained are also critical in the behaviour of the Finite Element Model.

Nonetheless, as emphasized in recent reviews of cranial and maxillofacial Finite Element studies (Voo *et al.,* 1996; Korioth *et al.,* 1997), expectations of high accuracy in all regions of biologic Finite Element Models are rarely achievable. Therefore the specific objectives of the study must be matched to available computational resources and the mesh design and boundary conditions optimized to shift the accuracy of the model toward regions of interest.

1. From a structural analytical viewpoint, geometry idealization, material data selection, and the assignment of boundary conditions of the present study are sound providing the mechanical consequences of Rapid Maxillary Expansion are investigated, which consequently makes the results qualitatively valid. Comparison with clinical and radiographic findings of a group of 49 patients which underwent this treatment approach offered a closer insight into the behaviour of the maxilla as a result of the application of the external loading from the jackscrew embedded within the appliance.
2. This approach could however be important as a preliminary step in the mathematical design optimization of maxillary expansion appliances. This methodology provides a reliable tool to directly compare stress and strain distributions, as well as the displacements generated by different Rapid Maxillary Expansion appliances.

As far as the objectives of the study are concerned:

1. "*When Rapid Maxillary Expansion is undertaken, the anatomical structures of the nasomaxillary complex have no bearing on the force necessary to separate the midpalatal suture.*" The force level required to separate the maxillary halves depends primarily on the resistance created by the surrounding anatomical structures. The parameters involved are numerous and highly individualised and consequently, absolute force values neither can be measured, nor are of use in the general clinical environment.

2. "*When Rapid Maxillary Expansion is undertaken, the various maxillofacial sutures have no effect on the expansion of the maxillary segments.*" This hypothesis is supported in relation to the frontomaxillary suture; the suture with the lacrimal bone and nasomaxillary suture, as well as the articulation of the pterygoid process of the sphenoid bone with the perpendicular plate of the palatine bone.

   This hypothesis is rejected in relation to the intermaxillary, the midpalatal and the transverse palatal suture, as well as the zygomaticomaxillary suture and the zygomatic arch. These sutures influence the qualitative, quantitative and directional behaviour of the maxilla during Rapid Maxillary Expansion.
3. "*When Rapid Maxillary Expansion is undertaken, the amount of force needed to successfully complete the process does not depend on the age of the patient and level of ossification of the midline palatal suture.*" Age and the level of ossification of the sutures would appear to influence the degree and the manner of midpalatal splitting.

Furthermore, from the present study it can be concluded that:

1. The pyramidal shape of the expansion observed between the two maxillary segments is a result of the different degrees of resistance that the midpalatal suture of the maxilla encounters along its length.
2. Dry skull material essentially substantiated the Finite Element Analysis findings. The displacements observed at the dry skull during the *in Vitro* Rapid Maxillary Expansion are approximated by the linear Finite Element Model (i.e. without taking under consideration relaxation period and tissue rebound phenomenon). However, in a clinical situation the phenomenon of tissue rebound is present when Rapid Maxillary Expansion treatment is undertaken. It also includes many biologic factors (i.e. soft tissue envelope) that influence and alter the behavior of the

human maxilla. It was impossible for all these factors to be included in the present study.

3. High levels of stress concentration were observed at the palate, where the external load is applied directly, the left articulation of the pterygoid process with the perpendicular plate of the palatine bone and the area of the right styloid process. This latter finding of the Finite Element Analysis is supported by the *in vitro* study, where sutural separation was observed bilaterally in the area of the base of the skull.
4. The expansion force created by opening the jackscrew within the Rapid Maxillary Expansion appliance is applied to the palatal side of the anchor teeth. The resultant dental effect of that force is buccal tipping of maxillary first permanent molars with consequent alveolar bending and bodily movement of maxillary first premolars in a buccal direction. The stresses that develop within the Periodontal Ligament are comparatively low - probably due to its remodeling properties.

The number of variables involved explain the individual variabilities in the treatment outcome and the low probability of accurate prediction of the stability of interarch expansion after Rapid Maxillary Expansion. Consequently, success of treatment should not be evaluated by gain in interarch dimension *per se*, but by harmonic adaptation of the dental unit in the new skeletal environment without violating basic biological principles (DanVardimon *et al.,* 1998).

6.2. Suggestions for further study:

The most significant positive contribution of Finite Element Analysis is the ability to predict events at sites at which measurements are likely to remain impossible in living humans. Currently, the approach is limited only by the computational power available to the individual experimenter, the availability

and reliability of suitable values for the many variables involved, and, in this present case, conditions of static loading.

- Establish the level of mesh refinement via a convergence test for an accurate Finite Element Model of the Craniofacial complex.
- To calculate the tissue rebound phenomenon in a clinical situation and the residual forces between each turn of the screw and introduce this information into the Finite Element Analysis of the Rapid Maxillary Expansion. This data will provide us with more accurate information as to stress distribution to the various craniofacial structures and the resultant displacements.
- If it was ethically acceptable, to obtain P-A cephalometric radiographs after each turn of the screw from a larger number of patients. This information would make the data obtained from the clinical findings and the Finite Element Analysis directly comparable and would lead to improvement of the Finite Element Model and consequently lead to better understanding of the behavior of the maxilla under expansion. Moreover, it may then be possible to customize the rapid maxillary appliance to the individual needs of each patient.

REFERENCES

Adkins MD., Nanda RS., Currier GF. "Arch perimeter changes on rapid palatal expansion." Am J Orthod Dentofacial Orthop 1990; 97: 194-199

Akita S., Hirano A. "Modified coronal incision: distribution of stress in the scalp and cranium." Cleft Palate Craniofac J 1993; 30 (4): 382-386

Alpern MC., Yurosko JJ. "Rapid palatal expansion in adults with and without surgery." Angle Orthod 1987; 57 (3): 245-263

Andriacchi TP., Galante JO., Belytschko TB., Hampton S. "A stress analysis of the femoral stem in total hip prostheses." J Bone Joint Surg Am 1976; 58 (5): 618-624

Angell EC. "Treatment of irregularities of the permanent or adult teeth." Dental Cosmos 1860; 1: 540-544

Askew MJ., Lewis JL. "Analysis of model variables and fixation post length effects on stresses around a prosthesis in the proximal tibia." J Biomech Eng 1981; 103 (4): 239-245

Athanasiou AE., Droschl H., Bosch C. "Data and patterns of transverse dentofacial structure of 6- to 15-year-old children: a posteroanterior cephalometric study." Am J Orthod Dentofacial Orthop 1992; 101 (5): 465-471

Athanasiou AE. "Orthodontic Cephalometry." Mosby-Wolfe, London, 1995

Athanasiou AE., Van der Meij AJW. "Posteroanterior (frontal) cephalometry." In: Athanasiou AE. (ed) Orthodontic Cephalometry, Mosby-Wolfe, London, 1995; pp141-162

Barber AF., Sims MR. "Rapid maxillary expansion and external root resorption in man: a scanning electron microscope study." Am J Orthod 1981; 79 (6): 630-652

Bartel DL., Ulsoy GA. "The effect of stem length and stem material on stresses in bone-prosthesis systems." Proc 21st Annual Meeting Orthopaedic Research Society; 1975

Bathe K., Wilson E. "Numerical Methods in Finite Element Analysis." Englewood Cliffs, NJ Prentice Hall, 1976

Battagel JM. "Tensor analysis of facial growth in males." Eur J Orthod 1995; 17 (3): 215-229

Beaupre GS., Orr TE., Carter DR. "An approach for time-dependent bone modeling and remodeling – application: a preliminary remodeling simulation." J Orthop Res 1990; 8 (5): 662-670

Bell WH., Epker BN. "Surgical-orthodontic expansion of the maxilla." Am J Orthod 1976; 70 (5): 517-528

Bell RA. "A review of maxillary expansion in relation to rate of expansion and patient's age." Am J Orthod 1982; 81 (1): 32-37

Bidez MW., Chen Y., McLoughlin SW., English CE. "Finite Element Analysis (FEA) studies in 2.5mm round bar design: the effects of bar length and material composition on bar failure." J Oral Implantol 1992; 18 (2): 122-128

Biederman W. "Rapid correction of Class III malocclusion by midpalatal expansion." Am J Orthod 1973; 63 (1): 47-55

Bishara SE., Staley RN. "Maxillary expansion: clinical implications." Am J Orthod Dentofacial Orthop 1987; 91 (1): 3-14

Björk A. "The principle of the Andreesen method of orthodontic treatment. A discussion based on cephalometric x-ray analysis of treated cases." Am J Orthod 1951; 37 (7): 437-458

Björk A. "Facial growth in man, studied with the aid of metallic implants." Acta Odontol Scand 1955; 13 (1): 9-34

Björk A. "Prediction of mandibular growth rotation." Am J Orthod 1969; 55 (6): 585-599

Björk A., Skieller V. "Facial development and tooth eruption. An implant study at the age of puberty." Am J Orthod 1972; 62 (4): 339-383

Björk A., Skieller V. "Growth in width of the maxilla studied by the implant method." Scand J Plast Reconstr Surg 1974; 8 (1-2): 26-33

Book D., Lavelle C. "Changes in craniofacial size and shape with two modes of orthodontic treatment." J Craniofac Genet Dev Biol 1988; 8 (3): 207-223

Bookstein FL. "The measurement of biological shape and shape change." In Levin S (ed): "Lecture Notes in Biomathematics." New York, Springer-Verlag, 1978

Bookstein FL. "On the cephalometrics of skeletal change." Am J Orthod 1982; 82 (3): 177-198

Bookstein FL. "The geometry of craniofacial growth invariants" Am J Orthod 1983; 83 (3): 221-234

Bookstein FL. "A statistical method for biological shape comparisons." J Theor Biol 1984; 107 (3): 475-520

Bookstein FL. "Tensor biometrics for changes in cranial shape." Ann Hum Biol 1984; 11 (5): 413-437

Bookstein FL., Chernoff B., Elder R., Humphries J., Smith G., Strauss R. "Morphometrics in evolutionary biology." Philadelphia, Academy of Natural Science, Special Publication No 15, 1985

Borchers L., Reichart P. "Three-dimensional stress distribution around a dental implant at different stages of interface development." J Dent Res 1983; 62 (2): 155-159

Braun S., Bottrel JA., Lee KG., Lunazzi JJ., Legan HL. "The biomechanics of rapid maxillary sutural expansion." Am J Orthod Dentofacial Orthop 2000; 118 (3): 257-261

Brekelmans WA., Poort HW., Sloof TJ. "A new method to analyse the mechanical behaviour of skeletal parts." Acta Orthop Scand 1972; 43 (5): 301-317

Brin I., Hirshfeld Z., Shanfeld JL., Davidovitch Z. "Rapid palatal expansion in cats: effect of age on sutural cyclic nucleotides." Am J Orthod 1981; 79 (2):162-175

Brosh T., Vardimon AD., Ergatudes C., Spiegler A., Lieberman M. "Rapid Palatal Expansion. Part 3: strains developed during active and retention phases." Am J Orthod Dentofacial Orthop 1998; 114 (2): 123-133

Brown TD., Way ME., Ferguson AB. "Stress transmission anomalies in femoral heads altered by aseptic necrosis." J Biomech 1980; 13 (8): 687-699

Bulman JS., Osborn JF. "Statistics in dentistry." Ed. British Dental Association, 1989

Byrum AG. "Evaluation of anterior-posterior and vertical skeletal change Vs dental change in rapid palatal expansion cases as studied by lateral cephalograms." Am J Orthod 1971; 60 (4): 419

Camacho DL., Hopper RH., Lin GM., Myers BS. "An improved method for finite element mesh generation of geometrically complex structures with application to the skullbase." J Biomech 1997; 30 (10): 1067-1070

Campen DH., Van Croon HW., Lindwer J. "Mechanical loosening of knee-endoprostheses with intermedullary stems: Influence of dynamic loading." 25th Annual Meeting of Orthopaedic Research Society, 1979; p: 98

Cangialosi TJ., Moss ML., McAlarney ME., Nirenblatt BD., Yuan M. "An evaluation of growth changes and treatment effects in Class II, Division 1 malocclusion with conventional roentgenographic cephalometry and finite element method analysis." Am J Orthod Dentofacial Orthop 1994; 105 (2): 153-160

Carter DR., Vasu R., Spengler DM., Dueland RT. "Stress fields in the unplated and plated canine femur calculated from in vivo strain measurements." J Biomech 1981; 14 (1): 63-70

Carter DR., Orr TE., Fyhrie DP. "Relationships between loading history and femoral cancellous bone architecture." J Biomech 1989; 22 (3): 231-244

Cattaneo PM., Dalstra M., Frich LH. "A three-dimensional finite element model from computed tomography data: a semi-automated method." Proc Inst Mech Eng (H) 2001; 215 (2): 203-213

Cattaneo PM., Dalstra M., Melsen B. "The transfer of occlusal forces through the maxillary molars: a finite element study." Am J Orthod Dentofacial Orthop 2003; 123 (4): 367-373

Ceylan I., Oktay H., Demirci M. "The effect of rapid maxillary expansion on conductive hearing loss." Angle Orthod 1996; 66 (4): 301-307

Chaconas SJ., Caputo AA., Davis JC. "The effects of orthopedic forces on the craniofacial complex utilising cervical and headgear appliances." Am J Orthod 1976; 69: 527-539

Chaconas SJ., Caputo AA. "Observation of orthopedic force distribution produced by maxillary orthodontic appliances." Am J Orthod 1982; 82 (6): 492-501

Chang JY., McNamara JA., Herberger TA. "A longitudinal study of skeletal side effects induced by RME." Am J Orthod Dentofacial Orthop 1997; 112 (3): 330-337

Chang YI., Shin SJ., Baek SH. "Three-dimensional finite element analysis in distal *en masse* movement of the maxillary dentition with the multiloop edgewise archwire." Eur J Orthod 2004; 26 (3): 339-345

Chao EYS., Malluege JK. "Pin-bone interface stresses in the application of external fixation and traction devices." Proceedings of the 27th Annual Meeting Orthopaedic Research Society Chicago, 1981; pp: 101

Chao EYS., An K-N. "Biomechanical analysis of external fixation devices for the treatment of open bone fractures." In: Gallagher RH., Simon BR., Johnson PC., Gross JF. (ed) "Finite Elements in Biomechanics." John Wiley, New York, 1982; pp: 195-222

Cheverud J., Lewis JL., Bachrach W., Lew WD. "The measurement of form and variation in form: an application of three-dimensional quantitative morphology by finite-element methods." Am J Phys Anthropol 1983; 62 (2): 151-165

Chin M., Toch BA. "Le Fort III advancement with gradual distraction using internal devices." Plast Reconstr Surg 1997; 100 (4): 819-830

Christiansen RL., Burstone CJ. "Centers of rotation within the periodontal space." Am J Orthod 1969; 55 (4): 353-369

Chung CH., Font B. "Skeletal and dental changes in the sagittal, vertical, and transverse dimensions after rapid palatal expansion.' Am J Orthod Dentofacial Orthop 2004; 126 (5): 569-575

Claes L., Palme U., Palme E., Kirschbaum U. "Biomechanical and mathematical investigations concerning stress protection of bone beneath internal fixation plates." In: Huiskes R., Van Campen DH., De Wijn JR. (ed) "Biomechanics: Principles and applications." Martinus Nijhoff, The Hague, 1982; pp: 325-330

Cleall JF., Bayne D., Posen J., Subtelny JD. "Expansion in the midpalatal suture in the monkey." Angle Orthodontist 1965; 35: 23-35

Coben SE. "The integration of facial skeleton variants." Am J Orthod 1955; 41: 407-434

Cook SD., Klawitter JJ., Weinstein AM. "The influence of design parameters on calcar stresses following femoral head arthroplasty." J Biomed Mater Res 1980; 14 (2): 133-144

Cook SD., Weinstein AM., Klawitter JJ. "A three dimensional finite element analysis of a porous rooted Co-Cr-Mo alloy dental implant." J Dent Res 1982; 61 (1): 25-29

Coolidge ED. "The thickness of the human periodontal membrane." J Am Dent Assoc. 1937; 24: 1260-1270

Cowin SC., Hegedus DH. "Bone remodelling I: a theory of adaptive elasticity." J Elasticity 1976; 6: 313-326

Cowin SC., Hart RT. "Errors in the orientation of the principal stress axes if bone tissue is modeled as isotropic." J Biomech 1990; 23 (4): 349-352

Crippen TE., Huiskes R., Chao EY. "Axisymmetric analysis of pin-bone interface stresses of external fixation devices." In: Van Buskirk WC., Woo SL-Y. (ed) "Biomechanics Symposium." American Society of Mechanical Engineers, New York, 1981; pp: 247-250

Croon HW., Campen DH., Van Klok J., Miehlke R. "Quasi two-dimensional FEM analysis and experimental investigations of the tibial part of knee endoprostheses with intramedullary stems." In: Huiskes R., Van Campen DH., De Wijn JR. (ed) "Biomechanics: Principles and applications." Martinus Nijhoff, The Hague, 1982; pp: 313-318

Cross DL. "Transverse dimensional changes following rapid maxillary expansion." [Doctor of Dental Surgery Thesis], University of Edinburgh, 1997

Cross DL., McDonald JP. "Effect of rapid maxillary expansion on skeletal, dental and nasal structures: a postero-anterior cephalometric study." Eur J Orthod 2000; 22 (5): 519-528

Dahlberg G. "Statistical methods for medical and biological students." New York, 1940, Interscience Publications

Daly CH., Nicholls JI., Nansen PD., Kydd WL. "The response of the maxillary central incisor to torsional loading." Proc Amer Conf Eng Med Biol 1974; 14: 288

da Silva Filho OG., Boas MC., Capelozza Filho L. "Rapid maxillary expansion in the primary and mixed dentitions: a cephalometric evaluation." Am J Orthod Dentofacial Orthop 1991; 100 (2): 171-179

da Silva Filho OG., Montes LA., Torelly LF. "Rapid maxillary expansion in the deciduous and mixed dentition evaluated through posteroanterior cephalometric analysis." Am J Orthod Dentofacial Orthop 1995; 107 (3): 268-275

Davis WM., Kronman JH. "Anatomical changes induced by splitting of the mid-palatal suture." Angle Orthod 1969; 39 (2): 126-132

de Clerck H., Dermaut L., Timmerman H. "The value of the macerated skull as a model used in orthopaedic research." Eur J Orthod 1990; 12 (2): 263-271

Derichsweiller H. "Die Gaumenrahtsprengung." Fortschritte der Kieferorthopadie 1953; Band 14, Heft

Desai CS., Abel JF. "Introduction of the Finite Element Method: A numerical method for engineering analysis." Van Norstrand-Teinhold Co (ed), New York, 1972

Doruk C., Sőkűcű O., Sezer H., Canbay EI. "Evaluation of nasal airway resistance during rapid maxillary expansion using acoustic rhinometry". Eur J Orthod 2004; 26 (4): 397-401

Downs WB. "Variations in facial relations: their significance in treatment and prognosis." Am J Orthod 1948; 34: 812-840

Droschl H. "The effect of heavy orthopedic forces on the maxilla in the growing *Saimiri scuireus* (squirrel monkey)." Am J Orthod 1973; 66: 449-461

Droschl H. "The effect of heavy orthopedic forces on the sutures of the facial bones." Angle Orthod 1975; 45 (1): 26-33

Ekström C., Henrikson CO., Jensen R. "Mineralization in the midpalatal suture after orthodontic expansion." Am J Orthod, 1977; 71 (4): 449-455

Enlow DH. "Wolff's law and the factor of architectonic circumstance." Am J Orthod 1968; 54 (11): 803-822

Evans FG. "Stress and strain in bones: their relation to fractures and osteogenesis." (ed.) Springfield, Illinois: Charles C. Thomas Publishing Co, 1957

Farah JW., Craig RG., Meroueh KA. "Finite element analysis of a mandibular model." J Oral Rehabil 1988; 15 (6): 615-624

Ferré JC., Legoux R., Helary JL., Albugues F., Le Floc'h C., Bouteyre J., Lumineau JP., Chevalier C., Le Cloarec AY., Orio E., Marquet F. "Study of the deformations of the isolated mandible under static constraints by simulation on a physicomathematical model." Anat Clin 1985; 7 (3): 183-192

Fried KH. "Palate-tongue relativity." Angle Orthod 1971; 41 (4): 308-323

Frost HM. "The Laws of Bone structure." Charles C. Thomas (ed), Springfield IL, 1964a

Frost HM. "Mathematical elements of lamellar bone remodelling." Charles C. Thomas (ed), Springfield IL, 1964b

Frost HM. "Vital biomechanics: proposed general concepts for skeletal adaptations to mechanical usage." Calcif Tissue Int 1988; 42 (3): 145-156

Fyhrie DP., Carter DR. "A unifying principle relating stress to trabecular bone morphology." J Orthop Res 1986; 4 (3): 304-317

Fyhrie DP., Hamid MS., Kuo RF., Lang SM. "Direct three dimensional finite element analysis of human vertebral cancellous bone." Transactions of 38th Annual Meeting of Orthopaedic Research Society 1992; 17: 551

Gabel AB. "A mathematical analysis of the function of the fibres of the periodontal membrane." J Periodontol 1956; 27: 191-198

Gardner GE., Kronman JH. "Cranioskeletal displacements caused by rapid palatal expansion in the rhesus monkey." Am J Orthod 1971; 59 (2): 146-155

Gault D., Brunelle F., Renier D., Marchac D. "The calculation of intracranial volume using CT scans." Childs Nerv Syst 1988; 4 (5): 271-273

Ghosh J., Nanda RS., Duncanson MG., Currier GF. "Ceramic bracket design: an analysis using the finite element method." Am J Orthod Dentofacial Orthop 1995; 108 (6): 575-582

Glassman AS., Nahigian SJ., Medway JM., Aronowitz HL. "Conservative surgical orthodontic adult rapid palatal expansion: sixteen cases." Am J Orthod 1984; 86 (3): 207-213

Goh GK., Kaan SK. "Dentofacial orthopaedic correction of maxillary retrusion with the protraction face mask – a literature review." Austr Orthod J 1992; 12: 143-150

Gosain AK., McCarthy JG., Glatt P., Stoffenberg D., Hoffmann RG. "A study of intracranial volume in Apert syndrome." Plast Recostr Surg 1995; 95 (2): 284-295

Graber TM., Swain BF. "Dentofacial Orthopedics." In: Graber TM (ed) "Current orthodontic concepts and techniques." Philadelphia, WB Saunders Company, 1975

Gravely JF., Benzies PM. "The clinical significance of tracing error in cephalometry." Br J Orthod 1974; 1 (3): 95-101

Gray LP. "Results of 310 cases of rapid maxillary expansion selected for medical reasons." J Laryngol Otol 1975; 89 (6): 601-614

Greenbaum KR., Zachrisson BU. "The effect of palatal expansion therapy on the periodontal supporting tissues." Am J Orthod 1982; 81 (1): 12-21

Grimm FM. "Bone bending, a feature of orthodontic tooth movement." Am J Orthod 1972; 62 (4): 384-393

Grossman W. "Rapid expansion in cleft palate cases." Trans Eur Orthod Soc 1963; 39: 366-372

Grummons DC., Kappeyne van de Copello MA. "A frontal asymmetry analysis." J Clin Orthod 1987; 21 (7): 448-465

Gryson JA. "Changes in mandibular interdental distance concurrent with rapid maxillary expansion." Angle Orthod 1977; 47 (3): 186-192

Guldberg RE., Hollister SJ. "Finite Element solution errors associated with digital image-based mesh generation." Bioengineering Conference of ASME 1994; Vol BED-28: 147-148

Gupta KK., Knoell AC., Grenoble DE. "Mathematical modeling and structural analysis of the mandible." Biomater Med Devices Artif Organs 1973; 1 (3): 469-479

Haas AJ. "Rapid expansion of the maxillary dental arch and nasal cavity by opening the midpalatal suture." Angle Orthod 1961; 31: 73-90

Haas AJ. "The treatment of maxillary deficiency by opening the midpalatal suture." Angle Orthod 1965; 35: 200-217

Haas AJ. "Palatal expansion: just the beginning of dentofacial orthopedics." Am J Orthod 1970; 57 (3): 219-255

Haas AJ. "Long-term posttreatment evaluation of rapid palatal expansion." Angle Orthod 1980; 50 (3): 189-217

Haas AJ., Andrew J. "Haas: entrevista." R Dental Press Orthodon Orthop Facial 2001; 6: 1-10

Halazonetis DJ. "Computer experiments using a two dimensional model of tooth support." Am J Orthod Dentofacial Orthop 1996; 109 (6): 598-606

Hampton SJ., Andriacchi TP., Galante JO. "Three dimensional stress analysis of the femoral stem of a total hip prosthesis." J Biomech 1980; 13 (5): 443-448

Hart RT., Davy DT., Heiple KG. "Mathematical modeling and numerical solutions for functionally dependent bone remodeling." Calcif Tissue Int 1984; 36 (Suppl 1): 104-109

Hart RT., Hennebel VV., Thongpreda N., Van Buskirk WC., Anderson RC. "Modeling the biomechanics of the mandible: a three-dimensional finite element study." J Biomech 1992; 25 (3): 261-286

Hartgerink DV., Vig PS., Abbott DW. "The effect of rapid maxillary expansion on nasal airway resistance." Am J Orthod Dentofacial Orthop 1987; 92 (5): 381-389

Harvold EP., Chierici G., Vargervik K. "Experiments on the development of dental malocclusions." Am J Orthod 1972; 61 (1):38-44

Haskell B., Day M., Tetz J. "Computer-aided modeling in the assessment of the biomechanical determinants of diverse skeletal patterns." Am J Orthod 1986; 89 (5): 363-382

Hay GE. "The equillibrium of a thin compressible membrane with application to the periodontal membrane." Canad J Res 1939; 17: 123

Hayes WC. "Theoretical modeling and design of implant systems." Proceedings Workshop on Mechanical Failure of Total Hip Replacement, American Academy of Orthopaedic Surgery, Chicago, 1978; pp:159-175

Hayes WC., Snyder B., Levine BM., Ramaswamy S. "Stress-morphology relationships in trabecular bone of the patella." In Gallacher RH., Simon BR., Johnson PC., Gross JF. (ed) "Finite Elements in Biomechanics." John Wiley, New York, 1982; pp: 223-268

Herold JS. "Maxillary expansion: a retrospective study of three methods of expansion and their long term sequelae." Br J Orthod 1989; 16 (3): 195-200

Hershey HG., Stewart BL., Warren DW. "Changes in nasal airway resistance associated with rapid maxillary expansion." Am J Orthod 1976; 69 (3): 274-284

Hicks EP. "Slow maxillary expansion. A clinical study of the skeletal versus dental response to low-magnitude force." Am J Orthod 1978; 73 (2): 121-141

Hobatho MC., Darmana R., Pastor P., Barrau JJ., Laroze S., Morucci JP. "Development of a three-dimensional finite element model of a human tibia using experimental modal analysis." J Biomech 1991; 24 (6): 371-383

Holberg C., Rudzki-Janson I. "Stresses at the Cranial Base induced by Rapid Maxillary Expansion." Angle Orthod 2006; 76: 543-550

Hollister SJ., Kikuchi N. "Direct analysis of trabecular bone stiffness and tissue level mechanics using an element-by-element homogenisation method." Transactions of 38th Annual Meeting of Orthopaedic Research Society 1992; 17: 559

Hollister SJ., Brennan JM., Kikuchi N. "Recent advances in computer methods in Biomechanics and Biomedical Engineering." Books and Journals Int Ltd, Swansea UK, 1992; pp: 308-317

Houston WJ. "The current status of facial growth prediction, a review." Br J Orthod 1979; 6 (1): 11-17

Houston WJ. "The analysis of errors in orthodontic measurements." Am J Orthod 1983; 83 (5): 382-390

Howe RP. "Palatal expansion using a bonded appliance. Report of a case." Am J Orthod 1982; 82 (6): 464-468

Hubbard RP. "Flexure of layered cranial bone." J Biomech 1971; 4 (4): 251-263

Huiskes R., Elangovan PT., Banens JPA., Slooff TJ. "Finite element computer methods for design and fixation problems of orthopaedic implants." In: Asmussen E., Jorgensen K. (ed.) "Biomechanics VI-B." University Park Press, Baltimore, 1978; pp: 229-238

Huiskes R., Janssen JD., Slooff TJ. "A detailed comparison of experimental and theoretical stress-analysis of a human femur." In: "Mechanical Properties of bone." ASME, New York, 1981

Huiskes R. "Principles and methods of solid biomechanics." In: Ducheyne P., Hastings G. (ed.) "Functional Behaviour of Orthopaedic Biomaterials: Vol 1. Fundamentals." CRC Press, Boca Raton FL, 1983

Huiskes R., Chao EY. "A survey of finite element analysis in orthopedic biomechanics: the first decade." J Biomech 1983; 16 (6): 385-409

Huiskes R., Weinans H., Grootenboer HJ., Dalstra M., Fudala B., Sloof TJ. "Adaptive bone-remodeling theory applied to prosthetic design analysis." J Biomech 1987; 20 (11-12): 1135-1150

Huiskes R., Weinans H., Grootenboer HJ., Summer DR., Fudala B., Turner HJ., Galante J. "Stress-shielding, stress-bypassing and bone resorption around 'press-fit' and bone ingrowth THA." Trans 35th Orthop Res Soc 1989a; 14: 529

Huiskes R., Weinans H., Dalstra M. "Adaptive bone remodeling and biomechanical design considerations for noncemented total hip arthroplasty." Orthopedics 1989b; 12 (9): 1255-1267

Huiskes R., Weinans H., vanRietbergen B., Summer DR., Turner HJ., Galante J. "Validation of strain-adaptive bone remodelling analysis to predict bone morphology around noncemented THA." Trans 37th Orthop Res Soc 1991; 16: 105

Inoue N., Oyama K., Ishiguro K., Azuma M., Ozaki T. "Radiographic observation of rapid expansion of human maxilla." Bull Tokyo Med Dent Univ 1970; 17 (3): 249-261

Inoue Y., Tsutsumi S., Tanne K., Ida K., Sakuda M. "Effects of principal stresses in periodontal tissues on canine retraction." J Dent Res 1988; 67: 168

Isaacson RJ., Murphy TD. "Some effects of rapid maxillary expansion in cleft lip and palate patients." Angle Orthod 1964; 34:143-154

Isaacson RJ., Wood JL., Ingram AH. "Forces produced by rapid maxillary expansion." Angle Orthod 1964; 34: 256-270

Işeri H., Tekkaya AE., Őztan Ő., Bigliç S. "Biomechanical effects of rapid maxillary expansion on the craniofacial skeleton, studied by the finite element method." Eur J Orthod 1998; 20 (4): 347-356

Ishiguro K., Krogman WM., Mazaheri M., Harding RL. "A longitudinal study of morphological craniofacial patterns via P-A x-ray headfilms in cleft patients from birth to six years of age." Cleft Palate J, 1976;13:104-126

Isotupa K., Koski K., Maekinen L. "Changing architecture of growing cranial bones at sutures as revealed by vital staining with alizarin red s in the rabbit." Am J Phys Anthropol 1965; 23: 19-22

Ivanovski V. "Removable rapid palatal expansion appliance." J Clin Orthod 1985; 19 (10): 727-728

Jackson GW., Kokich VG., Shapiro PA. "Experimental and post-experimental response to anteriorly directed extraoral force in young *Macaca nemestrina.*" Am J Orthod 1979; 75 (3): 318-333

Jacobs CR., Mandell JA., Beaupre GS. "A comparative study of automatic finite element mesh generation techniques in orthopaedic biomechanics." Bioengineering Conference of ASME 1993; Vol BED-24: 512-514

Jafari A., Sadashiva Shetty K. "Study of stress distribution and displacement of various craniofacial structures following application of transverse orthopedic forces – a three-dimensional FEM study." Angle Orthod 2003; 73: 12-20

Johansen VA., Hall SH. "Morphogenesis of the mouse coronal suture." Acta Anat (Basel) 1982; 114 (1): 58-67

Johnson DR., Moore WJ. "Anatomy for Dental Students." Oxford University Press (3rd ed.), Oxford, 1997

Jones ML., Ang S., Houston WJ. "Frames of reference for the measurement of occlusal change and the integration of data from orthodontic models and cephalometric radiographs." Br J Orthod 1980; 7 (4): 195-203

Jones ML. "Clinical assessment of the wider span palatal adhesive retainer." J Clin Orthod 1987; 21 (10): 740-742

Keyak JH., Skinner HB. "Three-dimensional finite element modelling of bone: effects of element size." J Biomed Eng 1992; 14 (6): 483-489

Khalil TB., Hubbard RP. "Parametric study of head response by finite element modelling." J Biomech 1977; 10: 119-132

Kingsley NW. "A treatise on oral deformities as a branch of mechanical surgery." New York, Appleton, 1880

Knoell AC. "A mathematical model of an *in vitro* human mandible." J Biomech 1977; 10 (3): 159-166

Knox J., Jones ML., Hubsch P., Middleton J., Kralj B. "An evaluation of the stresses generated in a bonded orthodontic attachment by three different load cases using the Finite Element Method of stress analysis." J Orthod 2000; 27 (1): 39-46

Korioth TW., Romilly DP., Hannam AG. "Three-dimensional finite element stress analysis of the dentate human mandible." Am J Phys Anthropol 1992; 88 (1): 69-96

Korioth TW., Versluis A. "Modeling the mechanical behavior of the jaws and their related structures by finite element (FE) analysis." Crit Rev Oral Biol Med 1997; 8 (1): 90-104

Korkhaus G. "Discussion of report: A review of orthodontic research (1946-1950)." Int Dent J 1953; 3: 356

Koski K. "Cranial growth centers – facts or fallacies." Am J Orthod 1968; 54: 566-583

Krabbel G., Appel H. "Development of a finite element model of the human skull." J Neurotrauma 1995; 12 (4): 735-742

Kragt G., Duterloo HS., Algra AM. "Initial displacements and variations of eigth human child skulls owing to high-pull headgear traction determined with laser holography." Am J Orthod 1986; 89: 399-406

Kraut RA. "Surgically assisted rapid maxillary expansion by opening the midpalatal suture." J Oral Maxillofac Surg 1984; 42 (10): 651-655

Krebs Å. "Expansion of the midpalatal suture studied by means of metallic implants." Trans Eur Orthod Soc 1958; 34: 163-171

Krebs Å. "Midpalatal suture expansion studied by the implant method over a seven-year period." Trans Eur Orthod Soc 1964; 40: 131-142

Kronfed R. "Histologic study of the influence of function on the human periodontal membrane." Journal of the American Dental Association 1931; 18: 142

Kudlick EM. "A study utilizing direct human skulls as models to determine how bones of the craniofacial complex are displaced under the influence of midpalatal expansion." [Master's Thesis] Rutherford, New Jersey: Fairleigh Dickinson University, 1973

Kummer BKF. "Biomechanics of bone: mechanical properties, functional structure, functional adaptation." In: Fung YC., Perrone N., Anliker M. (ed.) "Biomechanics: Its foundation and objectives." Prentice Hall, Englewood Cliffs, NJ., 1972; pp: 237-271

Kwak BM., Lim OK., Kim YY., Rim K. "An investigation of the effect of cement thickness on an implant by finite element stress analysis." Int Orthop (SICOT) 1979; 2: 315-319

Ladner PT., Muhl ZF. "Changes concurrent with orthodontic treatment when maxillary expansion is a primary goal." Am J Orthod Dentofacial Orthop 1995; 108 (2): 184-193

Lamparski DG., Rinchuse DJ., Close JM., Sciote JJ. "Comparison of skeletal and dental changes between 2-point and 4-point rapid palatal expanders." Am J Orthod Dentofacial Orthop 2003; 123 (3): 321-328

Langford SR., Sims MR. "Root surface resorption, repair, and periodontal attachment following rapid maxillary expansion in man." Am J Orthod 1982; 81 (2): 108-115

Langford SR. "Root resorption extremes resulting from clinical RME." Am J Orthod 1982; 81 (5): 371-377

Laptook T. "Conductive hearing loss and rapid maxillary expansion. Report of a case." Am J Orthod 1981; 80 (3): 325-331

Larrabee WF. " A finite element model of skin deformation I. Biomechanics of skin and soft tissue: a review." Laryngoscope 1986a; 96 (4): 399-405

Larrabee WF., Sutton D. " A finite element model of skin deformation II. An experimental model of skin deformation." Laryngoscope 1986b; 96 (4): 406-412

Larrabee WF., Galt JA. "A finite element model of skin deformation III. The finite element model." Laryngoscope 1986c; 96 (4): 413-419

Latham RA. "The development, structure and growth pattern of the human mid-palatal suture." J Anat 1971; 108 (1): 31-41

Lavelle CL. "An analysis of orthodontically induced changes in craniofacial form." Anat Anz 1988; 166 (1-5): 165-173

Lavelle C. "A retrospective cephalometric study of Class I patients." Br J Orthod 1989; 16 (1): 17-23

Lee KG., Ryu YK., Park YC., Rudolph DJ. "A study of holographic interferometry on the initial reaction of maxillofacial complex during protraction." Am J Orthod Dentofacial Orthop 1997; 111 (6): 623-632

Leong JC., Ma RY., Clark JA., Cornish LS., Yau AC. "Viscoelastic behavior of tissue in leg lengthening by distraction." Clin Orthop Relat Res 1979; 139: 102-109

Levine DL., Stoneking JE. "A three dimensional, finite element based, parametric study of an orthopaedic bone plate." In Simon BR (ed), International Conference Proceedings on Finite Elements in Biomechanics, University of Arizone Press, Tucson, 1980; pp: 713-728

Lewis JL. "Analytical methods in prosthesis design." Proceedings Workshop on Internal Joint Replacement, Northwestern University, Chicago, 1977; pp: 127-134

Lewis JL., Lew WD., Zimmerman JR. "A nonhomogeneous anthropometric scaling method based on finite element analysis." J Biomech 1980; 13 (10): 815-824

Lewis JL., Kramer GM., Wixson RL., Askew MJ. "Calcar loading by titanium total hip stems." Proceedings 27th Annual Meeting Orthopaedic Research Society, Chicago, 1981; p: 75

Lima AC., Lima AL., Filho RM., Oyen OJ. "Spontaneous mandibular arch response after rapid palatal expansion: a long-term study on Class I malocclusion." Am J Orthod Dentofacial Orthop 2004; 126 (5): 576-582

Linder-Aronson S., Lindgren J. "The skeletal and dental effects of rapid maxillary expansion." Br J Orthod 1979; 6 (1): 25-29

Lines PA. "Adult rapid maxillary expansion with corticotomy." Am J Orthod 1975; 67 (1): 44-56

Linge L. "Tissue reactions in facial sutures subsequent to external mechanical influences." In McNamara JA. (ed), "Factors affecting the growth of the midface. (Monograph No 6), Craniofacial Growth Series." Center for Human Growth and Development, The University of Michigan, Ann Arbor, 1976

Lohman A. "Treatment of narrow nasal passages." Dental Record, 1915; 36: 496-497

Lozanoff S., Diewert VM. "Measuring histological form change with finite element methods: an application using diazo-oxo-norleucine (DON) – treated rats." Am J Anat 1986; 177 (2): 187-201

Lozanoff S., Diewert VM. "A computer graphics program for measuring two- and three-dimensional form change in developing craniofacial cartilages using finite element methods." Comput Biomed Res 1989; 22 (1): 63-82

Lozanoff S., Jureczek S., Feng T., Padwal R. "Anterior cranial base morphology in mice with midfacial retrusion." Cleft Palate Craniofac J 1994; 31 (6): 417-428

Major PW., El Badrawy HE. "Maxillary protraction for early orthopedic correction of skeletal Class III malocclusion." Pediatr Dent 1993; 15 (3): 203-207

Marks LW., Gardner TN. "The use of strain energy as a convergence criterion in the finite element modelling of bone and the effect of model geometry on stress convergence." J Biomed Eng 1993; 15 (6): 474-476

McAlarney ME., Dasgupta G., Moss ML., Moss-Salentijn L. "Anatomical macroelements in the study of craniofacial rat growth." J Craniofac Genet Dev Biol 1992; 12 (1): 3-12

McCaffrey TV. "Nasal function and evaluation." In: Bailey BJ (ed.) "Head and neck surgery – otolaryngology." JB Lippincott, Philadelphia, 1993; pp: 264

McDonald JP. "The effect of rapid maxillary expansion on nasal airway resistance, craniofacial morphology and head posture." [PhD Thesis] University of Edinburgh, 1995

McDonald JP. "Airway problems in children – can the orthodontist help?" Ann Acad Med Singapore 1995; 24 (1): 158-162

McElhaney JH., Fogle JL., Melvin JW., Haynes RR., Roberts VL., Alem NM. "Mechanical properties on cranial bone." J Biomech 1970; 3 (5): 495-511

McGuinness NJP. "Three-dimensional orthodontic stress analysis in the periodontal ligament." [MSc Thesis] University of Wales, 1990

McGuinness NJ., Wilson AN., Jones ML., Middleton J. "A stress analysis of the periodontal ligament under various orthodontic loadings." Eur J Orthod 1991; 13 (3): 231-242

McGuinness N., Wilson AN., Jones M., Middleton J., Robertson NR. "Stresses induced by edgewise appliances in the periodontal ligament – a finite element study." Angle Orthod 1992; 62 (1): 15-22

McPherson GK., Kriewall TJ. "The elastic modulus of fetal cranial bone: a first step towards an understanding of the biomechanics of fetal head molding." J Biomech 1980; 13 (1): 9-16

McPherson GK., Kriewall TJ. "Fetal head molding: an investigation utilizing a finite element model of the fetal parietal bone." J Biomech 1980; 13 (1): 17-26

Mehta BV., Rajani S., Sinha G. "Comparison of image processing techniques (magnetic resonance imaging, computed tomography scan and ultrasound) for 3D modeling and analysis of the human bones." J Digit Imaging 1997; 10 (3)(Suppl 1): 203-206

Meijer HJ., Starmans FJ., Bosman F., Steen WH. "A comparison of three finite element models of an edentulous mandible provided with implants." J Oral Rehabil 1993; 20 (2): 147-157

Melsen B. "Effects of cervical anchorage during and after treatment: an implant study." Am J Orthod, 1978; 73 (5): 526-540

Melsen B., Melsen F. "The postnatal development of the palatomaxillary region studied on human autopsy material." Am J Orthod 1982; 82 (4): 329-342

Melvin JW., Robbins DH., Roberts VL. "The mechanical behaviour of the diploe layer of the human skull in compression." Dev Mech. 1969; 5: 811-818

Memikoglu TUT., Işeri H. "Effects of a bonded rapid maxillary expansion appliance during orthodontic treatment." Angle Orthodontist 1999; 69: 251-256

Meroueh KA., Watanabe F., Mentag PJ. "Finite element analysis of partially edentulous mandible rehabilitated with an osteointegrated cylindrical implant." J Oral Implantol 1987; 13 (2): 215-238

Middleton J., Jones M., Wilson A. "The role of the periodontal ligament in bone modeling: the initial development of a time-dependent finite element model." Am J Orthod Dentofacial Orthop 1996; 109 (2): 155-162

Miyasaka J., Tanne K., Yamagata Y., Sakuda M., Tsutsumi S. "Finite Element Analysis for biomechanical effects on Craniofacial Skeleton." Osaka University Press, Japan, 1986

Moaddab MB., Dumas AL., Chavoor AG., Neff PA., Homayoun N. "Temporomandibular joint: computed tomographic three-dimensional reconstruction." Am J Orthod 1985; 88 (4): 342-352

Mommaerts MY. "Transpalatal distraction as a method of maxillary expansion." British J Oral Maxillofac Surg 1999; 37 (4): 268-272

Mondro JF. "An improved direct-bonded palatal expansion appliance." J Clin Orthod 1977; 11: 203-206

Montgomery WM., Vig PS., Staab EV., Matteson SR. "Computed tomography: a three-dimensional study of the nasal airway." Am J Orthod 1979; 76 (4): 363-375

Moorrees CFA., Lebret L. "Mesh diagram and cephalometrics." Angle Orthod 1962; 32: 214-231

Moss ML. "The primacy of functional matrices in orofacial growth." Dent Pract Dent Rec 1968; 19 (2): 65-73

Moss ML. "New studies of cranial growth." Birth Defects Orig Artic Ser 1975; 11 (7): 283-295

Moss ML., Skalak R., Dasgupta G., Uilmann H. "Space, time, and space-time in craniofacial growth." Am J Orthod 1980; 77 (6): 591-612

Moss ML., Skalak R., Moss-Salentijn L., Dasgupta GM., Vilmann H., Mehta P. "The allometric center. The biological basis of an analytical model of craniofacial growth." Proc Finn Dent Soc 1981; 77 (1-3): 119-128

Moss ML., Skalak R., Shinozuka M., Patel H., Moss-Salentijn L., Vilmann H., Mehta P. "Statistical testing of an allometric centered model of craniofacial growth." Am J Orthod 1983; 83 (1): 5-18

Moss ML., Skalak R., Patel H., Shinozuka M., Moss-Salentijn L., Vilmann H. "An allometric network model of craniofacial growth." Am J Orthod 1984; 85 (4): 316-332

Moss ML., Shaklak R., Patel H., Sen K., Moss-Salentijn L., Shinozuka M., Vilmann H. "Finite element method modeling of craniofacial growth." Am J Orthod 1985; 87 (6): 453-472

Moss ML., Vilmann H, Moss-Salentijn L., Sen K., Pucciarelli HM., Skalak R. "Studies on orthocephalization: growth behavior of the rat skull in the period 13-49 days as described by the finite element method." Am J Phys Anthropol 1986; 72 (3): 323-342

Motoyoshi M., Shimazaki T., Sugai T., Namura S. "Biomechanical influences of head posture on occlusion: an experimental study using finite element analysis." Eur J Orthod 2002; 24 (4): 319-326

Moussa R., O'Reilly MT., Close JM. "Long-term stability of rapid palatal expander treatment and edgewise mechanotherapy." Am J Orthod Dentofacial Orthop 1995; 108 (5): 478-488

Movassaghi K., Altobelli DE., Zhou H. "Frontonasal suture expansion in the rabbit using titanium screws." J Oral Maxillofac Surg 1995; 53 (9): 1033-1042; discussion 1042-1043

Moyers RE., Bookstein FL. "The inappropriateness of conventional cephalometrics." Am J Orthod 1979; 75 (3): 599-617

Musson S. "A cephalometric study of growth changes in cleft lip and palate patients with the aid of tantalum implants." [MSc Thesis] University of Wales College of Medicine, 1985

Nanda R. "Protraction of maxilla in rhesus monkeys by controlled extraoral forces." Am J Orthod 1978; 74 (2): 121-141

Nanda R. "Biomechanical and clinical considerations of a modified protraction headgear." Am J Orthod 1980; 78 (2): 125-139

Nanda R., Hickory W. "Zygomaticomaxillary suture adaptations incident to anteriorly-directed forces in Rhesus monkeys." Angle Orthod 1984; 54 (3): 199-210

Odenrick L., Lilja E., Lindbäck KF. "Root surface resorption in two cases of rapid maxillary expansion." Br J Orthod 1982; 9 (1): 37-40

Owen DJR., Hinton EA. "A simple guide to Finite Elements." Prineridge Press Ltd., Swansea, 1980

Pavlin D., Vukicevic D. "Mechanical reactions of facial skeleton to maxillary expansion determined by laser holography." Am J Orthod 1984; 85 (6): 498-507

Persson M., Thilander B. "Palatal suture closure in man from 15 to 35 years of age." Am J Orthod 1977; 72 (1): 42-52

Pfaff W. "Stenosis of the Nasal Cavity caused by contraction of the palatal arch and abnormal position of the teeth: treatment by expansion of the maxilla." Dental Cosmos 1905; 45: 570-573

Pieper SD., Laub DR., Rosen JM. "A finite element facial model for simulating plastic surgery." Plast Reconstr Surg 1995; 96 (5): 1100-1105

Posnick JC., Bite V., Nakano P., Davis J., Armstrong D. "Indirect intracranial volume measurements using CT scans: clinical applications for craniosynostosis." Plast Reconstr Surg 1992; 89 (1): 34-45

Pritchard JJ., Scott JH., Girgis FG. "The structure and development of cranial and facial sutures." J Anat 1956; 90 (1): 73-86

Proffit WR. "Contemporary Orthodontics." (3rd Ed.) Mosby Inc., St. Louis, 2000

Rao SS. "The Finite Element Method in Engineering." New York, Pergamon Press, 1982

Remmler D., Olson L., Ekstrom R., Duke D., Matthews D., Ullrich CG. "Pre-surgical finite element analysis from routine computed tomography studies for craniofacial distraction: II. An engineering prediction model for gradual correction of asymmetric skull deformities." Plast Reconstr Surg 1998; 102 (5): 1395-1404

Remmler D., Olson L., Ekstrom R., Duke D., Matamoros A., Matthews D., Ullrich CG. "Pre-surgical CT/FEA for craniofacial distraction: I. Methodology, development and validation of the cranial finite element model." Med Eng Phys 1998; 20 (8): 607-619

Revelo B., Fishman LS. "Maturational evaluation of ossification of the midpalatal suture." Am J Orthod Dentofacial Orthop 1994; 105 (3): 288-292

Richtsmeier JT., Cheverud JM. "Finite element scaling analysis of human craniofacial growth." J Craniofac Genet Dev Biol 1986; 6 (3): 289-323

Ricketts RM., Bench RW., Hilgers JJ., Schulhof R. "An overview of computerised cephalometrics." Am J Orthod 1972; 61 (1): 1-28

Rieger MR., Fareed K., Adam WK., Tanquist RA. "Bone stress distribution for three endosseous implants." J Prosthet Dent 1989; 61 (2): 223-228

Roehrle H., Sollbach W., Gekeler J. "Stress analysis in artificial knee joints with fixed and movable axis using the finite element method." In: Huiskes R., Van Campen DH., De Wijn JR (ed.) "Biomechanics: Principles and Applications." Martinus Nijhoff, The Hague, 1982; pp: 305-312

Ruan JS., Khalil T., King AI. "Dynamic response of the human head to impact by three-dimensional finite element analysis." J Biomech Eng 1994; 116 (1): 44-50

Rubin C., Krishnamurthy N., Capilouto E., Yi H. "Stress analysis of the human tooth using a three-dimensional finite element model." J Dent Res 1983; 62 (3): 82-86

Rybicki EF., Simonen FA., Weis EB. "On the mathematical analysis of stress in the human femur." J Biomech 1972; 5 (2): 203-215

Rybicki EF., Simonen FA., Mills EJ., Hassler CR., Scoles P., Milne D., Weis EB. "Mathematical and experimental studies on the mechanics of plated transverse fractures." J Biomech 1974; 7 (4): 377-384

Sameshima GT., Melnick M. "Finite element-based cephalometric analysis." Angle Orthod 1994; 64: 343-350

Sandstrom RA., Klapper L., Papaconstantinou S. "Expansion of the lower arch concurrent with rapid maxillary expansion." Am J Orthod Dentofacial Orthop 1988; 94 (4): 296-302

Sarnäs KV., Björk A., Rune B. "Long term effect of rapid maxillary expansion studied in one patient with the aid of metallic implants and roentgen stereometry." Eur J Orthod 1992; 14 (6): 427-432

Sassouni V. "Roentgenographic cephalometric analysis of cephalo-facio-dental relationships." Am J Orthod 1955; 41: 734-742

Scholten R., Roehrle H., Sollbach W. "Analysis of stress distribution in natural and artificial hip joints using finite element method." S. Afr. Mech Eng 1978; 28: 220-225

Scott JH. "The growth of the human face." Proc R Soc Med 1954; 47 (2): 91-100

Scott JH. "The growth and function of the muscles of mastication in relation to the development of the facial skeleton and of the dentition." Am J Orthod 1954; 40: 429-449

Siegele D., Soltesz U., Scheicher H. "Dental implants with flexible inserts – a possibility to improve the stress distribution in the jaw." In: Perren SM., Schneider E. (ed.) "Biomechanics: Current Interdisciplinary Research." Dordrecht; 1985; pp: 271

Sih GC., Matic P., Berman AT. "Failure prediction of the total hip prosthesis system." J Biomech 1981; 14 (12): 833-841

Simon BR., Woo SL., Stanley GM., Olmstead SR., McCarty MP., Jemmott GF., Akeson WH. "Evaluation of one-, two-, and three-dimensional finite element and experimental models of internal fixation plates." J Biomech 1977; 10 (2): 79-86

Singh GD., McNamara JA., Lozanoff S. "Finite element analysis of the cranial base in subjects with Class III malocclusion." Br J Orthod 1997; 24 (2): 103-112

Skalak R. "Biomechanical considerations in osseointegrated prostheses." J Prosthet Dent 1983; 49 (6): 843-848

Skieller V. "Expansion of the midpalatal suture by removable plates, analysed by the implant method." Trans Eur Orthod Soc 1964; 40: 143-158

Skinner HB., Cook SD., Weinstein AM., Haddad RJ. "Stress changes in bone secondary to the use of a femoral canal plug with cemented hip replacement." Clin Orthop Relat Res 1982; 166: 277-283

Solow B., Tallgren A. "Head posture and craniofacial morphology." Am J Phys Anthropol 1976; 44: 417-436

Spolyar J. "The design, fabrication and use of a full coverage bonded rapid maxillary expansion appliance." Am J Orthod 1984; 86: 136-145

Sprawls P. "The principles of Computed Tomography Image Formation and Quality. Essentials of Body Computed Tomography." Saunders, 1990, pp:1-9

Starnbach H., Cleall J. "The effects of splitting the midpalatal suture on the surrounding sutures. (Abstr)" Am J Orthod 1964; 50: 923-924

Starnbach H., Bayne D., Cleall J., Subtelny JD. "Facioskeletal and dental changes resulting from rapid maxillary expansion." Angle Orthod 1966; 36 (2): 152-164

Storey E. "Tissue response to the movement of bones." Am J Orthod 1973; 64 (3): 229-247

Sung SJ., Baik HS., Moon YS., Yu HS., Cho YS. "A comparative evaluation of different compensating curves in the lingual and labial techniques using 3D FEM." Am J Orthod Dentofacial Orthop 2003; 123 (4): 441-450

Synge LL. "The tightness of the teeth, considered as a problem concerning the equilibrium of a thin incompressible elastic membrane." Philosoph Trans Roy Soc London, 1933; 435-477

Tanaka E., Tanne K., Sakuda M. "A three-dimensional finite element model of the mandible including the TMJ and its application to stress analysis in the TMJ during clenching." Med Eng Phys 1994; 16 (4): 316-322

Tanne K., Sakuda M. "Initial stress induced in the periodontal tissue at the time of the application of various types of orthodontic force: three-dimensional analysis by means of the finite element method." J Osaka Univ Dent Sch 1983; 23: 143-171

Tanne K., Miyasaka J., Yamagata Y., Sakuda M., Burstone CJ. "Biomechanical changes in the craniofacial skeleton due to rapid expansion appliances. (Abstract)" J Osaka Daikaku Shigaku Zasshi 1985; 30 (2): 345-356

Tanne K., Sakuda M., Burstone CJ. "Three-dimensional finite element analysis for stress in the periodontal tissue by orthodontic forces." Am J Orthod Dentofacial Orthop 1987; 92 (6): 499-505

Tanne K. "Stress distribution in the periodontal membrane associated with various moment to force ratios in orthodontic force systems." J Osaka Univ Dent Sch 1987; 27: 1-9

Tanne K., Miyasaka J., Yamagata Y., Sachdeva R., Tsutsumi S., Sakuda M. "Three-dimensional model of the human craniofacial skeleton: method and preliminary results using finite element analysis." J Biomed Eng 1988; 10 (3): 246-252

Tanne K., Hiraga J., Kakiuchi K., Yamagata Y., Sakuda M. "Biomechanical effect of anteriorly directed extraoral forces on the craniofacial complex: a study using the finite element method." Am J Orthod Dentofacial Orthop 1989; 95 (3): 200-207

Tanne K., Hiraga J., Sakuda M. "Effects of directions of maxillary protraction forces on biomechanical changes in craniofacial complex." Eur J Orthod 1989; 11 (4): 382-391

Tanne K., Nagataki T., Inoue Y., Sakuda M., Burstone CJ. "Patterns of initial tooth displacements associated with various root lengths and alveolar bone heights." Am J Orthod Dentofacial Orthop 1991; 100 (1): 66-71

Tanne K., Sakuda M. "Biomechanical and clinical changes of the craniofacial complex from orthopedic maxillary protraction." Angle Orthod 1991; 61 (2): 145-152

Tanne K., Shibaguchi T., Terada Y., Kato J., Sakuda J. "Stress levels in the PDL and biological tooth movement." In: (eds) "The Biological Mechanisms of Tooth Movement and Craniofacial Adaptations." 1992; pp: 201-209

Tanne K., Lu YC., Tanaka E., Sakuda M. "Biomechanical changes of the mandible from orthopaedic chin cup force studied in a three-dimensional finite element model." Eur J Orthod 1993; 15 (6): 527-533

Tanne K., Matsubara S., Sakuda M. "Location of the centre of resistance for the nasomaxillary complex studied in a three-dimensional finite element model." Br J Orthod 1995: 22 (3): 227-232

Tanne K., Tanaka E., Sakuda M. "Stress distributions in the TMJ during clenching in patients with vertical discrepancies of the craniofacial complex." J Orofac Pain 1995; 9 (2): 153-160

Tanne K., Matsubara S. "Association between the direction of orthopedic headgear force and sutural responses in the nasomaxillary complex." Angle Orthod 1996; 66 (2): 125-130

Tanne K., Tanaka E., Sakuda M. "Stress distribution in the temporomandibular joint produced by orthopedic chincup forces applied in varying directions: a three-dimensional analytic approach with the finite element method." Am J Orthod Dentofacial Orthop 1996; 110 (5): 502-507

Tarr RR., Clarke IC., Gruen TA., Sarmiento A. "Predictions of cement-bone failure criteria: three-dimensional finite element models versus clinical reality of total hip replacement." In: Gallagher RH., Simon BR., Johnson PC., Gross JF. (eds) "Finite Elements in Biomechanics." John Wiley, New York, 1982; pp:345-359

Ten Cate AR., Freeman E., Dickinson JB. "Sutural development: structure and its response to rapid expansion." Am J Orthod 1977; 71 (6): 622-636

Thörne H. "Experiences on widening the median maxillary suture." Trans Eur Orthod Soc 1956; 31: 279-290

Timms DJ. "Some medical aspects of rapid maxillary expansion." Br J Orthod 1974; 1: 127-132

Timms DJ. "A study of basal movement with rapid maxillary expansion." Am J Orthod 1980; 77 (5): 500-507

Turbyfill WJ. "The long term effect of rapid maxillary expansion." [Master's Thesis] Chapel Hill, North Carolina: University of North Carolina, 1976

Turner MJ., Clough RW., Martin HC., Topp LJ. "Stiffness and deflection analysis of complex structures." J Aero Sci 1956; 23: 805-823

Ulrich DE. "Mandibular width changes associated with maxillary expansion" [Master's Thesis] Chicago, Northwestern University, 1997

Umetani Y., Inou M. "Movement and function of mandible – a simplified mechano-morphological model of mandible." Anat Anaz 1988; 165 (2-3): 193-196

Valliappan S., Kjellberg S., Svensson NL. "Finite Element analysis of total hip prosthesis." In: Simon BR (ed.) International Conference Proceedings on Finite Elements in Biomechanics, University of Arizona Press, Tuscon, 1980; pp: 528-548

van Buskirk WC., Thongpreda N., Hart RT., Anderson RC., Carter R. "Biomechanics of the mandible." J Dent Res 1988; 67: 254

van der Klaauw CJ. "Cerebral skull and facial skull. A contribution to the knowledge of skull structure." Arch Neerl Zool 1945; 7: 16-37

van der Linden FP. "A new method to determine tooth positions and dental arch dimensions." J Dent Res 1972; 51 (4): 1104

van Rietbergen B., Weinans H., Huiskes R., Odgaard A. "A new method to determine trabecular bone elastic properties and loading using michromechanical finite-element models." J Biomech 1995; 28 (1): 69-81

van Rietbergen B., Müller R., Ulrich D., Rügsegger P., Huiskes R. "Tissue stresses and strain in trabeculae of a canine proximal femur can be quantified from computer reconstructions." J Biomech 1999; 32 (2): 165-173

van Rossen IP., Braak LH., de Putter C., de Groot K. "Stress-absorbing elements in dental implants." J Prosthet Dent 1990; 64 (2): 198-205

Vardimon AD., Brosh T., Spiegler A., Lieberman M., Pitaru S. "Rapid palatal expansion: Part 1. Mineralization pattern of the midpalatal suture in cats." Am J Orthod Dentofacial Orthop 1998; 113 (4): 371-378

Vardimon AD., Brosh T., Spiegler A., Lieberman M., Pitaru S. "Rapid palatal expansion. Part 2: Dentoskeletal changes in cats with patent versus synostosed midpalatal suture." Am J Orthod Dentofacial Orthop 1998; 113 (5): 488-497

Verna C., Dalstra M., Lee TC., Cattaneo PM., Melsen B. "Microcracks in the alveolar bone following orthodontic tooth movement: a morphological and morphometric study." Eur J Orthod 2004; 26 (5): 459-467

Verrue V., Dermaut L., Verhegghe B. "Three-dimensional finite element modelling of a dog skull for the simulation of initial orthopaedic displacements" Eur J Orthod, 2001; 23 (5): 517-527

Vichnin HH., Hayes WC., Lotke PA. "Parametric FE studies of tibial component fixation in the total condylar knee prosthesis." Proceedings 25th Annual Meeting Orthopaedic Research Society, Chicago, 1979; p: 99

Vichnin HH., Batterman SC. "Effects of cortical bone anisotropy on prosthesis stem stresses." Proceedings 28th Annual Meeting Orthopaedic Research Society, Chicago, 1982; p: 277

von Fraunhofer JA. "The finite element method of stress analysis and its application to dental problems." In: (ed.) "Scientific Aspects of Dental Materials." Butterworths, London and Boston, 1975; pp: 41

Voo K., Kumaresan S., Pintar FA., Yoganandan N., Sances A. "Finite-element models of the human head." Med Biol Eng Comput 1996; 34 (5): 375-381

Wagemans PA., van de Velde JP., Kuijpers-Jagtman AM. "Sutures and forces: a review." Am J Orthod 1988; 94 (2): 129-141

Walters RD. "Facial changes in the *Macaca Mulatta* monkey by orhtopedic opening of the midpalatal suture." Angle Orthod 1975; 45: 169-179

Warren DW. "Aerodynamic studies of upper airway: Implications for growth, breathing, and speech." In McNamara JA., Ribbens K. (eds), "Naso-respiratory function and craniofacial growth. (Monograph No 9), Craniofacial Growth Series." Center for Human Growth and Development, The University of Michigan, Ann Arbor, 1979

Wehrbein H., Yildizhan F. "The mid-palatal suture in young adults. A radiological-histological investigation." Eur J Orthod 2001; 23 (2): 105-114

Weinans H., Huiskes R., Grootenboer HJ. "The behavior of adaptive bone-remodeling simulation models." J Biomech 1992; 25 (12): 1425-1441

Wertz RA. "Changes in nasal airflow incident to rapid maxillary expansion." Angle Orthod 1968; 38 (1): 1-11

Wertz RA. "Skeletal and dental changes accompanying rapid midpalatal suture opening." Am J Orthod 1970; 58 (1): 41-66

Wertz RA., Dreskin M. "Midpalatal suture opening. A normative study." Am J Orthod Dentofacial Orthop 1977; 71: 367-381

William KR., Edmundson JT., Rees JS. "Finite Element Stress Analysis of restored teeth." Dent Material 1987; 3: 200-206

Williams S, Melsen B. "The interplay between sagittal and vertical growth factors. An implant study of activator treatment." Am J Orthod 1982; 81 (4): 327-332

Williams S., Leighton BC., Nielsen JH. "Linear evaluation of the development of sagittal jaw relationships." Am J Orthod 1985; 88 (3): 235-241

Wilson AN., Jones ML., Middleton J. "The effect of the periodontal ligament on bone remodelling." In: (eds) "Recent advances in Computer Methods in Biomechanics and Biomechanical Engineering." Books and Journals International, 1992; pp: 150-158

Wilson AN., Middleton J., Jones ML., McGuinness NJ. "The finite element analysis of stress in the periodontal ligament when subject to vertical orthodontic forces." Br J Orthod 1994; 21 (2): 161-167

Woo SL., Simon BR., Akeson WH., McCarty MP. "An interdisciplinary approach to evaluate the effect of internal fixation plate on long bone remodeling." J Biomech 1977; 10 (2): 87-95

Wright KW., Yettram AL. "Finite element stress analysis of Class I amalgam restoration subjected to setting and thermal expansion." J Dent Res 1978; 57 (5-6): 715-723

Yettram AL., Wright KW., Houston WJ. "Centre of rotation of a maxillary central incisor under orthodontic loading." Br J Orthod 1977; 4 (1): 23-27

Yettram AL., Wright KW. "Biomechanics of the femoral component of total hip prostheses with particular reference to the stress in the bone-cement." J Biomed Eng 1979; 1 (4): 281-285

Yettram AL., Wright KW. "Dependence of stem stress in total hip replacement on prosthesis and cement stiffness." J Biomed Eng 1980; 2 (1): 54-59

Zienkiewicz OC. "The Finite Element Method." (3rd Ed.) McGraw-Hill Book Company, London, 1977

Zimring JF., Isaacson RJ. "Forces produced by rapid maxillary expansion: part III. Forces present during retention." Angle Orthod 1965; 35: 178-186

APPENDIX:

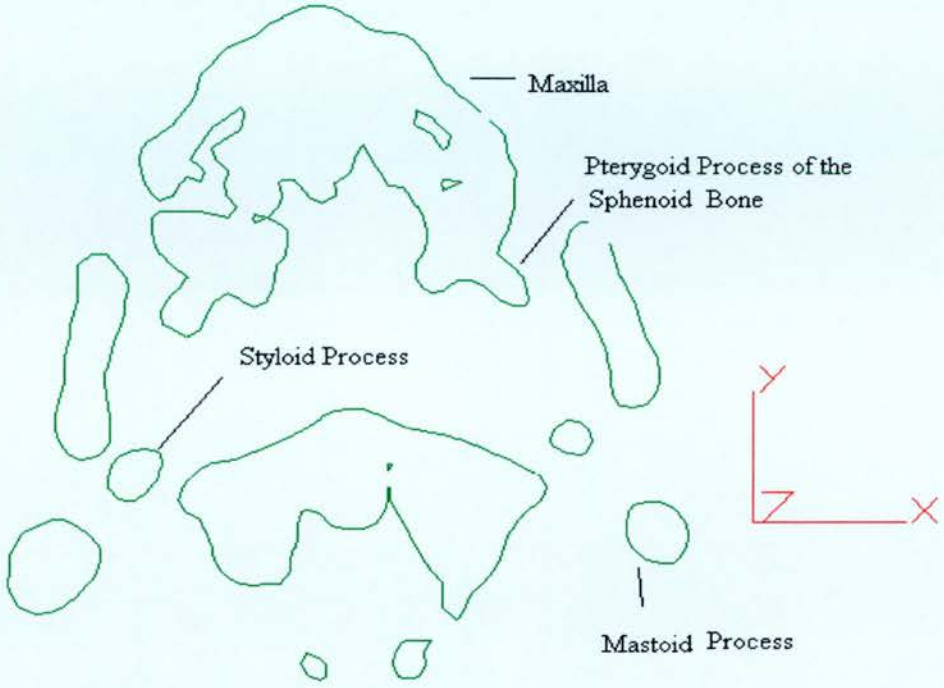

Appendix 1. Top view of section for Z=6

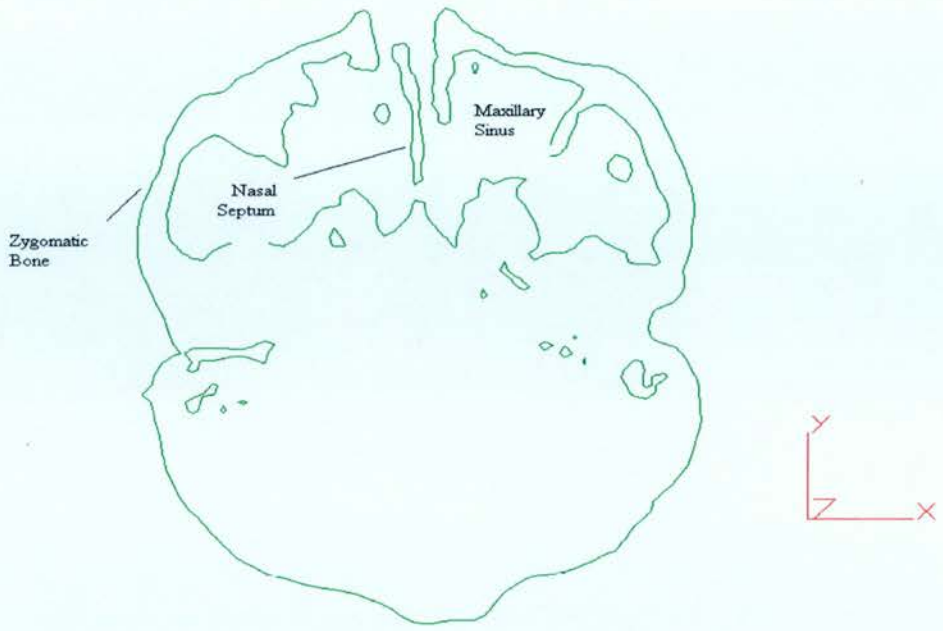

Appendix 2. Top view of section for Z=30

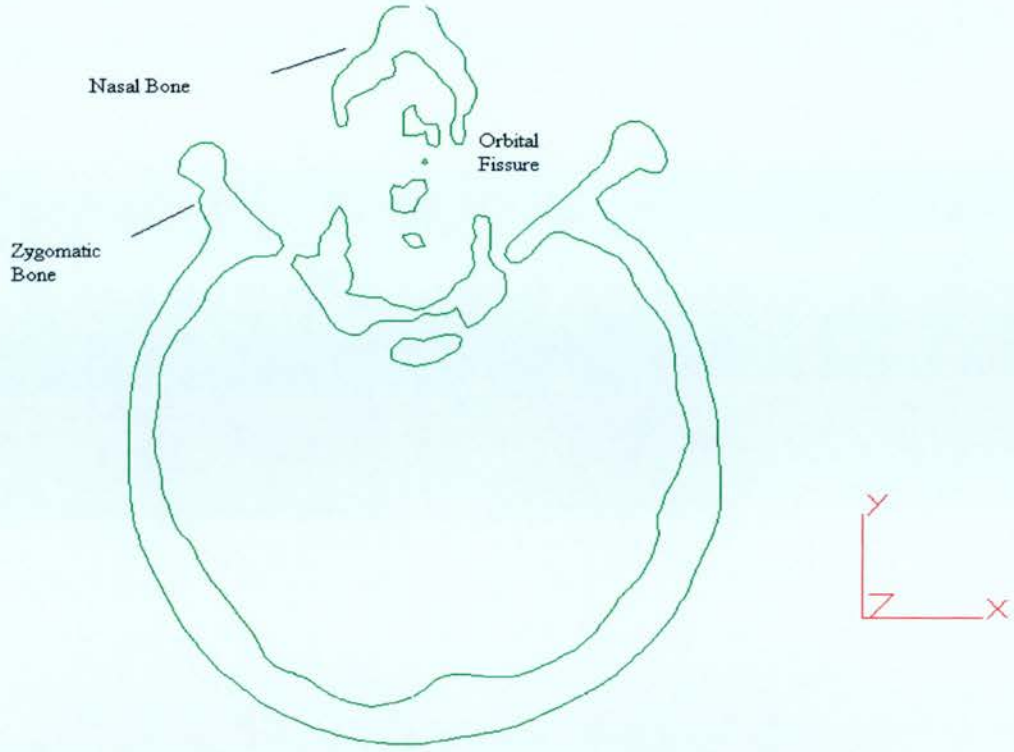

Appendix 3. Top view of section for Z=57

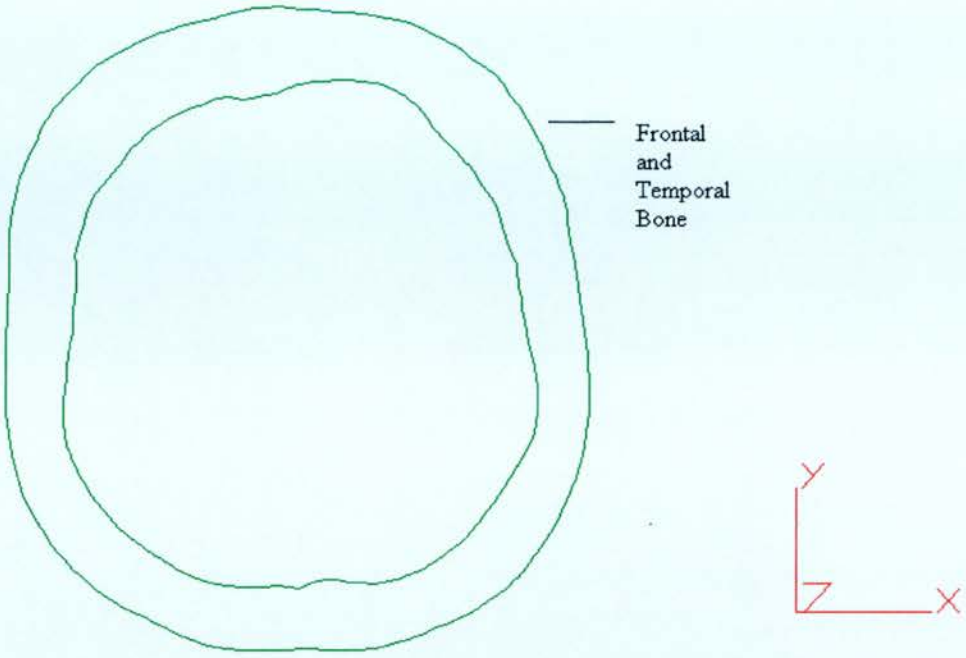

Appendix 4. Top view of section for Z=120

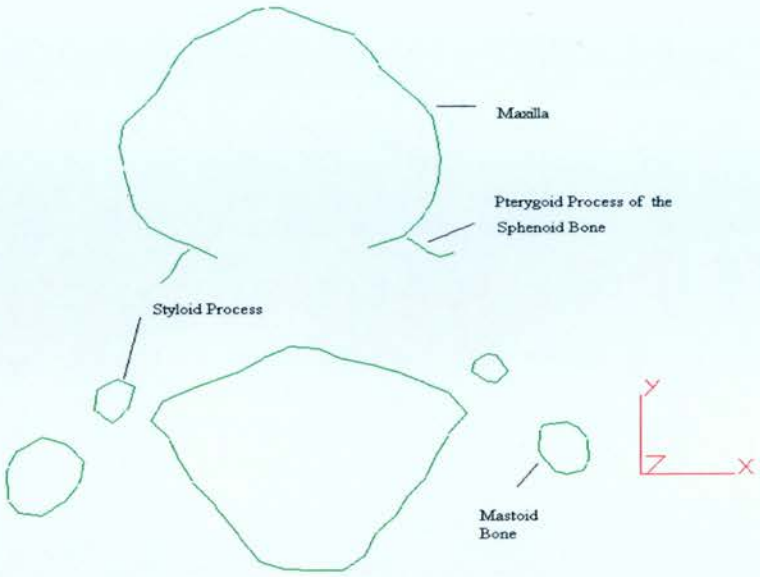

Appendix 5. Top view of section for Z=6

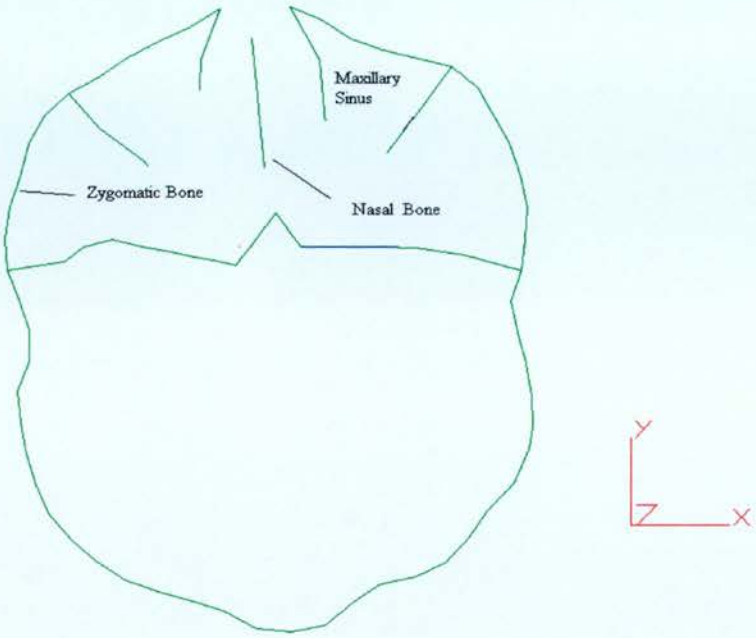

Appendix 6. Top view of section for Z=30

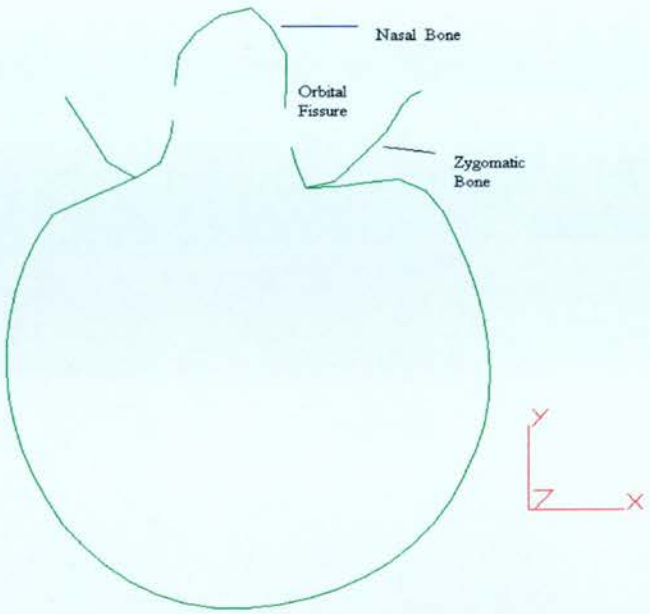

Appendix 7. Top view of section for Z=57

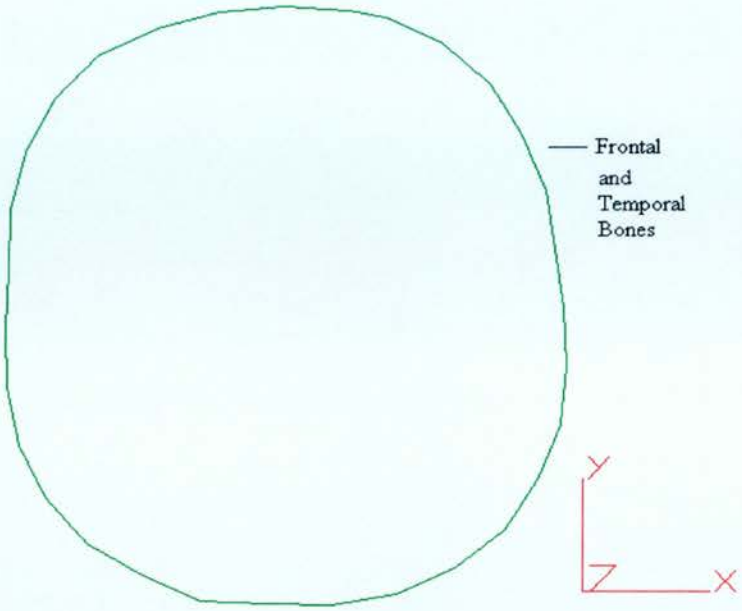

Appendix 8. Top view of section for Z=120

Appendix 9. Skeletal Landmarks used in digitising lateral cephalometric radiographs

Nr	Name	Definition
1	Sella (s)	The midpoint of the pituitary fossa (sella turcica); it is a constructed point in the median plane
2	Nasion (na)	The most anterior point of the frontonasal suture in the median plane (unilateral)
3	Posterior Nasal Spine (pns)	The intersection of a continuation of the anterior wall of the pterygopalatine fossa and the floor of the nose, marking the dorsal limit of the maxilla (unilateral)
4	Anterior Nasal Spine (ans or sp, spinal point)	This is the tip of the bony anterior nasal spine, in the median plane (unilateral)
5	A point (ss or subspinale) (Downs)	The point at the deepest midline concavity on the maxilla between Anterior Nasal Spine and Prosthion (unilateral)
6	Prosthion (Pr or Supradentale	The lowest and most anterior point on the alveolar portion of the premaxilla in the median plane between the upper central incisors (unilateral)
7	Infradentale (Id)	The highest and most anterior point on the alveolar process, in the median plane, between the mandibular central incisors (unilateral)
8	B point (B) (or sm, supramentale)	The point at the deepest midline concavity on the mandibular symphysis between Infradentale and Pogonion (unilateral) (Downs)
9	PM Protuberance Menti	Point on the chin, where the curvature changes from concave to convex, between B point and Pogonion
10	Pogonion (Pog)	The most anterior point of the bony chin in the median plane (unilateral)

11	Gnathion (Gn)	The most anterior and inferior point on the symphysis of the chin, and it is constructed by intersecting a line drawn peRMEndicular to the line connecting Me and Pog
12	Menton (Me)	The most inferior midline point on the mandibular symphysis (unilateral)
13	Mandibular Tangent Anterior	The lowest most point of the contour of the mandibular body between Menton and Antegonial notch
14	Antegonial Notch	
15	Mandibular Tangent Post	The lowest most point of the contour of the mandibular body posterior to Antegonial Notch
16	Gonion (Go)	The constructed point of intersection of the ramus plane and the mandibular plane
17	Articulare (Ar)	The point of intersection of the images of the posterior border of the condylar process of the mandible and the inferior border of the basilar part of the occipital bone (bilateral) (redefined by Coben after Björk)
18	Condylion (Co or cd)	The most superior point on the head of the condylar head (bilateral)
19	DC point (Ricketts)	Midpoint at the neck of the condyle
20	Xi point (Ricketts)	A point at the center of the mandibular ramus, opposite the mandibular foramen
21	Basion (Ba) (Coben)	The median point of the anterior margin of the foramen magnum can be located by following the image of the slope of the inferior border of the basilar part of the occipital bone to its posterior limit (unilateral)
22	Porion (Po) (anatomic)	The superior point of the external auditory meatus (bilateral)

23	Orbitale (Or)	The lowest point in the inferior margin of the orbit, midpoint between left and right images (bilateral)
24	PT point	A point at the foramen rotundum, at the most superior and posterior contour of the pterygomaxillary fissure
25	CF Pterygoidal distal	The most posterior point of the pterygomaxillary fissure
26	Pterygomaxillary fissure (Ptm)	A bilateral teardrop-shaped area of radioluscency, the anterior shadow of which represents the posterior surfaces of the tuberosities of the maxilla; the landmark is taken where the two edges, front and back, appear to merge inferiorly
38	Dorsum Sellae (Sp) (Sassouni Analysis)	The most posterior point on the internal contour of the sella turcica (unilateral)
39	Floor of Sella (Si) (Sassouni Analysis)	The lowermost point on the internal contour of the sella turcica (unilateral)
40	Clinoidale (Cl) (Sassouni Analysis)	The most superior point on the contour of the anterior clinoid (unilateral)
41	Sphenoethmoidal (SE) (Sassouni Analysis)	The intersection of the shadows of the greater wing of the sphenoid and the cranial floor as seen in the lateral cephalogram
42	Roof of the Orbit (RO) (Sassouni Analysis)	The uppermost point on the roof of the orbit (bilateral)
43	Supraorbitale (SOr) (Sassouni Analysis)	The most anterior point on the intersection of the shadow of the roof of the orbit and its lateral contour (bilateral)

Appendix 10. Dental Landmarks used in digitising lateral cephalometric radiographs

Nr	Name	Definition
27	Incision Superious Incisalis (Isi)	The incisal edge of the maxillary central incisor
28	Maxillary Central Incisor (U1)	The most labial point on the crown of the maxillary central incisor
29	Incision Superious Apicalis (Isa)	The root apex of the most anterior maxillary central incisor
30	Incision Inferious Apicalis (Iii)	The incisal edge of the most prominent mandibular central incisor
31	Mandibular Central Incisor (L1)	The most labial point on the crown of the mandibular central incisor
32	Incision Inferious Apicalis (Iia)	The root apex of the most anterior mandibular central incisor
33	Mandibular First Molar (L6)	The tip of the mesiobuccal cusp of the mandibular first permanent molar
34	Lower Molar Mesial Apex	The apex of the mesial root of the mandibular first permanent molar
35	Maxillary First Molar (U6)	The tip of the mesiobuccal cusp of the maxillary first permanent molar
36	Upper Molar Mesial Apex	The apex of the mesial root of the maxillary first permanent molar
37	Upper Molar Distal	Point on the distal surface of the maxillary first permanent molar crown

Appendix 11. Soft Tissue Landmarks used in digitising lateral cephalometric radiographs

Nr	Name	**Definition**
38	Glabella (G)	The most prominent point in the midsagittal plane of forehead
39	Soft Above Nasion	A point above Soft Nasion
40	Nasion Soft Tissue (Ns)	The point of deepest concavity of the soft tissue contour of the root of the nose
41	Soft Below Nasion	A point below Soft Nasion
42	Soft Bridge of Nose	A point on the bridge of the nose, approximately at the middle
43	Upper Nasal Tangent Point (unt)	The nasal tangent point of the nose frontal line
44	Pronasale (Pn)	The most prominent point of the nose
45	Lower Nasal Tangent Point (lnt)	The upper tangent point of the nose chin line
46	Subnasale (Sn)	The point where the lower border of the nose meets the outer contour of the upper lip
47	Superior Labial Sulcus (Sls)	The point of greatest concavity in the midline of the upper lip between subnasale and labrale superius
48	Soft Above Labrale Sup.	
49	Labrale Superious (Ls)	The median point in the upper margin of the upper membranous lip
50	Soft Below Labrale Sup	
51	Stomion Superious (Sts)	The lowest point of the upper lip
52	Stomion Inferious (Sti)	The highest point of the lower lip
53	Soft Above Labrale Inf.	
54	Labrale Inferious (Li)	The median point in the lower margin of the lower membranous lip

55	Soft Below Labrale Inf	
56	Inferior Labial Sulcus (Ils)	The point of greatest concavity in the midline of the lower lip between labrale inferious and menton
57	Pogonion Soft Tissue (Pos)	The most prominent point on the soft tissue contour of the chin
58	Gnathion Soft Tissue (Gns)	The soft tissue point overlying gnathion
59	Menton Soft Tissue (Ms)	The constructed point of intersection of a vertical co-ordinate from menton and the inferior soft tissuc contour of the chin
60	Submentale (sme)	The deepest point in the submental neck curvature

Appendix 12. Landmarks used in digitising Postero-anterior cephalometric radiographs

Nr	Name	Definition
1	Antegonion (ag)	The highest point in the antegonial notch (left & right)
2	Gonion (gon)	Point located at the gonial angle of the mandible (left & right)
3	Lateral Ramus (lr)	Point on the lateral border of the ramus, located between the condylar head and gonial angle (left & right)
4	Condyle Lateral (lc)	Point located at the lateral pole of the condylar head (left & right)
5	Condylar (cd)	The most superior point of the condylar head (left & right)
6	Body of the Mandible (mbdy)	Point located on the inferior surface of the body of the mandible between gonial angle and symphysis (left & right)
7	Prementon (pmen)	Point located on the inferior surface of the body of the mandible (left & right)
8	Mandibular Midpoint (m)	Located by projecting the mental spine on the lower mandibular border, peRMEndicular to the line ag-ag
9	Anterior Nasal Spine (ans)	The tip of the anterior nasal spine
10	Inferior Nasal Cavity (inc)	The most inferior aspect of the nasal cavity
11	Lateral Piriform Aperture (lpa)	The most lateral aspect of the piriform aperture (left & right)
12	Superior Nasal Cavity (snc)	The most superior aspect of the nasal cavity
13	Crista Galli	
14	Maxillare (mx)	The intersection of the lateral contour of the maxillary alveolar process and the lower contour of the maxillozygomatic process of the maxilla (left & right)
15	Mastoid Lateral (ma)	The most lateral point on the mastoid bone (left & right)
16	Point Zygomatic Arch (za)	Point at the most lateral border of the center of the zygomatic arch (left & right)

17	Zygomaticofrontal Lateral Suture point-out Left & Right (lzmf)	Point at the lateral margin of the zygomatico-frontal suture (left & right)
18	Zygomaticofrontal Medial Suture point-in Left & Right (mzmf)	Point at the medial margin of the zygomatico-frontal suture (left & right)
19	Inferio-Orbitale (io)	Most inferior point on the outline of the orbital (left & right)
20	Medio-Orbitale (mo)	The point on the medial orbital margin that is closest to the medial plane (left & right)
21	Superio-Orbitale (so)	Most superior point on the outline of the orbital (left & right)
22	Mandibular Molar (lm)	The most prominent lateral point on the buccal surface of the first permanent mandibular molar (left & right)
23	Lower Molar Apex (L6 apx)	Point located in the region of root apices of the mandibular first permanent molar (left & right)
24	Lower Molar Buccal Cusp (L6 tip)	Buccal cusp tip of the mandibular first permanent molar (left & right)
25	Lower Central Incisor Apex (L1 apx)	Root apex of the mandibular central incisor (left & right)
26	Lower Central Incisor Edge (L1 tip)	Central point of the incisal edge of mandibular central incisor (left & right)
27	MIL & MIR	Contact point of upper central incisors at the level of closest approximation
28	Upper Central Incisor Apex (U1 apx)	Root apex of the maxillary central incisor (left & right)
29	Upper Central Incisor Edge (U1 tip)	Central point of the incisal edge of maxillary central incisor (left & right)
30	Maxillary Molar (um)	The most prominent lateral point on the buccal surface of the first permanent maxillary molar (left & right)
31	Upper Molar Palatal Apex (U6 apx)	Point located in the region of root apices of the maxillary first permanent molar (left & right)
32	Upper Molar Palatal Cusp (U6 tip)	Palatal cusp tip of the maxillary first permanent molar (left & right)

Appendix 13. Statistical Tests

$$\text{Student t-test} = \frac{\text{difference between the means}}{\sqrt{(SE\eta_1)^2 + (SE\eta_2)^2}} \quad (1)$$

where $SE\eta_1$ and $SE\eta_2$ are the Standard Errors for the first and second mean values with $(\eta_1 + \eta_2 - 2)$ degrees of freedom.

A 99,5% confidence interval for the true difference between the population means before (μ_1) and after (μ_2) treatment

$$(\bar{\chi}_{after} - \bar{\chi}_{beforev}) - t_{\frac{1+\rho}{2}} \sqrt{\frac{s_1^2}{N_1} + \frac{s_2^2}{N_2}} < \mu_2 - \mu_1 < (\bar{\chi}_{after} - \bar{\chi}_{beforev}) + t_{\frac{1+\rho}{2}} \sqrt{\frac{s_1^2}{N_1} + \frac{s_2^2}{N_2}} \quad (2)$$

where $\bar{\chi}_{after}$, $\bar{\chi}_{before}$ are the mean values of the anomaly group before and after treatment; s^2_1, s^2_2 are respectively the variances of the same groups; and $t_{1+\rho/2}$ is the critical value of the student t-test for the probability $P=1+\rho/2$ and degrees of freedom defined by the following formula:

$$\nu = \frac{(\frac{S_1^2}{N_1} + \frac{S_2^2}{N_2})^2}{\frac{(S_1^2/N_1)^2}{N_1 - 1} + \frac{(S_2^2/N_2)^2}{N_2 - 1}} \quad (3)$$

$$t_0 = \frac{(\bar{\chi}_{after} - \bar{\chi}_{befrore\ v}) - (\mu_2 - \mu_1)}{\sqrt{\frac{s_1^2}{N_1} + \frac{s_2^2}{N_2}}} \quad (4)$$

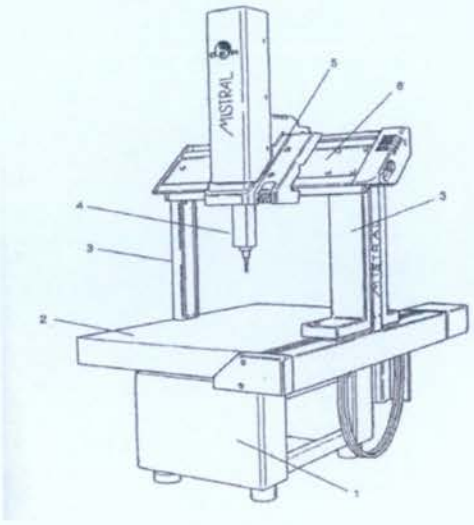

The constructing components of the Coordinate Measurement Machine (Mistral)

1. Base
2. Table from Granite
3. Main Carrier (vertical crossbar)
4. Measuring Column
5. Secondary Carrier
6. Main Carrier (horizontal crossbar)

Appendix 14. Coordinate Measurement Machine

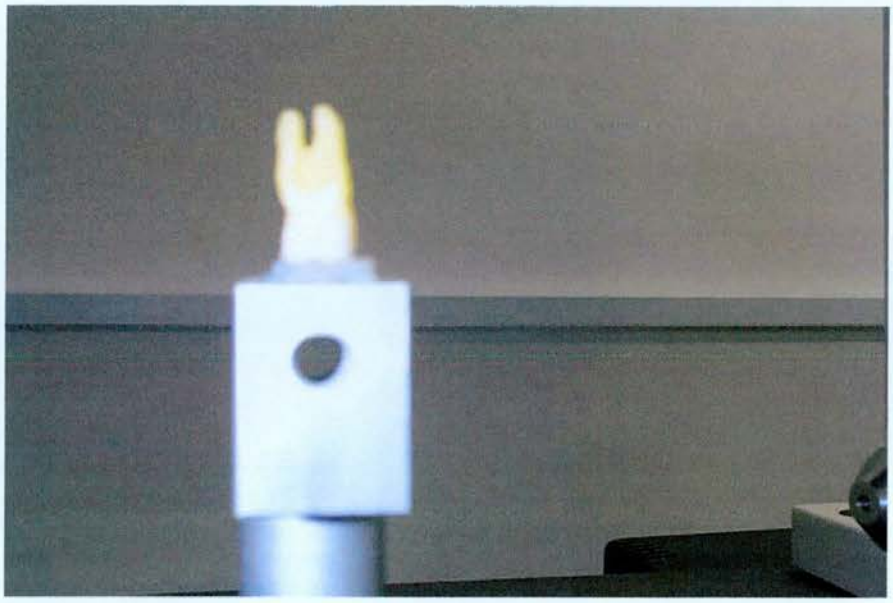

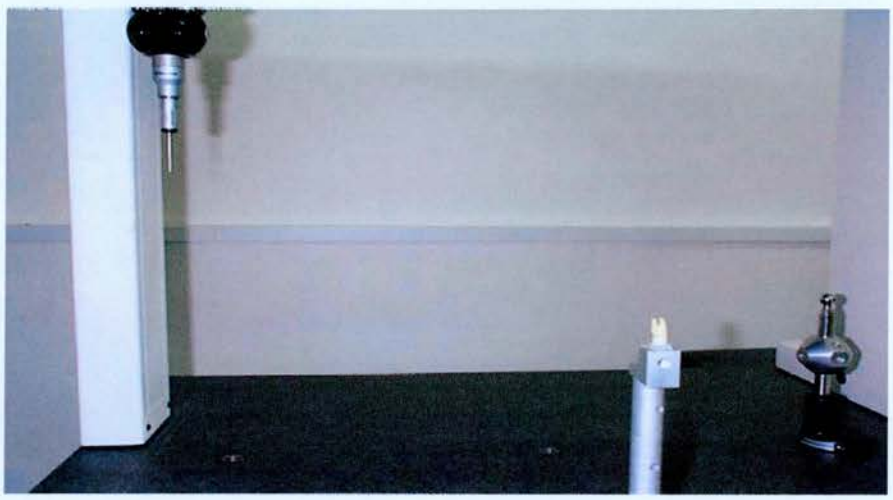

Appendix 15. Placement and scanning of the model of the tooth by the Coordinate Measurement Machine.

Instrument	Type	Manufacturer	Width of Measurement	Accuracy of the Instrument
Micrometer	Inside micrometer 5 – 30 mm	Mitutoyo	5 – 30 mm	0.01 mm
Digital Micrometer	MDC – 75M	Mitutoyo	50 – 75 mm	0.001 mm
Digital Gauge	500 – 181U	Mitutoyo	0 – 150 mm	0.01 mm

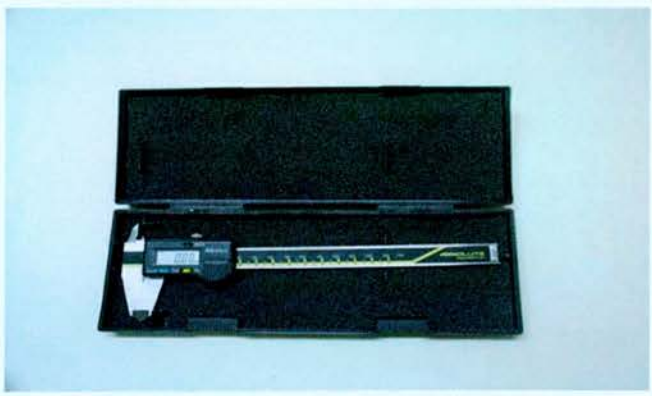

Appendix 16. Measuring devices used in the *in vitro* experimental application of the Rapid Maxillary Expansion

Appendix 17. Video image from the *in vitro* application of the Rapid Maxillary Expansion of the dry skull

Appendix 18. The Dry Skull before the application of the Rapid Maxillary Expansion forces

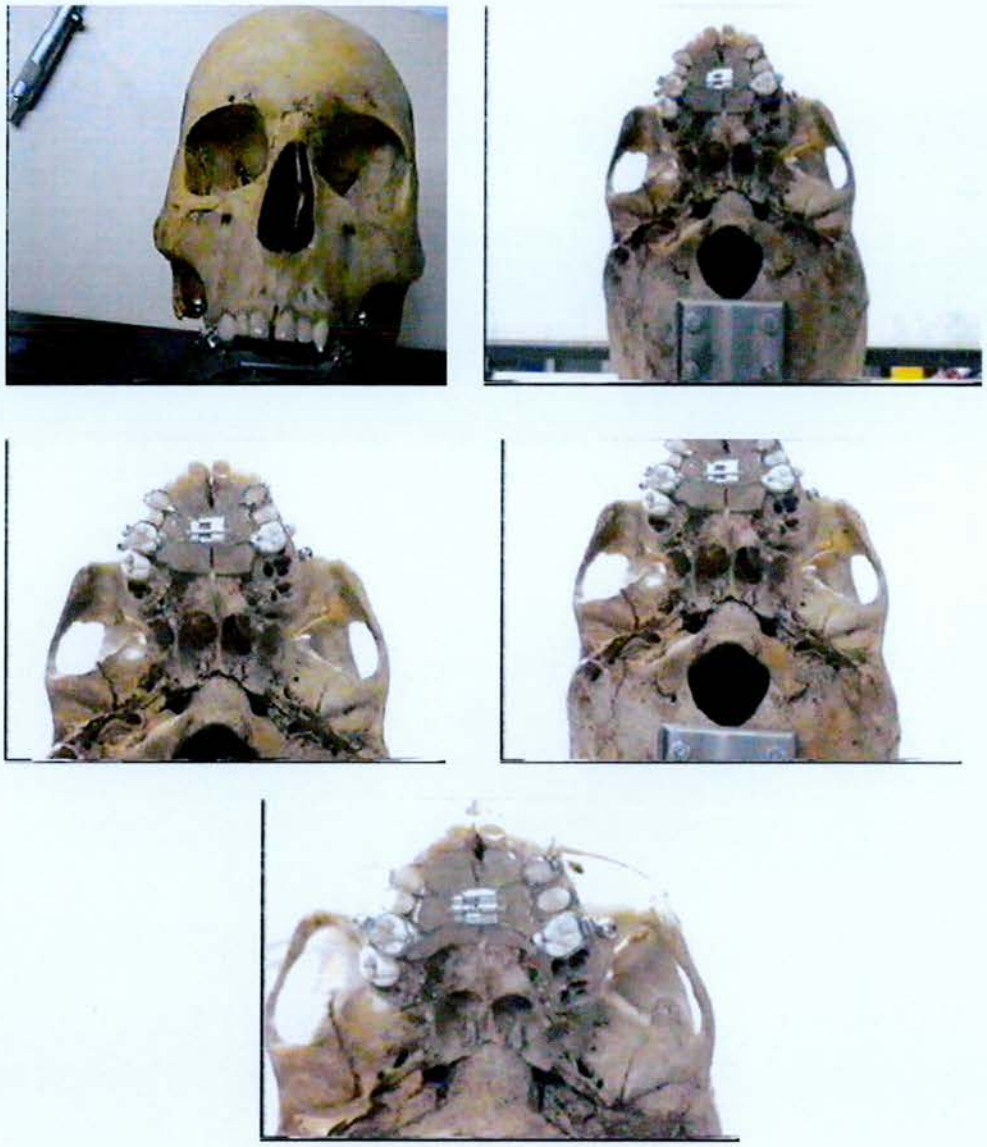

First Loading

Second Loading


Third Loading




Fourth Loading

Fifth Loading

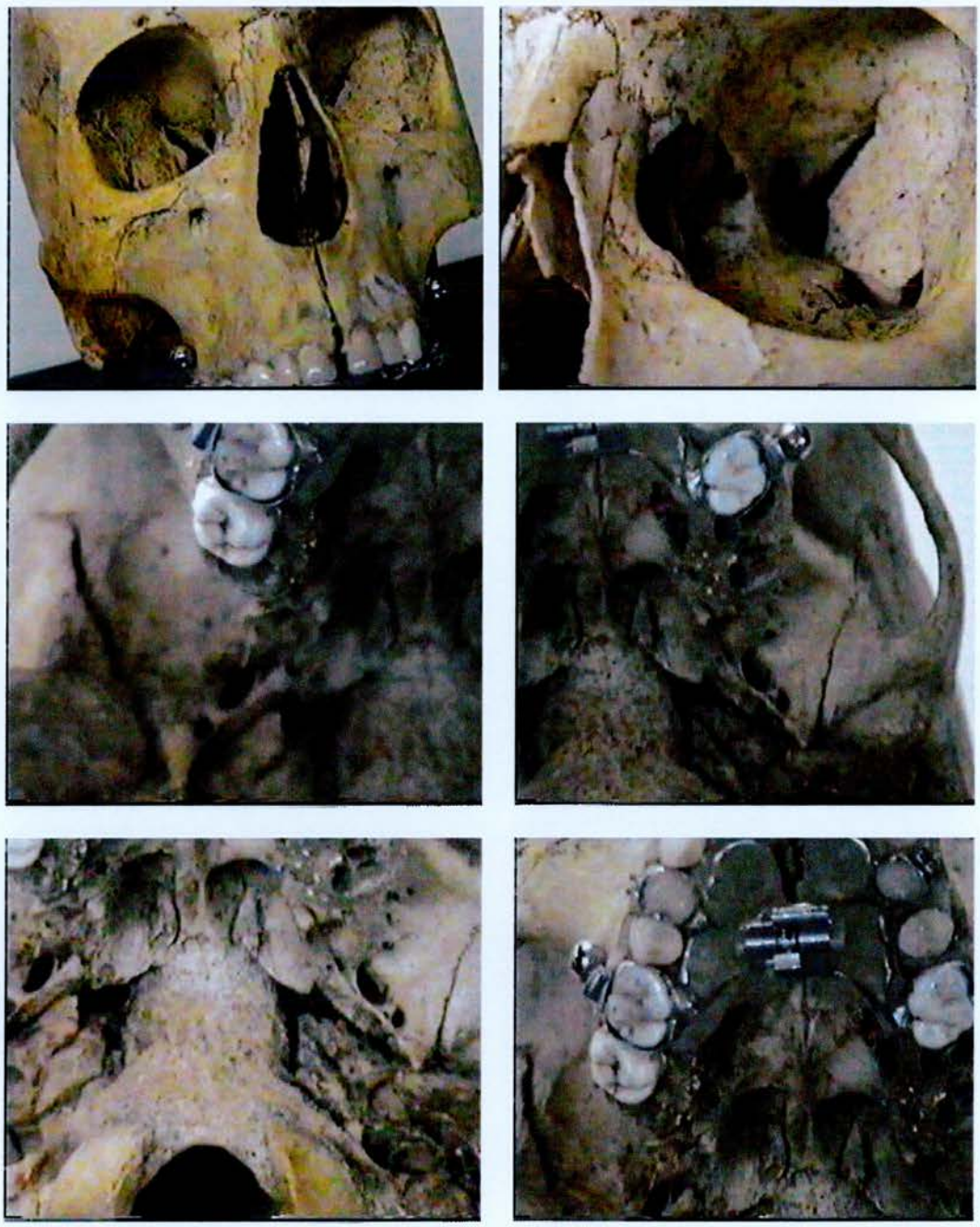

Sixth Loading

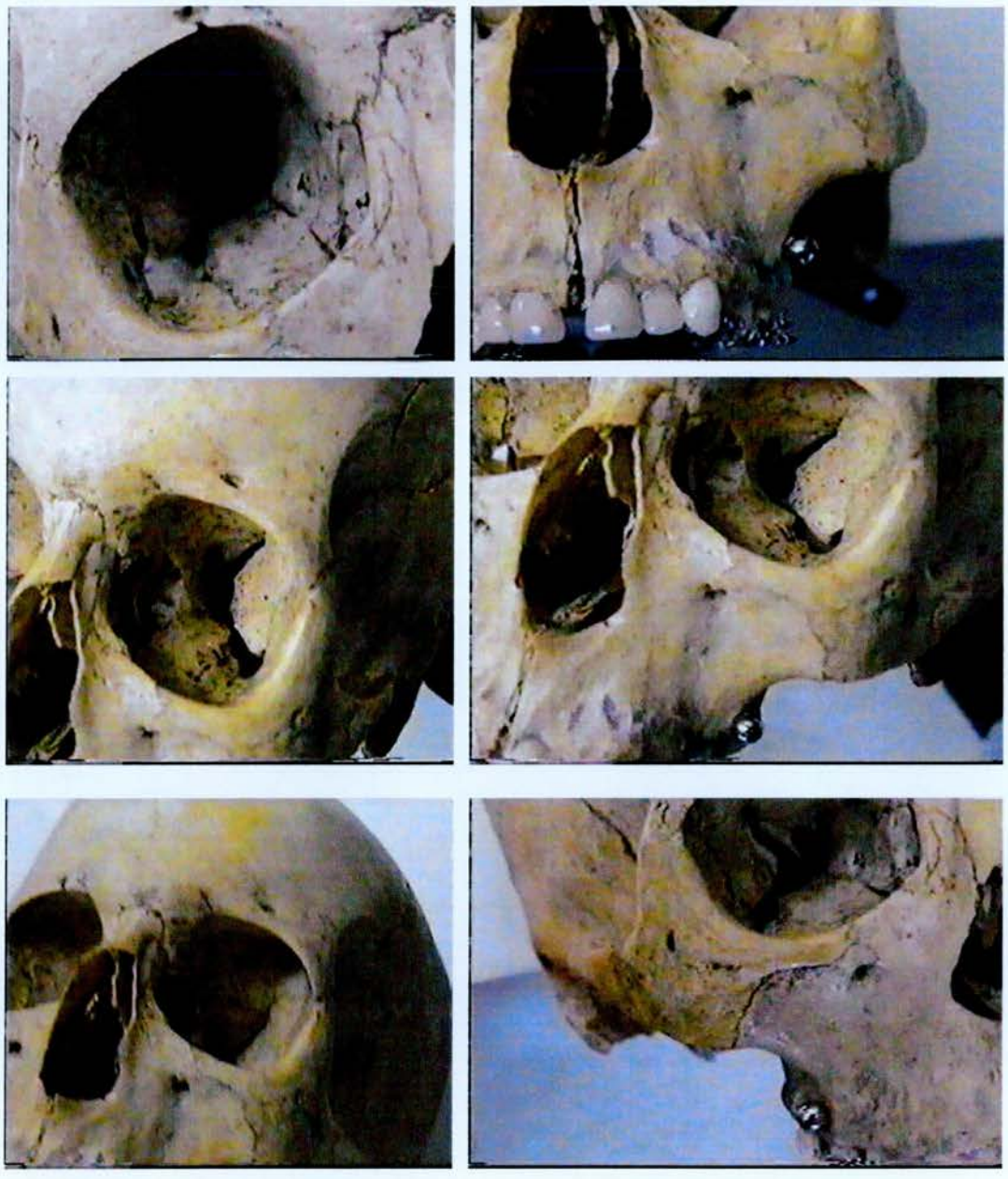

Seventh and ½ Loading

Appendix 19. *In vitro* application of the rapid maxillary expansion